How CD4+ T-cell help shapes functional and dysfunctional CD8+ T-cell differentiation

Busselaar, J.L.C.

How $CD4^+$ T-cell help shapes functional and dysfunctional $CD8^+$ T-cell differentiation

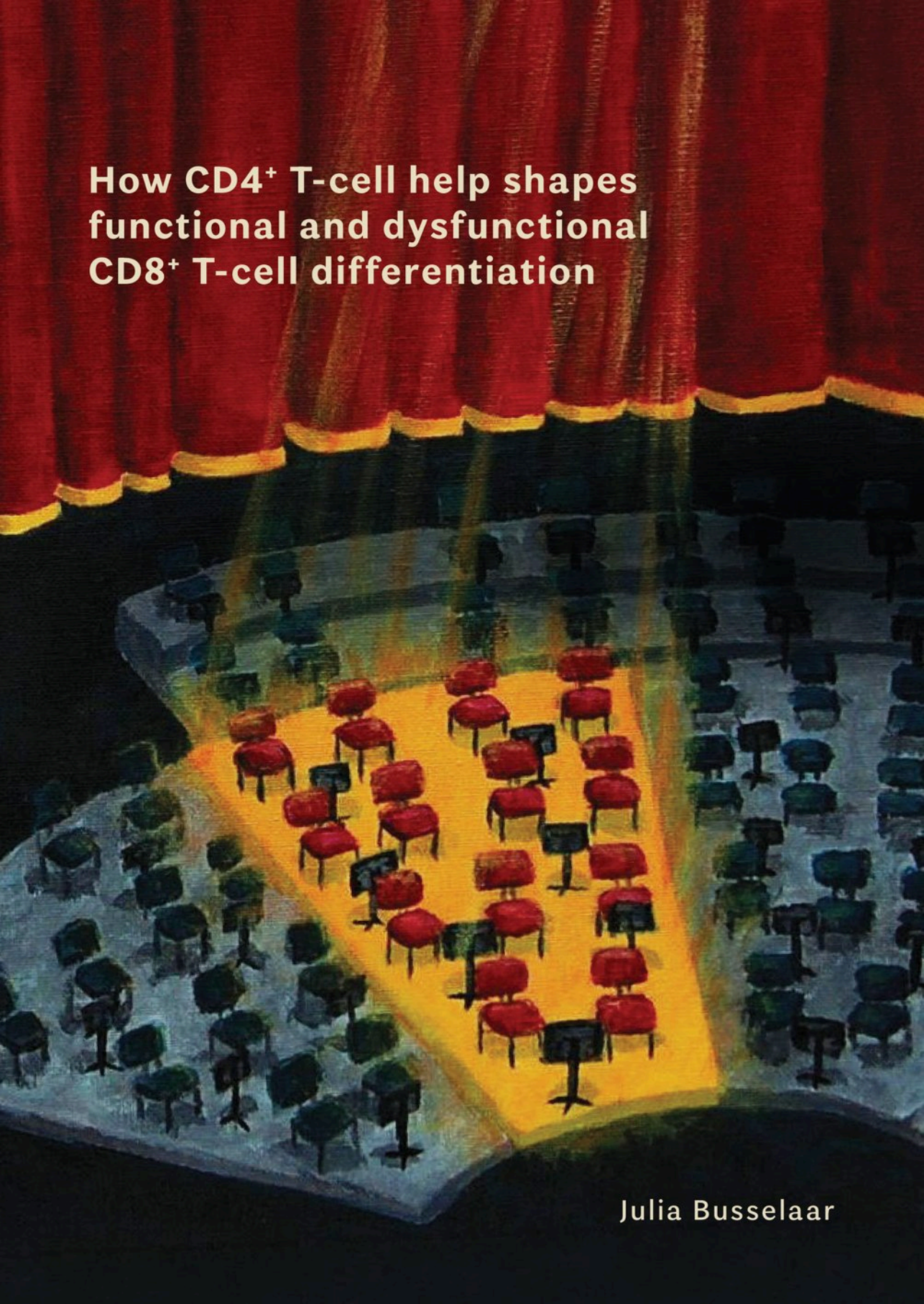

Julia Busselaar

How $CD4^+$ T-cell help shapes functional and dysfunctional $CD8^+$ T-cell differentiation

Julia Busselaar

About the cover

In the orchestra, second violins play the harmonic and rhythmic foundation of the music, supporting the main melody. While sometimes overlooked, this section is essential for the structure of the music and the depth of the sound. The second violin part often aligns in octaves with the first violins, providing the support they need to make their melody shine. Similarly, $CD4^+$ T cells support the immune response against cancer by providing help to $CD8^+$ T cells, the main effectors of anti-tumor immunity. $CD8^+$ T cells depend on $CD4^+$ T-cell help to reach their full cytotoxic potential, just like the first violins depend on the help of the second violins. Besides helping $CD8^+$ T cells, $CD4^+$ T cells can also help B cells or become regulatory T cells that dampen the immune response. In parallel, second violins can also support the lower string sections of the orchestra or add an extra layer of complexity to the music by playing a counter-melody.

ISBN: 978-94-6537-644-8

Cover artwork: Julia Busselaar
Cover and layout design: © Sıla Akçakoca, 2026 for Ridderprint
Print: Ridderprint | www.ridderprint.nl

How $CD4^+$ T-cell help shapes functional and dysfunctional $CD8^+$ T-cell differentiation

Proefschrift

ter verkrijging van

de graad van doctor aan de Universiteit Leiden,

op gezag van rector magnificus prof. dr. S. de Rijcke,

volgens besluit van het college voor promoties

te verdedigen op dinsdag 1 september 2026

klokke 14.30 uur

door

Julia Laura Charlotte Busselaar

geboren te Amsterdam

in 1994

Promotor

Prof. Dr. J.G. Borst

Tweede promotor

Prof. Dr. F.A. Ossendorp

Leden promotiecommissie

Prof. Dr. N.F. de Miranda	
Prof. Dr. A.N.M. Schumacher	
Prof. Dr. L. Meyaard	UMC Utrecht
Prof. Dr. D. Amsen	Sanquin, Universiteit van Amsterdam
Dr. D. Thommen	Nederlands Kanker Instituut

TABLE OF CONTENTS

Chapter 1

General Introduction & Scope of Thesis

T cells play a crucial role in the immunological protection of the host against infections and cancer. They can recognize pathogen-derived antigens expressed by infected cells, tumor-associated antigens or neoantigens expressed by cancer cells as a result of mutations. However, in cancer there are often barriers for an effective T-cell mediated immune response, which include a lack of non-self antigens, insufficient immune-activating signals, and an immune-suppressive tumor microenvironment (TME). Immune therapies aim to overcome these barriers and thereby to stimulate the host's immune system to fight the cancer. Clinical responses to immune therapies are variable, and a better fundamental understanding of the underlying immunological mechanisms is needed.

$CD8^+$ cytotoxic T lymphocytes (CTL) are particularly effective for anti-tumor immune responses, since they kill target cells upon recognition of intracellular antigens in the context of MHC class I (MHC-I) molecules, which are expressed by all nucleated cells including tumor cells. To undergo clonal expansion and gain effector functions, naïve tumor-specific $CD8^+$ T cells expressing a T cell receptor (TCR) that recognizes a specific (tumor) antigen, have to be activated (primed) by dendritic cells (DCs) in secondary lymphoid organs, generally the lymph node (LN). After priming, antigen recognition by a properly activated and differentiated antigen-specific $CD8^+$ T cell can lead to direct killing of the (tumor) target cell. However, $CD8^+$ T cells in cancer are often found in a dysfunctional or "exhausted" state, which is characterized by loss of effector function, loss of proliferation, and high expression of inhibitory receptors such as PD-1[1]. Upon interaction with their ligand, inhibitory receptors relay a negative signal that counteracts T cell activation, and thereby act as a brake or so-called "checkpoint" for anti-tumor immune responses. Immune checkpoint blockade (ICB) therapies, such as PD-1 blockade, aim to release this brake and thereby reactivate $CD8^+$ T cells within the tumor context[2].

$CD4^+$ T cells recognize antigens in the context of MHC class II (MHC-II), which is expressed by professional antigen-presenting cells (APCs), and typically not by solid tumor cells. $CD4^+$ T cells have a dual role in cancer: conventional helper T cells can help $CD8^+$ T cells or B cells, while regulatory T cells (Tregs) suppress the CTL response[3]. Tregs express high levels of the inhibitory receptor CTLA-4, which downregulates CD80/86 on DCs and thereby inhibits CD28 costimulation needed for CTL priming. CTLA-4 blockade is another checkpoint inhibition therapy, which aims to block this interaction and thereby allow for better activation of $CD8^+$ T cells. In comparison to CTLs, conventional $CD4^+$ T cells have generally received less attention within the ICB field, because most tumors are MHC-II negative and therefore not directly recognized by $CD4^+$ T cells. However, for an optimal anti-tumor $CD8^+$ T cell response, $CD4^+$ T-cell help via the DC interface is essential[4].

Priming of tumor-specific $CD8^+$ and $CD4^+$ T cells relies on antigen uptake by conventional (c) DCs in the tumor, DC activation and migration to the tumor-draining lymph node (TdLN) where tumor antigens are presented to T cells. In viral infection and vaccination settings, naïve $CD8^+$ and $CD4^+$ T cells are initially activated independently by migratory cDCs in distinct regions of the LN[5–7]. Type 1 cDCs (cDC1s), specialized in exogenous cell-derived antigen crosspresentation

on MHC-I, provide the first activation step for CD8⁺ T cells, while generally type 2 cDCs (cDC2s) initially activate CD4⁺ T cells via MHC-II[8,9]. The cDC1s subset can effectively present exogenous cell-derived antigens on both MHC-I and MCH-II, and thereby forms the platform for CD4⁺ T-cell help delivery to CD8⁺ T cells, as shown in mouse and human settings[5,6,10–12].

According to the two-step priming model[4], CD4⁺ T-cell help delivery likely takes place during the second step of T cell priming (Figure 1). This is supported by studies in infection and vaccination models, demonstrating that the initial activation of CD4⁺ and CD8⁺ T cells by migratory DCs takes place prior to CD4⁺ T-cell help delivery by resident cDC1s in distinct regions of the LN[5,6,13–15]. In cancer, initial priming of CD8⁺ T cells and delivery of CD4⁺ T-cell help also depend on crosspresenting cDC1s[10,12,16], but whether these events happen in two consecutive priming steps is less clear. A CD8⁺ T cell may receive its initial activation by one (migratory) cDC1, and the CD4⁺ T-cell help signal by another (resident) cDC1. However, these steps may also occur on the same 'helped', also called 'licensed' cDC1, that is interacting or has interacted with an activated CD4⁺ T cell. It has been proposed that cDC1s in cancer may also provide early activation signals for CD4⁺ T cells[10], although the possibility of their initial activation by cDC2s, as previously shown by others[17] was not excluded in this study.

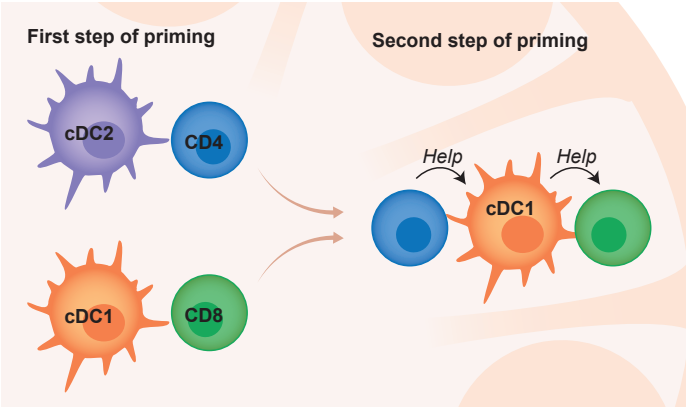

Figure 1. Two-step priming model of CD8⁺ and CD4⁺ T-cell activation in the LN.

Help signals (Figure 2) are relayed to the cDC1 via CD40 ligand (L) and type I interferon (IFN-I) produced by the activated CD4⁺ T cell[18–21]. These signals lead to increased survival, crosspresentation and upregulation of costimulatory molecules such as CD80/86 and CD70, as well as the production of cytokines such as IL-12 and IL-15 by the helped cDC1[4,12,22]. The delivery of these costimulatory and cytokine-mediated signals, in addition to the TCR-mediated activation signal via MHC-I, eventually results in the priming of 'helped' CD8⁺ T cells with optimal effector and memory functions [4,11]. Recent studies have suggested that in addition to cDC1 licensing, CD4⁺ T-cell help during priming may also be delivered to CD8⁺ T cells via cDC1-independent mechanisms, for example via other APCs such as monocyte-derived (Mo)DCs, or perhaps directly via CD4⁺ T-cell–derived IL-2[15,23].

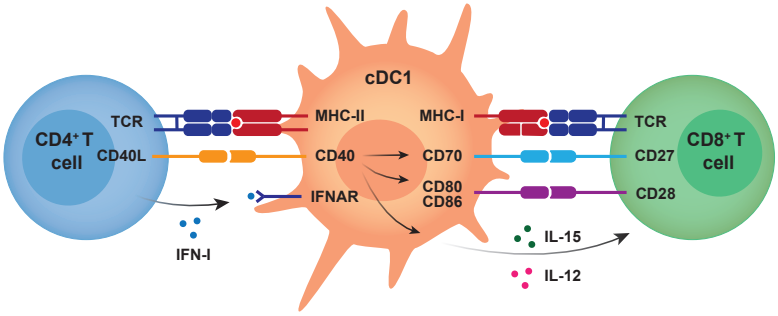

Figure 2. Signals involved in CD4$^+$ T-cell help delivery to CD8$^+$ T cells, mediated by cDC1.

Cancer immune therapies aim to improve tumor-specific CTL responses, by sustaining and activating previously primed tumor-specific CD8$^+$ T cells, or by new priming of such CD8$^+$ T cells. The importance of CD4$^+$ T-cell help for the anti-tumor CTL response is recognized mostly in the therapeutic vaccination field, where it has long been known that inclusion of MHC-II epitopes in the vaccine formulation improves CTL-mediated tumor control[24–26]. However, in the checkpoint inhibition field, the importance of CD4$^+$ T-cell help is not so generally considered. In recent years, accumulating evidence supports the idea that clinical efficiency of PD-1 blockade therapy does not solely depend on PD-1 expression on CD8$^+$ T cells, but also on PD-1 expression on conventional CD4$^+$ T helper cells[27,28]. Whether the spontaneous or ICB-induced priming of tumor-specific CD8$^+$ T cells happens in presence or absence of CD4$^+$ T-cell help, remains unclear.

In preclinical studies that investigate the role of CD4$^+$ T cells on CTL priming and differentiation, researchers often make use of antibody-based CD4$^+$ T-cell depletion in mouse models of chronic or acute infection[29–35]. These CD4$^+$ T-cell depletion experiments provide strong evidence for the importance of CD4$^+$ T-cell help for CTL effector and memory differentiation and function in the context of infection. However, the CD8$^+$ T-cell states in these type of experiments may additionally be affected by depletion of Tregs and/or the absence of CD4$^+$ T-cell-derived cytokines for CTL maintenance[15,36]. CD8$^+$ T-cell states may also be indirectly affected by the impact of CD4$^+$ T-cell depletion on antigen load or antigen persistence[37–39].

In order to specifically investigate CD8$^+$ T cells that are primed with or without CD4$^+$ T-cell help, outside the context of infection or chronic antigen stimulation, we made use of a DNA vaccination model wherein CD4$^+$ T cells are not depleted, but are simply engaged in the response or not via the addition of MHC-II restricted epitopes in the vaccine construct[40]. Using this model, our group has previously identified molecular mechanisms of CD4$^+$ T-cell help for the CD8$^+$ T-cell response during the effector phase. “Helped” CTLs undergo more clonal expansion, express higher levels of effector molecules such as Granzyme-B, IFNγ and TNF and are superior on a per-cell basis in antigen-specific killing of target cells[41]. They also show improved migratory and invasive capacities, which allows them to infiltrate tumors. On the other hand, “helpless” CD8$^+$ T

cells, primed in absence of CD4$^+$ T-cell help, expand less, show impaired cytotoxic and migratory function and have a higher expression of various inhibitory receptors including PD-1[41].

Besides shaping size and quality of the effector CTL pool, CD4$^+$ T-cell help also impacts CD8$^+$ T-cell memory. After antigen clearance and contraction of the effector CTL population, memory CD8$^+$ T cells persist long-term and respond efficiently upon secondary antigen encounter. Effector memory (T_{EM}) cells retain a phenotype resembling effector cells, and can rapidly respond to antigen by expressing cytolytic molecules. Central memory (T_{CM}) cells are characterized by their self-renewal capacities and robust clonal expansion upon antigen encounter, and are phenotypically more similar to naïve CD8$^+$ T cells[42]. In Chapter 2, we demonstrate that CD4$^+$ T-cell help during priming impacts CD8$^+$ T-cell memory by promoting the long-term maintenance, but not so much the gene expression profile of T_{CM} cells and by increasing and qualitatively altering the T_{EM} pool that transcriptionally and epigenetically resembles helped effector CTLs. Importantly, memory CD8$^+$ T cells that received help during priming, no longer depend on CD4$^+$ T-cell help during the secondary response, indicating that CD4$^+$ T-cell help improves CD8$^+$ T cell-intrinsic memory capacities.

After identifying the molecular mechanisms underlying CD4$^+$ T-cell help for effector and memory CD8$^+$ T-cell responses, we aimed to conceptualize an overarching model on how CD4$^+$ T-cell help shapes mature CD8$^+$ T-cell differentiation after antigen recognition in general. For therapeutic interventions, it is important to understand this differentiation process both in the context of an acute immune response such as after vaccination or transient infection, but also upon chronic immune stimulation as in the case of cancer or chronic infection.

When exhausted CD8$^+$ T cells were first discovered in the late 1990s[30], it was thought for years that these cells were derived from 'eroded' effector CTLs as a result of constant antigen stimulation[32]. However, in 2016 it was discovered that exhausted CD8$^+$ T cells do not derive from previously functional effector CTLs, but instead are generated from a population of PD-1$^+$TCF-1$^+$ 'stem-like' cells[33,43–45]. Many different names have been given to this population, such as 'memory-like', 'predysfunctional', 'precursor exhausted', 'progenitor exhausted (T_{PEX})', or simply TCF-1$^+$ CD8$^+$ T cells. Importantly, stem-like cells are the CD8$^+$ T cells responding to PD-(L)1 blockade therapy in preclinical tumor models[46,47]. In human cancer, effective PD-(L)1 blockade therapy induces proliferation and further differentiation of PD-1$^+$TCF-1$^+$ stem-like cells in the TdLN[48] or in intratumoral niches where they interact with DCs and CD4$^+$ T cells[49]. Thus, stem-like CD8$^+$ T cells are of particular interest for cancer immunotherapy.

In Chapter 3, we show that helpless CD8$^+$ T cells transcriptionally resemble stem-like cells. We compare the transcriptomic signature of helpless cells from our vaccination model to published signatures of predysfunctional stem-like cells from chronic infection and cancer. Based on the transcriptional overlap and supported by literature, we pose the hypothesis that stem-like CD8$^+$ T

cells equal helpless cells, and are generated as a result of priming in absence of $CD4^+$ T-cell help. Next, we provide experimental evidence for this hypothesis in Chapter 4. We show that upon priming, naïve $CD8^+$ T cells adopt an entire spectrum of differentiation states, ranging from lowly differentiated T_{CM} cells, to stem-like cells, T_{EM} cells and eventually terminally differentiated effector CTLs. The generation of this spectrum of $CD8^+$ T-cell states after priming, also known as the progressive differentiation model, has been proposed before and is supported by a large body of evidence epigenetic, transcriptomic and TCR tracing studies[50–54]. Until now, $CD8^+$ T-cell fate was proposed to be mainly dependent on TCR signaling strength. Our experiments argue that it is also dependent on $CD4^+$ T-cell help and all its associated signals, which shifts the CTL differentiation spectrum in the direction of a more effector-like state. We demonstrate that $CD4^+$ T-cell help is required for $CD8^+$ T cells to differentiate past the PD-1^+TCF-1^+ stem-like state towards the CTL effector state. We show that in an immunogenic tumor setting, tumor neoantigen-specific $CD8^+$ T cells that are spontaneously primed by the tumor have a stem-like, but not helped effector state, suggesting that $CD4^+$ T-cell help delivery is impaired. Our results support that stem-like $CD8^+$ T cells as found in cancer are in fact helpless cells that lie at an early stage on the 'normal' differentiation spectrum. Importantly, we show that helpless/stem-like cells are still able to complete their CTL differentiation when they are provided with help signals after initial priming.

That the second step of priming is not only important for $CD8^+$ T-cell differentiation but also for $CD4^+$ T-cell differentiation, is shown in Chapter 5. In type-1 immune responses raised against intracellular antigens, $CD4^+$ T cells differentiate into T helper 1 (Th1) cells that can deliver help to $CD8^+$ T cells, and T follicular helper (Tfh) cells that help the humoral response by promoting isotype class switching, somatic hypermutation and memory formation of B cells[55]. We show that upon initial activation, conventional $CD4^+$ T cells adopt a uncommitted Th1/Tfh phenotype. Interactions between $CD4^+$ T cells and cDC1s, which take place during the second step of priming, are dispensable for initial $CD4^+$ T-cell activation and formation of the uncommitted Th1/Tfh phenotype but essential for uncommitted $CD4^+$ T cells to differentiate into Th1 cells. The formation of Tfh cells on the other hand, depends on a second priming step on B cells.

One of the underlying mechanisms for impaired $CD4^+$ T-cell help in cancer may be a lack of inflammatory signals, such as type I interferon (IFN-I) in the TME. How this works is described in Chapter 6. We provide an overview of literature showing that IFN-I optimizes the help delivery capacity of cDC1, by promoting antigen presentation on MHC-I and MHC-II, costimulation and cytokine production. IFN-I also induces the expression of chemokines that are essential for the spatial organization of the help delivery platform within the LN. However, in a tumor setting the IFN-I pathway is often suppressed, resulting in suboptimal cDC1 activation and likely impaired delivery of $CD4^+$ T-cell help.

In recent years, evidence has accumulated showing that the target cells of PD-1 blockade therapy in cancer are not terminally exhausted CD8$^+$ T cells, as previously thought, but tumor-specific stem-like CD8$^+$ T cells[46]. Previous chapters have elaborated on stem-like cells being helpless CD8$^+$ T cells, indicating that it is the helpless cells are the likely target for PD-1 blockade therapy. Moreover, the PD-1/PD-L1 axis that is important for the response to ICB lies at the interface between tumor-specific T cells and cDC1, not at the interface between CTLs and their tumor target cells. The data that support this are reviewed in Chapter 7. We propose on basis of these data that PD-1 blockade leads to delivery of CD4$^+$ T-cell help for the CTL response, and discuss the clinical implications of this view.

Finally, Chapter 8 places the concepts and experimental findings as described in this thesis in the context of current literature.

References

1. Philip, M. & Schietinger, A. CD8+ T cell differentiation and dysfunction in cancer. *Nat. Rev. Immunol.* **22**, 209–223 (2022).
2. Waldman, A. D., Fritz, J. M. & Lenardo, M. J. A guide to cancer immunotherapy: from T cell basic science to clinical practice. *Nat. Rev. Immunol.* **20**, 651–668 (2020).
3. Speiser, D. E., Chijioke, O., Schaeuble, K. & Münz, C. CD4+ T cells in cancer. *Nat. Cancer* **4**, 317–329 (2023).
4. Borst, J., Ahrends, T., Bąbała, N., Melief, C. J. M. & Kastenmüller, W. CD4+ T cell help in cancer immunology and immunotherapy. *Nat. Rev. Immunol.* **18**, 635–647 (2018).
5. Eickhoff, S. *et al.* Robust anti-viral immunity requires multiple distinct T cell-dendritic cell interactions. *Cell* **162**, 1322–1337 (2015).
6. Hor, J. L. *et al.* Spatiotemporally distinct interactions with dendritic cell subsets facilitates CD4+and CD8+T cell activation to localized viral infection. *Immunity* **43**, 554–565 (2015).
7. Kitano, M. *et al.* Imaging of the cross-presenting dendritic cell subsets in the skin-draining lymph node. *Proc. Natl. Acad. Sci. U. S. A.* **113**, 1044–1049 (2016).
8. Wculek, S. K. *et al.* Dendritic cells in cancer immunology and immunotherapy. *Nat. Rev. Immunol.* **20**, 7–24 (2020).
9. Hilligan, K. L. & Ronchese, F. Antigen presentation by dendritic cells and their instruction of CD4+ T helper cell responses. *Cell. Mol. Immunol.* **17**, 587–599 (2020).
10. Ferris, S. T. *et al.* cDC1 prime and are licensed by CD4+ T cells to induce anti-tumour immunity. *Nature* **584**, 624–629 (2020).
11. Wu, R. & Murphy, K. M. DCs at the center of help: Origins and evolution of the three-cell-type hypothesis. *Journal of Experimental Medicine* **219**, 1–13 (2022).
12. Lei, X. *et al.* CD4+ helper T cells endow cDC1 with cancer-impeding functions in the human tumor micro-environment. *Nat. Commun.* **14**, 217 (2023).
13. Brewitz, A. *et al.* CD8+T cells orchestrate pDC-XCR1+dendritic cell spatial and functional cooperativity to optimize priming. *Immunity* **46**, 205–219 (2017).

14. Castellino, F. *et al.* Chemokines enhance immunity by guiding naive CD8+ T cells to sites of CD4+ T cell-dendritic cell interaction. *Nature* **440**, 890–895 (2006).

15. Jobin, K. *et al.* A distinct priming phase regulates CD8 T cell immunity by orchestrating paracrine IL-2 signals. *Science (1979).* **388**, (2025).

16. Roberts, E. W. *et al.* Critical Role for CD103+/CD141+ Dendritic Cells Bearing CCR7 for Tumor Antigen Trafficking and Priming of T Cell Immunity in Melanoma. *Cancer Cell* **30**, 324–336 (2016).

17. Binnewies, M. *et al.* Unleashing Type-2 Dendritic Cells to Drive Protective Antitumor CD4+ T Cell Immunity. *Cell* **177**, 556–571 (2019).

18. Lei, X. *et al.* CD4+ T cells produce IFN-I to license cDC1s for induction of cytotoxic T-cell activity in human tumors. *Cell. Mol. Immunol.* 1–19 (2024) doi:10.1038/s41423-024-01133-1.

19. Schoenberger, S. P., Toes, R. E. M., van der Voort, E. I. H., Offringa, R. & Melief, C. J. M. T-cell help for cytotoxic T lymphocytes is mediated by CD40–CD40L interactions. *Nature* **393**, 480–483 (1998).

20. Bennett, S. R. M. *et al.* Help for cytotoxic-T-cell responses is mediated by CD40 signalling. *Nature* **393**, 478–480 (1998).

21. Ridge, J. P., Di Rosa, F. & Matzinger, P. A conditioned dendritic cell can be a temporal bridge between a CD4+ T-helper and a T-killer cell. *Nature* **393**, 474–478 (1998).

22. Wu, R. *et al.* Mechanisms of CD40-dependent cDC1 licensing beyond costimulation. *Nat. Immunol.* **23**, 1536–1550 (2022).

23. Bosma, D. M. T. *et al.* CD4+ T-cell help delivery to monocyte-derived dendritic cells promotes effector differentiation of helper and cytotoxic T cells. *Immunol. Lett.* **275**, (2025).

24. Melief, C. J. M., Hall, T. Van, Arens, R., Ossendorp, F. & Burg, S. H. Van Der. Therapeutic cancer vaccines. *J. Clin. Invest.* **125**, 3401–3412 (2015).

25. Brightman, S. E., Naradikian, M. S., Miller, A. M. & Schoenberger, S. P. Harnessing neoantigen specific CD4 T cells for cancer immunotherapy. *J. Leukoc. Biol.* **107**, 625–633 (2020).

26. Tay, R. E., Richardson, E. K. & Toh, H. C. Revisiting the role of CD4+ T cells in cancer immunotherapy—new insights into old paradigms. *Cancer Gene Ther.* **28**, 5–17 (2021).

27. Zuazo, M. *et al*. Systemic CD4 Immunity as a Key Contributor to PD-L1/PD-1 Blockade Immunotherapy Efficacy. *Front. Immunol.* **11**, 3087 (2020).

28. Kumagai, S. *et al.* The PD-1 expression balance between effector and regulatory T cells predicts the clinical efficacy of PD-1 blockade therapies. *Nat. Immunol.* **21**, 1346–1358 (2020).

29. Matloubian, M., Concepcion, R. J. & Ahmed, R. CD4+ T cells are required to sustain CD8+ cytotoxic T-cell responses during chronic viral infection. *J. Virol.* **68**, 8056–8063 (1994).

30. Zajac, A. J. *et al.* Viral Immune Evasion Due to Persistence of Activated T Cells Without Effector Function. *Journal of Experimental Medicine* **188**, 2205–2213 (1998).

31. Barber, D. L. *et al.* Restoring function in exhausted CD8 T cells during chronic viral infection. *Nature* **439**, 682–687 (2006).

32. Wherry, E. J. *et al.* Molecular Signature of CD8+ T Cell Exhaustion during Chronic Viral Infection. *Immunity* **27**, 670–684 (2007).

33. Im, S. J. *et al.* Defining CD8+ T cells that provide the proliferative burst after PD-1 therapy. *Nature* **537**, 417–421 (2016).

34. Ghoneim, H. E. *et al.* De Novo Epigenetic Programs Inhibit PD-1 Blockade-Mediated T Cell Rejuvenation. *Cell* **170**, 142–157 (2017).

35. Hudson, W. H. *et al.* Proliferating Transitory T Cells with an Effector-like Transcriptional Signature Emerge from PD-1+ Stem-like CD8+ T Cells during Chronic Infection. *Immunity* **51**, 1043–1058 (2019).

36. Laidlaw, B. J., Craft, J. & Kaech, S. M. The multifaceted role of CD4 + T cells in the regulation of CD8 + T cell memory maturation. *Nat. Rev. Immunol.* **16**, 102–111 (2016).

37. Li, Y. *et al.* Persistent antigen and prolonged AKT–mTORC1 activation underlie memory CD8 T cell impairment in the absence of CD4 T cells. *The Journal of Immunology* **195**, 1591–1598 (2015).

38. Lu, Y.-J. *et al.* CD4 T cell help prevents CD8 T cell exhaustion and promotes control of Mycobacterium tuberculosis infection. *Cell Rep.* **36**, 109696 (2021).

39. van der Heide, V. *et al.* Prolonged but finite antigen presentation promotes reversible defects of "helpless" memory CD8+ T cells. *Immunity* **58**, 1742-1761.e14 (2025).

40. Ahrends, T. *et al.* CD27 Agonism Plus PD-1 Blockade Recapitulates CD4+ T-cell Help in Therapeutic Anticancer Vaccination. *Cancer Res.* **76**, 2921–2931 (2016).

41. Ahrends, T. *et al.* CD4+T cell help confers a cytotoxic T cell effector program including coinhibitory receptor downregulation and increased tissue invasiveness. *Immunity* **47**, 848–861 (2017).

42. Mueller, S. N., Gebhardt, T., Carbone, F. R. & Heath, W. R. Memory T Cell Subsets, Migration Patterns, and Tissue Residence. *Annu. Rev. Immunol.* **31**, 137–161 (2013).

43. Utzschneider, D. T. *et al.* T Cell Factor 1-expressing memory-like CD8+T cells sustain the immune response to chronic viral infections. *Immunity* **45**, 415–427 (2016).

44. He, R. *et al.* Follicular CXCR5-expressing CD8+ T cells curtail chronic viral infection. *Nature* **537**, 412–416 (2016).

45. Wu, T. *et al.* The TCF1-Bcl6 axis counteracts type I interferon to repress exhaustion and maintain T cell stemness. *Sci. Immunol.* **1**, eaai8593 (2016).

46. Chow, A., Perica, K., Klebanoff, C. A. & Wolchok, J. D. Clinical implications of T cell exhaustion for cancer immunotherapy. *Nat. Rev. Clin. Oncol.* **19**, 775–790 (2022).

47. Zebley, C. C., Zehn, D., Gottshalk, S. & Chi, H. T cell dysfunction and therapeutic intervention in cancer. *Nat. Immunol.* 1–11 (2024) doi:10.1038/s41590-024-01896-9.

48. Rahim, M. K. *et al.* Dynamic CD8+ T cell responses to cancer immunotherapy in human regional lymph nodes are disrupted in metastatic lymph nodes. *Cell* **186**, 1127–1143 (2023).

49. Magen, A. *et al.* Intratumoral dendritic cell–CD4+ T helper cell niches enable CD8+ T cell differentiation following PD-1 blockade in hepatocellular carcinoma. *Nat. Med.* **29**, 1389–1399 (2023).

50. Henning, A. N., Roychoudhuri, R. & Restifo, N. P. Epigenetic control of CD8+ T cell differentiation. *Nat. Rev. Immunol.* **18**, 340–356 (2018).

51. Dogra, P., Ghoneim, H. E., Abdelsamed, H. A. & Youngblood, B. Generating long-lived CD8(+) T-cell memory: Insights from epigenetic programs. *Eur. J. Immunol.* **46**, 1548–62 (2016).

52. Al Khabouri, S. & Gerlach, C. T cell fate mapping and lineage tracing technologies probing clonal aspects underlying the generation of CD8 T cell subsets. *Scand. J. Immunol.* **92**, (2020).

53. Pais Ferreira, D. *et al.* Central memory CD8+ T cells derive from stem-like Tcf7hi effector cells in the absence of cytotoxic differentiation. *Immunity* **53**, 985–1000 (2020).

54. Johnnidis, J. B. *et al.* Inhibitory signaling sustains a distinct early memory CD8+ T cell precursor that is resistant to DNA damage. *Sci. Immunol.* **6**, (2021).

55. Vinuesa, C. G., Linterman, M. A., Yu, D. & MacLennan, I. C. M. Follicular Helper T Cells. *Annu. Rev. Immunol.* **34**, 335–368 (2016).

Chapter 2

CD4$^+$ T-cell help creates memory CD8$^+$ T cells with innate and help-independent recall capacities

Tomasz Ahrends[1], Julia Busselaar[1], Tesa M. Severson[2], Nikolina Bąbała[1], Evert de Vries[1], Astrid Bovens[1], Lodewyk Wessels[2], Fred van Leeuwen[3] and Jannie Borst[1]

[1]Division of Tumor Biology and Immunology,

[2]Division of Molecular Carcinogenesis, Oncode Institute,

[3]Division of Gene Regulation, The Netherlands Cancer Institute-Antoni van Leeuwenhoek, Amsterdam, The Netherlands.

Nature Communications 2019;10(1): 5531

Abstract

CD4⁺ T-cell help is required for the generation of CD8⁺ cytotoxic T lymphocyte (CTL) memory. Here we use genome-wide analyses to show how CD4⁺ T-cell help delivered during priming promotes memory differentiation of CTLs. Help signals enhance IL-15-dependent maintenance of central memory T (T_{CM}) cells. More importantly, help signals critically regulate the size and function of the effector memory T (T_{EM}) cell pool. Helped T_{EM} cells can produce Granzyme B and IFNγ upon antigen-independent, innate-like recall by IL-12 and IL-18. In addition, helped memory CTLs express the effector program characteristic of helped primary CTLs upon recall with MHC class I-restricted antigen, likely due to epigenetic imprinting and sustained mRNA expression of effector genes. Our data thus indicate that during priming, CD4⁺ T-cell help optimizes CTL memory by creating T_{EM} cells with innate and help-independent antigen-specific recall capacities.

Introduction

Immunological memory is classically attributed to cells of the adaptive immune system. It is based on clonal expansion of antigen-specific lymphocytes, long-term maintenance of at least part of this antigen-specific lymphocyte pool as memory cells and the intrinsic ability of memory cells to respond more efficiently to renewed antigen encounter[1]. Memory CD8+ T cells can also be reactivated by cytokines in an antigen-independent manner[2].

A single activated CD8+ cytotoxic T lymphocyte (CTL) can give rise to both effector and memory cells[3]. The differentiation path of a given CD8+ T cell is graded from less to more differentiated, culminating in the terminally differentiated effector cell that is short-lived. Compared to effector cells, memory CD8+ T cells reportedly exhibit less differentiated phenotypes, can self-renew, have high proliferative potential and increased longevity[4]. Memory CD8+ T cells are discerned into central (T_{CM}), effector (T_{EM}) and tissue-resident (T_{RM}) cells[5]. T_{CM} cells and T_{EM} cells can be discriminated based on expression of homing receptors that allow T_{CM} cells to circulate through lymph nodes, while T_{EM} cells primarily circulate through non-lymphoid tissues and spleen.

Whether a primed CD8+ T cell becomes a short-lived effector cell (SLEC), or a memory precursor cell (MPEC) is decided upon by specific transcription factors that act in pairs to determine opposite cell fates by directing specific gene expression programs[3,6]. For example, the balance between Blimp-1 and Bcl-6 is decisive for an effector versus memory T-cell fate. Cell fate decisions are largely based on gene transcription that is orchestrated at the epigenetic level[7]. Epigenetic processes, such as DNA methylation, histone acetylation, and histone methylation confer chromatin states of a gene that facilitate or prohibit transcription. Recent data reveal a coupling between the master regulators of transcription and epigenetic modification[6,8].

Memory CD8+ T cells have an intrinsic ability to more efficiently expand and display effector functions upon secondary stimulation. Certain genes are more readily expressed in activated memory T cells as compared to activated naïve T cells[7,9]. This may be due to the fact that these genes are epigenetically poised, which means that they have an open chromatin state, but low gene expression in the steady-state memory phase[9]. For example, the promotor regions of the *Il2* and *Ifng* genes are more rapidly demethylated upon recall[10,11]. Alternatively, genes can already be expressed in steady-state memory cells at the mRNA level, but not at the protein level. Recall with antigen, but also with cytokines can induce protein translation from such transcripts and thereby efficient recall of functions[12].

Intrinsic memory qualities are instilled into CD8+ T cells during the priming phase, a phenomenon termed memory programming[13]. The generation and programming of memory CD8+ T cells relies on "help" signals that are delivered by CD4+ T cells during priming[14–17]. These help signals are relayed from the CD4+ T cell to the CD8+ T cell via an XCR1+ lymph-node resident dendritic

cell (DC), as established in the mouse[17,18]. The DC is conditioned by the $CD4^+$ T cell to deliver certain costimulatory signals and cytokines that orchestrate CTL effector- and memory differentiation[14,15,17,19]. We have recently identified by transcriptomic and functional analyses the gene expression program underlying CTL effector differentiation as instructed by $CD4^+$ T-cell help[20].

We here present the impact of $CD4^+$ T-cell help on the gene expression program of steady-state memory $CD8^+$ T cells and secondary effector CTLs. We demonstrate that help delivered during priming promotes the size of both T_{CM} and T_{EM} pools, but primarily alters the intrinsic functionality of T_{EM} cells. Remarkably, help signals confer cytokine-induced and help-independent recall capacities to $CD8^+$ memory T cells and allow them to "remember" that they have received help during priming.

Results

Help endows $CD8^+$ T cells with intrinsic memory capacity

To determine how $CD4^+$ T-cell help delivered during priming impacts $CD8^+$ T-cell memory, we used a mouse model of therapeutic vaccination. A comparative setting was created using two plasmid (p)DNA vaccines that encode the human papilloma virus (HPV) E7 protein either with the immunodominant, MHC class I-restricted epitope $E7_{48-57}$ alone (No Help), or in conjunction with exogenous, HPV-unrelated MHC class II-restricted helper epitopes (Help)[21]. As shown before[20–22], inclusion of helper epitopes in the vaccine significantly increased the magnitude of the primary H-$2D^b$/$E7_{48-57}$ (E7)-specific $CD8^+$ T cell response (Figure 1A, Supplementary Figure 1A, B). Help also significantly increased the total numbers of E7-specific $CD8^+$ T cells with a SLEC phenotype ($CD127^-$ $KLRG1^+$), as well as those with MPEC phenotype ($CD127^+KLRG1^-$) (Supplementary Figure 1C).

To examine the impact of help delivered during priming on the memory $CD8^+$ T-cell response, mice were primed with either Help or No Help vaccine and recalled with No Help vaccine in conjunction with i.p. injection of lipopolysaccharide (LPS)[22]. Mice primed with the Help vaccine had a significantly higher recall response to H-$2D^b$/$E7_{48-57}$ than mice primed with No Help vaccine (Figure 1A). At the peak of the secondary response, the frequencies of $CD8^+$ T cells expressing Granzyme B (Figure 1B), IFNγ and TNFα (Figure 1C) in blood, draining lymph node (dLN) and spleen were significantly higher after priming with Help as compared to No Help vaccine. Accordingly, an in vivo cytotoxicity assay revealed that - at the peak of the secondary response - injected $E7_{49-57}$ peptide-loaded target cells were killed much more efficiently in mice primed with the Help vaccine, than in mice primed with the No Help vaccine (Figure 1D, E). Thus, $CD4^+$ T-cell help delivered during priming improved the secondary $CD8^+$ T-cell response to MHC class I-restricted antigen only.

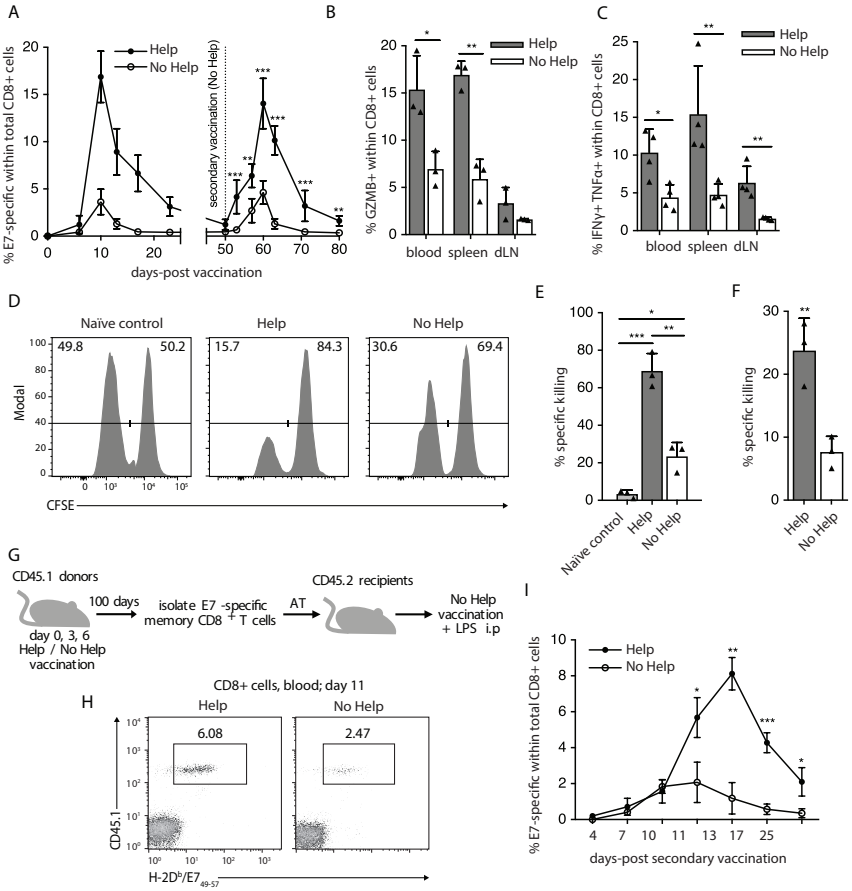

Figure 1. CD4+ T-cell help instills intrinsic recall capacities into CD8+ T cells. (A-F) Mice were vaccinated intra-epidermally with a DNA construct encoding HPV-E7 with (Help) or without (No Help) MHC class II-restricted epitopes on days 0, 3 and 6. On day 50, mice were rechallenged with No Help vaccine and i.p. lipopolysaccharide (LPS) injection. (A) Percentage of H-2D^b/E7$_{49-57}$ tetramer$^+$ cells among total CD8$^+$ T cells in blood at indicated days after first vaccination (n=7 per group). (B, C) In a separate experiment, on day 10 after rechallenge, frequencies of Granzyme B (GZMB)$^+$ cells (B) and IFNγ$^+$TNFα$^+$ cells (C) within total CD8$^+$ T cells in indicated tissues were determined by flow cytometry (n=3-4). (D, E) In a separate experiment, mice (n=3) were injected i.v on day 10 after rechallenge with a 1:1 ratio of splenocytes loaded with E7$_{49-57}$ peptide (CTL target) or not (control) and labeled with a low or high dose of carboxyfluorescein succinimidyl ester (CFSE), respectively. Naive recipient mice were used as control. After 15 h, percentage of specific in vivo target cell killing was determined by flow cytometric analysis of splenocytes. (D) Representative histograms of CFSE$^+$ cells. (E) Bar diagram quantitatively depicting all results. (F) In a separate experiment, E7-specific CD8$^+$ T cells were isolated from spleen at day 10 after rechallenge (n=3). T cells were incubated in vitro at a 1:1 ratio with E7$_{49-57}$-peptide-loaded or non-loaded splenocytes and specific killing of target cells was analyzed 12 h later. (G-I) CD45.1$^+$ donor mice received Help or No Help vaccine. At day 100, E7-specific (memory) CD8$^+$ T cells were isolated from spleens and injected i.v. in equal numbers into CD45.2$^+$ recipient mice (n=4 per group). One day later, recipient mice were rechallenged. (G) Experimental set up. (H) Representative flow cytometry plots indicating frequencies of CD45.1$^+$ E7-specific CD8$^+$ T cells in blood at day 11 after rechallenge. (I) Frequencies of CD45.1$^+$ E7-specific CD8$^+$ T cells in blood at indicated days after vaccination. Data in this figure are from one experiment representative of at least two experiments. Error bars indicate SD, *p<0.05, **p<0.01, ***p<0.001 (unpaired two-tailed Student's t test).

The secondary $CD8^+$ T-cell response might be improved because help signals lead to increased numbers of $E7_{48-57}$-specific memory $CD8^+$ T cells and/or improve their cell-intrinsic capacity to undergo a secondary response. *In vitro,* secondary responder CTLs that had received help during priming could kill target cells more efficiently than equal numbers of helpless secondary responder CTLs (Figure 1F), arguing that help signals improved memory CTL function on a per-cell basis. To examine this further, we performed an adoptive transfer experiment. Memory $CD8^+$ T cells isolated from mice primed either with Help or No Help vaccine were transferred in equal numbers to naïve recipient mice that were subsequently challenged with No Help vaccine (Figure 1G). Memory $CD8^+$ T cells isolated from mice primed with Help vaccine expanded significantly more than those primed with No Help vaccine (Figure 1H, I). Thus, $CD4^+$ T-cell help delivered during priming instills into memory $CD8^+$ T cells cell-intrinsic capacities for $CD4^+$ T-cell help-independent secondary expansion and display of cytotoxic effector function.

Help supports $CD8^+$ T_{EM} and T_{CM} formation and maintenance

We next tested in the same vaccination settings how $CD4^+$ T-cell help impacted the establishment and maintenance of $CD8^+$ T_{EM} and T_{CM} subpopulations in secondary lymphoid tissues and blood. The frequencies of E7-specific $CD8^+$ T cells with a T_{EM} phenotype ($CD44^+CD62L^-$) and a T_{CM} phenotype ($CD44^+CD62L^+$) were determined by flow cytometry. At day 50, the frequency of E7-specific T_{EM} cells among total $CD8^+$ T cells in the dLN was significantly lower after No Help vaccination than after Help vaccination (Figure 2A, B). At the same time point, there were no significant differences in the frequencies of E7-specific T_{CM} cells in the two vaccination settings (Figure 2A, B). At day 120, however, the frequencies of both E7-specific T_{EM} cells and T_{CM} cells were significantly lower after No Help vaccination than after Help vaccination (Figure 2B). Likewise in the spleen, only the T_{EM} cell pool was significantly smaller after No Help vaccination than after Help vaccination at day 50 (Figure 2C, D), while at day 120, both T_{EM} and T_{CM} pools were significantly smaller after No Help vaccination than after Help vaccination (Figure 2D).

T_{EM} cells circulate through the blood and secondary lymphoid organs[4,5] and accordingly, the beneficial influence of help on the size of the T_{EM} cell pool in blood was evident both at day 50 and day 120 (Figure 2E, F). At both time points, frequencies of T_{CM} cells in blood were very low, in agreement with their preferential localization to secondary lymphoid organs[4,5] (Figure 2E, F). In the bone marrow, T_{EM} frequencies were reduced in the helpless population as compared to the helped population on day 50 and this difference was more significant on day 120 (Supplementary Figure 2A, B). We next examined the effect of $CD4^+$ T-cell help on the generation of memory $CD8^+$ T cell subsets in a model of overt inflammation. Mice were infected with the acute lymphocytic choriomeningitis virus (LCMV) strain Armstrong and depleted for $CD4^+$ T cells (No Help) or not (Help). At day 50 after infection we analyzed frequencies of GP33- and NP396-specific T_{EM} and T_{CM} cells in the spleen. Similarly to the vaccination model, help resulted in increased frequencies of both virus-specific memory subsets (Supplementary Figure 2C). Thus,

CD4+ T-cell help delivered during priming improved generation of the CD8+ T_{EM} population and long-term maintenance of both CD8+ T_{EM} and T_{CM} populations.

Memory CD8+ T cells are known to undergo antigen-independent homeostatic proliferation driven by IL-15[23]. At day 50 after vaccination, IL2RB (CD122), the common β chain of the IL-2- and IL-15 receptors, was expressed at significantly higher levels at the cell surface of helped as compared to helpless E7-specific T_{CM} cells, in both dLN and spleen (Figure 2G, H). In T_{EM} cells, however, "help" did not affect the cell surface expression of IL2RB (Figure 2G, H). These data suggested that IL-15 receptor signaling was instrumental in maintaining T_{CM} cells in dLN and spleen after Help vaccination. To test this, we performed an intervention experiment with neutralizing antibody to IL-15. $OVA_{257-264}$/H-2K^b-specific OT-I T cells were transferred into CD45.2+ recipient mice that received Help or No Help vaccine encoding the $OVA_{257-264}$ epitope. The primary response showed the impact of help on the OT-I T cell response (Supplementary Figure 2D). Next, mice were treated from day 20 to 50 with control antibody or neutralizing antibody to IL-15 (Figure 2I). At day 100, the size of the T_{CM} and T_{EM} cell pools in dLN and spleen was determined. IL-15 neutralization had significantly diminished the size of the T_{CM} cell pools after Help vaccination, but did not affect the T_{CM} cell pools after No Help vaccination (Figure 2J). The T_{EM} cell populations in dLN and spleen were unaffected by IL-15 neutralization after Help or No Help vaccination (Figure 2K). These data indicate that help signals delivered during priming lead to upregulation of IL2RB on CD8+ T_{CM} cells, which likely increases their capacity for IL-15-driven long-term survival *in vivo*. The same help signals apparently promote long-term survival of CD8+ T_{EM} cells by an IL-15-independent mechanism.

Help predominantly affects the transcriptome of T_{EM} cells

To gain insight into the molecular mechanisms by which CD4+ T-cell help altered the cell-intrinsic functionality of steady-state CD8+ T_{EM} and T_{CM} cells, we performed gene expression profiling. E7-specific memory CD8+ T_{EM} and T_{CM} cells were flow cytometrically isolated at day 100 from the spleens of mice that had received Help or No Help vaccine, mRNA was isolated and subjected to sequencing (RNAseq). This unbiased, genome-wide analysis revealed that CD4+ T-cell help affected T_{CM} cells much less than T_{EM} cells (Figure 3A, B). In T_{CM} cells, we found only 193 genes with significant differential expression between the comparative groups (Figure 3A; Supplementary Data 1), but in T_{EM} cells, we found 2522 differentially expressed genes (Figure 3B; Supplementary Data 2). Importantly, the effect size was also larger in the latter case. This is confirmed by hierarchical clustering and inspection of the resulting heatmap, revealing that T_{EM} cells dramatically change their gene expression profile as a result of CD4+ T-cell help, while T_{CM} cells do so to a much lesser extent (Figure 3C).

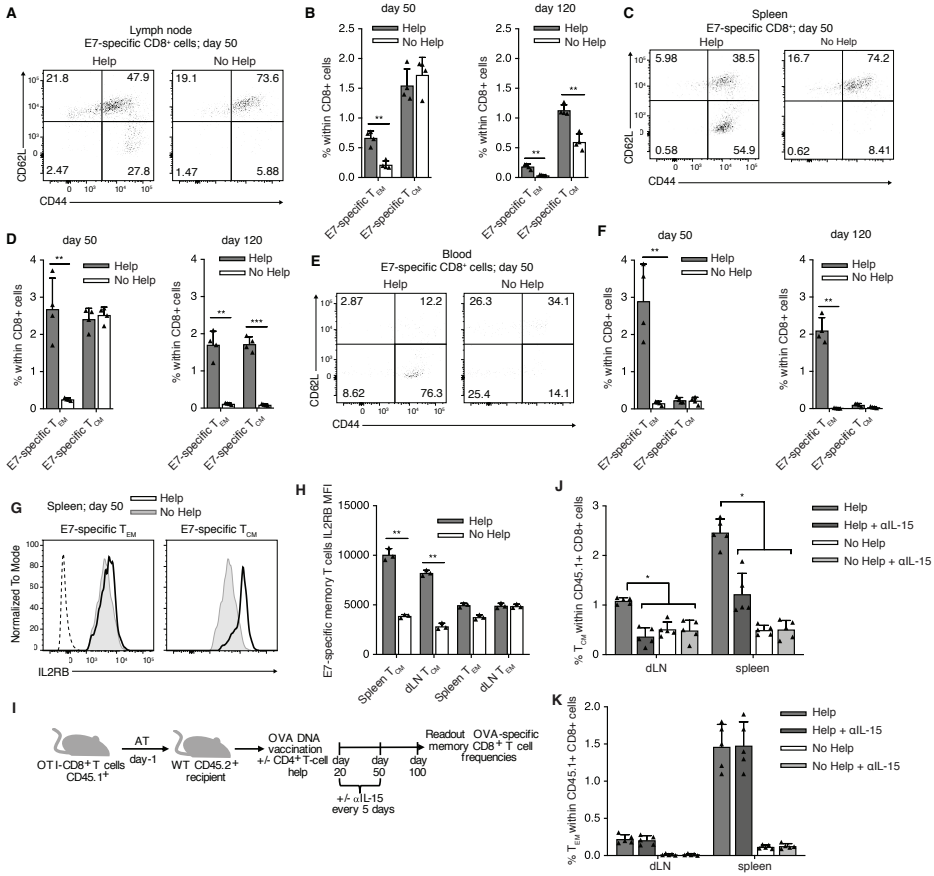

Figure 2. CD4⁺ T-cell help supports formation of CD8⁺ T_{CM} and T_{EM} cells. (A-F) Mice (n=4 per group) received Help or No Help vaccine on days 0, 3 and 6 and were analyzed on day 50 or 120. (A, C, E) Representative flow cytometric plots indicating within the H-2D^b/E7$_{49\text{-}57}$ tetramer$^+$ CD8$^+$ population frequencies of cells with an effector memory T (T_{EM}) phenotype (CD44$^+$CD62L$^-$) or central memory T (T_{CM}) phenotype (CD44$^+$CD62L$^+$), as determined in draining lymph node (dLN) (A), spleen (C) and blood (E). (B, D, F) Quantification of frequencies of E7-specific CD44$^+$CD62$^-$ T_{EM} and CD44$^+$CD62$^+$ T_{CM} phenotype CD8$^+$ T cells determined in dLN (B), spleen (D) and blood (F). (G, H) Cell surface expression of IL2RB (CD122) as determined by flow cytometry on E7-specific CD8$^+$ T_{CM} and T_{EM} cell subsets in spleen at day 50. (G) Primary data. Filled grey: No Help; open black line: Help. Dotted line: unstained control. (H) Quantification of mean fluorescence intensity (MFI) for n=3. (I) Experimental set up. CD45.1+ OT-I T cells were adoptively transferred into CD45.2+ recipient mice (n=5 per group) that 1 day later received OVA-encoding Help or No Help vaccine. From day 20 onwards, indicated groups were treated with isotype control antibody or neutralizing αIL-15 antibody every 5 days until day 50. (J, K) Frequencies of CD45.1+ TCM cells (J) and TEM cells (K) were determined at day 100 in dLN and spleen. Data in this figure are from one experiment representative of two experiments. Error bars indicate SD, *p<0.05, **p<0.01, ***p<0.001 (unpaired two-tailed Student's t test).

Ingenuity pathway analysis (IPA) gave insight in the many molecules that were differentially expressed in helped versus helpless T_{EM} cells (Figure 3D). Genes with increased expression included those encoding transcription factors Tbet (*Tbx21*), Blimp-1 (*Prdm1*), Runx1 and Id2 known to be involved in CD8+ T cell effector function[6]. In addition, transcription factors Tcf-1 (*Tcf7*) and TOX (*Tox*), which are associated with decreased CD8+ T cell effector functions and an exhausted phenotype[24–26], were specifically downregulated in T_{EM} cells as a result of CD4+ T-cell help. Transcripts encoding the cytotoxic effector molecules Granzyme A, Granzyme B (*Gzma, Gzmb*), Perforin (*Prf1*), IFNγ, Fas ligand (*Faslg*) and Trail (*Tnfsf10*) were upregulated, indicating increased cytotoxic potential. Transcripts encoding the IL-2 receptor α chain (*Il2ra*), IL-12 receptor β chain (*Il12rb1, 2*) and IL-18 receptor α chain (*Il18r1*) were upregulated, which fits with memory T cell survival and function[2,27,28]. Several chemokine receptor transcripts were upregulated, including *Cx3cr1* that we previously found to report CD4+ T-cell help in effector CTLs[21]. Other interesting features included the upregulation of Pycard (Asc), Caspase-1 (*Casp-1*) and NOD-like receptors (*Nlrc3, 5*) that can together create "inflammasome" structures leading to pro-IL1β processing[29], which suggests an innate-type alarm state of helped T_{EM} cells.

These findings suggested that helped T_{EM} cells have a more effector-like phenotype than their non-helped counterparts. To examine this, we compared by Gene Set Enrichment Analysis (GSEA) the Help versus No Help T_{EM} gene expression profiles to a published gene expression profile characteristic of effector CD8+ T cells[30]. This gene set consisted of the top 200 up- and downregulated genes in effector (day 8) versus memory (day >30) virus-specific CD8+ T cells isolated after acute LCMV-Armstrong infection. The effector CD8+ T cell gene set was indeed enriched in the expression profile of helped steady-state T_{EM} cells (Figure 3E), indicating a more effector-like phenotype in this population.

To examine whether helped T_{EM} cells, isolated at the steady-state memory phase, resembled helped CTLs, isolated at the primary effector phase, we performed hierarchical clustering of all genes that were differentially expressed as a result of help in primary CTLs or in T_{EM} cells. A number of these genes was differentially expressed both in helped primary CTLs and helped T_{EM} cells (Figure 3F, clusters 1 and 4), suggesting that part of the help signature seen in primary effectors is maintained in steady-state $T_{EM.}$ Other gene expression differences resulting from help were more pronounced in T_{EM} cells than in primary CTLs (Figure 3F, clusters 2 and 3). This included the upregulation of transcripts for various Killer cell lectin-like receptors, the chemokine receptor CX3CR1, and cytokine receptors: IL2R, IL12R and IL18R (Figure 3F). Taken together, these results show that besides increasing the size of the T_{EM} pool, CD4+ T-cell help delivered during priming also creates a T_{EM} population with distinct, more effector-like properties.

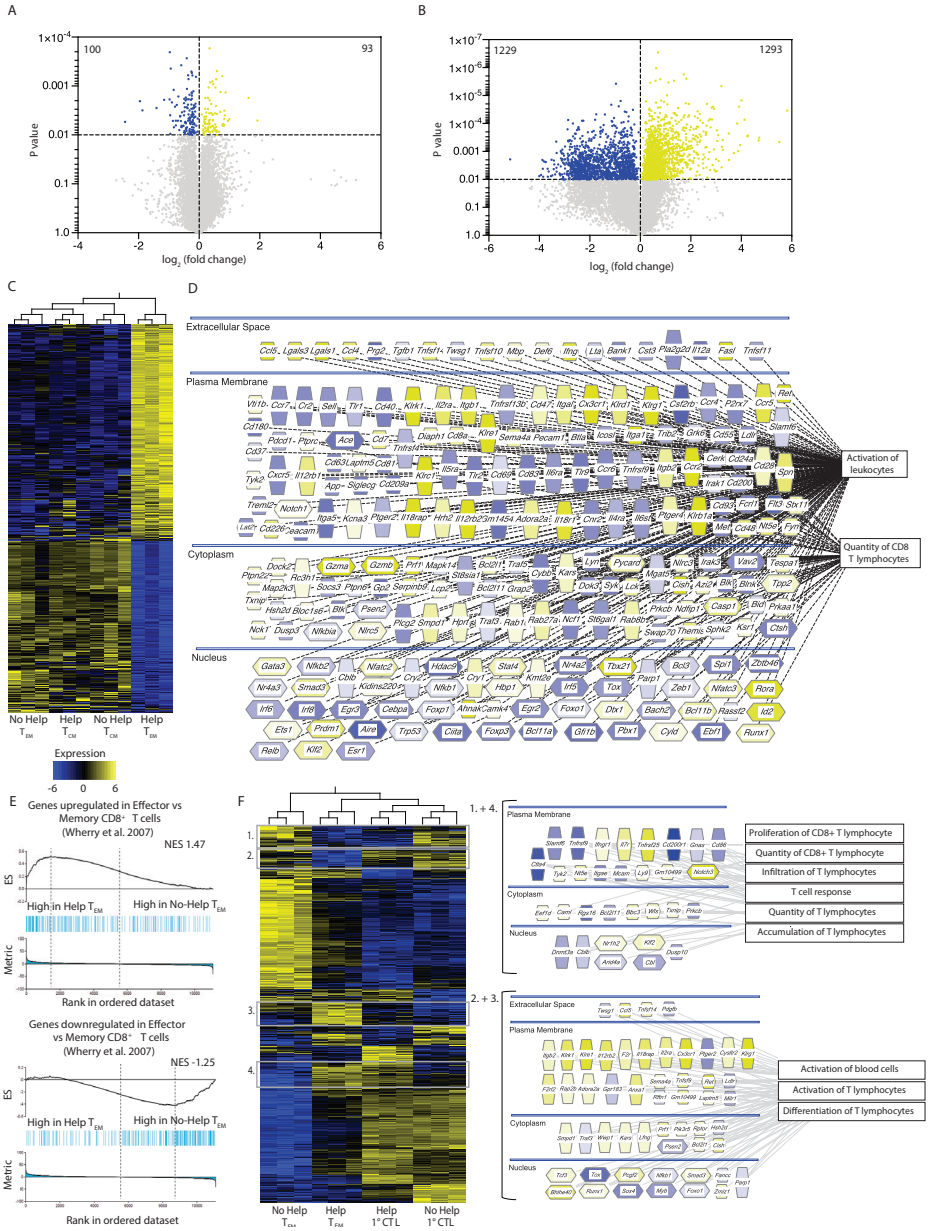

Figure 3. CD4⁺ T-cell help primarily alters the steady-state transcriptome of T_{EM} CD8⁺ T cells. (A, B) Volcano plots depicting results of comparative transcriptome analysis of steady-state E7-specific CD8⁺ T_{CM} cells (A) and T_{EM} cells (B) isolated from spleen at day 100 after primary vaccination with Help or No Help vaccine (n=3 mice per group). Blue and yellow dots indicate transcripts with significant differential expression (p<0.01). See also Supplementary Data 1 and 2. (C) Hierarchical clustering and heat map of the differentially expressed genes in steady-state T_{EM} and T_{CM} cells taken from the Help versus No Help vaccination settings. (D) Molecules differentially expressed in steady-state T_{EM} cells after Help versus No Help vaccination, as assigned to the indicated functional categories and annotated for subcellular localization by IPA. (E) Gene Set Enrichment Analysis (GSEA) of published gene sets listing the top 200 up- or downregulated genes in effector CD8⁺ T cells

(day 8 after LCMV-Armstrong infection)[30] within the gene expression profile of helped versus helpless T_{EM} cells in steady-state. ES, enrichment score; NES, normalized enrichment score. (F) Hierarchical clustering and heat map of genes differentially expressed in steady-state T_{EM} cells taken at day 100 after primary vaccination with Help or No Help vaccine, as determined here and genes differentially expressed in primary CTLs taken at day 10 from the same settings, as determined previously[20]. Numbers and adjacent boxes (right panels) indicate Cluster 1, denoting molecules differentially expressed in both helped versus helpless T_{EM} cells and primary CTLs and Cluster 2, denoting molecules only differentially expressed in helped versus helpless T_{EM} cells, as assigned to the indicated functional categories and annotated for subcellular localization by IPA.

Help promotes innate memory function of CD8+ T cells

The transcriptome data from T_{EM} cells suggested that helped memory cells have increased sensitivity to IL-12 and IL-18, since the receptors for these cytokines were upregulated (Figure 3F). It has been reported that combined stimulation with IL-12 and IL-18 can reactivate memory CD8+ T cells in an antigen non-specific manner, enabling them to exert effector functions[2,27,28]. We therefore tested whether help created this type of innate memory. For this purpose, we generated OVA-specific CD8+ memory T cells by adoptive transfer of OT-I T cells and vaccination with OVA-encoding Help or No Help vaccine (Figure 4A). At day 100, the cell surface expression of both IL-18Rα chain (Figure 4B) and IL-12Rβ chain (Figure 4C) was significantly higher on helped than on helpless memory OT-I T cells in dLN, spleen and blood. To test the innate recall function, steady-state memory OT-I cells taken from dLN and spleen were stimulated *in vitro* with IL-12 and IL-18. The frequency of memory cells that could produce IFNγ (Figure 4D, E) or Granzyme B (Figure 4F) was significantly higher in the helped population as compared to the helpless population. This feature was characteristic for memory OT-I cells, as opposed to naïve cells. Also upon *in vitro* stimulation with cognate antigen (SIINFEKL), the frequency of IFNγ producing OT-I cells was higher in the helped memory population compared to the helpless or the naive populations (Figure 4G).

We also tested *in vivo* whether help signals optimized memory CD8+ T cells for antigen-independent, innate responsiveness. For this purpose, OT-I T cells were transferred into recipient mice that were then vaccinated with OVA-encoding Help or No Help vaccine. After 50 days, these mice were vaccinated with HPV-E7-encoding Help vaccine (Figure 4H). In this setting, the CD4+ T cell response is an antigen-specific memory response, since the same helper epitopes are present in the OVA- and E7-encoding DNA vaccines. The memory CD8+ T cells formed after OVA vaccination might be recalled in an antigen-independent manner, by cytokines such as IL-12 and IL-18 made by CD4+ T cell-activated DCs. To test the role of IL-12, neutralizing anti-IL-12 mAb was injected upon recall. At day 10 after secondary vaccination, the frequency of memory OT-I T cells that produced IFNγ upon non-cognate recall was significantly higher in the helped than in the helpless group (Figure 4I, J). Moreover, treatment with neutralizing αIL-12 antibody significantly reduced IFNγ production by helped OT-I T cells, while not affecting the response of helpless cells (Figure 4I, J). In conclusion, delivery of CD4+ T-cell help during priming generated memory CD8+ T cells with innate-like recall capacities, being able to produce Granzyme B and IFNγ upon restimulation by cytokines, in the absence of cognate antigen.

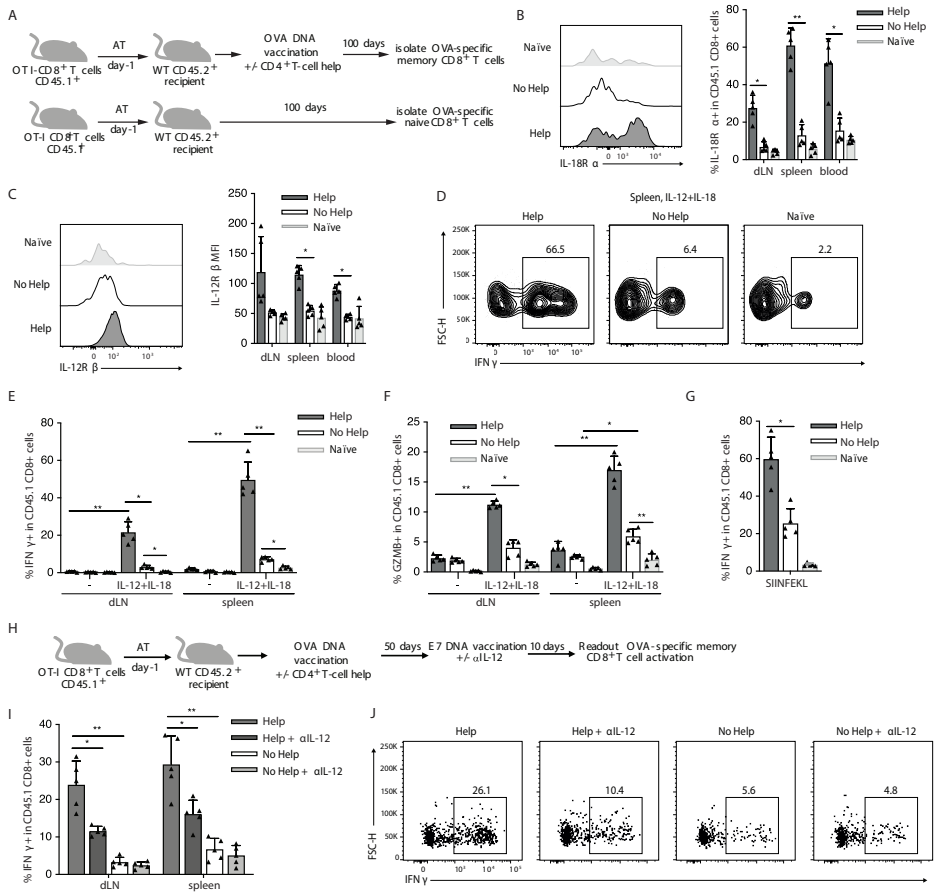

Figure 4. CD4⁺ T-cell help promotes innate recall function of memory CD8⁺ T cells. (A) Experimental set up. CD45.1⁺ OT-I T cells were adoptively transferred into CD45.2⁺ recipient mice (n=5 per group) that 1 day later received OVA-encoding Help or No Help pDNA vaccine. At day 100 after primary vaccination, flow cytometry was performed in blood and CD45.1⁺ OT-I T cells were flow cytometrically isolated from dLN and spleen and directly analyzed or incubated for 5 h with IL-12 and IL-18 or OVA peptide. Unvaccinated recipient mice were used to isolate naïve OT-I T cells. (B) Representative flow cytometric plots (left panel) and percentage of IL18Rα expressing cells within CD45.1⁺ OT-I cells in indicated organs (right panel). (C) Representative flow cytometric plots (left panel) and MFI of IL-12Rβ expressed on CD45.1⁺ OT-I T cells in indicated organs (right panel). (D-G) Primary flow cytometric data (D) and frequencies of IFNγ-producing (E, G) or Granzyme B (GZM-B)-producing (F) OT-I T cells in dLN and spleen, as determined after in vitro stimulation with IL-12 + IL-18 (D-F) or OVA peptide (SIINFEKL) (G). (H) Experimental set up. CD45.1⁺ OT-I T cells were adoptively transferred into CD45.2⁺ recipient mice (n=5 per group) that 1 day later received OVA-encoding Help or No Help pDNA vaccine. At day 50 after primary vaccination, mice were rechallenged with E7-encoding Help vaccine and injected with isotype control or neutralizing mAb to IL-12, 4 times, every 3 days. At day 10 after secondary vaccination, total dLN and spleen cells were incubated for 5 h with GolgiPlug (no cytokines or antigens were added). (I) Frequencies of IFNγ-producing CD45.1⁺ OT-I T cells isolated from indicated organs. (J) Representative flow cytometric analysis of cells isolated from spleen. Data are from one experiment representative of two experiments. Error bars indicate SD, *p<0.05, **p<0.01, ***p<0.001 (unpaired two-tailed Student's t test).

Helped memory CD8+ T cells are help-independent upon recall

We have previously identified the molecular program instilled into primary CTL effectors by CD4+ T-cell help[20]. Here, we examined which transcriptional program unfolded in memory CD8+ T cells after antigen rechallenge as a result of help delivered during priming. Mice that had been vaccinated with Help or No Help vaccine were rechallenged with No Help vaccine. At day 10 after rechallenge, E7-specific CD8+ T cells were isolated from the spleen and analyzed by transcriptomics. Statistical analysis of normalized transcript read counts indicated differential expression of 1315 genes (Figure 5A, Supplementary Data 3). Of these, 391 genes were also differentially expressed as a result of help in the primary CTL response (Supplementary Data 4). We have previously described many of these transcripts as part of the signature of helped CTLs and showed for a number of these their importance in dictating the cytotoxic and migratory potential of CTLs in a tumor model[20]. Part of this signature were transcripts encoding cytotoxic effector molecules (*Ifng, Gzma, Gzmb*), the effector marker KLRG1 (*Klrg1*), transcription factor Tbet (*Tbx21*), receptors for IL-2, IL-12 and IL-18 (*Il2ra, Il12rb, Il18r*) and chemokine receptor CX3CR1 (*Cx3cr1*) that were all upregulated as a result of "help" (Figure 5B). Moreover, transcripts encoding coinhibitory receptors PD-1, LAG3, BTLA, CD200(R) (*Pdcd1, Lag3, Btla, Cd200, Cd200r*) and transcription factors EOMES, ID3 TCF7, TOX (*Eomes, Id3, Tcf7, Tox*) that have all been connected to CTL dysfunction[31] were similarly downregulated in "helped" CTLs in primary and secondary responses (Figure 5C). Many differences in gene expression observed between Help and No Help conditions were more pronounced in the secondary response (Figure 5B, C). Thus, CD8+ T cells that receive help during priming acquire the intrinsic ability to adopt a helped gene expression program after recall.

Next, we compared gene expression profiles of helped T_{EM} cells to those of helped primary and secondary effectors. Hierarchical clustering of differentially expressed genes revealed that expression profiles of helped secondary effectors were similar to those of T_{EM} cells that had received help during priming (Figure 5D). Fold-changes of differentially expressed genes in the Help versus No Help setting were correlated between the T_{EM} population and primary effectors, and this correlation was even stronger between T_{EM} cells and secondary effectors (Figure 5E). These findings suggest that helped secondary effectors are largely derived from helped T_{EM} cells.

Altogether, these data indicate that delivery of CD4+ T-cell help during priming favor the formation of T_{EM} cells that maintain an imprint of help[20] and can express the program characteristic of helped, more potent primary effectors upon recall with MHC class I restricted peptide only.

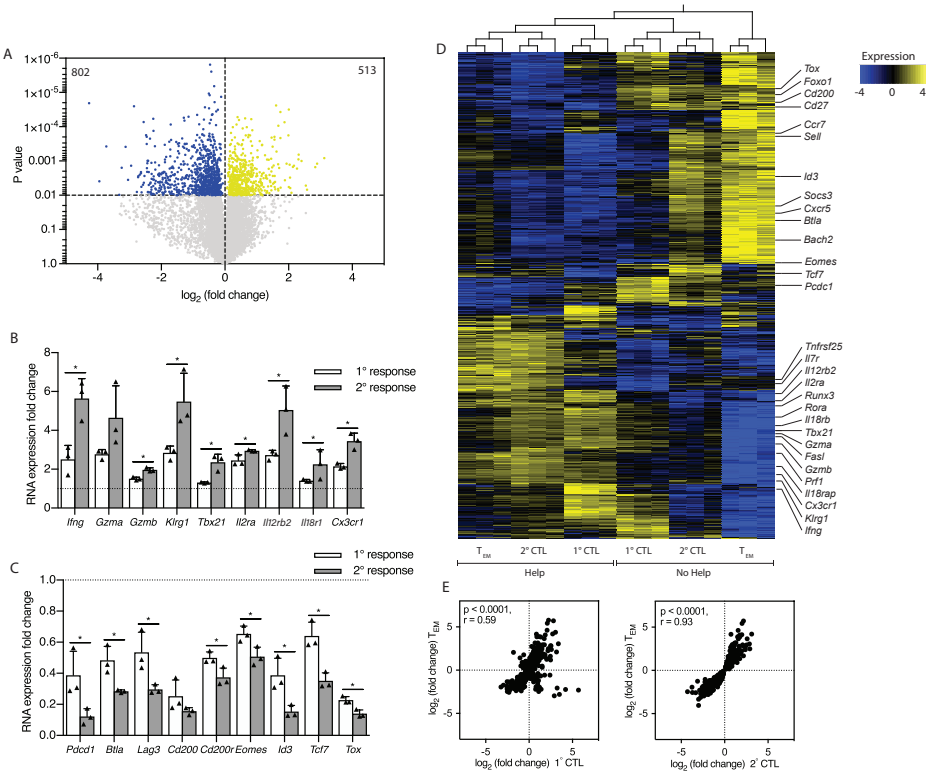

Figure 5. Helped memory CD8⁺ T cells express the Help signature genes after recall with MHC class I-restricted peptide only. Mice received primary vaccination with Help or No Help vaccine and were recalled at day 50 with No Help vaccine + LPS, as outlined in Figure 1A. At day 10 of the secondary response, E7-specific CD8⁺ T cells were flow cytometrically isolated form the spleen (n=3) and samples were processed for RNAseq. (A) Volcano plot depicting results of comparative transcriptome analysis of helped versus helpless secondary effectors. Blue and yellow dots indicate transcripts with significant differential expression between the two groups ($p<0.01$) See also Supplementary Data 3. (B, C) Fold change in mRNA expression of a number of signature genes differentially expressed in the Help versus No Help setting of the primary response (1°), as determined before[20] or the secondary response (2°), as determined here. (D) Hierarchical clustering of genes that were differentially expressed in the Help versus No Help groups in steady-state T_{EM} (Figure 3), primary (1°) CTLs[20] or secondary (2°) CTLs (Figure 5A). Certain genes of known or suspected functional or diagnostic relevance are annotated. (E) Correlation between log_2 fold changes in mRNA expression of genes differentially expressed in helped versus helpless T_{EM} cells and primary (1°) CTLs (left panel) or secondary (2°) CTLs (right panel). Error bars indicate SD, *$p<0.05$ (unpaired two-tailed Student's t test).

Helped memory cells display epigenetic imprinting of help

The data outlined above argue that memory CTLs "remember" that they have been helped during priming and are consequently help-independent after recall. We characterized the epigenetic states of helped and helpless steady-state memory CTLs to examine a potential epigenetic basis for this. Cells were isolated from spleen based on CD8 and H-2D^b/E7$_{48-57}$-tetramer staining at day 100 after vaccination. Given the low numbers of cells recovered, we used an ultra-low-input protocol for native chromatin immunoprecipitation (ULI-NChIP)[32], with antibodies against H3K4me3 and H3K27me3. These two histone marks characterize permissive and repressed chromatin states that respectively favor and deter gene transcription[33]. After high throughput DNA sequencing, on average 54662 H3K4me3 and 104758 H3K27me3 peaks (FDR<0.01) were identified in helped and helpless steady-state memory CTL samples. Principal component analysis (PCA) showed that these CTL populations had distinct profiles for both epigenetic marks (Figure 6A).

We identified consensus peaks in chromatin of helped or helpless memory CTLs that contained significantly different amounts of H3K4me3 and H3K27me3 deposition (FDR<0.05) (Figure 6B, C, Supplementary Data 5, 6). These differentially modified regions (DMRs) were annotated to the nearest transcriptional start sites (TSSs). Genes that were significantly enriched in H3K4me3 marks in helped memory CTLs were assigned by IPA to the top functional categories (z-score>2) 'stimulation of T lymphocytes', 'cytotoxicity' and 'activation of lymphocytes' (Figure 6D). The epigenetic marks were congruent with the previously defined help gene expression program[20] being opened in helped memory cells, as indicated by an open configuration of *Ifng, Gzma Gzmb, Prf1* genes encoding cytotoxic effector molecules and transcription factors *Tbx21 and Prdm1* (Figure 6D). H3K4me3 deposition positively correlated with differential mRNA expression in helped versus helpless steady-state T_{EM} and T_{CM} cells, while H3K27me3 deposition negatively correlated with differential mRNA expression in these populations (Figure 6E, F). These data argue that CD4+ T-cell help brings about epigenetic changes that allow memory CTLs to display a helped phenotype at steady state and after recall in the absence of help signals.

Discussion

Therapeutic vaccines against cancer or pathogens aim to raise CTL responses. A historical disconnect between the fields of vaccinology and immunology has reportedly delayed the development of effective synthetic T cell inducing vaccines[34,35]. Vaccinology currently focuses on incorporating innate DC-activating signals into such vaccines[35]. However, helper epitopes must also be included[36]. Moreover, it should be ensured that both CTL- and helper epitopes reach the appropriate DCs[37,38]. Recent intravital imaging studies showed CD4+ T-cell help is transmitted from a CD4+ T cell to the CD8+ T cell by a lymph node-resident cDC1[18,39]. This event occurs during a second step of priming, after the naïve CD8+ and CD4+ T cells have been activated by a (migratory) conventional (c)DC1, or cDC2, respectively, that has been stimulated by innate signals[17,18,39,40].

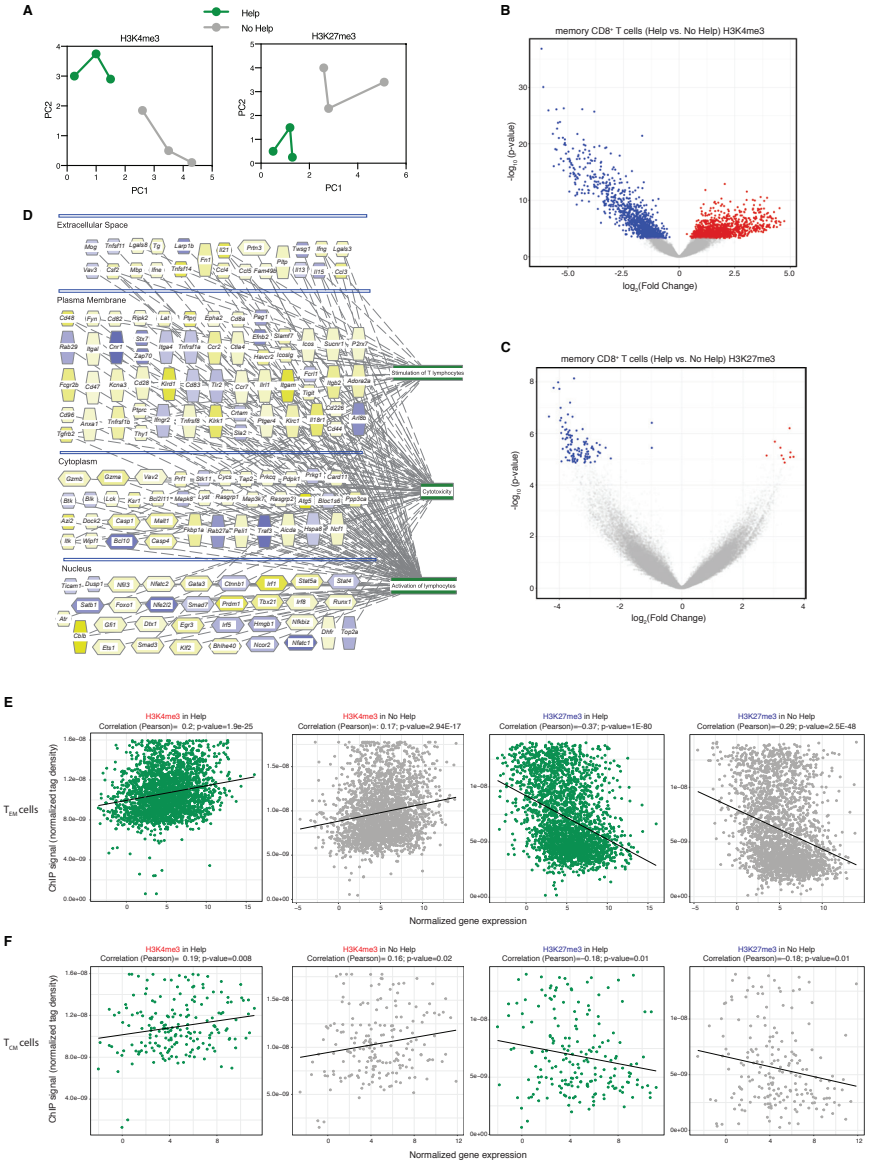

Figure 6. Help delivered during priming leaves an epigenetic imprint in steady-state memory cells. Mice (n=3 per group) received Help or No Help vaccine on days 0, 3 and 6. At day 100, E7-specific memory CD8$^+$ T cells were isolated from the spleens and subjected to ChIPseq analysis with antibodies against H3K4me3 and H3K27me3. (A) PCA plots depicting results of ChIPseq analysis. (B, C) Volcano plots depicting differentially modified regions (DMRs) as designated by H3K4me3 (B) or H3K27me3 (C) marks. Blue and red dots indicate DMRs with significant differential modifications (FDR<0.05). (D) Molecules differentially modified by H3K4me3 in helped memory E7-specific CD8$^+$ T cells, as assigned to functional categories and annotated for subcellular localization by IPA. (E, F) Correlation between differential mRNA expression in helped versus non-helped T_{EM} (E) and T_{CM} (F) cells and histone methylation in gene bodies and regions maximally 1 kb upstream from the TSS. Normalized tags of H3K4me3 and H3K27me3 are shown versus average normalized mRNA expression values in helped versus non-helped T_{EM} (E) and T_{CM} (F) cells (described in Figure 5).

The help signals lead to upregulation of IL-12 or IL-15 and the costimulatory ligands CD80/86 and CD70 on the LN-resident cDC1[15,17]. As a result, the CD8+ T cell receives costimulatory input via CD28, CD27 and cytokine receptors that lead to optimal CTL effector differentiation[17,20]. The consensus has been that primary CTL responses benefit from help only when innate DC-activating signals are lacking[41]. However, we have recently demonstrated by transcriptome analysis that CD4+ T-cell help optimizes the quality of the primary CTL response after both DNA vaccination and virus infection, by similar molecular mechanisms[20].

CD4+ T-cell help optimizes many intrinsic properties of the CTL, including its cytotoxic, migratory and invasive capacities[20]. We determined that the second step of priming is a "checkpoint" for CTL functionality, since CTLs raised in the absence of help had an overall dysfunctional phenotype, characterized by low expression of cytotoxic effector molecules and increased expression of PD-1, BTLA and other coinhibitory molecules at the cell surface, which prevented them from killing target cells. The impact of help on the primary CTL effector capabilities as demonstrated in our study was not vaccination model-specific, but had a general validity. We showed in the same study that the helped versus helpless gene expression profile could also be identified by transcriptomics in CTLs raised against the acute virus strain LCMV-Armstrong. Moreover, the same traits were identified by gene array in a different vaccination model by other researchers[42].

Pioneering studies showed that CD4+ T-cell help delivered during priming promotes formation and maintenance of the memory CD8+ T cell pool, but this was not specified to memory T cell subsets at the time[43,44]. We show here that CD4+ T-cell help primarily increases the steady-state CD8+ T_{EM} cell pool and has a relatively minor effect on the T_{CM} pool. IL-15 receptor signaling upregulates anti-apoptotic Bcl-2 proteins and has been implicated in the survival of memory CD8+ T cells[45,46]. We found that CD4+ T-cell help increased expression of the IL-2Rβ (CD122) chain on steady-state CD8+ T_{CM} cells and not on T_{EM} cells. Accordingly, IL-15 drove the maintenance of helped T_{CM} cells, but not T_{EM} cells, in agreement with earlier findings[46]. This result suggests, in agreement with another report[47], that T_{EM} cells rely on other, yet undefined, help-dependent mechanisms for their long-term survival.

Helped T_{EM} cells had upregulated transcripts encoding many molecules implicated in cytotoxic functions, including Granzyme A and B, Perforin, Fas ligand, Trail and IFNγ. Increased "surveillance" activity was also suggested by upregulation of transcripts encoding inflammasome components Pycard (Asc), Caspase-1 and NOD-like receptors that regulate IL-1 production[29]. Memory CD8+ T cells are known to acquire functional properties characteristic of innate immune cells, allowing them to protect against pathogens unrelated to the ones responsible for priming[27,28]. In specific cellular niches, these pathogens would evoke the production of cytokines that locally activate memory CD8+ T cells, reportedly to produce IFNγ[2]. In memory CD8+ T cells, a pool of presynthesized *Ifng* mRNA is available that is freed for rapid translation into protein upon recall[12]. A combination

of IL-12 and IL-18 was found to be particularly potent in inducing antigen-independent IFNγ production by memory CD8$^+$ T cells[27]. We accordingly found that helped memory CD8$^+$ T cells responded to combined stimulation by IL-12 and IL-18 by IFNγ and Granzyme B protein production. We did not specify in these experiments whether T_{EM} cells were responsible for this response, but this is likely, because T_{EM} (and not T_{CM}) cells showed help-dependent upregulation of IL-12Rβ and IL18Rα chains, and previous studies have demonstrated that T_{EM} cells are more responsive to IL-12 than T_{CM} cells[48]. We also show that helped memory cells responded *in vivo* - in an IL-12-dependent manner - to recall by non-cognate antigen. The intra-epidermal vaccination procedure presumably evokes a cytokine alert in the keratinocytes where the vaccine DNA is expressed[37], which explains this response. The ability of helped T_{EM} cells to mount more efficient innate recall responses than helpless T_{EM} cells may not only be due to increased expression of specific cytokine receptors, but also to other cell-intrinsic alterations, which we show here to be many.

We performed epigenetic analysis on total steady-state CD8$^+$ memory T cells, since the cell input was too small to do this for separate T_{EM} and T_{CM} subsets. However, the genes that were epigenetically altered as a result of help signals were differentially expressed in T_{EM} cells and not in T_{CM} cells. This result argues that primarily the T_{EM} cell pool was epigenetically modified as a result of help signals delivered during priming. The genes that were epigenetically modified to facilitate transcription fell in the functional categories “stimulation/activation of lymphocytes” and “cytotoxicity”, again indicating a higher alert state of helped T_{EM} cells. The epigenetic marks correlated with gene expression. Helped T_{EM} cells were transcriptionally distinct from either helped or helpless T_{CM} cells (Figure 3C), indicating that they constituted cells with a unique differentiation state.

Once helped during priming, memory CD8$^+$ T cells no longer require help to undergo secondary expansion upon recall with cognate antigen[43,44,49,50]. In our vaccination model, TLR stimulation was required to recall helped memory CD8$^+$ T cells with the No Help vaccine. Likely, this promoted antigen presentation and/or other functions of DCs that play a key role in initiating secondary T cell responses[51]. Helped memory CD8$^+$ T cells were superior over their helpless counterparts in secondary expansion and cytotoxicity, due to cell-intrinsic mechanisms. This memory programming of CD8$^+$ T cells by CD4$^+$ T-cell help has been described many years ago[13], but we identify here its molecular basis. Helped memory CTLs expressed, after recall in absence of help signals, the signature gene set identified in helped primary CTLs. The gene signature characteristic for helped secondary effectors was in large part already present in steady-state helped T_{EM} cells (Figure 5D). These data, together with the epigenetic data we provide, argue that CD8$^+$ T cells acquire, as a result of help signals delivered during priming, a unique T_{EM} cell differentiation program that allows them to perform specific surveillance functions at steady-state and to display a helped gene expression program after recall in the absence of help signals.

Methods

Mice

Gender-matched, 7-9 week-old mice were maintained under specific-pathogen free conditions, in accordance with national regulations for animal testing and research. Ethical approval for this study was granted by the institutional Experimental Animal Committee (DEC) of the Netherlands Cancer Institute. C57BL/6JRj mice were purchased from Janvier Laboratories. CD45.1+ and OT-I;CD45.1+ mice were bred in-house.

Vaccination

For vaccination, we used the HELP-E7SH and E7SH DNA vaccines[21,22]. OVA DNA vaccines were generated by the C-terminal addition of the $OVA_{257-264}$ coding sequence to the HELP-E7SH and E7SH DNA constructs. For DNA "tattoo" vaccination, the hair on a hind leg was removed using depilating cream (Veet) on day –1. On days 0, 3, and 6, mice were anesthetized, and 15 µl of a 2 mg/ml DNA solution in 10 mM Tris-HCl, 1 mM EDTA, pH 8.0, was applied to the hairless skin with a Permanent Make Up tattoo machine (Amiea, MT Derm GmbH), using a sterile disposable 9-needle bar with a needle depth of 1 mm and oscillating at a frequency of 100 Hz for 45 sec. For rechallenge (at day 50 after primary vaccination), the hair removal step was repeated, and mice received a single DNA tattoo and an i.p. injection with 5 µg LPS from E. coli 055:B5 (Sigma) in 100 µl Hank's Buffered Salt Solution (HBSS) on the next day (day 0, rechallenge).

Antibody treatments

Neutralizing mAb to IL-15 (GRW15PLZ, Thermo Fisher Scientific) was injected i.p as described[52] at 5 µg per injection, 3 times per week from day 20 to day 50 after primary vaccination. Neutralizing mAb to IL-12p75 (R2-9A5, Bio X Cell) or isotype control mAb (LTF-2, Bio X Cell) were injected i.p. at 500 µg per mouse in 100 µl HBSS on days 0, 3, 6 and 9.

Tissue preparation and flow cytometry

Peripheral blood cells were obtained by tail bleeding; spleen, inguinal lymph nodes, and bone marrow were passed through a 70 µm cell strainer (BD Falcon). After erythrocyte lysis, cell suspensions were washed and stained with relevant mAbs and phycoerythrin-conjugated H-$2D^b$/$E7_{49-57}$ or H-$2K^b$/$OVA_{257-264}$ tetramers. For intracellular staining of transcription factors, cells were fixed and permeabilized with the FOXP3/transcription factor staining buffer set (Thermo Fisher Scientific). Flow cytometry was performed using the LSRFortessa (BD Biosciences) and data were analyzed with FlowJo software (Tree Star Inc.). Live cells were selected based on near-infra red dye (Life Technologies) exclusion. Antibody details are listed in Supplementary Data 8.

Isolation of antigen-specific CD8$^+$ T cells

At day 50 or 100 after primary vaccination, or at day 10 after secondary vaccination, mice were sacrificed, spleens were isolated and passed through 70 µm cell strainer (BD Falcon). After erythrocyte lysis, cell suspensions were washed, stained with anti-CD8α mAb (53-6.7, eBioscience), anti-CD44 (IM7, eBioscience) and anti-CD62L (MEL-14, BD Pharmingen) and PE-conjugated H-2D^b/E7$_{49\text{-}57}$ or H-2K^b/OVA$_{257\text{-}264}$ tetramers and sorted on a BD FACSAria Fusion cell sorter. Live cells were selected based on propidium iodide exclusion. All samples were maintained at 4^{o}C for the duration of the sort, and purity was at 95%-98% for all samples. Isolated cells were subsequently used for *in vivo*, *in vitro*, RNAseq or ChIPseq assays.

In vivo cytotoxicity assay

Splenocytes from naive mice were labeled *ex vivo* with 0.1 µM carboxyfluorescein succinimidyl ester (CFSE; Life Technologies) and pulsed with 5 µM E7$_{49\text{-}57}$ peptide (specific target) or labeled with 1 mM CFSE and left unpulsed (control). Subsequently, 5 x 10^6 cells of each population were injected retro-orbitally (r.o.) in the same recipient mouse, and 16 h later, spleens were analyzed by flow cytometry. Percent killing was calculated as follows: 100 – ([(% specific targets in vaccinated recipients/% control targets in vaccinated recipients)/(% specific targets in control recipients/% control targets in control recipients)] x 100).

In vitro cytotoxicity assay

To create target cells, splenocytes from naïve mice were labeled with 0.1 µM Cell Trace Violet (CTV; Thermo Fisher Scientific) and pulsed with 5 µM E7$_{49\text{-}57}$ peptide (specific target) or labeled with 1 µM CFSE (Thermo Fisher Scientific) and left unpulsed (control target). Subsequently, 5000 *ex vivo* isolated H-2D^b/E7$_{49\text{-}57}$-specific CD8$^+$ T cells were mixed with equal numbers of the two target cell populations in 1:1 ratio and incubated at 37^{o}C, 5% CO_2 for 12 h. Cells were then analyzed by flow cytometry. Percent killing was calculated as follows: 100 – ([(% specific targets /% control targets)/(% control targets in absence of effectors/% specific targets in absence of effectors)] x 100).

Adoptive transfer experiments

E7-specific memory CD8$^+$ T cells that had been flow cytometrically sorted *ex vivo* with MHC tetramers were injected at 1 x 10^5 cells per mouse r.o. into naïve WT C57BL/6 mice. Naïve OT-I CD8$^+$ T cells that carry a transgenic Vα2/Vβ5 TCR specific for H-2K^b/OVA$_{257\text{-}264}$ were purified to 95% homogeneity form spleens of OT-1;CD45.1$^+$ mice with the CD8$^+$ T cell Isolation Kit (Miltenyi Biotec) and injected r.o. into WT C57BL/6 mice at 1.5 x 10^5 cells per mouse. One day later, mice received DNA vaccination, unless indicated otherwise.

In vitro restimulation assay

Prior to cytokine detection with the BD Cytofix/Cytoperm Kit (BD Biosciences), cells were incubated for 16 h with or without $E7_{49-57}$ peptide (RAHYNIVTF) or for 5 h with 5 ng/ml recombinant IL-12 p70 (Thermo Fisher Scientific) and 10 ng/ml IL-18 (MBL) in the presence of GolgiPlug in IMDM with 8% FCS or GolgiPlug in medium alone.

RNA sequencing (RNAseq)

For isolation of T_{CM} and T_{EM} cells, H-$2D^b$/$E7_{49-57}$-specific $CD8^+$ T cells were flow cytometrically sorted based on anti-CD8, anti-CD62L, anti-CD44 and tetramer staining from 3 mice per experimental group. Cells were resuspended in Trizol (Ambion Life Technologies) and total RNA was extracted according to the manufacturer's protocol. Quality and quantity of the total RNA was assessed by the 2100 Bioanalyzer using a Nano chip (Agilent). Only RNA samples having an RNA Integrity Number (RIN) > 8 were subjected to library generation. Strand-specific cDNA libraries were generated using the TruSeq Stranded mRNA sample preparation kit (Illumina) according to the manufacturer's protocol. The libraries were analyzed for size and quantity of cDNAs on a 2100 Bioanalyzer using a 7500 chip (Agilent), diluted and pooled at 10 nM in multiplex sequencing pools. The libraries were sequenced as 50 base single reads in two lanes on a HiSeq2500 with V3 chemistry (Illumina).

Chromatin immunoprecipitation sequencing (ChIPseq)

Between 6-9 x 10^4 E7-specific memory $CD8^+$ T cells per sample were subjected to ULI-NChIP procedure[32]. For each immunoprecipitation, 0.25 µg of αH3K4me3 mAb (#9272, Cell Singaling Technology), or 0.25 µg of αH3K27me3 mAb (C15410069, Diagenode) was used. Input DNA for each sample was used as a control. Quality control metrics of ChIPseq experiment are summarized in Supplementary Data 7.

RNAseq analysis

Illumina adapter sequences were trimmed from Fastq files using trimmomatic (v. 0.36) with 4-base wide sliding window, to trim reads when the average quality per base drops below 15. Any reads remaining below ≤ 36 bases long were filtered out. Adapter-trimmed files were aligned to GRCm38.77 with STAR (v. 2.5.3a). Using the genes (GRCm38.77.gtf), HTSeq-count was used in intersection-strict mode for exon feature type to generate a count matrix for all samples. Differential expression analysis was performed using Qlucore Omics Explorer (v. 3.4). Genes with less than 5 reads in at least one of the samples were discarded. Mapping quality threshold was set to 10. TNM normalization method was applied. Differential expression with two-group comparison was considered significant at $P<0.01$. GSEA was performed using Qlucore Omics Explorer. Functional classification of the genes and identification of enriched signaling pathways was performed using IPA software (Qiagen).

ChIPseq analysis

Single-end fastq files were aligned to mm10 (GrCm38.77) using bwa (v. 0.7.17). Resulting alignments were filtered for mapping quality > MQ20 using samtools (v. 1.5). Peak calling for H3K27me3 ChIP-seq was performed using MACS2 (v. 2.1.1) with detection for broad peaks using input for normalization. For H3K4me3 we performed narrow peak calling using MACS (v. 2.1.1) with input normalization. For differential binding, we used the R package Diffbind (v. 2.2.1) to determine differentially bound peaks found in all replicates for “No Help” vs “Help” with the EdgeR method. We annotated the bound regions using BEDTools (v. 2.17.0) closest Bed reporting the first feature against a file of genes and locations determined from GRCm38.77 gtf file selecting for ‘gene_name’. To show correlation of ChIP-sequencing tags versus mRNA expression, we merged the replicates for each cell type using samtools and counted reads in the gene body including 1000 bp upstream from the TSS from the merged alignments. Data were normalized by dividing by region size and library read count. For each gene, normalized tags are shown versus average normalized gene expression values for “No Help” vs “Help” cell types of both ChIP-sequencing marks (H3K27me3 and H3K4me3). Table for quality control metrics was produced with the R package ChIPQC for ChIP-seq experiments. To generate PCA plots, reads were counted in 10kb bins across the genome for each sample using deepTools (v. 2.5.7) multiBamSummary bins function. The binned counts were output to a table and log transformed. PCA was carried out on these data using R function prcomp.

Statistical analysis

Data was analyzed with GraphPad Prism software using unpaired two-tailed Student’s t or one-way ANOVA test. Error bars in figures indicate SD. A P value < 0.05 was considered statistically significant; *P < 0.05, **P <0.005, ***P < 0.001 and ****P < 0.0001.

Data availability

RNAseq and ChIPseq data have been deposited in the GEO database under the accession code GSE118160. All other data supporting findings in this study are available from the corresponding author upon request.

Acknowledgements

The authors thank Eliza-Marie Malipaard for helpful discussions and Genomics, FACS, and Experimental Animal facilities of our institute for technical assistance.

This research was supported by grant NKI 2012-5397 and 2017-11079 of the Dutch Cancer Society to J.B.

Author Contributions

Study design and experimental design: T.A. and J.Bo.; Performing experiments: T.A., N.B., A.B., E.d.V.; Data analysis: T.A., J.Bu., T.M.S.; Manuscript writing: T.A., J.Bu., J.Bo.; Experimental advice, critical reading and editing of the manuscript: L.W., F.v.L., T.M.S.

Competing Interests

The authors declare no competing interests.

References

1. Farber, D. L., Netea, M. G., Radbruch, A., Rajewsky, K. & Zinkernagel, R. M. Immunological memory: lessons from the past and a look to the future. *Nature Reviews Immunology* **16**, 124–128 (2016).
2. Lauvau, G., Boutet, M., Williams, T. M., Chin, S. S. & Chorro, L. Memory CD8+ T Cells: Innate-Like Sensors and Orchestrators of Protection. *Trends in Immunology* **37**, 375–385 (2016).
3. Kaech, S. M. & Cui, W. Transcriptional control of effector and memory CD8+ T cell differentiation. *Nature Reviews Immunology* **12**, 749–761 (2012).
4. Joshi, N. S. & Kaech, S. M. Effector CD8 T cell development: a balancing act between memory cell potential and terminal differentiation. *Journal of Immunology* **180**, 1309–15 (2008).
5. Mueller, S. N., Gebhardt, T., Carbone, F. R. & Heath, W. R. Memory T Cell Subsets, Migration Patterns, and Tissue Residence. *Annual Review of Immunology* **31**, 137–161 (2013).
6. Gray, S. M., Kaech, S. M. & Staron, M. M. The interface between transcriptional and epigenetic control of effector and memory CD8+ T-cell differentiation. *Immunological reviews* **261**, 157–68 (2014).
7. Weng, N., Araki, Y. & Subedi, K. The molecular basis of the memory T cell response: differential gene expression and its epigenetic regulation. *Nature Reviews Immunology* **12**, 306–315 (2012).
8. Shin, H. M. *et al.* Epigenetic modifications induced by Blimp-1 regulate CD8+ T cell memory progression during acute virus infection. *Immunity* **39**, 661–675 (2013).
9. Araki, Y. *et al.* Genome-wide Analysis of Histone Methylation Reveals Chromatin State-Based Regulation of Gene Transcription and Function of Memory CD8+ T Cells. *Immunity* **30**, 912–925 (2009).
10. Kersh, E. N. *et al.* Rapid demethylation of the IFN-gamma gene occurs in memory but not naive CD8 T cells. *Journal of immunology (Baltimore, Md. : 1950)* **176**, 4083–93 (2006).
11. Northrop, J. K., Thomas, R. M., Wells, A. D. & Shen, H. Epigenetic remodeling of the IL-2 and IFN-gamma loci in memory CD8 T cells is influenced by CD4 T cells. *Journal of immunology (Baltimore, Md. : 1950)* **177**, 1062–9 (2006).
12. Salerno, F. *et al.* Translational repression of pre-formed cytokine-encoding mRNA prevents chronic activation of memory T cells. *Nature Immunology* **19**, 828–837 (2018).
13. Masopust, D., Kaech, S. M., Wherry, E. J. & Ahmed, R. The role of programming in memory T-cell development. *Current Opinion in Immunology* **16**, 217–225 (2004).

14. Castellino, F. & Germain, R. N. Cooperation between CD4+ and CD8+ T cells: when, where, and how. *Annual Review of Immunology* **24**, 519–40 (2006).

15. Bedoui, S., Heath, W. R. & Mueller, S. N. CD4+ T-cell help amplifies innate signals for primary CD8+ T-cell immunity. *Immunol Rev* **272**, 52–64 (2016).

16. Laidlaw, B. J., Craft, J. & Kaech, S. M. The multifaceted role of CD4 + T cells in the regulation of CD8 + T cell memory maturation. *Nat Rev Immunol* **16**, 102–111 (2016).

17. Borst, J., Ahrends, T., Bąbała, N., Melief, C. J. M. & Kastenmüller, W. CD4+ T cell help in cancer immunology and immunotherapy. *Nat Rev Immunol* **18**, 635–647 (2018).

18. Eickhoff, S. *et al.* Robust anti-viral immunity requires multiple distinct T cell-dendritic cell interactions. *Cell* **162**, 1322–1337 (2015).

19. Greyer, M. *et al.* T Cell Help Amplifies Innate Signals in CD8+DCs for Optimal CD8+T Cell Priming. *Cell Reports* **14**, 586–597 (2016).

20. Ahrends, T. *et al.* CD4+T cell help confers a cytotoxic T cell effector program including coinhibitory receptor downregulation and increased tissue invasiveness. *Immunity* **47**, 848–861 (2017).

21. Oosterhuis, K., Aleyd, E., Vrijland, K., Schumacher, T. N. & Haanen, J. B. Rational Design of DNA Vaccines for the Induction of Human Papillomavirus Type 16 E6-and E7-Specific Cytotoxic T-Cell Responses. *Human Gene Therapy* **23**, 3001–1312 (2012).

22. Ahrends, T. *et al.* CD27 Agonism Plus PD-1 Blockade Recapitulates CD4+ T-cell Help in Therapeutic Anticancer Vaccination. *Cancer Res* **76**, 2921–2931 (2016).

23. Surh, C. D. & Sprent, J. Homeostasis of naive and memory T cells. *Immunity* **29**, 848–62 (2008).

24. Utzschneider, D. T. *et al.* T Cell Factor 1-expressing memory-like CD8+T cells sustain the immune response to chronic viral infections. *Immunity* **45**, 415–427 (2016).

25. Khan, O. *et al.* TOX transcriptionally and epigenetically programs CD8+ T cell exhaustion. *Nature* **571**, 211–218 (2019).

26. Alfei, F. *et al.* TOX reinforces the phenotype and longevity of exhausted T cells in chronic viral infection. *Nature* **571**, 265–269 (2019).

27. Freeman, B. E., Hammarlund, E., Raué, H.-P. & Slifka, M. K. Regulation of innate CD8+ T-cell activation mediated by cytokines. *Proceedings of the National Academy of Sciences of the United States of America* **109**, 9971–6 (2012).

28. Soudja, S. M., Ruiz, A. L., Marie, J. C. & Lauvau, G. Inflammatory monocytes activate memory CD8(+) T and innate NK lymphocytes independent of cognate antigen during microbial pathogen invasion. *Immunity* **37**, 549–62 (2012).

29. Rathinam, V. A. K. & Fitzgerald, K. A. Inflammasome Complexes: Emerging Mechanisms and Effector Functions. *Cell* **165**, 792–800 (2016).

30. Wherry, E. J. *et al.* Molecular Signature of CD8+ T Cell Exhaustion during Chronic Viral Infection. *Immunity* **27**, 670–684 (2007).

31. Philip, M. & Schietinger, A. Heterogeneity and fate choice: T cell exhaustion in cancer and chronic infections. *Current Opinion in Immunology* **58**, 98–103 (2019).

32. Brind'Amour, J. *et al.* An ultra-low-input native ChIP-seq protocol for genome-wide profiling of rare cell populations. *Nature Communications* **6**, 1–8 (2015).

33. van Leeuwen, F. & van Steensel, B. Histone modifications: From genome-wide maps to functional insights. *Genome Biology* **6**, 113 (2005).

34. Gilbert, S. C. T-cell-inducing vaccines - what's the future. *Immunology* **135**, 19–26 (2012).

35. O'Hagan, D. T., Friedland, L. R., Hanon, E. & Didierlaurent, A. M. Towards an evidence based approach for the development of adjuvanted vaccines. *Current Opinion in Immunology* **47**, 93–102 (2017).

36. Melief, C. J. M., Hall, T. Van, Arens, R., Ossendorp, F. & Burg, S. H. Van Der. Therapeutic cancer vaccines. *J Clin Invest* **125**, 3401–3412 (2015).

37. Babala, N. *et al.* Subcellular Localization of Antigen in Keratinocytes Dictates Delivery of CD4 + T-cell Help for the CTL Response upon Therapeutic DNA Vaccination into the Skin. *Cancer Immunol Res* **6**, 835–847 (2018).

38. Hos, B. J., Tondini, E., van Kasteren, S. I. & Ossendorp, F. Approaches to Improve Chemically Defined Synthetic Peptide Vaccines. *Frontiers in Immunology* **9**, 884 (2018).

39. Hor, J. L. *et al.* Spatiotemporally distinct interactions with dendritic cell subsets facilitates CD4+and CD8+T cell activation to localized viral infection. *Immunity* **43**, 554–565 (2015).

40. Brewitz, A. *et al.* CD8+T cells orchestrate pDC-XCR1+dendritic cell spatial and functional cooperativity to optimize priming. *Immunity* **46**, 205–219 (2017).

41. Bevan, M. J. Helping the CD8(+) T-cell response. *Nature Reviews Immunology* **4**, 595–602 (2004).

42. Provine, N. M. *et al.* Immediate Dysfunction of Vaccine-Elicited CD8 + T Cells Primed in the Absence of CD4 + T Cells. *The Journal of Immunology* **197**, 1809–1822 (2016).

43. Shedlock, D. J. & Shen, H. Requirement for CD4 T cell help in generating functional CD8 T cell memory. *Science (1979)* **300**, 337–9 (2003).

44. Sun, J. C. & Bevan, M. J. Defective CD8 T cell memory following acute infection without CD4 T cell help. *Science* **300**, 339–42 (2003).

45. Wu, T.-S. *et al.* Reduced Expression of Bcl-2 in CD8 + T Cells Deficient in the IL-15 Receptor α-Chain. *The Journal of Immunology* **168**, 705–12 (2002).

46. Castro, I., Yu, A., Dee, M. J. & Malek, T. R. The Basis of Distinctive IL-2– and IL-15–Dependent Signaling: Weak CD122-Dependent Signaling Favors CD8 + T Central-Memory Cell Survival but Not T Effector-Memory Cell Development. *The Journal of Immunology* **187**, 5170–5182 (2011).

47. Schenkel, J. M. *et al.* IL-15-Independent Maintenance of Tissue-Resident and Boosted Effector Memory CD8 T Cells. *Journal of Immunology* **196**, 3920–6 (2016).

48. Herndler-Brandstetter, D. *et al.* KLRG1+ Effector CD8+ T Cells Lose KLRG1, Differentiate into All Memory T Cell Lineages, and Convey Enhanced Protective Immunity. *Immunity* **48**, 716-729.e8 (2018).

49. Janssen, E. M. *et al.* CD4+ T cells are required for secondary expansion and memory in CD8+ T lymphocytes. *Nature* **421**, 852–856 (2003).

50. Cullen, J. G. *et al.* CD4+ T help promotes influenza virus-specific CD8+ T cell memory by limiting metabolic dysfunction. *Proc Natl Acad Sci U S A* **116**, 4481–4488 (2019).

51. Zammit, D. J., Cauley, L. S., Pham, Q.-M. & Lefrançois, L. Dendritic cells maximize the memory CD8 T cell response to infection. *Immunity* **22**, 561–70 (2005).

52. Reyes, J. L. *et al.* Neutralization of IL-15 abrogates experimental immune-mediated cholangitis in diet-induced obese mice. *Scientific Reports* **8**, 1–12 (2018)

Supplementary Figures

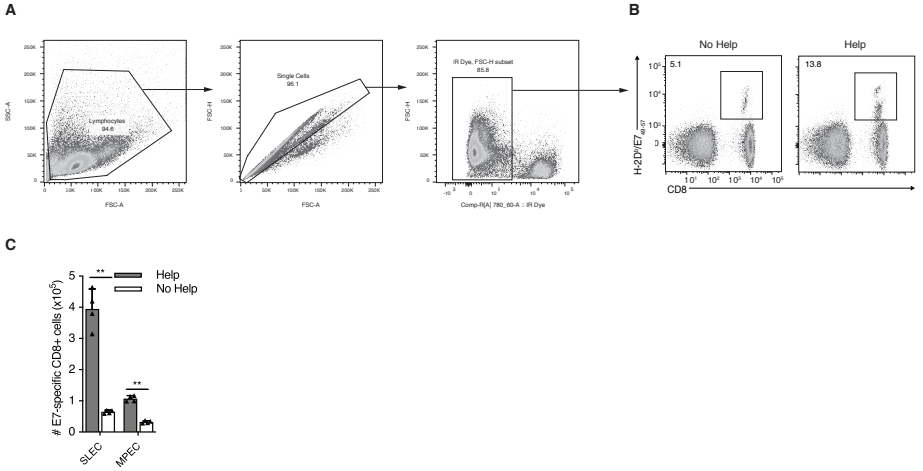

Supplementary Figure 1. (A, B, C) Mice (n=4 per group) were vaccinated as described for Figure 1. (A) Representative flow cytometry gating strategy. 3 initial steps of the gating strategy were used in all experiments. (B) Representative flow cytometric plots indicating in the boxes H-2D^b/E7$_{49\text{-}57}$ (E7)-specific CD8$^+$ T cells as measured in the spleen at the peak of the primary response (day 10). (B) Absolute numbers (#) of E7-specific CD8$^+$ T cells among CD127$^-$KLRG1$^+$ SLECs and CD127$^+$KLRG1$^-$ MPECs, as measured in the spleen at day 10 after primary vaccination. Error bars indicate SD, **p < 0.01 (unpaired two-tailed Student's t test).

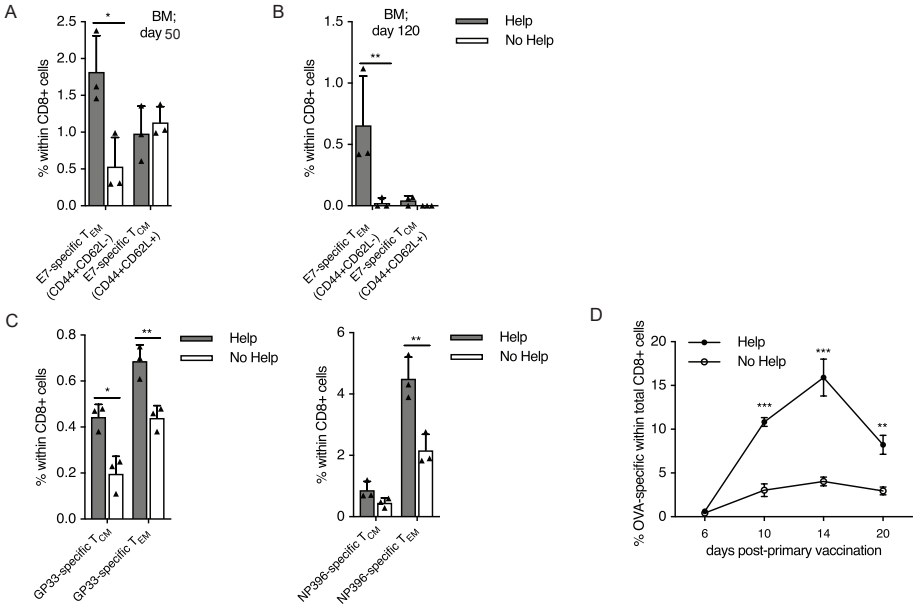

Supplementary Figure 2. (A,B) Mice (n=5 per group) received Help or No Help vaccine on days 0, 3 and 6 and were analyzed on days 50 or 120. Quantification of frequencies of E7-specific $CD44^+CD62^-$ T_{EM} and $CD44^+CD62^+$ TCM phenotype $CD8^+$ T cells determined in BM at day 50 (A) and day 120 (B). (C) Mice were infected with 10^5 PFU of LCMV Armstrong i.p. At day 2 before and days 2 and 4 after the infection, mice were injected i.v. with depleting anti-CD4 mAb (GK1.5) at 200 µg per mouse (No Help) or with isotype control antibody (Help). Graphs indicate frequencies of GP33- and NP396-specific T_{EM} ($CD62L^-CD44^+$) and T_{CM} ($CD62L^+CD44^+$) cells at day 50 post-infection. (D) $CD45.1^+$ OT-I T cells were adoptively transferred into $CD45.2^+$ recipient mice (n=5 per group) that 1 day later received OVA-encoding Help or No Help pDNA vaccine. Depicted is the percentage of H-2Kb/OVA257-264 tetramer+ cells among total $CD8^+$ T cells in the blood at the indicated days after the vaccination. Error bars indicate SD, *p < 0.05, **p < 0.01, ***p < 0.001 (unpaired two-tailed Student's t test).

Description of Supplementary Tables

Supplementary Table 1

All 193 genes that were found to be differentially expressed between helped and helpless E7-specific T_{CM} cells at the steady-state, as described in Figure 3.

Supplementary Table 2

All 2522 genes that were found to be differentially expressed between helped and helpless E7-specific T_{EM} cells at the steady-state, as described in Figure 3.

Supplementary Table 3

All 1315 genes differentially expressed between helped and helpless effector CTLs in the secondary response, as described in Figure 5.

Supplementary Table 4

All 391 genes differentially expressed between helped and helpless effector CTLs in both primary and secondary response, as described in Figure 5.

Supplementary Table 5

All 4643 differentially modified regions (DMR) as designated by H3K4me3 marks between helped and helpless memory cells, as described in Figure 6.

Supplementary Table 6

All 882 differentially modified regions (DMR) as designated by H3K27me3 marks between helped and helpless memory cells, as described in Figure 6.

Supplementary Table 7

Summary of quality control metrics of ChIPseq experiment described in Figure 6. Peaks = number of peaks called in the sample, Reads = reads in the library, Dup% = number of duplicate reads, ReadL = read length, FragL = fragment length, RelCC = relative cross-coverage score, SSD = squared sum of deviations, RiP% = percent reads in peaks.

Supplementary Table 8

Details of antibodies used for flow cytometric analysis.

All supplementary Tables are available at DOI 10.1038/s41467-019-13438-1

Chapter 3

Helpless priming sends $CD8^+$ T cells on the road to exhaustion

Julia Busselaar[1], Sun Tian[2], Hans van Eenennaam[3] and Jannie Borst[1]*

[1] Department of Immunology, Leiden University Medical Center, Leiden, The Netherlands;
[2]Aduro Biotech Europe BV, Oss The Netherlands;
[3]AIMM Therapeutics BV, Amsterdam, The Netherlands

Frontiers in Immunology 2020; 11: 592569
DOI: 10.3389/fimmu.2020.592569

Abstract

Persistent antigen exposure in chronic infection and cancer has been proposed to lead to cytotoxic T lymphocyte (CTL) “exhaustion”, i.e. loss of effector function and disease control. Recent work identifies a population of poorly differentiated TCF-1^{+}PD-1^{+} CD8^{+} T cells as precursors of the terminally exhausted CTL pool. These “predysfunctional” CTLs are suggested to respond to PD-1 targeted therapy by giving rise to a pool of functional CTLs. Supported by gene expression analyses, we present a model in which lack of CD4^{+} T-cell help during CD8^{+} T cell priming results in the formation of predysfunctional CTLs. Our model implies that predysfunctional CTLs are formed during priming and that the remedy for CTL dysfunction is to provide “help” signals for generation of optimal CTL effectors. We substantiate that this may be achieved by engaging CD4^{+} T cells in new CD8^{+} T cell priming, or by combined PD-1 blocking and CD27 agonism with available immunotherapeutic antibodies.

Introduction

In chronic infection and cancer, CD8+ T cells upregulate coinhibitory receptors and display impaired proliferative and cytotoxic capacities, a phenomenon described as "T cell exhaustion". T cell exhaustion is considered a crucial factor in limiting clinical responses to immunotherapy, but this T cell state is not well understood. Some experts do not envision functions for exhausted T cells, while others surmise a role in host protection[1]. Recent data illuminate how exhausted CD8+ T cells are formed. The original model proposed that exhausted CD8+ T cells develop from effector T cells as a result of chronic stimulation via their T cell antigen receptor (TCR)[2]. However, new transcriptomic analyses, that include TCR-based lineage tracing, argue that exhausted CD8+ T cells are not derived from functional effector cells. Rather, CD8+ T cells can attain a "predysfunctional" state early after infection or tumorigenesis that may progress into a terminally exhausted state. It is considered that predysfunctional cells may also be "reinvigorated" to become CTL effectors. Blockade of the PD-1/PD-L1 coinhibitory axis may lead to such reinvigoration. Knowledge about the exact molecular and cellular mechanisms underlying CD8+ T cell predysfunction, exhaustion and reinvigoration are clinically relevant in chronic infection and cancer, and likely also in auto-immune and inflammatory diseases.

Here, we first discuss the recent literature on CD8+ T cell predysfunction and exhaustion in a key mouse model of chronic virus infection. This work has recently led to the concept that predysfunction and exhaustion represent aspects of a CD8+ T-cell differentiation pathway, distinct from effector and memory differentiation. By connecting studies on infection and cancer, we integrate supporting arguments for this concept. We synthesize these recent insights into a model of progressive fate commitment of primed CD8+ T cells. Supported by gene expression analyses, we introduce the novel perspective that the predysfunctional differentiation state results from CD8+ T-cell priming in the absence of CD4+ T-cell help. This viewpoint implies that reinvigoration of predysfunctional CD8+ T cells may be achieved by addition of help signals. We rationalize that PD-1 targeted checkpoint blockade may lead to delivery of "help" signals and may be supported by engagement of specific T cell costimulatory receptors.

Help delivery during CD8+ T cell priming

Priming of CD4+ and CD8+ T cells relies on three key signals: TCR engagement by peptide/MHC complexes, costimulation by CD28 and members of the TNF receptor family, as well as specific cytokine signaling. Dendritic cells (DC) can supply these signals, provided that the DC is of the appropriate subset and adequately activated, by pathogen- or danger-derived signals or by CD4+ T cells. In secondary lymphoid organs, CD4+ and CD8+ T cells engage in successive antigen-specific interactions with different DC subtypes. Migratory DCs deliver the antigen from the site of infection, while lymph node-resident DCs pick up the antigen locally. CD4+ and CD8+ T cells

are initially activated independent from each other, in different regions of the lymph node by migratory conventional (c)DC1 and cDC2 subsets[3–5]. After this first step of priming, a second step of priming takes place on lymph node-resident cDC1s. In this interaction, CD4$^+$ T-cell help is delivered that is essential for optimal differentiation of CD8$^+$ T cells into CTL effector- and memory cells[6] (Figure 1). CD4$^+$ and CD8$^+$ T cells that have undergone the first step of priming produce specific chemokines that attract lymph node-resident cDC1[3,4,7]. In case the cDC1 co-presents recognizable MHC class II- and MHC class I- restricted antigens, it can relay help signals from the CD4$^+$ T cell to the CD8$^+$ T cell. Plasmacytoid (p)DCs likely promote this scenario by the production of type I interferon (IFN), which optimizes maturation and antigen crosspresentation by cDC1s[8].

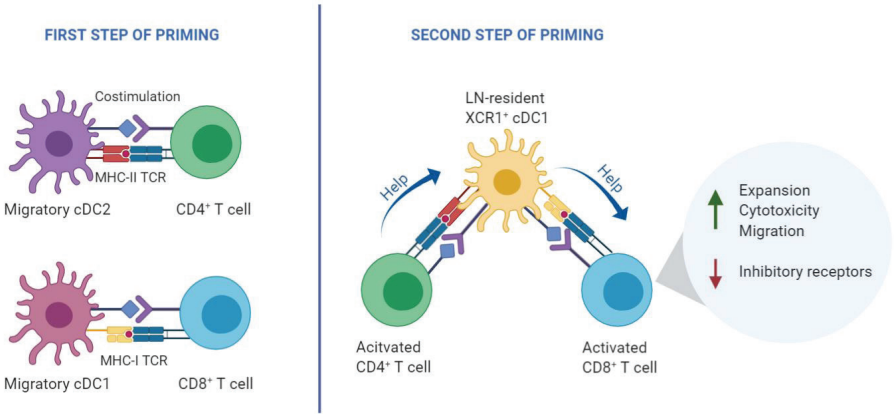

Figure 1. Two-step priming model. During the first step of T cell priming (left), CD8$^+$ T cells and CD4$^+$ T cells are initially activated independently by different DC subtypes that present antigen on MHC class I and class II, respectively. In the second step of priming (right), recently activated CD4$^+$ and CD8$^+$ T cells interact with the same lymph node-resident cDC1 co-expressing MHC class I and MHC class II epitopes. Helped CD8$^+$ T cells undergo optimal priming by signaling via various co-stimulatory and cytokine signals that emerge from the helped cDC1, resulting in an optimal CTL effector program[6].

Upon cognate contact with the CD4$^+$ T cell, the lymph node-resident cDC1 gains expression of various cytokines and co-stimulatory ligands that in concert optimize the CD8$^+$ T cell response[6]. Interaction between CD40 ligand on the CD4$^+$ T cell and CD40 on the cDC1 amplifies production of IL-12 and IL-15 by the DC, which improves clonal expansion and effector differentiation of CD8$^+$ T cells[9,10]. Furthermore, CD40 signaling in DCs upregulates CD80/CD86 and CD70, which relay costimulatory signals via CD28 and CD27, respectively[11–13]. In both CD4$^+$ and CD8$^+$ T cells, CD28 costimulation amplifies the TCR signal and drives cell division[14], while CD27 costimulation promotes cell survival and effector differentiation[15–18]. CD27 costimulation of CD8$^+$ T cells is a key effector pathway of CD4$^+$ T-cell help. It promotes CTL differentiation and survival, likely directly, but also by increasing expression of the IL-2 receptor alpha chain, IL-2 and the IL-12 receptor,

leading to autocrine IL-2 signaling and responsiveness to DC-derived IL-12[18–21]. IL-21 production by CD4+ T cells also promotes CTL effector differentiation[22].

By transcriptomic analyses in mice, we have discovered how help signals impact effector and memory gene expression programs of CD8+ T cells[18,23]. At the effector stage, "helped" versus "helpless" CTLs differentially expressed about 1000 transcripts, encoding proteins enabling critical CTL functions, such as cytotoxicity and migratory abilities. From functional studies in a tumor model, we concluded that CD4+ T-cell help confers upon CTLs the exact properties desired for effective anti-tumor immunity, as defined by Chen and Mellman in "The cancer immunity cycle"[24]. Conversely, helpless CTLs proved to have a dysfunctional phenotype characterized by low cytotoxic capacity and high expression of PD-1 and other co-inhibitory receptors[18], classifying them as "exhausted", according to the original definition. Other authors defined by micro-array similar gene expression features in helpless CTLs, which proved to resemble exhausted CTLs, as defined in a mouse model of chronic LCMV infection[25]. In conclusion, there appears to be a connection between helpless priming of CD8+ T cells and acquisition of the exhausted state. This connection will be clarified in this Hypothesis and Theory article.

Antigen-specific CD8+ T cell fates in chronic infection

Exhaustion

Exhaustion of antigen-specific CD8+ T cells was first described in mouse models of chronic infection with LCMV[26]. Exhausted virus-specific CD8+ T cells were defined by a diminished ability to display effector functions such as IFNγ production, and high expression of co-inhibitory receptors such as PD-1. It was proposed that virus-specific effector CD8+ T cells gradually turn into exhausted cells upon chronic engagement of the TCR by persistent viral antigen. Observations that TCR-regulated transcription factors contribute to exhaustion led to this idea[27–29]. In agreement with TCR signaling driving exhaustion, the exhausted virus-specific CD8+ T cell fraction was found to increase in time upon viral persistence[30]. However, virus-specific CD8+ T cells can already show impaired effector functions from the beginning of a chronic infection, suggesting causes other than chronic antigen exposure[30]. Adoptive transfer experiments demonstrated that exhausted CD8+ T cells in chronic LCMV infections derive from the same progenitors as memory cells and not from terminally differentiated (KLRG1^{hi}) effector T cells[31]. This finding suggested that exhausted CD8+ T cells in chronic infection do not follow a normal effector differentiation path[32].

Predysfunction

Despite the persistence of viral antigen, not all virus-specific CD8+ T cells in chronic infection acquire a terminally exhausted phenotype. A subset of virus-specific CD8+ T cells in chronic LCMV infection was found to proliferate and give rise to terminally exhausted cells[33]. Other authors

defined in the same model a small "memory-like" subpopulation within the virus-specific CD8$^+$ T cell pool that retained proliferative capacities and could re-expand upon secondary infection in an antigen-free host[34]. Later, this proliferative population was found to express the transcription factor TCF-1[35,36] and the chemokine receptor CXCR5[37,38]. These studies report that TCF-1$^+$ CXCR5$^+$ CD8$^+$ T population is self-sustaining and constantly replenishes the exhausted CD8$^+$ T cell pool. This population is described by different nomenclature (Table 1), but throughout this article, we will use the term "predysfunctional". The predysfunctional population is established early in chronic infection with LCMV strain clone 13, before the peak of the T cell response, but is not seen in acute infection with LCMV strain Armstrong[39]. TCF-1 is also expressed in memory T cells in acute infection, but predysfunctional TCF1$^+$ T cells in chronic infection can be identified by co-expression of CXCR5, Slamf6 and PD-1[22,38]. TCF-1 signaling represses effector differentiation and is thereby essential for generation and maintenance of predysfunctional T cells[36,40,41].

From predysfunction to exhaustion

Antigenic stimulation of predysfunctional TCF-1$^+$CXCR5$^+$ CD8$^+$ T cells can drive their differentiation into TCF-1$^-$ CXCR5$^-$ "terminally exhausted" cells[33,42,43]. During this differentiation process, predysfunctional cells transiently acquire a more effector-like gene signature[40,43,44]. Terminally exhausted CD8$^+$ T cells are short-lived and display higher expression of coinhibitory receptors than TCF-1$^+$ predysfunctional cells[35–38]. Conversion from a predysfunctional to a terminally exhausted state is associated with epigenetic and transcriptional changes involving genes encoding coinhibitory receptors, effector molecules and effector-associated transcription factors[44–46]. The transcription factor TOX plays a critical role in epigenetic imprinting of dysfunction in the TCF-1$^+$ subset and induces fate commitment to a terminally exhausted phenotype[39,47–50]. Both the establishment of the predysfunctional population and the TOX-driven commitment to exhaustion are part of a differentiation path that is separate from effector differentiation, occurring in early stages of chronic LCMV infection[39,40,47]. Together, these findings provide strong support for the notion that terminally exhausted T cells found in chronic infections are derived from a population of predysfunctional cells, instead of from functional effectors. Similar processes likely take place in human, where virus-specific predysfunctional and terminally exhausted CD8$^+$ T cell populations have been identified in patients with chronic hepatitis C virus (HCV) infection [35]. Also, CXCR5$^+$ CD8$^+$ T cells were found in patients infected with human immunodeficiency virus (HIV) or chronic hepatitis B virus (HBV)[51,52].

Table 1: Definitions of predysfunctional CD8+ T cell populations in chronic infection and cancer.

Population name	Markers	Source	References
Memory-like	TCF-1^{+}	LCMV-c13	[32,34,35,58]
		Human HCV	[35]
		Human melanoma	[74]
Stem-like	CXCR5^{+}TIM3^{-}	LCMV-c13	[38,45]
		Human NSCLC	[63]
	PD-1^{+}CD101^{-}TIM3^{-}	LCMV-c13	[43]
	TIM3^{-}CD28^{+}	Human kidney cancer	[64]
	TCF-1^{+}	B16-gp33	[72]
Progenitor-like	TCF-1^{high}TIM3^{low}	LCMV-c13	[36]
		Human melanoma	[36]
	Tcf7+Tox+	LCMV-c13	[39]
Progenitor	TCF-1^{+}	LCMV-c13	[49,59,85,87]
	Ly108^{+} (Slamf6^{+})	LCMV-c13	[22]
Progenitor exhausted	Slamf6^{+}TIM3^{-}	LCMV-c13; B16-OVA	[46]
	TCF-1^{+}PD-1^{+}	Human melanoma	[46]
Precursor	T-bet^{high}Eomes^{low}	LCMV-c13	[33]
Memory precursor-like	PD-1^{-}TCF-1^{+}	MC38-OVA	[73]
Precursor exhausted	KLRG1^{-}PD-1^{+} Ly108^{+}	LCMV-c13	[40]
	TCF-1^{+}	LCMV-c13	[86]
Stem cell-like exhausted	CXCR5^{+}TIM3^{-}	LCMV-c13	[41]
Pre-exhausted	*GZMK+, ZNF683+*	Human NSCLC	[66]
Predysfunctional	multiple	Human cancers	[69]
Early dysfunctional	CD38^{low}CD101^{low}	ASTxCre-ER^{T2}	[61,62]
Transitional	*GZMK+*	Human melanoma	[65]
		Human HCC	[68]
Follicular cytotoxic	CXCR5^{+}	LCMV-13	[37,99]
		LCMV-DOCILE; HIV	[51]
		Human CHB	[52]

The listed populations have in common that they sustain the CTL response in presence of persistent antigen, and form the progenitors of the terminally exhausted population, as originally shown by Utzschneider et al. (2016), Wu et al. (2016), He et al. (2016) and Im et al. (2016) and corroborated by Miller et al. (2019) and Zander et al. (2019). Other cited papers consider the defined population to be predysfunctional based on the markers and the proliferative/"stem-like" phenotype described in the original papers. In the papers describing human single cell RNAseq data, the predysfunctional population is defined by intermediate expression of inhibitory receptor genes, low expression of effector-associated genes, and TCR sharing with the terminally exhausted population.

Reinvigoration

Importantly, PD-1 blockade unleashes the expansion potential of predysfunctional, but not terminally exhausted virus-specific CD8$^+$ T cells[35,37,38]. Predysfunctional TCF-1$^+$ CD8$^+$ T cells express PD-1 that supports the maintenance of this population early during chronic LCMV infection [40]. Chronic virus infections (LCMV clone 13, HIV) induce chromatin accessibility and permanent demethylation of the *Pdcd1* locus (encoding PD-1), causing exhausted CD8$^+$ T cells to stably express PD-1 at high levels[53,54]. Terminally exhausted CD8$^+$ T cells express higher levels of PD-1 and other coinhibitory receptors than predysfunctional cells[35–37]. In the terminally exhausted population, efficacy and durability of virus-specific CD8$^+$ T cell reinvigoration by PD-1 blockade proved to be limited by the epigenetic landscape, including chromatin accessibility and *de novo* DNA methylation[55,56]. Taken together, these results argue that the predysfunctional virus-specific CD8$^+$ T cell population in chronic infection is reinvigorated by PD-1 blockade. Predysfunctional cells respond to PD-(L)1 blockade by undergoing proliferation, as well as differentiation towards a terminally exhausted phenotype[46]. During this differentiation, cells pass through an intermediate or "transitory" state, characterized by a transcriptional signature that resembles that of effector CTLs[43,44]. While these effector-like CD8$^+$ T cells that are reinvigorated by PD-1 blockade are able to produce cytokines and contribute to virus control, they retain expression of inhibitory receptors and eventually convert to a terminally exhausted state upon persistent antigen exposure[43].

Proposition: Helpless priming generates predysfunctional CD8$^+$ T cells

Establishing a chronic infection in mouse models is often aided by depleting CD4$^+$ T cells[26,30,38,56,57], suggesting a link between the absence of CD4$^+$ T-cell help and infections persisting chronically. Decreased antigen presentation and decreased costimulatory signaling by DCs during priming promote the formation of TCF-1$^+$ cells, suggesting that this population may be generated as a result of suboptimal priming[58]. Importantly, CD4$^+$ T-cell depletion in chronic LCMV infection impaired the generation of terminally differentiated effector CD8$^+$ T cells, but not of predysfunctional TCF-1$^+$ CD8$^+$ T cells[59]. This finding indicates that the predysfunctional TCF-1$^+$ CD8$^+$ T cell population is formed independently of CD4$^+$ T-cell help. We propose that this population is formed as a result of helpless priming and provide supporting evidence in this Perspective.

As a model to study CD4$^+$ T-cell help for the CTL response, our group made use of a therapeutic DNA vaccination scheme in mice. We used a comparative setting with two vaccines that encode an immunodominant MHC-I restricted peptide from the human papillomavirus (HPV) E7 protein to prime CD8$^+$ T cells, either with or without HPV-unrelated immunodominant MHC-II restricted peptides to induce CD4$^+$ T-cell help[60]. Genome-wide mRNA deep sequencing of HPV-E7-specific CD8$^+$ T cells at the effector stage of the CTL response yielded "Help" and "No Help" signatures[18]. Helpless CTLs expressed many genes characteristic of the predysfunctional CD8$^+$ T-cell subset at a higher level than helped CTLs,

including *Tcf7* (encoding TCF-1), *Tox*, *Pdcd1* (encoding PD-1), *Cxcr5* and *Slamf6* (Figure 2A)[18]. We therefore hypothesized that predysfunctional CD8+ T cells found in chronic LCMV infection are cells that have not experienced CD4+ T-cell help during priming. To test this, we determined how predysfunctional CD8+ T cells defined in literature and helpless CD8+ T cells defined in our study are related at the gene expression level, by Gene Set Enrichment Analysis (GSEA). A published gene expression signature characteristic for the predysfunctional TCF-1+ CD8+ T-cell population in chronic LCMV infection[35] in mice thus proved to be enriched in the No Help gene expression signature of antigen-specific CD8+ T cells from our vaccination study (Figure 2B). Additionally, using another published dataset from chronic LCMV infection[46], we determined a "No Help score" as a measure of correlation with our No Help gene expression signature. This analysis demonstrated that predysfunctional TCF-1+ CD8+ T cells display a higher No Help score than TCF-1- terminally exhausted cells, indicating that predysfunctional CD8+ T cells are transcriptionally more similar to helpless CD8+ T cells (Figure 2C).

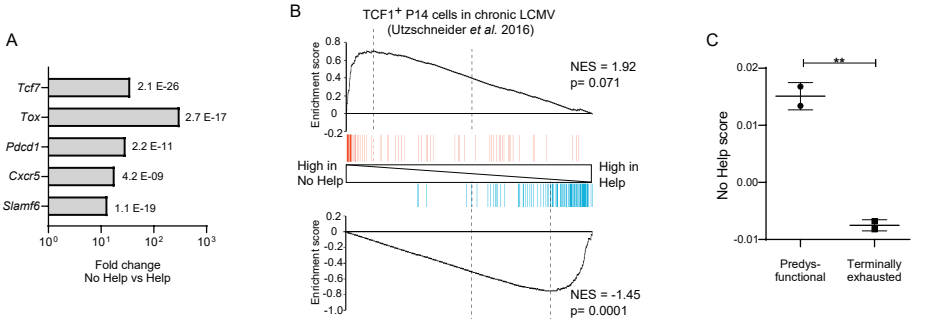

Figure 2. Predysfunctional TCF-1+ CD8+ T cells in a chronic LCMV infection model display a gene expression signature characteristic of helpless antigen-specific CD8+ T cells in a vaccination model. The transcriptional "No Help" signature was determined by differential gene expression (False discovery rate (FDR)<0.01) of antigen-specific CTLs raised in No Help versus Help vaccination settings (GEO database GSE89665)[18]. (A) Differential expression of selected genes characteristic of predysfunctional TCF-1+CD8+ T cells (Table 1) in No Help versus Help settings. FDR is depicted per gene. (B) GSEA of the top 200 upregulated (red)- or downregulated (blue) genes from Tcf7+ versus Tcf7- virus-specific CD8+ T cells in chronic LCMV infection[35] within the gene expression profiles of CD8+ T cells from the No Help versus Help vaccination settings. NES = normalized enrichment score. (C) No Help score in predysfunctional TCF-1+TIM3- and terminally exhausted TCF-1-TIM3+ CD8+ T cells from a setting of chronic LCMV infection (GEO database GSE122713)[46]. The No Help score was calculated as the difference of correlations in gene expression between a given population and No Help or Help vaccination settings. A higher No-Help score indicates greater transcriptional similarity to helpless CD8+ T cells. *P<0.05, **P<0.01, ***P<0.001 by Student's t-test.

CD8$^+$ T cell dysfunction in cancer

The parallel

In cancer, tumor antigen-specific CD8$^+$ T cells may be chronically stimulated within the tumor micro-environment (TME), which theoretically can lead to exhaustion, as it does in mouse models of chronic virus infection. However, in the LCMV models, infection is systemic and analysis is generally focused on CD8$^+$ T cells from the spleen. This milieu is distinct from the TME in partially undefined aspects. In both environments, specific conditions are created by interplay between infected cells or growing tumor cells, immune cells and non-immune cells. Intratumoral CD8$^+$ T cells are known to be exposed to various suppressive immune cell types, inhibitory molecules, hypoxia, metabolites and nutrient deprivation[2].

Mouse models

Using a mouse model of tamoxifen-inducible liver cancer, Schietinger *et al*. showed that tumor antigen-specific CD8$^+$ T cells taken from the TME early during tumorigenesis could be reinvigorated by PD-1 blockade or recall in an antigen-free host. Late in tumor development, however, these cells could no longer be rendered functional. It was found that tumor-specific CD8$^+$ T cells in the TME over time acquire a fixed dysfunctional phenotype[61]. Follow-up research in this model showed that tumor-specific CD8$^+$ T cells in the TME first attain a reversible dysfunctional state and next enter a epigenetically fixed dysfunctional state[62]. These data are in agreement with a transition from predysfunction to exhaustion.

In a murine melanoma model, single-cell transcriptomics revealed that among CD8$^+$ tumor infiltrating lymphocytes (TILs), TCF-1$^+$ predysfunctional and TCF-1$^-$ terminally exhausted cell subsets can be discerned that are analogous to those defined in chronic LCMV infection. Adoptive transfer experiments demonstrated that TCF-1$^+$ CD8$^+$ T cells can persist long-term inside a tumor and give rise to terminally exhausted cells[46]. Like in chronic infection, transcriptional and epigenetic changes underlying this conversion depended on the transcription factor TOX[48,50].

Human cancer

Also in human cancer, there is increasing evidence for the existence of predysfunctional and terminally exhausted CD8$^+$ T cell populations. In non-small cell lung cancer (NSCLC), CXCR5 expression was selectively found on CD8$^+$ TILs and not on CD8$^+$ T cells from healthy tissue or blood[63]. In kidney cancer, TCF-1$^+$TIM3$^-$CD28$^+$ predysfunctional TILs were found to reside in niches that are rich in antigen-presenting cells, while PD-1$^+$TIM3$^+$ terminally exhausted cells were distributed throughout the tumor tissue. Transcriptional and epigenetic profiles of these human TIL subsets proved to be similar to those described in the mouse. Importantly, TCR repertoire overlap between the two populations indicated that TCF-1$^+$ predysfunctional TILs are indeed the progenitors of terminally exhausted TILs[64]. TCR repertoire overlap between a terminally

exhausted TIL population, characterized by high expression of coinhibitory receptor genes, and a predysfunctional TIL population, characterized by expression of *GZMK*, was also found in human melanoma[65], NSCLC[66], colorectal cancer (CRC)[67] and hepatocellular carcinoma (HCC)[68]. These findings are consistent with a model where also in human cancer, exhausted TILs derive from a predysfunctional population. However, a strict division of the human TIL pool into predysfunctional or terminally exhausted may be an oversimplification. Rather, CTL dysfunction in human TILs covers a spectrum of differentiation states, ranging from predysfunctional to terminally exhausted[69].

The question remains whether the active CTLs that display effector functions in human tumors are generated from a separate CD8+ T cell pool, or are connected to the (pre)dysfunctional pool. In CRC, HCC and NSCLC studies, TCR sharing was found between *GZMK*+ predysfunctional TILs and *CX3CR1+* effector populations found in blood and normal tissue[66–68]. These results support a model in which the predysfunctional population forms a branchpoint from which differentiation trajectories of effector versus exhausted CD8+ T cells emanate, possibly reflecting CD8+ T cells after the first step of priming that subsequently receive CD4+ T-cell help, versus CD8+ T cells that do not. However, it was not determined in those studies whether the T cells that shared TCRs were tumor-specific. In melanoma, intratumoral *GZMH*+ effector CTLs did not share TCRs with the predysfunctional or exhausted CD8+ TIL population, indicating that they formed a separate lineage[65]. Interestingly, in this study, tumor reactivity was enriched in the dysfunctional but not in the cytotoxic TIL population, suggesting that the cytotoxic population consists of bystander cells that do not recognize the tumor, as was demonstrated before[70,71]. These data argue that in melanoma, persistent tumor antigen recognition drives the conversion of helpless tumor-specific TILs from the predysfunctional to the terminally exhausted state, while the tumor may also harbor helped bystander cells with an effector phenotype[69]. Whether tumor-specific dysfunctional TILs can differentiate within the TME into competent effector CTLs remains to be investigated.

Reinvigoration

In mouse models of melanoma, the TCF-1+ predysfunctional CD8+ TILs proved to be the responders to PD-1 blockade and necessary for tumor control[46,72,73]. In melanoma patients, an increased fraction of TCF-1+ predysfunctional CD8+ TILs is a positive predictor for response to PD-(L)1 targeted therapy[46,74]. In a murine liver cancer model, CD101 and CD38 marked predysfunctional versus terminally exhausted TILs. These markers were heterogeneously expressed by PD-1^{high} TILs from melanoma and NSCLC patients, suggesting that the human PD-1^{high} TIL population consists of a mixture of predysfunctional and terminally exhausted cells[62].

Helplessness and predysfunction in cancer

$CD4^+$ T-cell help is less likely to be delivered in cancer than in infection for the following reasons: Tumor cells generally do not express PAMPs and may only exude DAMPs under specific circumstances. Therefore, they are less likely to activate migratory DCs than infected cells. Furthermore, in the suppressive TME, migratory cDC2s, which are essential for the priming of $CD4^+$ T cells[75], are reportedly suppressed by Tregs, resulting in suboptimal priming of $CD4^+$ helper T cells in the tumor-draining lymph node[76]. Also, DC-activating signals such as type I IFN that promote crosspresentation functions of the lymph node-resident cDC1[8], are often lacking. In the blood of melanoma patients, tumor reactivity of CTLs was found to be enriched in the PD-1^+ population[77]. These data led us to hypothesize that helpless priming may contribute to the dysfunctional phenotype of $CD8^+$ T cells in cancer.

To test this hypothesis, we performed bioinformatic analyses using our previously defined No Help versus Help signatures of mouse $CD8^+$ T cells and datasets from mouse and human cancer. GSEA showed that gene sets characteristic of predysfunctional TCF-1^+ $CD8^+$ TILs from a gp33 antigen bearing B16 melanoma mouse model[72] were enriched in the No Help gene expression signature (Figure 3A). In an ovalbumin (OVA) antigen-bearing B16 melanoma model from a different research group[46], TCF-1^+ $CD8^+$ TILs displayed a higher No Help score than TCF-1^- $CD8^+$ TILs (Figure 3B). These results indicate that also in mouse cancer models, dysfunctional TCF-1^+ $CD8^+$ TILs display a gene expression profile that resembles that of helpless cells. In NSCLC patients, the presence of PD-1^{high} TILs was a positive predictor of response to PD-1 blockade therapy. Importantly, PD-1^{high} TIL cells displayed higher intrinsic tumor reactivity compared to TIL populations with intermediate or no PD-1 expression from the same tumor[78]. We used the published gene expression profiles from these matched TIL subsets to calculate their No Help score. Among these patients' TIL populations, the transcriptome of PD-1^{high} TILs was most similar to that of helpless vaccine antigen-specific $CD8^+$ T cells (Figure 3C). These data from human cancer support our hypothesis that dysfunctional tumor-reactive $CD8^+$ T cells are cells that have lacked help during priming.

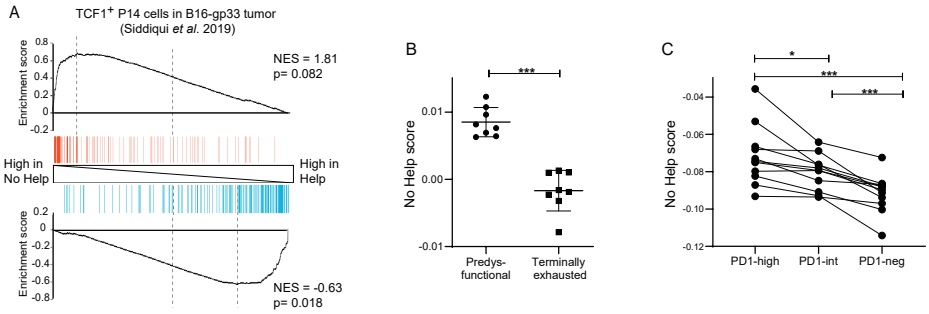

Figure 3. Predysfunctional TCF-1$^+$ CD8$^+$ T cells in human cancer display a gene expression signature characteristic of helpless antigen-specific CD8$^+$ T cells in a mouse vaccination model. (A) GSEA showing enrichment of the top 200 upregulated (red) or downregulated (blue) genes in gp33-specific TCF-1$^+$ CD8$^+$ T cells in a murine B16-gp33 tumor model[72] within the gene expression profiles of vaccine antigen-specific CD8$^+$ T cells in No Help versus Help settings[18]. (B) No Help scores, defined in our vaccination model, determined in the transcriptomes of predysfunctional TCF-1$^+$TIM3$^-$ and terminally exhausted TCF-1$^-$TIM3$^+$ tumor antigen-specific CD8$^+$ T cells from a murine B16-OVA tumor model (GEO database GSE122713)[46]. (C) No Help score defined as in (B), determined in the transcriptome of patient-matched PD-1-high, PD-1-intermediate, and PD-1-negative CD8$^+$ TILs in human melanoma (GEO database GSE99531)[78]. *P<0.05, **P<0.01, ***P<0.001 by Student's t-test (B) or one-way ANOVA (C).

Helpless dysfunction model

We present a novel model posing that virus-specific or tumor-specific, predysfunctional TCF-1$^+$ CD8$^+$ T cells in chronic infection or cancer result from priming in the absence of CD4$^+$ T-cell help. CD4$^+$ T-cell help delivered during priming optimizes effector differentiation of antigen-specific CD8$^+$ T cells[18,59]. Additionally, CD4$^+$ T-cell help promotes effector memory CD8$^+$ T cell (T_{EM}) generation, and renders these T_{EM} cells more effector-like on a per-cell basis[23]. These results are in line with a previously proposed progressive differentiation model for primed CD8$^+$ T cells[79], adding that CD4$^+$ T-cell help shifts differentiation of primed CD8$^+$ T cells towards a more effector-like state (Figure 4).

By optimizing CTL function, CD4$^+$ T-cell help contributes to antigen clearance, which is necessary for proper memory formation[80,81]. CD4$^+$ T-cell help also promotes the long-term maintenance of T_{CM} cells and is necessary for open configuration of gene loci encoding CTL effector molecules in memory CD8$^+$ T cells[23,82,83]. The epigenetic imprinting induced by help signals during priming allows memory cells to rapidly exert effector functions upon reactivation in a CD4$^+$ T helper cell-independent manner[23,84].

In the absence of CD4$^+$ T-cell help, effector differentiation of CD8$^+$ T cells is incomplete, resulting in predysfunctional CTLs that have limited cytotoxic and migratory potential and express coinhibitory receptors[18,25], which prohibits antigen clearance. The chronic stimulation of memory precursor cells impairs the formation of a memory pool and instead drives their differentiation into predysfunctional CTLs, as seen in chronic infection and cancer[32,85]. These

predysfunctional TCF-1$^+$ cells have self-maintaining properties and form the progenitors of the terminally exhausted TCF-1$^-$ CD8$^+$ T cell pool[86]. Exhausted CD8$^+$ T cells differ in their epigenetic and transcriptional states from predysfunctional CD8$^+$ T cells. They have a further developed effector differentiation program, but are fixed in their dysfunctional state[87].

Overcoming CTL dysfunction by help signals

Based on our model, we propose that in chronic infection and cancer, CTL dysfunction can be overcome by help signals. In that scenario, help signals would enable the CTLs to progress further towards a terminal effector differentiation state. Adoptive transfer of CD4$^+$ T cells has been shown to increase proliferation of pre-existing TCF-1$^+$ CD8$^+$ T cells in chronic LCMV infection[59]. Also, adoptive transfer of IL-21-producing CD4$^+$ T cells into tumor-bearing mice induced generation of a CX3CR1$^+$ effector CD8$^+$ T cell pool, leading to improved tumor control[22]. Using help signals to alleviate CTL dysfunction is not yet incorporated into clinical protocols. In the clinic, PD-1 blockade is used as method to “reinvigorate” dysfunctional CTLs.

We here propose that PD-1 blockade recapitulates aspects of CD4+ T-cell help and acts on the predysfunctional/helpless CD8$^+$ T cell population. As reviewed in the preceding sections, in chronic LCMV infection and cancer, PD-1 blockade induced proliferation of predysfunctional TCF-1$^+$ CD8$^+$ T cells. The question is whether PD-1 blockade is sufficient to overcome lack of help and - by association – to convert predysfunctional CTLs into fully functional effectors. In chronic LCMV infection, established through transient CD4$^+$ T-cell depletion, PD-L1 blockade promoted differentiation of predysfunctional CD8$^+$ T cells into transitional cells that displayed a more effector-like phenotype and contributed to virus control. However, eventually these cells became terminally exhausted[43]. Blockade of the PD-L1/PD-1 axis in a helpless setting increases the magnitude of the antigen-specific CD8$^+$ T-cell response, but in contrast to CD4$^+$ T-cell help, it did not rescue the formation of the effector population that conferred protection against chronic infection and cancer[22]. These results suggest that predysfunctional/helpless cells cannot be rescued by PD-1 blockade alone.

The prevailing view is that PD-1 blockade relieves pre-existing dysfunctional CTLs from suppression in the TME. However, accumulating data argue that PD-1 blockade can also facilitate *de novo* CTL priming. Firstly, PD-(L)1 targeted immunotherapy can be effective while PD-L1 is not expressed in the tumor[88]. Secondly, PD-1 signaling impedes TCR as well as CD28 signaling, indicating that it can also impact on costimulation at the T cell/DC interface[89]. In agreement with this, tumor regression upon PD-1 blockade in mouse colon carcinoma depended on CD28 co-stimulation[90]. Thirdly, the response to PD-1 blockade in mouse colon carcinoma was found to depend on influx of newly activated CD8$^+$ T cells from tumor draining lymph nodes[91].

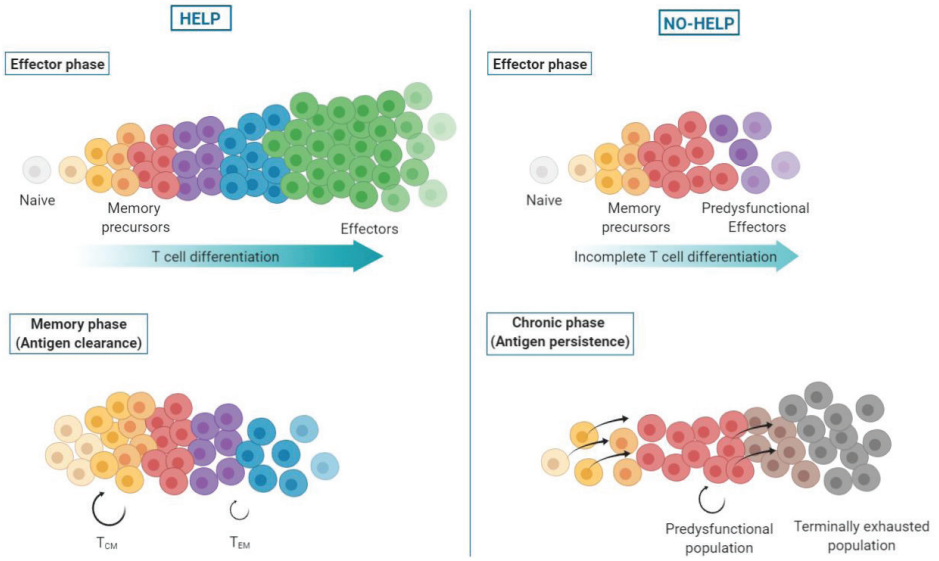

Figure 4. Helpless dysfunction model. Upon priming of CD8⁺ T cells, a differentiation spectrum is formed, ranging from uncommitted memory precursors to terminally differentiated effector cells. In presence of CD4⁺ T-cell help signals (left), the antigen-specific CD8⁺ T-cell population attains higher differentiation states, with the majority of cells becoming terminally differentiated, short-lived effector CTLs. These helped CTLs clear the antigen source and die. When antigen wanes, memory precursor cells persist and form helped central (T_{CM}) and effector memory (T_{EM}) CD8⁺ T cells. In absence of help signals (right), antigen-specific CD8⁺ T cells undergo incomplete effector differentiation and terminally differentiated effector CTLs are lacking. Instead, predysfunctional effector CTLs are formed that are less committed ("memory-like"), i.e. have not fully unfolded their effector program and express coinhibitory receptors. In addition, formation of effector memory CD8⁺ T cells is impaired. As a result, antigen persists and continuous TCR stimulation of memory precursor cells drives their differentiation into predysfunctional CTLs that self-maintain or differentiate into terminally exhausted cells.

Recent data from human cancer also argue that PD-1 blockade promotes CD8⁺ T cell priming: In basal cell carcinoma, new CD8⁺ T-cell clones entered the upon tumor PD-1 blockade[92]. TCR repertoire analysis argued that these clones pre-existed in blood and entered the tumor after treatment[93]. PD-1 is expressed rapidly after stimulation of naive CD8⁺ T cells, and inhibits effector differentiation during priming[94]. We found that in the CD4⁺ T-cell help-dependent second step of priming, CD8⁺ T cells downregulate PD-1, whereas helpless cells maintain high PD-1 expression[18]. This supports a model in which PD-1 serves as a checkpoint in the two-step T-cell priming process.

We have shown in the mouse vaccination model, that the effects of CD4⁺ T-cell help on the CTL response could be mimicked by combined PD-1-blockade and CD27 agonism[95]. We and others have shown that delivery of CD4⁺ T-cell help is highly dependent on CD70-CD27 signaling and CD27 agonism installs a large part of the "helped" gene signature into CD8⁺ T cells during priming[12,16–18]. The combined effect of PD-1 blockade and CD27 agonism likely recapitulates

combined CD28 and CD27 costimulation that are known to complement each other in generation of the CTL effector pool[15]. The collective data make a strong case for combining CD27 agonism with PD-(L)1 blockade in cancer immunotherapy.

Concluding remarks

We here present our hypothesis that CD8$^+$ T cell priming in the absence of CD4$^+$ T-cell help leads to CD8$^+$ T cell dysfunction. We pose that exhausted antigen-specific CD8$^+$ T cells observed in infection and cancer derive not from previous active CTLs, but from helpless CD8$^+$ T cells that emerge from the priming process in a dysfunctional state. We pose that provision of CD4$^+$ T-cell help, or the signals that mediate the priming of fully functional "helped" CD8$^+$ T cells will be crucial for the development of effective immunotherapeutic strategies in chronic infection and cancer. In immunotherapy, reverting exhausted cells back to a functional phenotype is considered an important challenge[1]. Alternatively, we argue that in patients with immunogenic cancer types, *de novo* priming of helped CD8$^+$ T cells will be beneficial for tumor control. For this purpose, potential approaches are antigen-agnostic PD-1/CD27 targeting, or antigen-informed therapeutic vaccination. Such vaccines should contain MHC-I and MHC-II epitopes to activate both CD8$^+$ and CD4$^+$ T cells. Other strategies include specific targeting of antigens and activation signals to XCR1$^+$ cDC1s. In these approaches, evaluation of the transcriptional help signature in tumor-specific CD8$^+$ T cells is a potential diagnostic tool.

Methods

No Help CD8$^+$ T cell gene expression signature

RNAseq fastq files of samples of helped CD8$^+$ T cells (n=3) and samples of non-helped CD8$^+$ T cells (n=3) were retrieved from GEO database (GSE89665)[18]. FASTQ files were aligned to the mouse genome mm10 (GRCm38.77) using HISAT2 v2.1.0[96], and number of reads was assigned to genes by using featureCounts v1.6.1[97]. Reads mapped to genes were normalized and differentially expressed gene analysis between non-helped CD8$^+$ T cells and helped CD8$^+$ T cell was performed using edgeR package in R Bioconductor[98]. The false discovery rate (FDR) < 0.01 was used as the criteria to select statistically differentially expressed gene lists. In total, a list of 1331 genes were found differentially expressed between non-helped condition and helped condition (FDR<0.01), and represents the No Help signature.

Calculation of No Help score in published CD8$^+$ T-cell expression signatures

RNAseq fastq files were retrieved from GEO database (GSE99531, GSE122713)[46,78]. FASTQ files were aligned to the mouse genome mm10 using HISAT2 v2.1.0[96], and number of reads was assigned to genes by using featureCounts v1.6.1[97]. Genes with all zero counts were removed.

The raw counts were normalized by count per million (CPM) methods[98]. For each sample, a "No-Help score" was determined by nearest centroid method on the 1331 genes from the No Help signature. In short, No Help score was calculated as the difference of Pearson correlations in normalized read counts between a given population and No Help or Help vaccination settings. A higher No-Help score indicates greater transcriptional similarity to helpless CD8+ T cells.

Gene Set Enrichment Analysis

RNAseq files of helped or non-helped CD8 T cells, aligned to the mouse genome mm10, were imported into Qlucore Omics Explorer. Genes with less than 5 reads in at least one of the samples were discarded. Mapping quality threshold was set to 10. TNM normalization method was applied. Gene Set Enrichment Analysis was performed using published gene sets of the top 200 up- and downregulated genes from *Tcf7*-GFP+ versus *Tcf7*-GFP- P14 cells in chronic LCMV infection[35] or B16-gp33 tumor model[72].

Statistical analysis

Data was analyzed with GraphPad Prism software using unpaired two-tailed Student's t-test, or repeated measures one-way ANOVA with Tukey's multiple comparison test. A P value < 0.05 was considered statistically significant; *P < 0.05, **P <0.005 and ***P < 0.001.

Illustrations

Illustrations in Figures 1 and 4 were created with BioRender.

Data availability

All datasets analyzed in this article can be found in the Gene Expression Omnibus (https://www.ncbi.nlm.nih.gov/geo/).

Acknowledgements

We thank Paul Vink and Lars Guelen (Aduro Biotech) for their support of this project. This work was financially supported by grant 11079 from the Dutch Cancer Society.

Author contributions

JuB performed data analysis and wrote the paper. ST performed data analysis. JaB contributed to writing the paper. HvE critically reviewed the paper.

Competing Interests

HvE and ST have been employees of Aduro Biotech. HvE has stocks and/or stock options in Aduro Biotech, Inc. The other authors do not have any financial competing interests. Both company-employed authors declare that their employment does not alter their adherence to the policies of Frontiers in Immunology.

References

1. Blank, C. U. *et al.* Defining 'T cell exhaustion'. *Nature Reviews Immunology* **19**, 665–674 (2019).
2. Xia, A., Zhang, Y., Xu, J., Yin, T. & Lu, X.-J. T cell dysfunction in cancer immunity and immunotherapy. *Frontiers in Immunology* **10**, 1719 (2019).
3. Eickhoff, S. *et al.* Robust anti-viral immunity requires multiple distinct T cell-dendritic cell interactions. *Cell* **162**, 1322–1337 (2015).
4. Hor, J. L. *et al.* Spatiotemporally distinct interactions with dendritic cell subsets facilitates CD4+and CD8+T cell activation to localized viral infection. *Immunity* **43**, 554–565 (2015).
5. Kitano, M. *et al.* Imaging of the cross-presenting dendritic cell subsets in the skin-draining lymph node. *Proc Natl Acad Sci U S A* **113**, 1044–1049 (2016).
6. Borst, J., Ahrends, T., Bąbała, N., Melief, C. J. M. & Kastenmüller, W. CD4+ T cell help in cancer immunology and immunotherapy. *Nat Rev Immunol* **18**, 635–647 (2018).
7. Castellino, F. & Germain, R. N. Cooperation between CD4+ and CD8+ T cells: when, where, and how. *Annu Rev Immunol* **24**, 519–40 (2006).
8. Brewitz, A. *et al.* CD8+T cells orchestrate pDC-XCR1+dendritic cell spatial and functional cooperativity to optimize priming. *Immunity* **46**, 205–219 (2017).
9. Greyer, M. *et al.* T Cell Help Amplifies Innate Signals in CD8+DCs for Optimal CD8+T Cell Priming. *Cell Rep* **14**, 586–597 (2016).
10. Agarwal, P. *et al.* Gene Regulation and Chromatin Remodeling by IL-12 and Type I IFN in Programming for CD8 T Cell Effector Function and Memory. *The Journal of Immunology* **183**, 1695–1704 (2009).
11. Prilliman, K. R. *et al.* Cutting Edge: A Crucial Role for B7-CD28 in Transmitting T Help from APC to CTL. *The Journal of Immunology* **169**, 4094–4097 (2002).
12. Taraban, V. Y., Rowley, T. F. & Al-Shamkhani, A. Cutting Edge: A critical role for CD70 in CD8 T cell priming by CD40-licensed APCs. *The Journal of Immunology* **173**, 6542–6546 (2004).
13. Sanchez, P. J., McWilliams, J. A., Haluszczak, C., Yagita, H. & Kedl, R. M. Combined TLR/CD40 Stimulation Mediates Potent Cellular Immunity by Regulating Dendritic Cell Expression of CD70 In Vivo. *The Journal of Immunology* **178**, 1564–1572 (2007).
14. Acuto, O. & Michel, F. CD28-mediated co-stimulation: a quantitative support for TCR signalling. *Nature Reviews Immunology* **3**, 939–951 (2003).
15. Hendriks, J., Xiao, Y. & Borst, J. CD27 Promotes Survival of Activated T Cells and Complements CD28 in Generation and Establishment of the Effector T Cell Pool. *The Journal of Experimental Medicine* **198**, 1369–1380 (2003).

16. Bullock, T. N. J. & Yagita, H. Induction of CD70 on dendritic cells through CD40 or TLR stimulation contributes to the development of CD8 + T cell responses in the absence of CD4 + T cells. *The Journal of Immunology* **174**, 710–717 (2005).

17. Feau, S., Garcia, Z., Arens, R., Yagita, H. & Borst, J. The CD4 + T-cell help signal is transmitted from APC to CD8 + T- cells via CD27–CD70 interactions. *Nature Communications* **3**, (2012).

18. Ahrends, T. *et al.* CD4+T cell help confers a cytotoxic T cell effector program including coinhibitory receptor downregulation and increased tissue invasiveness. *Immunity* **47**, 848–861 (2017).

19. Obar, J. J. *et al.* CD4+ T cell regulation of CD25 expression controls development of short-lived effector CD8+ T cells in primary and secondary responses. *Proceedings of the National Academy of Sciences* **107**, 193–198 (2010).

20. Wilson, E. B. & Livingstone, A. M. Cutting Edge: CD4 + T Cell-Derived IL-2 Is Essential for Help-Dependent Primary CD8 + T Cell Responses. *The Journal of Immunology* **181**, 7445–7448 (2008).

21. Peperzak, V., Xiao, Y., Veraar, E. A. M. & Borst, J. CD27 sustains survival of CTLs in virus-infected nonlymphoid tissue in mice by inducing autocrine IL-2 production. *The Journal of Clinical Investigation* **120**, 168–178 (2010).

22. Zander, R. *et al.* CD4+ T Cell Help Is Required for the Formation of a Cytolytic CD8+ T Cell Subset that Protects against Chronic Infection and Cancer. *Immunity* **51**, 1028–1042 (2019).

23. Ahrends, T. *et al.* CD4+ T cell help creates memory CD8+ T cells with innate and help-independent recall capacities. *Nature Communications* **10**, 5531 (2019).

24. Chen, D. S. & Mellman, I. Oncology meets immunology: the cancer-immunity cycle. *Immunity* **39**, 1–10 (2013).

25. Provine, N. M. *et al.* Immediate Dysfunction of Vaccine-Elicited CD8 + T Cells Primed in the Absence of CD4 + T Cells. *The Journal of Immunology* **197**, 1809–1822 (2016).

26. Zajac, A. J. *et al.* Viral Immune Evasion Due to Persistence of Activated T Cells Without Effector Function. *Journal of Experimental Medicine* **188**, 2205–2213 (1998).

27. Martinez, G. J. *et al.* The transcription factor NFAT promotes exhaustion of activated CD8+ T cells. *Immunity* **42**, 265–278 (2015).

28. Chen, J. *et al.* NR4A transcription factors limit CAR T cell function in solid tumours. *Nature* **567**, 530–534 (2019).

29. Man, K. *et al.* Transcription factor IRF4 promotes CD8+ T cell exhaustion and limits the development of memory-like T cells during chronic infection. *Immunity* **47**, 1129–1141 (2017).

30. Wherry, E. J. *et al.* Molecular Signature of CD8+ T Cell Exhaustion during Chronic Viral Infection. *Immunity* **27**, 670–684 (2007).

31. Angelosanto, J. M., Blackburn, S. D., Crawford, A. & Wherry, E. J. Progressive loss of memory T cell potential and commitment to exhaustion during chronic viral infection. *Journal of Virology* **86**, 8161–8170 (2012).

32. Speiser, D. E. *et al.* T cell differentiation in chronic infection and cancer: Functional adaptation or exhaustion? *Nature Reviews Immunology* **14**, 768–774 (2014).

33. Paley, M. A. *et al.* Progenitor and Terminal Subsets of CD8+ T Cells Cooperate to Contain Chronic Viral Infection. *Science* **338**, 1220–1225 (2012).

34. Utzschneider, D. T. *et al.* T cells maintain an exhausted phenotype after antigen withdrawal and population reexpansion. *Nature Immunology* **14**, 603–610 (2013).

35. Utzschneider, D. T. *et al.* T Cell Factor 1-expressing memory-like CD8+T cells sustain the immune response to chronic viral infections. *Immunity* **45**, 415–427 (2016).

36. Wu, T. *et al.* The TCF1-Bcl6 axis counteracts type I interferon to repress exhaustion and maintain T cell stemness. *Sci Immunol* **1**, eaai8593 (2016).

37. He, R. *et al.* Follicular CXCR5-expressing CD8+ T cells curtail chronic viral infection. *Nature* **537**, 412–416 (2016).

38. Im, S. J. *et al.* Defining CD8+ T cells that provide the proliferative burst after PD-1 therapy. *Nature* **537**, 417–421 (2016).

39. Yao, C. *et al.* Single-cell RNA-seq reveals TOX as a key regulator of CD8+ T cell persistence in chronic infection. *Nature Immunology* **20**, 890–901 (2019).

40. Chen, Z. *et al.* TCF-1-Centered Transcriptional Network Drives an Effector versus Exhausted CD8 T Cell-Fate Decision. *Immunity* **51**, 840–855 (2019).

41. Shan, Q. *et al.* Ectopic Tcf1 expression instills a stem-like program in exhausted CD8+ T cells to enhance viral and tumor immunity. *Cellular & Molecular Immunology* (2020) doi:10.1038/s41423-020-0436-5.

42. Utzschneider, D. T. *et al.* High antigen levels induce an exhausted phenotype in a chronic infection without impairing T cell expansion and survival. *Journal of Experimental Medicine* **213**, 1819–1834 (2016).

43. Hudson, W. H. *et al.* Proliferating Transitory T Cells with an Effector-like Transcriptional Signature Emerge from PD-1+ Stem-like CD8+ T Cells during Chronic Infection. *Immunity* **51**, 1043–1058 (2019).

44. Beltra, J.-C. *et al.* Developmental relationships of four exhausted CD8+ T Cell subsets reveals underlying transcriptional and epigenetic landscape control mechanisms. *Immunity* **52**, 825–841 (2020).

45. Jadhav, R. R. *et al.* Epigenetic signature of PD-1+ TCF1+ CD8 T cells that act as resource cells during chronic viral infection and respond to PD-1 blockade. *Proceedings of the National Academy of Sciences of the United States of America* **116**, 14113–14118 (2019).

46. Miller, B. C. *et al.* Subsets of exhausted CD8+ T cells differentially mediate tumor control and respond to checkpoint blockade. *Nature Immunology* **20**, 326–336 (2019).

47. Khan, O. *et al.* TOX transcriptionally and epigenetically programs CD8+ T cell exhaustion. *Nature* **571**, 211–218 (2019).

48. Scott, A. C. *et al.* TOX is a critical regulator of tumour-specific T cell differentiation. *Nature* vol. 571 270–274 Preprint at https://doi.org/10.1038/s41586-019-1324-y (2019).

49. Alfei, F. *et al.* TOX reinforces the phenotype and longevity of exhausted T cells in chronic viral infection. *Nature* **571**, 265–269 (2019).

50. Seo, H. *et al.* TOX and TOX2 transcription factors cooperate with NR4A transcription factors to impose CD8+ T cell exhaustion. *Proceedings of the National Academy of Sciences of the United States of America* **116**, 12410–12415 (2019).

51. Leong, Y. A. *et al.* CXCR5+ follicular cytotoxic T cells control viral infection in B cell follicles. *Nature Immunology* **17**, 1187–1196 (2016).

52. Jiang, H. *et al.* CXCR5+CD8+T cells indirectly offer B cell help and are inversely correlated with viral load in chronic hepatitis B infection. *DNA and Cell Biology* **36**, 321–327 (2017).

53. Youngblood, B. *et al.* Chronic virus infection enforces demethylation of the locus that encodes PD-1 in antigen-specific CD8+ T cells. *Immunity* **35**, 400–412 (2011).

54. Sen, D. R. *et al.* The epigenetic landscape of T cell exhaustion. *Science* **354**, 1165–1169 (2016).

55. Pauken, K. E. *et al.* Epigenetic stability of exhausted T cells limits durability of reinvigoration by PD-1 blockade. *Science* **354**, 1160–1165 (2016).

56. Ghoneim, H. E. *et al.* De Novo Epigenetic Programs Inhibit PD-1 Blockade-Mediated T Cell Rejuvenation. *Cell* **170**, 142–157 (2017).

57. Matloubian, M., Concepcion, R. J. & Ahmed, R. CD4+ T cells are required to sustain CD8+ cytotoxic T-cell responses during chronic viral infection. *J Virol* **68**, 8056–8063 (1994).

58. Snell, L. M. *et al.* CD8+ T Cell Priming in Established Chronic Viral Infection Preferentially Directs Differentiation of Memory-like Cells for Sustained Immunity. *Immunity* **49**, 678–694 (2018).

59. Kanev, K. *et al.* Proliferation-competent Tcf1+ CD8 T cells in dysfunctional populations are CD4 T cell help independent. *Proceedings of the National Academy of Sciences of the United States of America* **116**, 20070–20076 (2019).

60. Oosterhuis, K., Aleyd, E., Vrijland, K., Schumacher, T. N. & Haanen, J. B. Rational Design of DNA Vaccines for the Induction of Human Papillomavirus Type 16 E6-and E7-Specific Cytotoxic T-Cell Responses. *Hum Gene Ther* **23**, 3001–1312 (2012).

61. Schietinger, A. *et al.* Tumor-specific T cell dysfunction is a dynamic antigen-driven differentiation program initiated early during tumorigenesis. *Immunity* **45**, 389–401 (2016).

62. Philip, M. *et al.* Chromatin states define tumour-specific T cell dysfunction and reprogramming. *Nature* **545**, 452–456 (2017).

63. Brummelman, J. *et al.* High-dimensional single cell analysis identifies stem-like cytotoxic CD8+ T cells infiltrating human tumors. *The Journal of experimental medicine* **215**, 2520–2535 (2018).

64. Jansen, C. S. *et al.* An intra-tumoral niche maintains and differentiates stem-like CD8 T cells. *Nature* **576**, 465–470 (2019).

65. Li, H. *et al.* Dysfunctional CD8 T cells form a proliferative, dynamically regulated compartment within human melanoma. *Cell* **176**, 775–789 (2019).

66. Guo, X. *et al.* Global characterization of T cells in non-small-cell lung cancer by single-cell sequencing. *Nature Medicine* **24**, 978–985 (2018).

67. Zhang, L. *et al.* Lineage tracking reveals dynamic relationships of T cells in colorectal cancer. *Nature* **564**, 268–272 (2018).

68. Zheng, C. *et al.* Landscape of infiltrating T cells in liver cancer revealed by single-cell sequencing. *Cell* **169**, 1342–1356 (2017).

69. van der Leun, A. M., Thommen, D. S. & Schumacher, T. N. CD8+ T cell states in human cancer: insights from single-cell analysis. *Nature Reviews Cancer* **20**, 218–232 (2020).

70. Scheper, W. *et al.* Low and variable tumor reactivity of the intratumoral TCR repertoire in human cancers. *Nature Medicine* **25**, 89–94 (2019).

71. Simoni, Y. *et al.* Bystander CD8+ T cells are abundant and phenotypically distinct in human tumour infiltrates. *Nature* **557**, 575–579 (2018).

72. Siddiqui, I. *et al.* Intratumoral Tcf1+PD-1+CD8+ T cells with stem-like properties promote tumor control in response to vaccination and checkpoint blockade immunotherapy. *Immunity* **50**, 195–211 (2019).

73. Kurtulus, S. *et al.* Checkpoint blockade immunotherapy induces dynamic changes in PD-1 – CD8 + tumor-infiltrating T cells. *Immunity* **50**, 181–194 (2019).

74. Sade-Feldman, M. *et al.* Defining T cell states associated with response to checkpoint immunotherapy in melanoma. *Cell* **175**, 998–1013 (2018).

75. Gerner, M., Casey, K. A., Kastenmuller, W. & Germain, R. N. Dendritic cell and antigen dispersal landscapes regulate T cell immunity. *Journal of Experimental Medicine* **214**, 3105–3122 (2017).

76. Binnewies, M. *et al.* Unleashing Type-2 Dendritic Cells to Drive Protective Antitumor CD4+ T Cell Immunity. *Cell* **177**, 556–571 (2019).

77. Gros, A. *et al.* Prospective identification of neoantigen-specific lymphocytes in the peripheral blood of melanoma patients. *Nature Medicine* **22**, 433–438 (2016).

78. Thommen, D. S. *et al.* A transcriptionally and functionally distinct PD-1+ CD8+ T cell pool with predictive potential in non-small-cell lung cancer treated with PD-1 blockade. *Nature Medicine* **24**, 994–1004 (2018).

79. Restifo, N. P. & Gattinoni, L. Lineage relationship of effector and memory T cells. *Curr Opin Immunol* **25**, 556–563 (2013).

80. Kim, J. *et al.* Memory programming in CD8+ T-cell differentiation is intrinsic and is not determined by CD4 help. *Nat Commun* **6**, 7994 (2015).

81. Li, Y. *et al.* Persistent antigen and prolonged AKT–mTORC1 activation underlie memory CD8 T cell impairment in the absence of CD4 T cells. *The Journal of Immunology* **195**, 1591–1598 (2015).

82. Northrop, J. K., Wells, A. D. & Shen, H. Cutting Edge: Chromatin remodeling as a molecular basis for the enhanced functionality of memory CD8 T cells. *The Journal of Immunology* **181**, 865–868 (2008).

83. Northrop, J. K., Thomas, R. M., Wells, A. D. & Shen, H. Epigenetic remodeling of the IL-2 and IFN-gamma loci in memory CD8 T cells is influenced by CD4 T cells. *J Immunol* **177**, 1062–9 (2006).

84. Cullen, J. G. *et al.* CD4+ T help promotes influenza virus-specific CD8+ T cell memory by limiting metabolic dysfunction. *Proc Natl Acad Sci U S A* **116**, 4481–4488 (2019).

85. Philip, M. & Schietinger, A. Heterogeneity and fate choice: T cell exhaustion in cancer and chronic infections. *Curr Opin Immunol* **58**, 98–103 (2019).

86. Kallies, A., Zehn, D. & Utzschneider, D. T. Precursor exhausted T cells: key to successful immunotherapy? *Nature Reviews Immunology* vol. 20 128–136 Preprint at https://doi.org/10.1038/s41577-019-0223-7 (2020).

87. Mann, T. H. & Kaech, S. M. Tick-TOX, it's time for T cell exhaustion. *Nature Immunology* **20**, 1090–1099 (2019).

88. Chen, D. S. & Mellman, I. Elements of cancer immunity and the cancer-immune set point. *Nature* **541**, 321–330 (2017).

89. Hui, E. *et al.* T cell costimulatory receptor CD28 is a primary target for PD-1-mediated inhibition. *Science* **355**, 1428–1433 (2017).

90. Kamphorst, A. O. *et al.* Rescue of exhausted CD8 T cells by PD-1–targeted therapies is CD28-dependent. *Science* **355**, 1423–1427 (2017).

91. Fransen, M. F. *et al.* Tumor-draining lymph nodes are pivotal in PD-1/PD-L1 checkpoint therapy. *JCI Insight* **3**, e124507 (2018).

92. Yost, K. E. *et al.* Clonal replacement of tumor-specific T cells following PD-1 blockade. *Nature Medicine* **25**, 1251–1259 (2019).

93. Wu, T. D. *et al.* Peripheral T cell expansion predicts tumour infiltration and clinical response. *Nature* **579**, 274–278 (2020).

94. Ahn, E. *et al.* Role of PD-1 during effector CD8 T cell differentiation. *Proceedings of the National Academy of Sciences* **115**, 4749–4754 (2018).

95. Ahrends, T. *et al.* CD27 Agonism Plus PD-1 Blockade Recapitulates CD4+ T-cell Help in Therapeutic Anticancer Vaccination. *Cancer Res* **76**, 2921–2931 (2016).

96. Kim, D., Langmead, B. & Salzberg, S. L. HISAT: A fast spliced aligner with low memory requirements. *Nature Methods* **12**, 357–360 (2015).

97. Liao, Y., Smyth, G. K. & Shi, W. FeatureCounts: an efficient general purpose program for assigning sequence reads to genomic features. *Bioinformatics* **30**, 923–930 (2014).

98. Robinson, M. D., McCarthy, D. J. & Smyth, G. K. edgeR: A Bioconductor package for differential expression analysis of digital gene expression data. *Bioinformatics* **26**, 139–140 (2010).

99. Yu, D. & Ye, L. A portrait of CXCR5+ follicular cytotoxic CD8+ T cells. *Trends in Immunology* **39**, 965–979 (2018)

Chapter 4

Stem-like PD-1$^+$TCF-1$^+$ CD8$^+$ T cells result from helpless priming and rely on CD4$^+$ T-cell help to complete their cytotoxic effector differentiation

Julia Busselaar[1]*, Douwe M. T. Bosma[1]*, Mo D. Staal[1], Xin Lei[1], Yanling Xiao[1] and Jannie Borst[1]

[1]Department of Immunology and Oncode Institute, Leiden University Medical Center, Leiden, The Netherlands
*Shared first authors

The Journal of Immunotherapy of Cancer 2026; 14(4): e014041
DOI: 10.1136/jitc-2025-014041

Abstract

Antigen-specific CD8$^+$ T cells can be in a stem-like PD-1$^+$TCF-1$^+$ differentiation state that progresses into terminal exhaustion in cancer and chronic infection. These stem-like cells are important, since they are the responders to PD-1 targeted immunotherapy and a potential resource for anti-tumor immunity. We use a mouse vaccination model to delineate by spectral flow cytometry and single cell RNA sequencing the effects of CD4$^+$ T-cell help during priming on the differentiation fate of stem-like CD8$^+$ T cells. We use bioinformatic analysis to extrapolate our data to mouse models of cancer and chronic infection. We next explore CD8$^+$ T-cell differentiation states and delivery of CD4$^+$ T-cell help in the immunogenic MC38 tumor model. Upon vaccination in absence of help signals, stem-like CD8$^+$ T cells do not further differentiate and accumulate in the draining lymph node. When help signals are delivered, stem-like CD8$^+$ T cells proliferate and differentiate into circulating cytotoxic effector cells. Stem-like CD8$^+$ T cells raised by vaccination in presence or absence of CD4$^+$ T-cell help have an identical transcriptome, which they share with stem-like CD8$^+$ T cells defined in mouse models of cancer and chronic infection. The immunogenic MC38 tumor harbors endogenous helper epitopes, but primes stem-like CD8$^+$ T cells rather than helped cytotoxic effectors. Therapeutic vaccination with endogenous helper epitopes does not improve MC38 tumor control. Intra-tumoral expression of strong, exogenous helper epitopes as present in our vaccine improves tumor control, but does not efficiently convert stem-like tumor-specific CD8$^+$ T cells into helped cytotoxic effectors. Our data argue that stem-like CD8$^+$ T cells are helpless cells that lie at the bifurcation point of CD8$^+$ T-cell effector- and exhaustion trajectories. Even though the immunogenic MC38 tumor expresses helper epitopes, it primarily raises stem-like CD8$^+$ T cells, indicating that help delivery is impaired in this tumor context. Promoting the efficient delivery of help signals to stem-like tumor-specific CD8$^+$ T cells to drive their expansion and differentiation into cytotoxic effectors is therefore an important therapeutic challenge in cancer and other conditions that lead to T-cell exhaustion.

Introduction

In a CTL response that results in antigen clearance, differentiation of newly activated CD8+ T cells is described as a trajectory ranging from the naïve state, via central memory (T_{CM}) and effector memory (T_{EM}) precursor states to a terminally differentiated effector CTL state[1,2]. When antigen persists, such as in chronic infection and cancer, CD8+ T cells differentiate along an exhaustion trajectory, characterized by poor cytolytic function and expression of coinhibitory receptors, including PD-1[3]. "Stem-like", "(pre)dysfunctional" or "progenitor exhausted (Tpex)" cells lie early in this trajectory, marked by co-expression of transcription factor TCF-1 and PD-1, next to CXCR5 and SLAMF6[4,5]. Stem-like CD8+ T cells are of interest, since they respond to PD-1-targeted immune checkpoint blockade (ICB) to generate functional CTLs in mouse models and are associated with ICB response in human cancer[6]. Recent meta-analyses of mRNA- and TCR sequencing (seq) datasets have mapped stem-like CD8+ T cells at the branchpoint of differentiation trajectories towards either the functional CTL effector state or the terminally exhausted state[7,8]. Stem-like cells are formed during both acute and chronic infection, consistent with the concept that they can differentiate into either cell state[9,10]. To improve immunotherapy strategies, it is crucial to know how stem-like CD8+ T cells can be instructed to become competent CTL effectors[3,6].

We here test the hypothesis that stem-like CD8+ T cells lie on a potentially productive CTL effector differentiation trajectory that can be completed when CD4+ T-cell help signals are provided[11]. During priming in lymph nodes (LNs), CD4+ T cells can deliver "help" for the CTL response, via conventional (c) dendritic cells (DCs). CD4+ and CD8+ T cells are initially activated separately, in distinct regions of the LN by migratory cDCs. When conditions permit, activated CD4+ and CD8+ T cells are subsequently guided by chemokine cues to recognize their respective antigens on the same cDC1[12]. In this cellular scenario, help for the CTL response is delivered[13,14]. The CD4+ T cell "licenses" the cDC1 to relay help signals to CD8+ T cells, by endowing it with optimal antigen cross-presentation and cross-priming capacity, which is facilitated by costimulatory molecules such as CD70, as well as specific cytokines and chemokines[15–19]. Help signals instruct the CD8+ T cell to acquire optimal CTL effector[20] and effector memory[21] differentiation programs, hallmarked in the primary effector phase by downregulation of inhibitory receptors and increased cytotoxic, migratory and invasive capacities, which are pivotal for tumor control[20]. Conversely, "helpless" CTLs, i.e. CD8+ T cells primed in absence of CD4+ T-cell help, have all the typical hallmarks of CTL dysfunction[11,20,22].

Inflammatory signals, in particular IFN-I, make a key contribution to cDC1 licensing[17,23]. IFN-I acts in synergy with CD4+ T-cell mediated CD40 signaling to induce the gene expression program of the licensed cDC1[19]. Innate signaling by IFN-I as elicited e.g. by virus infections often seems to compensate for CD4+ T-cell help in the primary CTL response, but help is generally required for generation of adequate CD8+ T-cell memory[14,24]. This conundrum has recently been solved by the finding that CD4+ T-cell help does improve the primary CTL response to virus infection, but

this contribution is obscured when conventional and regulatory CD4$^+$ T cells are co-depleted to eliminate "help"[25]. In chronic LCMV infection, CD4$^+$ T-cell depletion promotes CD8$^+$ T-cell exhaustion[26] and reduces formation of virus-controlling effector CTLs, but not stem-like cells[27,28]. These data suggest that lack of help promotes CD8$^+$ T-cell differentiation along the exhaustion trajectory when antigen persists.

Based on these concepts, we have postulated that stem-like cells as found in chronic infection and cancer may result from helpless priming[11]. Here, we tested the impact of CD4$^+$ T-cell help on formation and fate of stem-like CD8$^+$ T cells in a well-defined vaccination model, in which we previously determined at the molecular level how CD4$^+$ T-cell help improves function of CD8$^+$ T-cell effector and effector memory cells[20,21]. We demonstrate that PD-1$^+$TCF-1$^+$ stem-like CD8$^+$ T cells lie on a potentially productive effector differentiation trajectory that is completed in non-tumor-bearing mice when help signals are delivered by vaccination. However, in an immunogenic MC38 tumor context, help delivery and CTL effector differentiation are impaired, both before and after therapeutic vaccination, even when a CD4$^+$ T-cell response to tumor-intrinsic epitopes takes place.

Results

Stem-like CD8$^+$ T cells predominate after priming in absence of CD4$^+$ T-cell help

To compare CD8$^+$ T-cell responses in presence or absence of CD4$^+$ T-cell help, we use two DNA vaccines: one encoding the immunodominant E7$_{48\text{-}57}$ peptide of human papilloma virus (HPV) that only primes E7-specific CD8$^+$ T cells (No Help) and one additionally encoding HPV-unrelated MHC-II restricted helper epitopes P30/PADRE that also primes CD4$^+$ T cells[29,30] (Help) (Figure 1A). The plasmid DNA is "tattooed" into the epidermis, resulting in antigen expression in keratinocytes and efficient T-cell priming by migratory cDCs in the skin-draining inguinal LN[29,31]. Mice are vaccinated at day 0, 3 and 6, after which the antigen-specific CD8$^+$ T-cell response is followed by H-2D^b/E7$_{48\text{-}57}$ (E7) tetramer staining (Supplementary Figure 1A-C). In this transparent model, antigen is only transiently present during priming[31,32] and the impact of CD4$^+$ T cells during priming on long-term CD8$^+$ T-cell fate is tested by their vaccine-based engagement in the response[29,30].

As previously shown[20,29], the E7-specific CD8$^+$ T-cell response to No Help vaccination was lower and of shorter duration than the response to Help vaccination (Figure 1B) and at day 10, the frequency of E7-specific CD8$^+$ T cells was significantly lower in the No Help setting than in the Help setting in blood and spleen (Figure 1C). Moreover, in the No Help setting PD-1, TCF-1 and SLAMF6 that identify the stem-like state[6,28,33] were expressed at higher levels on E7-specific CD8$^+$ T cells in the dLN, which is the priming site (Figure 1D).

An extensive antibody panel was used to distinguish E7-specific CD8+ T-cell differentiation states[2,34] after Help or No Help vaccination in blood, spleen, dLN and ndLN. At day 10 after vaccination, clustering analysis and dimension reduction on cumulative E7-tetramer+ CD8+ T cells resulted in 10 clusters (Figure 1E), which were differentially distributed between vaccination settings (Figure 1F, Supplementary Figure 1D) and between organs (Supplementary Figure 1D, E). Cluster 1 cells were higher in frequency among tetramer+ CD8+ T cells (Figure 1G) and total CD8+ T cells (Supplementary Figure 1F) after Help than after No Help vaccination and were mostly found in the circulation, i.e. in blood and spleen**.** Cluster 1 cells were characterized by low expression of CD62L and TCF-1 and high expression of KLRG1 and CX3CR1 (Figure 1H), consistent with a terminally differentiated, short-lived effector CTL state[35,36]. In LNs, Cluster 6 cells were higher in frequency among tetramer+ CD8+ T cells (Figure 1I) and total CD8+ T cells (Supplementary Figure 1F) in the No Help setting than in the Help setting and characterized by high levels of TCF-1, SLAMF6 and PD-1 and low levels of KLRG1 and CX3CR1 (Figure 1H), indicating the stem-like phenotype[6,28,33]. Consistent with vaccination rather than chronic antigen exposure, exhausted CD8+ T cells with a PD-1^{high}TIM3+TCF-1- phenotype[4] were not observed (Supplementary Figure 1G). These results indicate that in presence of CD4+ T-cell help during priming, CD8+ T cells can terminally differentiate into CTL effector cells that distribute systemically through blood and spleen. In absence of CD4+ T-cell help, primed CD8+ T cells accumulate in the PD-1+TCF-1+ stem-like state in LNs.

CD4+ T-cell help shifts the CD8+ T-cell differentiation spectrum towards the effector state

To analyze the effects of CD4+ T-cell help on the CTL differentiation spectrum, we mapped the antigen-specific CD8+ T-cell clusters as defined in Figure 1 using the Wanderlust algorithm that aligns cells to a unified trajectory based on overlap in marker expression[37]. This procedure generated a CTL differentiation trajectory ranging from the naïve state (CD44-CD62L+) to the short-lived effector state (KLRG1+CX3CR1+) (Figure 2A). After Help vaccination, CD8+ T cells in dLN, spleen and blood had a higher mean trajectory score than after No Help vaccination (Figure 2B), indicating that on average, CD4+ T-cell help shifts the differentiation state of CD8+ T cells towards completion of the trajectory.

To visualize the calculated trajectory along the progressive differentiation path as described in literature[1,2,34], we mapped protein expression of differentiation markers of naïve (CD44-CD62L+TCF-1+), T stem cell memory (T_{SCM})/T_{CM} precursor (CD44+CD62L+TCF-1+), stem-like (PD-1+TCF-1+SLAMF6+), T_{EM} precursor (CD44+CD62L-) and effector (KLRG1+CX3CR1+) cell states against the trajectory (Figure 2C, Supplementary Figure 2). PD-1 and SLAMF6 were upregulated halfway through the trajectory, in CD8+ T cells that retained TCF-1 expression, corroborating that PD-1+TCF-1+SLAMF6+ stem-like cells are in an early differentiation state. These cells highly expressed proliferation marker Ki67, in agreement with literature data[33,38,39]. Further differentiation along the trajectory towards effector cells was associated with downregulation of PD-1, TCF-1 and SLAMF6 and upregulation of CX3CR1 and KLRG1 (Figure 2C).

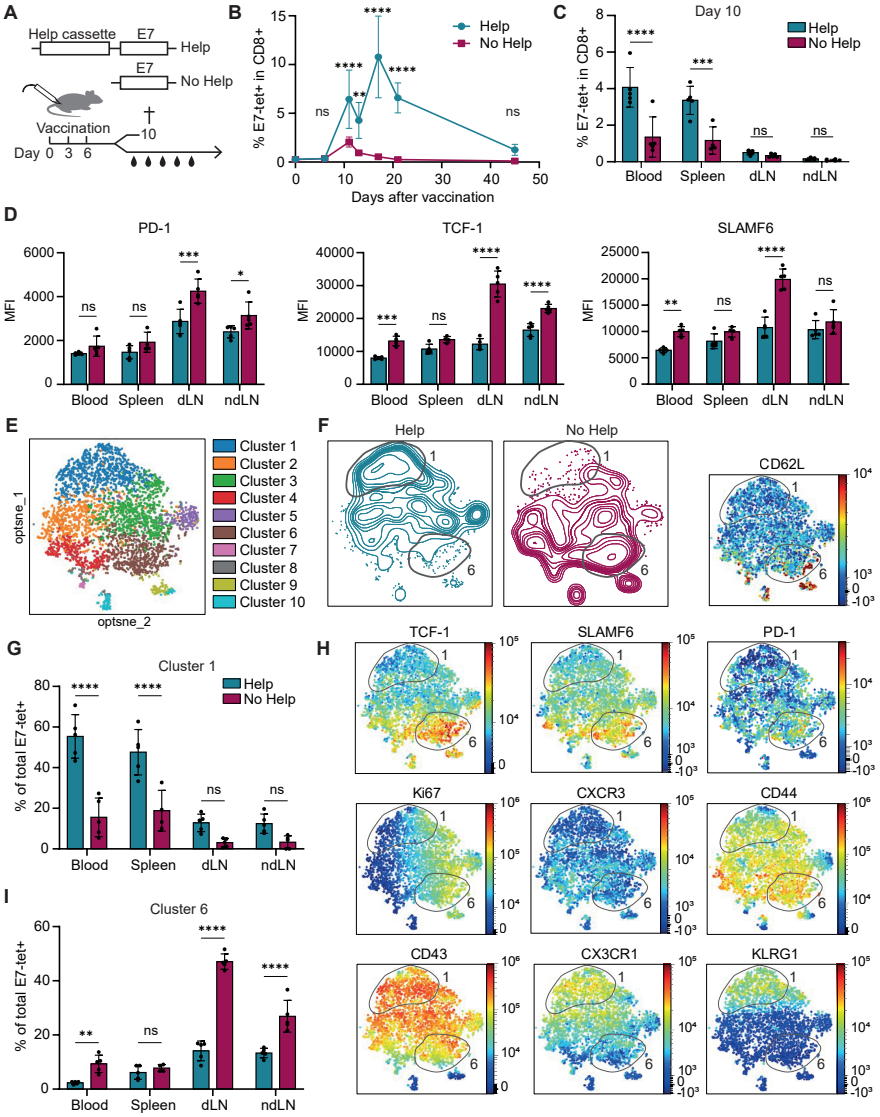

Figure 1. Stem-like CD8⁺ T cells predominate after priming in absence of CD4⁺ T-cell help. (A) Vaccination model. (B-I) The response of E7-tetramer⁺ CD8⁺ T cells to vaccination was analyzed by flow cytometry with antibodies to differentiation markers. (B, C) Percentage of E7-tetramer⁺ CD8⁺ T cells in indicated organs at the indicated days after the first vaccination. (D) Median Fluorescence Intensity (MFI) of indicated markers on E7-tetramer⁺ CD8⁺ T cells at day 10. (E, F) Opt-SNE visualization of E7-tetramer⁺ CD8⁺ T cells at day 10. FlowSom clustering of cells from all experimental settings (E) and distribution of cells from the two vaccination settings (F). Clusters 1 and 6 are encircled. (G, I) Frequencies of E7-tetramer⁺ CD8⁺ T cells in Cluster 1 (G) and Cluster 6 (I) per organ. (H) Differentiation marker expression on cumulative E7-tetramer⁺ CD8⁺ T cells from all experimental settings visualized by opt-SNE. Data are from 1 experiment, representative of at least 2 independent experiments with n=5 mice per group. Error bars indicate SD. Statistical significance was calculated by two-way ANOVA and Sidak's multiple comparisons test. ns, not significant, *P < 0.05, **P <0.005, ***P < 0.001 and ****P < 0.0001. See also Supplementary Figure 1.

Next, we plotted antigen-specific CD8+ T cells, harvested from blood, spleen and LNs after Help or No Help vaccination, against this differentiation spectrum based on their trajectory score (Figure 2D). Blood and spleen harbored cells with a high trajectory score of 0.8-1.0 (Figure 2D), corresponding to a KLRG1+CX3CR1+ phenotype (Figure 2C) after Help vaccination, while this population was much smaller after No Help vaccination. In LNs, cells had a lower trajectory score ranging from 0.3 to 0.8 (Figure 2B, D), predominated by the PD-1+TCF-1+SLAMF6+ phenotype (Figure 2C), both after Help and No Help vaccination. However, after Help vaccination, the LN cells had differentiated further than after No Help vaccination (Figure 2B, D).

We conclude that antigen-primed CD8+ T cells can differentiate into CD44+CD62L+ T_{CM} precursor and PD-1+TCF-1+SLAMF6+ stem-like populations irrespective of CD4+ T-cell help, but require CD4+ T-cell help to become CD44+CD62L- T_{EM} precursor and KLRG1+CX3CR1+ short-lived CTL effector cells.

Stem-like CD8+ T cells turn into effector cells upon receiving CD4+ T-cell help

If stem-like CD8+ T cells are indeed incompletely differentiated, one would expect them to arise earlier after priming than help-dependent effector CTLs. To test this assumption, we vaccinated mice under Help or No Help conditions and analyzed antigen-specific CD8+ T cells in the dLN at multiple successive days after the first vaccination (Figure 3A). After Help vaccination, E7-specific CD8+ T cells strongly increased in number from day 6 onwards, while after No Help vaccination the response was lower and more belated (Figure 3B). To exclude background tetramer staining of naïve CD8+ T cells, especially at early time points, we only included clusters that increased in size after vaccination (Supplementary Figure 3). Clustering and dimension reduction of cumulative responding CD8+ T cells indicated distinct phenotypes in Help and No Help settings, as expected (Figure 3C). We dissected responder CD8+ T cells into stem-like (TCF-1+SLAMF6+) and effector (GZMB+) subsets (Figure 3D, E) and analyzed the generation of these two populations over time. After Help vaccination, the stem-like population initially predominated, but from day 6 onwards it decreased, while the effector population increased (Figure 3F). After No Help vaccination, in contrast, the stem-like population steadily increased to form the majority of the E7-specific CD8+ T-cell pool in the dLN, while the effector cell population remained small (Figure 3G). These results indicate that stem-like CD8+ T cells are generated early after priming, in both presence and absence of CD4+ T-cell help. However, only in presence of CD4+ T-cell help, these cells in time further differentiate into effector CTLs.

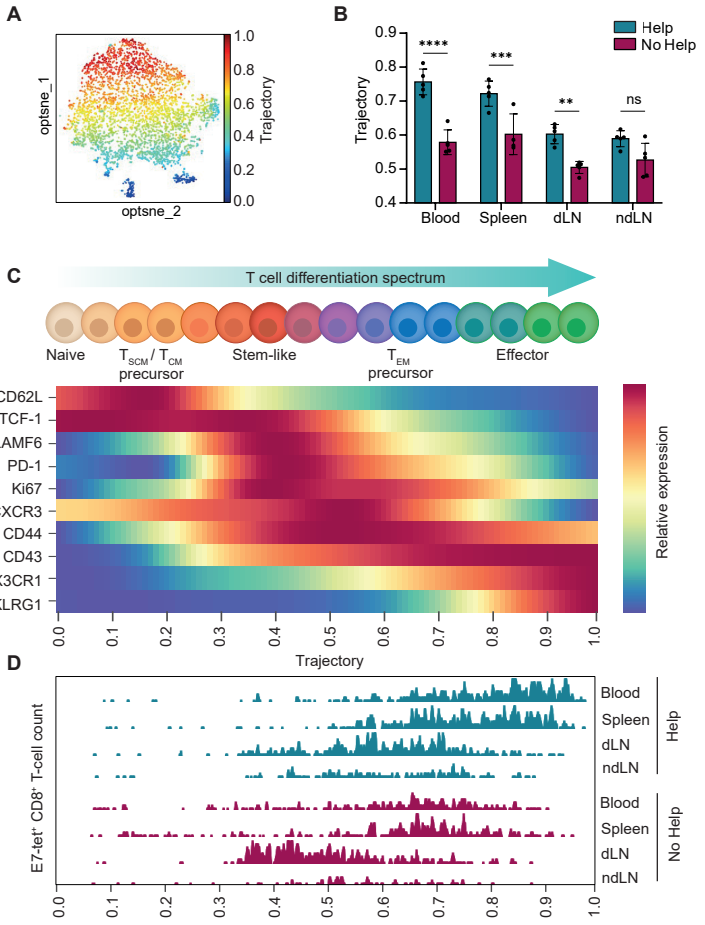

Figure 2. CD4⁺ T-cell help shifts the CD8⁺ T-cell differentiation spectrum towards the effector state. Mice were vaccinated and analyzed at day 10 as outlined in Figure 1 (same experiment). (A) Wanderlust trajectory shown as color gradient within opt-SNE visualization of all E7-tetramer⁺ CD8⁺ T cells from all organs. (B) Mean trajectory score of E7-tetramer⁺ CD8⁺ T cells from indicated organs. (C) CD8⁺ T-cell differentiation states as defined in literature were mapped to the trajectory axis based on marker expression. Heat map shows relative expression level of differentiation markers on E7-tetramer⁺ CD8⁺ T cells, as determined per marker on lowest and highest level observed. (D) Distribution of E7-tetramer⁺ CD8⁺ T cells from indicated organs after Help or No Help vaccination along the differentiation trajectory. Data are from 1 experiment, representative of 2 independent experiments with n=5 mice per group. Error bars indicate SD. Statistical significance was calculated by two-way ANOVA and Sidak's multiple comparisons test. ns, not significant, *P < 0.05, **P< 0.005, ***P < 0.001 and ****P <0.0001. See also Supplementary Figure 2.

It is an important question whether stem-like CD8+ T cells primed in absence of CD4+ T-cell help can still complete their effector differentiation when help signals are delivered after priming. To test this, we used adoptive transfer with OT-I T cells that express a transgenic TCR recognizing the ovalbumin $(OVA)_{257/264}$/H-2K^b complex (Figure 3H). CD45.2+ mice received 10^5 naïve CD45.1+ OT-I cells and OVA-No Help vaccine encoding the $OVA_{257/264}$ epitope. At day 10, CD45.1+CD44+SLAMF6+ stem-like OT-I cells were flow sorted from pooled dLNs (Supplementary Figure 4A) and transferred at 10^4 per mouse into CD45.2+ secondary recipient mice. The next day, so still in the effector phase of the response, these mice received either control OVA-No Help or test OVA-Help vaccine with the same helper epitopes as in the E7 Help vaccine. The vaccine encoded both helper and CTL epitopes to enable communication between CD4+ T cells and CD8+ T cells at the cDC1 interface[13,14]. Transferred stem-like OT-I T cells clonally expanded upon OVA-Help vaccination, but not upon OVA-No Help vaccination (Figure 3I, J, Supplementary Figure 4B). After Help vaccination, a proportion of the transferred OT-I T cells gained the help-dependent KLRG1+CX3CR1+ effector phenotype as compared to the OT-I population at transfer (Figure 3K, L, Supplementary Figure 4C), primarily in blood and spleen (Figure 3M). Together, these results demonstrate that helpless stem-like CD8+ T cells can still respond to help signals after initial priming by expansion, CTL effector differentiation and systemic dissemination.

Combined scRNAseq and TCRseq analyses support that stem-like CD8+ T cells differentiate into CTL effectors upon CD4+ T-cell help delivery

To test directly whether addition of CD4+ T-cell help signals leads to the transition of stem-like CD8+ T cells into effector CTLs, we performed single cell RNA sequencing (scRNAseq) and TCR sequencing (TCRseq). For this purpose, mice received E7-Help or E7-No Help vaccine and at day 5 or day 10, activated CD3+CD44+CD62L- T cells were sorted by flow cytometry from both dLN and ndLN (Supplementary Figure 5). This resulted in eight samples that were labeled with distinct hashtag oligonucleotides (HTO)-conjugated antibodies before performing scRNAseq and TCRseq on pooled cells (Supplementary Figure 6A, B). For analysis, we used CD8+ T cells isolated from dLNs at days 5 and 10 after Help vaccination and at day 10 after No Help vaccination, since these HTO groups yielded sufficient CD8+ T-cell numbers as identified based on *Cd8a* and *Cd8b1* expression (Supplementary Figure 6C, D).

Whole transcriptome-based clustering of 3051 CD8+ T cells pooled from these three experimental conditions identified seven distinct cell states (Figure 4A), based on specific transcripts (Supplementary Table 1). Naive cells (Cluster 0) and T_{CM} cells (Cluster 1) were identified by co-expression of *Sell* (encoding CD62L), *Il7r* and *Ly6c2*, while naive cells expressed higher levels of *Lef1* and *Ccr7* and T_{CM} cells expressed *Eomes* (Figure 4B). Stem-like cells (Cluster 2) were identified by high expression of *Tcf7* (encoding TCF-1), *Id3* and *Slamf6,* next to *Sell*, *Lef1* and *Ccr7*. CTL effector cells (Cluster 3) were characterized by expression of *Gzmb*, *Gzmk*, *Id2* and *Tbx21* (encoding T-bet), and expressed various killer lectin receptor (KLR) genes such as *Klrc1* and *Klrk1* and proliferation-associated genes including *Mki67, Tk1 and Kif11*. Some smaller clusters were characterized by expression of KLRs (Cluster 4), protein/RNA biosynthesis genes (Cluster 5), and IFN-I responsive genes (Cluster 6).

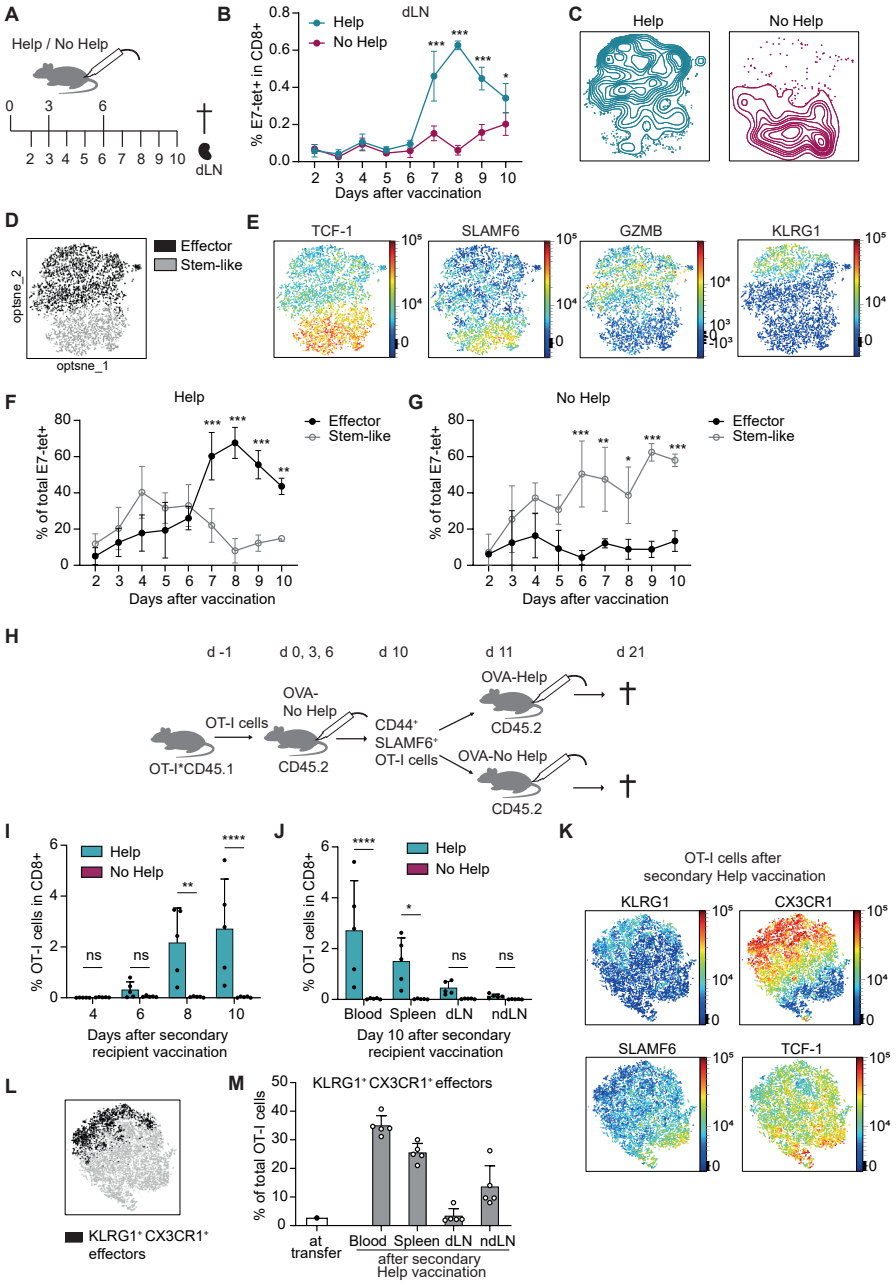

Figure 3. Formation of effector but not stem-like CD8⁺ T cells relies on CD4⁺ T-cell help. (A) Experimental setup for panels B-G. At different time points after Help or No Help vaccination, E7-specific CD8⁺ T cells in the dLN were analyzed by flow cytometry with the differentiation marker panel. (B) Frequency of E7-tetramer⁺ CD8⁺ T cells in dLNs. (C-E) Opt-SNE visualization of all responding E7-tetramer⁺ CD8⁺ T cells (see Supplementary Figure 3) in the dLN at all time points. (C) Distribution of responder CD8⁺ T cells from Help versus No

Help vaccination settings. (D) Visualization of stem-like (TCF-1+SLAMF6+) and effector (GZMB+) clusters. (E) Visualization of differentiation marker expression. (F, G) Frequency of stem-like and effector populations as defined in C-E within total responder E7-tetramer+ CD8+ T cells. (H) Experimental setup for panels I-M. (I, J) Frequency of OT-I (CD45.1+OVA-tetramer+ CD8+) T cells in secondary recipients, as measured in indicated organs at indicated time points. (K, L) Opt-SNE visualization of OT-I T cells in secondary recipients at day 10 after Help vaccination. (K) Expression of differentiation markers across opt-SNE. (L) Visualization of the KLRG1+CX3CR1+ effector population. (M) Frequency of KLRG1+CX3CR1+ effector cells (as defined in L) within the OT-I T cell population in indicated organs after secondary Help vaccination, and frequency of KLRG1+CX3CR1+ cells in the pooled OT-I population at transfer (as identified by manual gating). Data from B-G and I-M are each from 1 experiment, representative of 2 independent experiments with n=3-5 mice per group. Error bars indicate SD. Statistical significance was calculated by two-way ANOVA and Sidak's multiple comparisons test. ns, not significant, *P < 0.05, **P < 0.005, ***P < 0.001 and ****P < 0.0001. See also Supplementary Figure 3 and 4.

Clonal expansion within each CD8+ T-cell cluster was assessed by TCRseq analysis. Expanded clones, defined as TCR clonotypes containing ≥ 2 cells, were quantified for each cluster (Supplementary Figure 7A). This analysis revealed that, in agreement with proliferation marker expression, the effector population (Cluster 3) displayed much higher clonal expansion than any of the other clusters, both by number of distinct expanded clones and number of individual cells per clonotype (Figure 4C, Supplementary Figure 7B). The great majority of expanded TCR clonotypes were exclusively present in Cluster 3, while some were shared between Clusters 2 and 3 (Supplementary Figure 7C).

Pseudotime analysis based on calculating gene expression changes associated with dynamic biological processes[40] identified the stem-like population (Cluster 2) as an intermediate state between the naive (Cluster 0) and effector (Cluster 3) CD8+ T-cell differentiation states (Figure 4D, E). Importantly, effector CD8+ T cells lying at the end of the differentiation trajectory (Cluster 3) were abundantly present in the day 10 Help condition but mostly lacking in the day 10 No Help condition (Figure 4D). Under Help conditions, Cluster 3 effector cells increased in frequency from day 5 tot day 10 after vaccination (Figure 4F). Accordingly, CD8+ T cells from the day 10 Help condition showed a higher median pseudotime score as compared to cells from the other two experimental conditions (Figure 4E). They also showed a higher number of distinct expanded clones (Supplementary Figure 7D, E), and a higher number of cells per TCR clonotype (Supplementary Figure 7F), in agreement with clonal expansion being most prominent in Cluster 3 (Figure 4C). Stem-like CD8+ T cells (Cluster 2) were generated both under No Help and Help conditions (Figure 4D, F) but predominated under No Help conditions at day 10 (Figure 4F). Importantly, Cluster 2 stem-like CD8+ T cells from Help and No Help conditions had indiscernible transcriptomes at day 10 (Figure 4G). Differential gene expression analysis between Cluster 2 and 3 followed by Ingenuity Pathway Analysis (IPA) showed that functional qualities of helped CD8+ T cells, such as cytotoxicity, cell migration and proliferation, were acquired upon differentiation from the stem-like to the effector state (Supplementary Figure 8A-D, Supplementary Table 2). These findings agree with our earlier study in the same vaccination model, where we used bulk

RNAseq of primed CD8$^+$ T cells from the No Help and Help settings at day 10 in the spleen to define the CTL effector differentiation program installed as a result of CD4$^+$ T-cell help[20].

Taken together, the current results show at the single cell level that the differentiation spectrum of CD8$^+$ T cells primed in presence of CD4$^+$ T-cell help includes both stem-like and effector cells, with effector cells expanding and predominating in time. In absence of help, the same stem-like CD8$^+$ T cells are formed that do not further differentiate into effector cells.

Stem-like CD8$^+$ T cells that predominate after helpless priming transcriptionally resemble stem-like CD8$^+$ T cells in chronic infection and cancer

Next, we determined how the stem-like and helped effector CD8$^+$ T-cell states from our vaccination system relate to CD8$^+$ T-cell states found in infection and cancer. We used primary data from mouse acute (Armstrong) and chronic (clone 13, CD4$^+$ T-cell depleted) LCMV infection models generated by Pritykin *et al.*[7] (Figure 5A). This study showed that the TCF-1$^+$ progenitor/stem-like state of CD8$^+$ T cells is epigenetically and transcriptionally comparable in classical models of chronic infection and cancer in mice. This study[7] and others[8,10] also demonstrated that the stem-like CD8$^+$ T-cell state lies at the basis of trajectories towards either effector CD8$^+$ T cells, as found in acute infection, or terminally exhausted CD8$^+$ T cells, as found in chronic infection and cancer (Figure 5B). We used the top 200 signature genes of the TCF-1$^+$ progenitor state defined by Pritykin *et al.* (Supplementary Table 3) to determine similarity to Cluster 2 and Cluster 3 cells from our vaccination model by module scoring. The TCF-1$^+$ progenitor signature was clearly enriched in the stem-like Cluster 2 cells predominating after No Help vaccination (Figure 5C). Furthermore, the gene signature of effector CTLs responding to acute LCMV infection (Supplementary Table 3) was enriched in effector Cluster 3 cells that predominate after Help vaccination (Figure 5C).

We also investigated at the whole transcriptome level how stem-like CD8$^+$ T cells raised in our vaccination model compared to those raised by a tumor. For this purpose, we used a dataset derived from a genetically engineered mouse model of spontaneous lung cancer (KP-NINJA), wherein tumor cells express LCMV-derived foreign antigens[41] (Figure 5D). The authors showed that tumor-specific PD-1$^+$TCF-1$^+$ stem-like cells accumulated in the tumor-draining LN (TdLN), and that these largely shared their transcriptome with stem-like CD8$^+$ T cells from chronic LCMV infection. Module score analysis showed that the top-100 gene expression signature of TdLN-derived stem-like CD8$^+$ T cells (Supplementary Table 3) was highly enriched in the stem-like CD8$^+$ T cells raised in our vaccination model (Figure 5E, F). These data extrapolate our findings to a large array of data from commonly used mouse models of (chronic) infection and cancer, making it plausible that the TCF-1$^+$ progenitor from which both effector and exhausted cells can arise equals a primed CD8$^+$ T cell that has not (yet) received CD4$^+$ T-cell help to differentiate into an effector CTL.

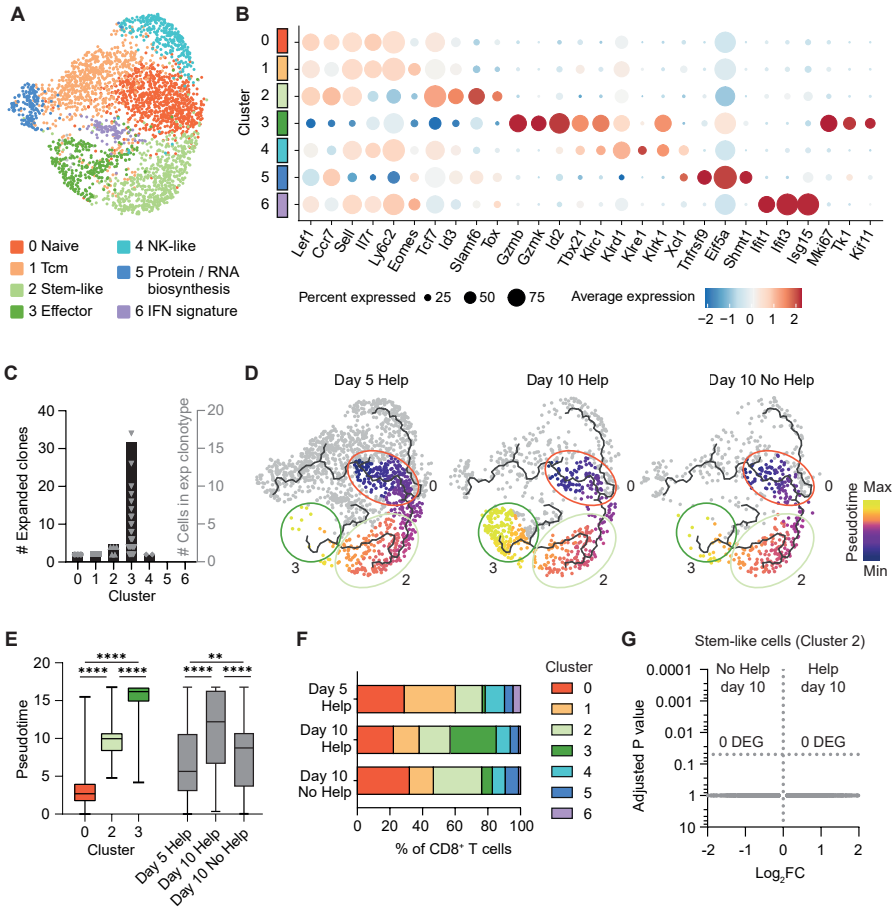

Figure 4. Combined scRNAseq and TCRseq support conversion of stem-like CD8⁺ T cells into CTL effectors upon CD4⁺ T-cell help delivery. Mice received Help or No Help vaccine (n=3 per group) and at days 5 and 10, activated CD3⁺CD44⁺CD62L⁻ T cells were flow cytometrically sorted from dLN and ndLN (See Supplementary Figure 5), labeled with different HTOs and subjected to 10x Genomics scRNAseq and coupled TCRseq (See Supplementary Figure 6). (A) UMAP projection and clustering of CD8⁺ T cells (defined in Supplementary Figure 6) from days 5 and 10 Help and day 10 No Help settings. (B) Level and frequency of CD8⁺ T-cell differentiation marker gene transcript expression, as identified by scRNAseq per CD8⁺ T-cell cluster. (C) TCR clonotype analysis. Number (#) of expanded CD8⁺ T-cell clonotypes (bars, left y-axis) as deduced from TCRseq per cluster, based on ≥ 2 cells with the same TCR, and number (#) of cells per expanded clonotype (symbols, right y-axis) per cluster (See also Supplementary Figure 7). (D) UMAPs showing pseudotime within the differentiation trajectory branch from naïve to effector gene expression profile, as based on scRNAseq data from the cumulative day 5 Help and day 10 Help and No Help conditions, plotted per indicated experimental condition. (E) Box plot showing pseudotime per cluster and per experimental condition. Statistical significance was calculated between clusters or between experimental conditions by two-way ANOVA and Sidak's multiple comparisons test. **P < 0.005 and ****P < 0.0001. (F) Distribution of CD8⁺ T cells over the different clusters (defined in A) per experimental condition. (G) Volcano plot showing 0 differentially expressed genes (DEG) between CD8⁺ cells within Cluster 2 from the day 10 Help versus No Help settings.

In an extension of the model of Pritykin *et al.*[7] and others[8,10], based on our current findings and review of the literature, we propose the following model: During CD8⁺ T-cell priming, stem-like cells are generated prior to delivery of CD4⁺ T-cell help signals. In case help signals are subsequently delivered, these stem-like cells are driven along a progressive differentiation trajectory into fully functional effector CTLs. When help signals are lacking and stem-like CD8⁺ T cells are exposed to chronic antigen stimulation under conditions as found in chronic infection and cancer, they follow the differentiation trajectory towards terminal exhaustion (Figure 5G).

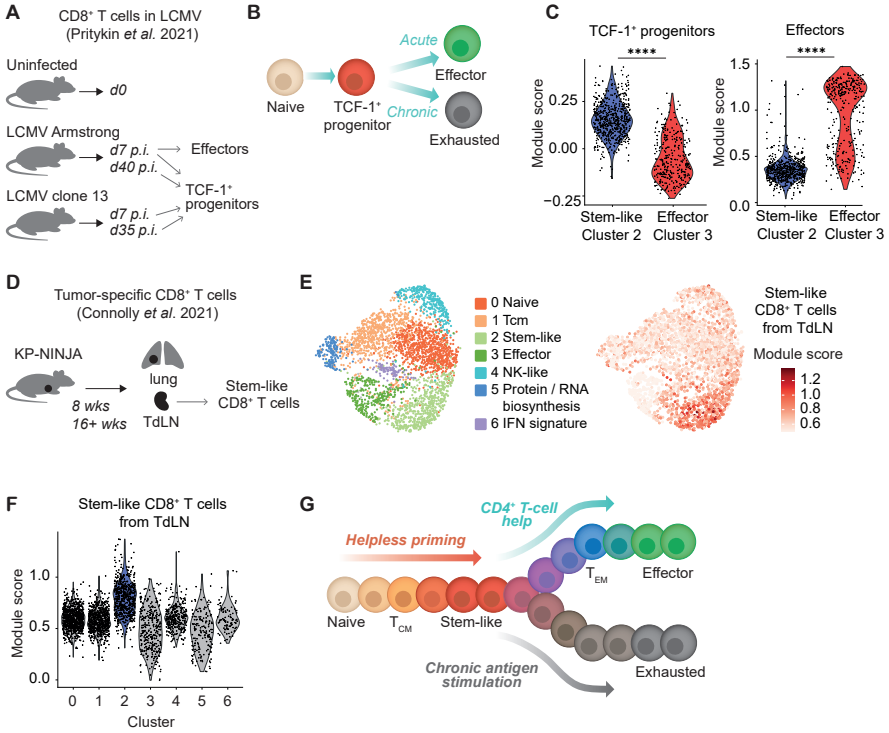

Figure 5. Stem-like CD8⁺ T cells that predominate after helpless priming transcriptionally resemble stem-like CD8⁺ T cells in chronic infection and cancer. (A) Outline of experimental conditions that generated the virus-specific CD8⁺ T cells analyzed by scRNAseq in Pritykin et al.[7]. (B) Differentiation model proposed by Pritykin et al.[7] and others[8,10]. (C) Violin plots showing module scores of the top 200 marker genes for CD8⁺ TCF-1⁺ progenitor cells (cluster 9, left panel) and effector cells (cluster 6, right panel) from Pritykin et al.[7] per CD8⁺ T cell in the stem-like Cluster 2 and helped effector Cluster 3 as defined in our vaccination model. Statistical significance was calculated by Mann-Whitney test. ****P < 0.0001. (D) Outline of experimental conditions that generated the tumor antigen-specific CD8⁺ T cells analyzed by scRNAseq in Connolly et al.[41]. (E, F) Module score of the top 100 marker genes for stem-like CD8⁺ T cells from TdLN (cluster 4, Connolly et al.[41]) per CD8⁺ T cell present in Cluster 2 and 3 in our vaccination model (Figure 4), as shown by UMAP (E) and violin plots (F). (G) Proposed model for CD8⁺ T-cell differentiation, wherein the PD-1⁺TCF-1⁺ stem-like state lies at the branchpoint of CD4⁺ T-cell help-dependent effector CTL differentiation and chronic antigen-driven CD8⁺ T-cell exhaustion in e.g. chronic infection and cancer.

The immunogenic MC38 tumor induces priming of neoantigen-specific stem-like, but not helped effector CD8+ T cells

We found earlier that therapeutic vaccination with the Help construct led to control of the HPV-E7+ TC-1 lung carcinoma, while No Help vaccination led to tumor outgrowth[29]. TC-1 tumor control after therapeutic Help vaccination was attributed to downregulation of inhibitory receptors, increased cytotoxicity and tumor invading capacities of CTLs as instructed by CD4+ T-cell help[20]. TC-1 is not spontaneously immunogenic and classifies as a lymphocyte-depleted, myeloid-rich tumor[42]. To investigate whether a spontaneously immunogenic tumor invites CD4+ T-cell help for the CTL response, we here used the T-cell infiltrated MC38 colon carcinoma model. MC38 tumor cells express defined MHC-I and MHC-II-restricted neoepitopes[43–45], which might enable spontaneous delivery of CD4+ T-cell help to the CTL response. To compare the differentiation states of CD8+ T cells raised by the MC38 tumor or by Help vaccination, we used a DNA vaccine encoding defined MC38-derived, MHC-I-restricted Rpl18 and Adpgk neoantigens[44] in conjunction with the Help cassette (Help-RA) (Figure 6A). Frequencies of Rpl18-tetramer+ CD8+ T cells spontaneously raised by MC38 tumors at day 15 were similar to those raised by Help vaccination at day 10 in blood, spleen and dLN. Rpl18-specific CD8+ T cells were also clearly detectable within the MC38 tumor (Figure 6B). We next compared neoantigen-specific CD8+ T-cell differentiation states in the MC38 and vaccination settings by flow cytometry (Supplementary Figure 9). In spleen and dLN of tumor-bearing mice, the frequency of PD-1+TCF-1+SLAMF6+ stem-like cells within the Rpl18-specific CD8+ T-cell pool was significantly higher than in vaccinated mice (Figure 6C). Conversely, in Help-RA vaccinated mice, the frequency of KLRG1+CX3CR1+ effector cells within the Rpl18-specific CD8+ T-cell pool was significantly higher than in tumor-bearing mice (Figure 6D). These results indicate that the MC38 tumor predominantly induces priming of stem-like CD8+ T cells and not help-dependent effector CTLs. Accordingly, the frequency of GZMB+ cells among Rpl18-specific CD8+ T cells and their GZMB protein levels were higher after vaccination than after MC38 tumor implantation (Figure 6E-G). Also, the frequencies of IFNγ+TNFα+ cells within total CD8+ T cells were higher in vaccinated mice than in tumor-bearing mice (Figure 6H, I). This reflected improved functional capacity rather than increased size of the responder population, since the frequency of antigen-specific CD8+ T cells in spleen was similar after vaccination or tumor inoculation (Supplementary Figure 9D).

Within the MC38 tumor, the great majority of Rpl18-specific CD8+ tumor infiltrating lymphocytes (TILs) expressed PD-1 and none of these cells had the KLRG1+CX3CR1+ helped effector phenotype (Supplementary Figure 9E-I), even though a fraction of them expressed GZMB (Supplementary Figure 9F). Also in the total CD8+ TIL population, GZMB+PD-1+ cells were found, while cells with a KLRG1+CX3CR1+ helped effector phenotype were lacking (Supplementary Figure 9H, I). Among Rpl18-specific TILs, the frequency of PD-1^{high}TIM3+TCF-1- exhausted cells[4] increased from day 7 to day 15 (Figure 6J), while the population of stem-like PD-1^{int}TCF-1+SLAMF6+ TILs decreased (Figure 6K), in line with the concept that stem-like cells become exhausted upon chronic antigen exposure in the TME. Accordingly, the frequency of Rpl18-specific GZMB+ TILs also decreased

upon tumor progression (Figure 6L). Among total CD8$^+$ TILs, a small proportion retained the capacity to produce IFNγ and TNFα after *in vitro* stimulation (Figure 6M).

We conclude that tumor-specific CD8$^+$ T cells primed by MC38 reach a stem-like differentiation state that develops into exhaustion in the TME, while they do not reach an effector differentiation state.

Delivery of CD4$^+$ T-cell help to CD8$^+$ T cells is impaired in the MC38 tumor context

We next tested whether therapeutic vaccination could deliver help to MC38-specific CD8$^+$ T cells. For this purpose, we used a 'neoHelp' cassette encoding MC38-derived MHC-II-restricted neoantigens Ddr2, Zmiz1 and Pcdh18[45] either alone (neoHelp), or in conjunction with MC38-derived MHC-I-restricted neoantigens Rpl18 and Adpgk (neoHelp-RA) (Figure 7A). Helper epitope vaccination did not change the frequency or the effector phenotype of Rpl18-specific CD8$^+$ T cells in blood over time compared to the empty vector (EV) control group (Figure 7B-D), nor did it improve survival of MC38 tumor-bearing mice (Figure 7E). Outside a tumor context, neoHelp-RA vaccination increased the frequency of Rpl18-specific CD8$^+$ T cells and their GZMB expression as compared to RA vaccination, but did not increase the formation of Rpl18-specific CD8$^+$ T cells with a KLRG1$^+$CX3CR1$^+$ effector phenotype (Supplementary Figure 10A-D). These data indicate that the neoantigen helper epitopes were functional, but not optimal in inducing CTL effector differentiation.

We therefore used another approach to introduce help for the CTL response by expressing in wild-type (wt) MC38 cells the strong helper epitopes P30 and PADRE as present in our standard vaccine Help cassette (Figure 7F). Next, we compared tumor-specific CD8$^+$ T-cell responses and tumor outgrowth in the MC38 wt and MC38-Help settings. The exogenous helper epitopes in the MC38-Help tumor were immunogenic as shown by the presence of a FOXP3$^-$CD44$^+$PADRE-tetramer$^+$ CD4$^+$ T-cell population in the spleen of mice bearing the MC38-Help tumor, but not the MC38 wt tumor (Figure 7G, Supplementary Figure 11A). Outgrowth of MC38-Help tumors was less efficient than that of MC38 wt tumors, resulting in lower tumor weight by day 15 and tumor clearance in 2 out of 10 mice (Figure 7H, I). The frequency of Rpl18-specific cells among CD8$^+$ TILs was higher in MC38-Help than in MC38 wt by day 15 (Figure 7J). However, the frequency of KLRG1$^+$CX3CR1$^+$ helped effector cells among Rpl18-tetramer$^+$ CD8$^+$ TILs was not different between the tumor settings (Figure 7K). Overall, the differentiation state of Rpl18-specific CD8$^+$ T cells in MC38 wt and MC38-Help tumors did not differ as assessed by the panel of differentiation markers, and most cells expressed PD-1 (Supplementary Figure 11B-E). The frequency of GZMB$^+$ cells among Rpl18-tetramer$^+$ CD8$^+$ TILs and total CD8$^+$ TILs was also not different between the two tumor settings (Figure 7L, Supplementary Figure 11F) and these cells were of a KLRG1$^-$CX3CR1$^-$PD-1$^+$ phenotype (Supplementary Figure 11G-I). CD8$^+$ TILs in both tumor settings had similar phenotypes, were largely PD-1$^+$ and cells with a KLRG1$^+$CX3CR1$^+$ helped effector phenotype were lacking. Likewise, the frequencies of CD8$^+$ TILs capable of producing IFNγ and TNFα upon *ex vivo* stimulation with Rpl18 and Adpgk neoantigen peptides did not differ (Supplementary Figure 11J).

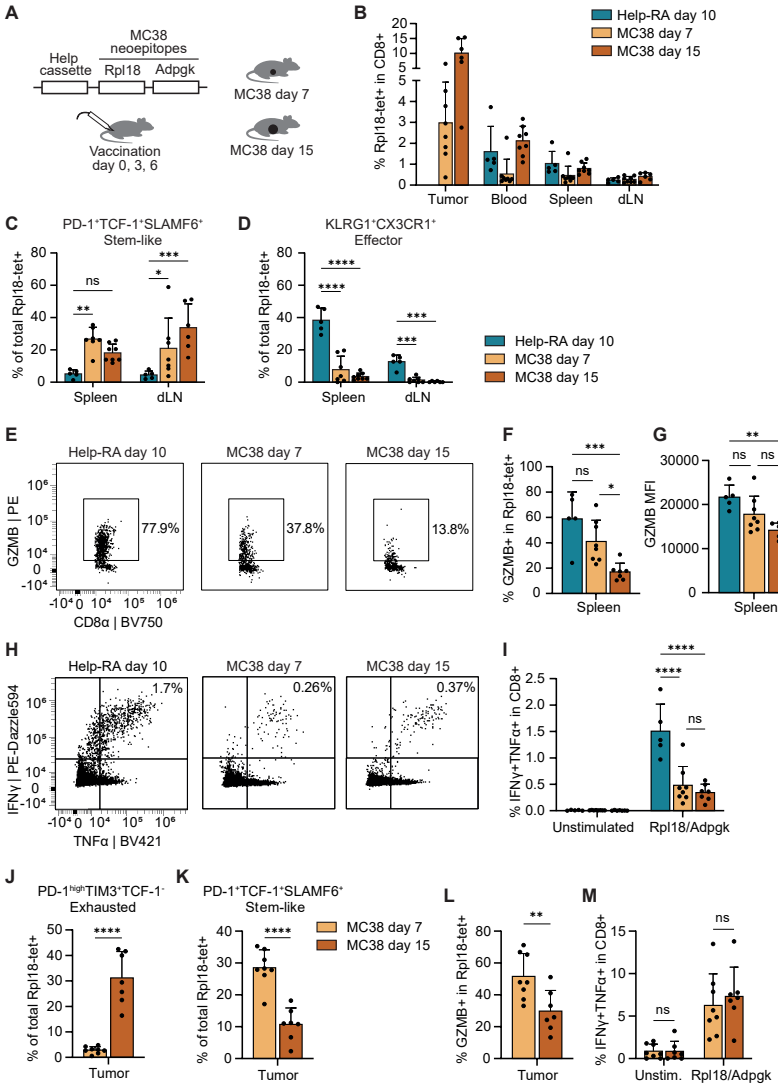

Figure 6. The MC38 tumor induces priming of neoantigen-specific stem-like, but not helped effector CD8⁺ T cells. (A) Experimental setup, mice were vaccinated or implanted with the MC38 tumor. (B) Frequency of Rpl18-tetramer⁺ CD8⁺ T cells in indicated tissues and the MC38 tumor. (C, D) Frequency of PD-1⁺TCF-1⁺ stem-like (C) and KLRG1⁺CX3CR1⁺ effector cells (D) within the Rpl18-specific CD8⁺ T-cell pool in the indicated organs. (E-G) Frequency of Granzyme-B (GZMB)⁺ cells within the Rpl18-specific CD8⁺ T cell population in spleen (E, F), and MFI of GZMB in this population (G). (H, I) Frequency of IFNγ⁺TNFα⁺ cells within the CD8⁺ T cell population from spleen after ex vivo stimulation with Rpl18 and Adpgk neoantigen peptides. (J, K) Frequency of PD-1^{hi}TIM3⁺TCF-1⁻ exhausted (J) and PD-1⁺TCF-1⁺ stem-like cells (K) within the CD8⁺ TIL pool on day 7 or 15 after tumor inoculation. (L) Frequency of GZMB⁺ cells within Rpl18-specific CD8⁺ TILs. (M) Frequency of IFNγ⁺TNFα⁺ cells within CD8⁺ TILs upon ex vivo restimulation with Rpl18 and Adpgk peptides. Data in A-D and E-M are from 2 separate experiments with n=5-8 mice per group. Error bars indicate SD. Statistical significance was calculated by two-way (B-D, I, M) or one-way (F, G) ANOVA and Sidak's multiple comparisons test, or unpaired t-test (J, K). ns, not significant, *P < 0.05, **P < 0.005, ***P < 0.001 and ****P < 0.0001. See also Supplementary Figure 9.

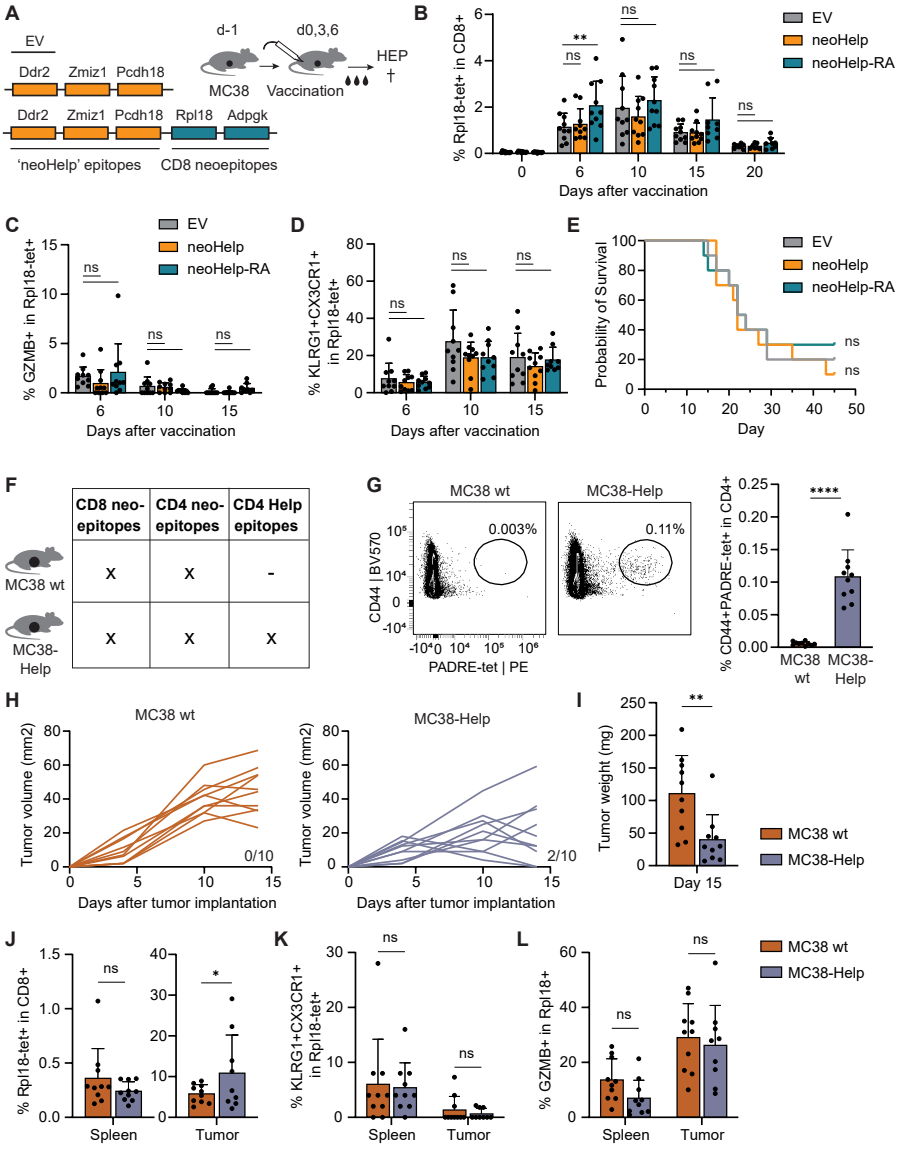

Figure 7. Delivery of CD4⁺ T-cell help to CD8⁺ T cells through vaccination or helper epitope expression is impaired in the MC38 tumor context. (A) Experimental outline. Mice were s.c. inoculated with 300.000 MC38 tumor cells on day -1, and vaccinated on day 0, 3, and 6 with DNA encoding empty vector (EV), neoHelp (MC38-derived MHC-II restricted neoepitopes mutated Ddr2, Zmiz1 and Pcdh13) or neoHelp-Rpl18-Adpgk (neoHelp-RA, containing both MC38-derived MHC-II and MHC-I restricted neoepitopes). Tumor outgrowth, survival and MC38-specific (Rpl18-tetramer⁺) CD8⁺ T-cell responses in blood were assessed over time. (B) Frequency of Rpl18-tetramer⁺ CD8⁺ T cells in blood at various timepoints. (C, D) Frequency of Granzyme-B (GZMB)⁺ cells (C) and KLRG1⁺CX3CR1⁺ effector cells (D) within the Rpl18-tetramer⁺ CD8⁺ T cell pool. (E) Survival plot. (F) MC38 tumor cells for which endogenous MHC-I and MHC-II restricted neoepitopes have been defined were transduced to stably express the Help cassette (P30/PADRE) as present in our vaccine, resulting in the MC38-Help tumor line. (G-L) Mice were

inoculated with 300.000 MC38 or MC38-Help cells (legend for all panels as indicated in Panels D and I) at day 0 and analyzed at day 15. (G) Frequency of CD44+PADRE-tetramer+ among CD4+ T cells in spleen. (H) Outgrowth of MC38 and MC38-Help tumors until day 15. Numbers of mice with complete tumor clearance are indicated. (I) Tumor weight at day 15. (J) Frequency of Rpl18-tetramer+ CD8+ T cells in spleen and tumor. (K) Frequency of KLRG1+CX3CR1+ effector cells within the Rpl18-specific CD8+ T-cell pool in the indicated organs. (L) Frequency of Granzyme-B (GZMB)+ cells within Rpl18-specific CD8+ T cells in spleen and tumor. Data in B-E are from 1 experiment with n=10 mice per group. Data in G-L are from 1 experiment representative of 2 independent experiments with n=10 mice per group. Error bars indicate SD. Statistical significance was calculated by two-way ANOVA and Sidak's multiple comparisons test (B-D, J-L), Mantel-Cox log-rank test (E) or unpaired t-test (G, I). In B-E, statistical significance was calculated in comparison to the EV group. ns, not significant, *P < 0.05, **P < 0.005, ***P < 0.001 and ****P < 0.0001. See also Supplementary Figure 11.

In conclusion, deliberate expression of strong helper epitopes in MC38 tumor cells raised tumor-specific CD4+ T cells and increased the frequency of tumor-specific CD8+ T cells. However, these CD8+ T cells lacked the helped effector phenotype, suggesting that CD4+ T-cell help was not efficiently delivered in this tumor context. Tumor control was moderately improved, which may have been due to the increase in tumor-specific CD8+ T cells resulting from help signals, but also to CD4+ T-cell help delivered to B cells or myeloid cells.

Discussion

By bulk RNAseq, we have shown that CD4+ T-cell help downregulates coinhibitory receptors on primed CD8+ T cells and strongly promotes their cytotoxic and migratory capacities[20]. Here, we define in the same model at the single cell level that CD4+ T-cell help promotes the differentiation of CD8+ T cells from the stem-like to the CTL effector state, which is accompanied by clonal expansion. Our results are in line with the linear model of CD8+ T-cell differentiation, which proposes a spectrum of CD8+ T cell states ranging from stem-like memory populations with low differentiation states to (short-lived) effector T cells with a terminal differentiation state[1,2,46,47]. Our data explain the increased functionality that we and others have described for helped CD8+ T cells[20–22] as a shift in this differentiation spectrum towards the effector state. The here determined nature of this shift also explains our earlier finding that CD4+ T-cell help increased the number and functionality of T_{EM} cells, but not of more stem-like T_{CM} cells[21].

Importantly, we did not exclusively raise effector CTLs upon Help vaccination, but cells ranging along the entire CD8+ T-cell differentiation spectrum, including stem-like cells. On phenotypic and transcriptomic level, stem-like cells from the Help and No Help vaccination settings were identical, suggesting that these cells have received the same signals during priming. We propose therefore that stem-like cells generated after Help vaccination also represent helpless cells, that have undergone the first step of priming but have not yet received CD4+ T-cell help. After Help vaccination, stem-like cells in the dLN turn into effector cells over time, in accordance with the idea that help is delivered in a second step of priming[14].

The progressive differentiation model proposes that CD8$^+$ T-cell fate is mainly determined by TCR signaling strength and inflammatory signals during priming[1,2]. We specify here that effector differentiation additionally depends on CD4$^+$ T-cell help that allows cDC1s to provide specific cytokine- and costimulatory signals to CD8$^+$ T cells[13–15,20]. We propose that the final differentiation fate of CD8$^+$ T cells is determined by the integration of TCR, costimulatory and cytokine signals received during both the first and the second priming steps. This would also explain why CTL responses are differentially dependent on CD4$^+$ T-cell help in diverse infection, tumor or vaccination settings, that vary in the amounts of antigen and inflammatory signals they elicit[24]. Our findings support that CD8$^+$ stem-like cells lie on the trajectory towards effector differentiation but can alternatively differentiate towards terminal exhaustion upon persistent antigen exposure, as recently suggested[7,10]. The fact that CD8$^+$ T-cell exhaustion in mouse models of chronic LCMV infection is exacerbated by CD4$^+$ T-cell depletion[26] fits in our concept that the stem-like cells that lie at the beginning of the exhaustion trajectory equal helpless cells.

Adoptive transfer showed that stem-like CD8$^+$ T cells formed after No Help vaccination could further proliferate and complete their CTL effector differentiation after Help vaccination. Ideally, CD4$^+$ T-cell help will improve the endogenous CD8$^+$ T-cell response in chronic infection and cancer. Adoptive transfer of virus-specific CD4$^+$ T cells in chronic LCMV infection indeed improved proliferative and cytotoxic capacities of stem-like CD8$^+$ T cells[27,28]. Also, adoptive transfer of neoantigen-specific CD4$^+$ T cells or expression of MHC-II-restricted neoantigens by tumor cells increased CTL activity and tumor control in mouse tumor models[48,49]. However, we found that expression of endogenous or exogenous helper epitopes by MC38 tumor cells failed to induce the helped CTL effector phenotype. The tumor-endogenous helper epitopes may have been too weak, since they also did not raise helped effector CD8$^+$ T cells outside the tumor context. Exogenous helper epitopes did increase the frequency of tumor-specific CD8$^+$ T cells raised, which likely contributed to the observed reduction in tumor outgrowth. MC38 cannot be directly recognized by CD4$^+$ T cells since it lacks MHC-II[29], but CD4$^+$ T cells may also have contributed indirectly via help to myeloid cells or B cells[50].

In the lymphocyte-depleted HPV-E7$^+$ TC-1 lung carcinoma model, raising a helped CTL response by therapeutic vaccination with our Help-E7 vaccine led to tumor control, while the No Help vaccine had no effect[20,29]. However, in the MC38 tumor context, where tumor-specific CD8$^+$ T cells are spontaneously primed, it appears challenging to transmit CD4$^+$ T-cell help signals. These findings are in line with a recent study showing that tumor-specific CD4$^+$ T cells raised by MC38 and other tumors acquire a dysfunctional state already in the dLN that is in part imposed by Tregs[51]. Tumors often lack inflammatory signals such as IFN-I and induce Treg responses[52,53], which attenuate DC activation and hamper delivery of CD4$^+$ T-cell help[12,19,51]. It will be of interest to understand the limitations and possibilities for delivery of help to the CTL response in cancers with different, defined TME types.

The validity of our CD8+ T-cell differentiation model should be further investigated in other settings, such as viral infection and human cancer. Nevertheless, we propose that helpless priming may be causally related to CD8+ T-cell exhaustion, since lack of helped effector CTLs will lead to antigen persistence[11]. We hope that our study contributes to a theoretical framework on CTL effector differentiation that provides a rationale to optimize immunotherapeutic strategies.

Methods

Mice

Female 8-10-week-old C57BL/6JRj mice obtained from Janvier Laboratories and OT-I (Tg(TcraTcrb)1100Mjb) mice on a CD45.1+ C57BL/6 background (bred in-house) were housed in individually ventilated cages under specific pathogen free conditions. Animal experiments were approved by the Experimental Animal Committee of Leiden University Medical Center and performed in accordance with national and European regulations. Cages were allocated randomly to experimental groups.

Vaccination

For intra-epidermal DNA vaccination, hair was removed from the right hind leg with depilating cream (Veet, Reckitt Benckiser) on day 0 and on days 0, 3, and 6, 15 µl of a 2 mg/ml plasmid DNA solution in H_2O was applied into the hairless skin of anesthetized mice with a Permanent Make Up tattoo device (Cheyenne, MT Derm GmbH), using a sterile disposable nine-needle bar with a needle depth of 1 mm and oscillating at a frequency of 100 Hz for 45 s, as described[26,27]. Plasmid DNA vaccines used were Help-E7SH (Help) and E7SH DNA (No Help)[29,30], OVA-Help and OVA-No Help[20], Rpl18-Adpgk-Help, and neoHelp and neoHelp-RA (Supplementary Methods).

Tumor challenge

The murine MC38-L colorectal carcinoma cell line was obtained from Leiden University Medical Center and has been characterized regarding neoepitope expression[44,45,54]. The MC38-Help cell line was created by transducing MC38-L cells with lentivirus encoding EF1a-Help-3xFLAG-IRES-eGFP (Supplementary Methods). Mice were injected subcutaneously in the right flank with 300.000 live MC38 or MC38-Help cells (LUMC) in 100 µl Hank's buffered salt solution (HBSS, Gibco). Tumor sizes were measured 3 times per week by caliper, and a tumor volume of 1000 mm^3 was maintained as humane endpoint.

Tissue processing and flow cytometry

Peripheral blood cells were obtained by tail vein bleeding in Microvette CB300 LH tubes (Sarstedt) and erythrocytes were removed by incubating twice in Red Blood Cell lysis buffer (Santa Cruz) for 1 min at room temperature. Spleens were passed through a 70 µm cell strainer (BD Falcon)

and erythrocytes were lysed for 5 min at room temperature. Right (dLN) and left (ndLN) inguinal LNs were digested into single cell suspensions with 100 µg/ml Liberase TL (Roche) in Dulbecco's Modified Eagle Medium (DMEM, Gibco) for 30 min at 37°C and passed through a 70 µm cell strainer. Tumors were isolated after perfusion of sacrificed mice with 15 ml phosphate buffered saline (PBS) with 2 mM ethylenediaminetetraacetic acid (EDTA, Santa Cruz). Tumors were mechanically disaggregated by scalpel and digested into single cell suspensions with 100 µg/ml Liberase TL (Roche) with 10 µg/ml DNAse I (Sigma) in DMEM (Gibco) for 30 min at 37°C. Tumors were passed through a 70 µm cell strainer. For flow cytometry, cells were washed with FACS buffer (PBS + 2% FCS) and stained for 1 h at room temperature with 1:200 PE-conjugated I-Ab/AKFVAAWTLKAA (PADRE) tetramers (NIH) or for 30 min on ice with 1:1000 LIVE/DEAD Near IR dye (Invitrogen) or 1:500 Zombie UV (Biolegend), 1:100 APC-conjugated H-2D^b/E7$_{49\text{-}57}$ tetramers, APC-conjugated H-2K^b/OVA$_{257\text{-}264}$ tetramers or APC-conjugated H-2K^b/KILTFDRL (mutated Rpl18) tetramers (produced in-house at LUMC) and monoclonal antibodies (mAbs) for surface staining (Supplementary Methods). For intracellular staining, cells were fixed and permeabilized with the FOXP3/transcription factor staining buffer set (eBioscience), according to the manufacturer's protocol and stained with antibodies for 30 min on ice (Supplementary Methods). Flow cytometry was performed using a 3-laser or 5-laser Aurora (Cytek) and SpectroFlow software.

Ex vivo restimulation

Ex vivo restimulation of splenocyte or tumor cell suspensions was performed as described [44]. In brief, cells of the DC line D1 were seeded in a 96-wells plate at 50.000 cells per well in conditioned medium and loaded with 1 mg/ml mutated Rpl18 and mutated Adpgk peptide or left unloaded, and incubated overnight at 37°C. The next day, 500.000 splenocytes or tumor cells were seeded on D1 cells and preincubated for 1 h at 37°C. Subsequently, GolgiPlug (BD Biosciences) was added at a final dilution of 1:1000 and left for 5 h at 37°C until analysis.

Adoptive cell transfer

OT-I CD8$^+$ T cells, carrying a transgenic Vα2/Vβ5 TCR recognizing OVA$_{257\text{-}264}$/H-2K^b, were isolated to more than 90% purity from spleens of naïve OT-I;CD45.1$^+$ C57BL/6 mice using a negative selection MACS CD8α$^+$ T-cell Isolation Kit (Miltenyi). OT-I cells were retro-orbitally (r.o.) injected at 10^5 cells per mouse into WT CD45.2$^+$ C57BL/6 mice on day -1, after which mice were vaccinated with OVA-No Help construct[20] on day 0, 3 and 6. On day 10, CD45.1$^+$ CD44$^+$ SLAMF6$^+$ helpless CD8$^+$ T cells were sorted from dLN on a 3-laser FACSAria II (BD Biosciences). Cells were r.o. injected at 10^4 cells per mouse into WT C57BL/6 mice, which were vaccinated once with OVA-Help or OVA-No Help on the next day.

Flow cytometry data analysis

Flow cytometry data were analyzed with OMIQ software and FlowAI[55] was used to remove events showing anomalies in flow rate, signal acquisition and dynamic range. After manual gating of tetramer$^+$ CD8$^+$ T cells (Supplementary Figure 1A) and conventional marker expression analysis,

subsampling was performed to select maximally 150 tetramer+ CD8+ T cells from each sample. Samples containing <5 total tetramer+ CD8+ T cells were excluded from further analysis. FlowSom[56] was used for K-means clustering of tetramer+ CD8+ T cells, including all markers except live/dead, CD4, CD8, FOXP3 and tetramer. Optimal t-distributed stochastic neighbor embedding (opt-SNE)[57] was used for dimension reduction and visualization of the data, using the same markers. Wanderlust[37] was used for trajectory analysis, using the same markers except Ki67, and using Cluster 10 (CD44-CD62L+ naive cells) as starting point. FlowSom clustering of all tetramer+ CD8+ cells from dLN at day 2-10 and 3 naïve LNs was done for the analysis of antigen-specific CD8+ T-cell populations on consecutive days after vaccination. Responding tetramer+ CD8+ T cells were selected for analysis by including clusters that showed <20% frequency in naïve LNs and a change in frequency between different time points after vaccination (Supplementary Figure 3D).

Statistical analysis

Data were analyzed with GraphPad Prism software using two-way ANOVA and Sidak's multiple comparisons test, unless indicated otherwise. Bars indicate means, error bars indicate SD. A P value < 0.05 was considered statistically significant; ns, not significant, *P < 0.05, **P < 0.005, ***P < 0.001 and ****P < 0.0001. Sample size was calculated a priori using G*Power software, using previous results of E7-specific CD8+ T-cell frequencies between Help and No Help[20] for power calculations.

Sample and library preparation for scRNAseq and TCRseq

Mice were vaccinated under Help or No Help conditions at day 0, 3, and 6 and were sacrificed at day 5 or day 10 after first vaccination, after which dLN and ndLN were isolated (Supplementary Figure 5). For each experimental condition, LNs from 3 individual mice were pooled to reduce biological variability, resulting in 8 samples (Supplementary Figure 6A). Samples were stained with the following mAbs: 1:100 CD19-PerCP/Vio700 (clone REA749, Miltenyi), 1:100 CD3-BV421 (clone 17A2, Biolegend), 1:100 CD44-PE/Cy7 (clone IM7, eBioscience), 1:100 CD62L-FITC (clone MEL-14, eBioscience). For each sample, activated T cells (CD19-CD3+CD44+CD62L-) were sorted on a 3-laser FACSAria II (BD Biosciences) and labeled with a distinct hashtag oligonucleotide (HTO)-conjugated mAb to MHC-I/CD45 (TotalSeq C0301 to C0307 and C0309, Biolegend), after which all 8 samples were pooled. scRNAseq libraries were prepared using a 10X Chromium single cell 5' v2 chemistry kit (10X Genomics) and TCRseq libraries were prepared using a 10X Chromium single cell V(D)J enrichment kit for mouse T cells (10X Genomics), according to the manufacturer's protocols. Sequencing was performed on a NovaSeq6000 system (Illumina). A total of 25,000 cells was used for sequencing, with a median sequencing depth of 11,196 reads per cell.

scRNAseq analysis

Analysis of scRNAseq and TCRseq data was performed using CellRanger (10X Genomics, v6.0.1) and Seurat (v4.3.0) in R (v4.2.3). For details, see Supplementary Methods. In summary, scRNAseq and TCRseq reads were aligned to the mouse reference genome mm10, TCR and BCR genes were

removed from the gene expression count matrix, and the dataset was analyzed using the standard Seurat pipeline. HTO demultiplexing was performed (Supplementary Figure 6B) and dataset was filtered based on number of RNA features, number of RNA counts, mitochondrial gene expression and expression of genes associated with B cells or APCs. Cell cycle scores for G2/M and S phase were assigned based on expression of G2/M and S phase genes, and these scores were regressed out during clustering. $CD8^+$ T-cell clusters were selected on presence of *Cd8a, Cd8b1* and absence of *Cd4* transcripts (Supplementary Figure 6C). Within the $CD8^+$ T-cell subset, number of cells per HTO was determined (Supplementary Figure 6D). HTOs containing <30 $CD8^+$ T cells were excluded from further analysis. Cluster 7, consisting of 52 $CD8^+$ T cells that showed only cell cycle genes as markers, was excluded, since cell cycle genes were regressed out during clustering. TCRseq analysis was performed using Loupe VDJ Browser (v5.0.0, 10X Genomics). Expanded clones were identified as TCR clonotypes containing 2 or more cells. TCR sequences from Loupe VDJ Browser, and UMAP projection and cluster annotation from Seurat were visualized together using Loupe Browser (v6.4.1, 10X Genomics). To quantify expanded clonotypes per differentiation cluster, only cells that grouped together in the UMAP with their assigned cluster were included. Seurat and Monocle3 (v1.3.1) in R were used for trajectory analysis. Ingenuity Pathway Analysis (Qiagen) was used for functional classification of differentially expressed genes between Cluster 2 and Cluster 3. For comparison of our scRNAseq data to published gene signatures, top 200 marker genes of TCF-1^+ progenitor (cluster 9) and effector (cluster 6) $CD8^+$ T cells from chronic and acute LCMV infection were downloaded from Table S5 from Pritykin *et al*. 2021[7]. These top 200 genes were used to calculate a module score for each cell in our dataset. The same method was performed using top 100 marker genes of stem-like $CD8^+$ T cells from the TdLN, (cluster 4) as published by Connolly *et al.* 2021[41], which were kindly provided to us by the authors.

Data availability

The scRNAseq and scTCRseq data utilized in Figure 4 have been deposited in the GEO database with the accession number GSE249046.

Acknowledgements

We thank Kees Franken for manufacturing tetramers, Mart de Boo for helping with tissue processing, Fiamma Salerno and Elselien Frijlink for scientific discussions, Ferry Ossendorp for advice on the tumor model, Susan Kloet for advise on scRNAseq, Tom de Wit for help with sorting, Evert de Vries for general support, Nikhil Yoshi and Kelli Connolly for sharing their dataset, and the Flow Cytometry Facility, Leiden Genome Technology Center, and Experimental Animal Facility of our institute for technical assistance.

Author Contributions

Study design: J.Bo, J.Bu; experimental design and performing experiments: J.Bu, D.B., M.S., Y.X, X.L; data analysis: J.Bu; manufacturing DNA vaccines: M.S.; paper writing: J.Bu, J.Bo; critical reading and editing of the paper: D.B., M.S., X.L, Y.X; supervision: J.Bo.

Competing Interests

The authors declare no competing financial interests in relation to the work described.

Funding

This research was supported by Oncode and grants 2017-11079 and 2017-10894 of the Dutch Cancer Society to J. Borst.

References

1. Henning, A. N., Roychoudhuri, R. & Restifo, N. P. Epigenetic control of CD8+ T cell differentiation. *Nat. Rev. Immunol.* **18**, 340–356 (2018).
2. Kaech, S. M. & Cui, W. Transcriptional control of effector and memory CD8 + T cell differentiation. *Nat. Rev. Immunol.* **12**, 749–761 (2012).
3. Philip, M. & Schietinger, A. CD8+ T cell differentiation and dysfunction in cancer. *Nat. Rev. Immunol.* **22**, 209–223 (2022).
4. Gebhardt, T., Park, S. L. & Parish, I. A. Stem-like exhausted and memory CD8+ T cells in cancer. *Nat. Rev. Cancer* **23**, 780–798 (2023).
5. Zehn, D., Thimme, R., Lugli, E., de Almeida, G. P. & Oxenius, A. 'Stem-like' precursors are the fount to sustain persistent CD8+ T cell responses. *Nat. Immunol.* **23**, 836–847 (2022).
6. Chow, A., Perica, K., Klebanoff, C. A. & Wolchok, J. D. Clinical implications of T cell exhaustion for cancer immunotherapy. *Nat. Rev. Clin. Oncol.* **19**, 775–790 (2022).
7. Pritykin, Y. *et al.* A unified atlas of CD8 T cell dysfunctional states in cancer and infection. *Mol. Cell* **81**, 2477–2493 (2021).
8. Zheng, L. *et al.* Pan-cancer single-cell landscape of tumor-infiltrating T cells. *Science (1979).* **374**, 6474 (2021).
9. Broomfield, B. J. & Groom, J. R. Defining the niche for stem-like CD8+ T cell formation and function. *Curr. Opin. Immunol.* **89**, 102454 (2024).
10. McManus, D. T. *et al.* An early precursor CD8+ T cell that adapts to acute or chronic viral infection. *Nature* **640**, 772–781 (2025).

11. Busselaar, J., Tian, S., van Eenennaam, H. & Borst, J. Helpless Priming Sends CD8+ T Cells on the Road to Exhaustion. *Front. Immunol.* **11**, 592569 (2020).

12. Busselaar, J., Sijbranda, M. & Borst, J. The importance of type I interferon in orchestrating the cytotoxic T-cell response to cancer. *Immunol. Lett.* **270**, 106938 (2024).

13. Wu, R. & Murphy, K. M. DCs at the center of help: Origins and evolution of the three-cell-type hypothesis. *Journal of Experimental Medicine* **219**, 1–13 (2022).

14. Borst, J., Ahrends, T., Bąbała, N., Melief, C. J. M. & Kastenmüller, W. CD4+ T cell help in cancer immunology and immunotherapy. *Nat. Rev. Immunol.* **18**, 635–647 (2018).

15. Ferris, S. T. *et al.* cDC1 prime and are licensed by CD4+ T cells to induce anti-tumour immunity. *Nature* **584**, 624–629 (2020).

16. Lei, X. *et al.* CD4+ helper T cells endow cDC1 with cancer-impeding functions in the human tumor micro-environment. *Nat. Commun.* **14**, 217 (2023).

17. Lei, X. *et al.* CD4+ T cells produce IFN-I to license cDC1s for induction of cytotoxic T-cell activity in human tumors. *Cell. Mol. Immunol.* 1–19 (2024) doi:10.1038/s41423-024-01133-1.

18. Wu, R. *et al.* Mechanisms of CD40-dependent cDC1 licensing beyond costimulation. *Nat. Immunol.* **23**, 1536–1550 (2022).

19. Gressier, E. *et al.* CD4+ T cell calibration of antigen-presenting cells optimizes antiviral CD8+ T cell immunity. *Nat. Immunol.* **24**, (2023).

20. Ahrends, T. *et al.* CD4+ T cell help confers a cytotoxic T cell effector program including coinhibitory receptor downregulation and increased tissue invasiveness. *Immunity* **47**, 848–861 (2017).

21. Ahrends, T. *et al.* CD4+ T cell help creates memory CD8+ T cells with innate and help-independent recall capacities. *Nat. Commun.* **10**, 5531 (2019).

22. Provine, N. M. *et al.* Immediate dysfunction of vaccine-elicited CD8 + T cells primed in the absence of CD4 + T cells. *The Journal of Immunology* **197**, 1809–1822 (2016).

23. Brewitz, A. *et al.* CD8+T cells orchestrate pDC-XCR1+dendritic cell spatial and functional cooperativity to optimize priming. *Immunity* **46**, 205–219 (2017).

24. Wiesel, M. & Oxenius, A. From crucial to negligible: Functional CD8+ T-cell responses and their dependence on CD4+ T-cell help. *Eur. J. Immunol.* **42**, 1080–1088 (2012).

25. Jobin, K. *et al.* A distinct priming phase regulates CD8 T cell immunity by orchestrating paracrine IL-2 signals. *Science (1979).* **388**, (2025).

26. Wherry, E. J. *et al.* Molecular Signature of CD8+ T Cell Exhaustion during Chronic Viral Infection. *Immunity* **27**, 670–684 (2007).

27. Kanev, K. *et al.* Proliferation-competent Tcf1+ CD8 T cells in dysfunctional populations are CD4 T cell help independent. *Proc. Natl. Acad. Sci. U. S. A.* **116**, 20070–20076 (2019).

28. Zander, R. *et al.* CD4+ T Cell Help Is Required for the Formation of a Cytolytic CD8+ T Cell Subset that Protects against Chronic Infection and Cancer. *Immunity* **51**, 1028–1042 (2019).

29. Ahrends, T. *et al.* CD27 Agonism Plus PD-1 Blockade Recapitulates CD4+ T-cell Help in Therapeutic Anticancer Vaccination. *Cancer Res.* **76**, 2921–2931 (2016).

30. Oosterhuis, K., Aleyd, E., Vrijland, K., Schumacher, T. N. & Haanen, J. B. Rational design of DNA vaccines for the induction of human papillomavirus type 16 E6-and E7-specific cytotoxic T-cell responses. *Hum. Gene Ther.* **23**, 3001–1312 (2012).

31. Babala, N. *et al.* Subcellular Localization of Antigen in Keratinocytes Dictates Delivery of CD4 + T-cell Help for the CTL Response upon Therapeutic DNA Vaccination into the Skin. *Cancer Immunol. Res.* **6**, 835–847 (2018).

32. Bins, A. D. *et al.* A rapid and potent DNA vaccination strategy defined by in vivo monitoring of antigen expression. *Nat. Med.* **11**, 899–904 (2005).

33. Schenkel, J. M. *et al.* Conventional type I dendritic cells maintain a reservoir of proliferative tumor-antigen specific TCF-1+ CD8+ T cells in tumor-draining lymph nodes. *Immunity* **54**, 2338–2353 (2021).

34. Gattinoni, L., Speiser, D. E., Lichterfeld, M. & Bonini, C. T memory stem cells in health and disease. *Nat. Med.* **23**, 18–27 (2017).

35. Joshi, N. S. *et al.* Inflammation Directs Memory Precursor and Short-Lived Effector CD8+ T Cell Fates via the Graded Expression of T-bet Transcription Factor. *Immunity* **27**, 281–295 (2007).

36. Gerlach, C. *et al.* The Chemokine Receptor CX3CR1 Defines Three Antigen-Experienced CD8 T Cell Subsets with Distinct Roles in Immune Surveillance and Homeostasis. *Immunity* **45**, 1270–1284 (2016).

37. Bendall, S. C. *et al.* Single-Cell Trajectory Detection Uncovers Progression and Regulatory Coordination in Human B cell Development. *Cell* **157**, 714 (2014).

38. Siddiqui, I. *et al.* Intratumoral Tcf1+PD-1+CD8+ T cells with stem-like properties promote tumor control in response to vaccination and checkpoint blockade immunotherapy. *Immunity* **50**, 195–211 (2019).

39. Beltra, J.-C. *et al.* Developmental relationships of four exhausted CD8+ T Cell subsets reveals underlying transcriptional and epigenetic landscape control mechanisms. *Immunity* **52**, 825–841 (2020).

40. Trapnell, C. *et al.* The dynamics and regulators of cell fate decisions are revealed by pseudotemporal ordering of single cells. *Nat. Biotechnol.* **32**, 381–386 (2014).

41. Connolly, K. A. *et al.* A reservoir of stem-like CD8 + T cells in the tumor-draining lymph node preserves the ongoing antitumor immune response. *Sci. Immunol.* **6**, 64 (2021).

42. Frijlink, E. *et al.* PD-1 or CTLA-4 blockade promotes CD86-driven Treg responses upon radiotherapy of lymphocyte-depleted cancer in mice. *Journal of Clinical Investigation* **134**, (2024).

43. Yadav, M. *et al.* Predicting immunogenic tumour mutations by combining mass spectrometry and exome sequencing. *Nature* **515**, 572–576 (2014).

44. Hos, B. J. *et al.* Identification of a neo-epitope dominating endogenous CD8 T cell responses to MC-38 colorectal cancer. *Oncoimmunology* **9**, e1673125 (2020).

45. Hos, B. J. *et al.* Cancer-specific T helper shared and neo-epitopes uncovered by expression of the MHC class II master regulator CIITA. *Cell Rep.* **41**, 111485 (2022).

46. Johnnidis, J. B. *et al.* Inhibitory signaling sustains a distinct early memory CD8+ T cell precursor that is resistant to DNA damage. *Sci. Immunol.* **6**, (2021).

47. Pais Ferreira, D. *et al.* Central memory CD8+ T cells derive from stem-like Tcf7hi effector cells in the absence of cytotoxic differentiation. *Immunity* **53**, 985–1000 (2020).

48. Brightman, S. E. *et al.* Neoantigen-specific stem cell memory-like CD4+ T cells mediate CD8+ T cell-dependent immunotherapy of MHC class II-negative solid tumors. *Nat. Immunol.* **24**, 1345–1357 (2023).

49. Alspach, E. *et al.* MHC-II neoantigens shape tumour immunity and response to immunotherapy. *Nature* **574**, 696–701 (2019).

50. Speiser, D. E., Chijioke, O., Schaeuble, K. & Münz, C. CD4+ T cells in cancer. *Nat. Cancer* **4**, 317–329 (2023).

51. Guo, M. *et al.* Molecular, metabolic, and functional CD4 T cell paralysis in the lymph node impedes tumor control. *Cell Rep.* **42**, 113047 (2023).

52. Luca, B. A. *et al.* Atlas of clinically distinct cell states and ecosystems across human solid tumors. *Cell* **184**, 5482–5496 (2021).

53. Combes, A. J. *et al.* Discovering dominant tumor immune archetypes in a pan-cancer census. *Cell* **185**, 184–203 (2022).

54. Schrörs, B. *et al.* MC38 colorectal tumor cell lines from two different sources display substantial differences in transcriptome, mutanome and neoantigen expression. *Front. Immunol.* **14**, (2023).

55. Monaco, G. *et al.* flowAI: automatic and interactive anomaly discerning tools for flow cytometry data. *Bioinformatics* **32**, 2473–2480 (2016).

56. Van Gassen, S. *et al.* FlowSOM: Using self-organizing maps for visualization and interpretation of cytometry data. *Cytometry Part A* **87**, 636–645 (2015).

57. Belkina, A. C. *et al.* Automated optimized parameters for T-distributed stochastic neighbor embedding improve visualization and analysis of large datasets. *Nat. Commun.* **10**, 5415 (2019).

Supplementary Figures

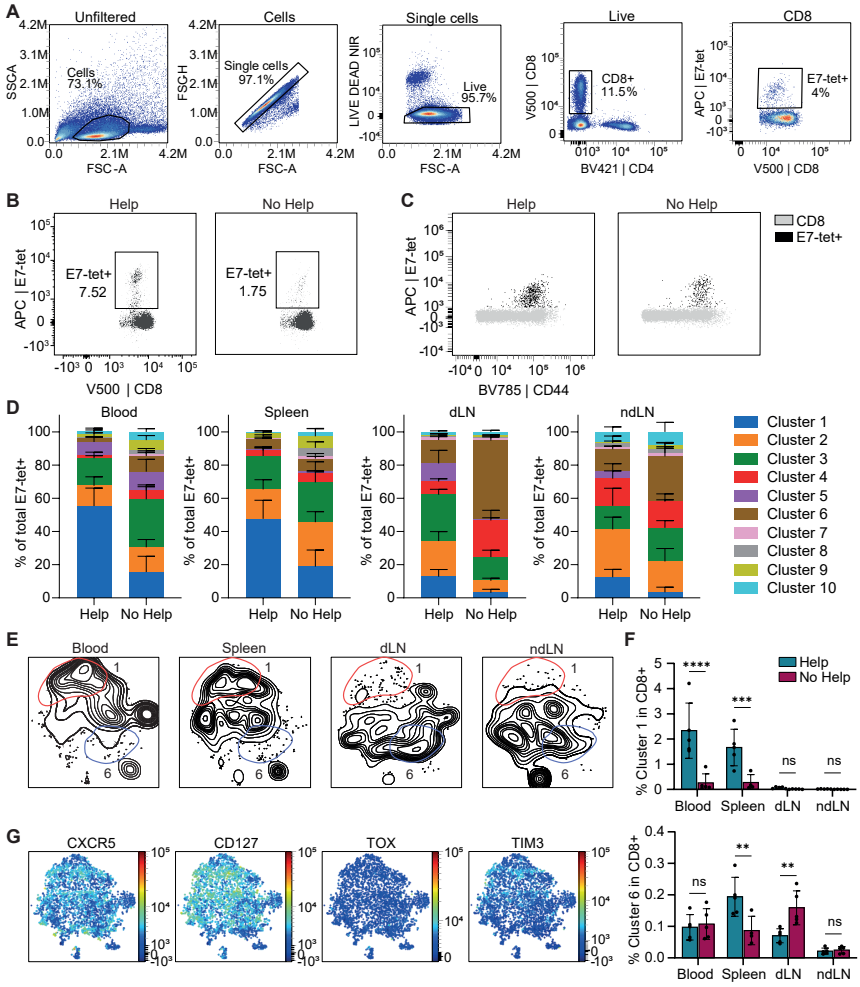

Supplementary Figure 1. Gating and phenotyping of antigen-specific CD8⁺ T cells after Help and No Help vaccination. Mice were vaccinated under Help or No Help conditions at day 0, 3, and 6 and sacrificed at day 10 after which blood, spleen, dLN and ndLN were analyzed as described in Figure 1. (A) Gating strategy for antigen-specific (E7-tetramer⁺) CD8⁺ T cells at day 10 after vaccination. Gating strategy is shown for 1 blood sample, but was used consistently for all experiments and organs. (B-C) Representative FACS plots from one mouse per group, showing E7-tetramer⁺ CD8⁺ cells in blood at day 11 after vaccination (B) and CD44 expression in E7-tet⁺ and total CD8⁺ in spleen at day 10 (C). (D-G) Opt-SNE visualization and FlowSom clustering of E7-tetramer⁺ CD8⁺ T cells at day 10 after Help or No Help vaccination was performed as shown in Figure 1E. (D) Frequency of tetramer⁺ CD8⁺ T cells per cluster per organ. (E) Distribution of cells from different organs across opt-SNE. (F) Frequency of Cluster 1 and Cluster 6 E7-tetramer+ cells in total CD8+ T cells per organ after Help versus No Help vaccination. (G) Expression of additional differentiation markers on cumulative E7-tetramer⁺ CD8⁺ T cells from all experimental settings visualized by opt-SNE. Data are from 1 experiment, representative of 2 independent experiments with n=5 mice per group. ns, not significant, **P <0.005, ***P < 0.001 and ****P < 0.0001.

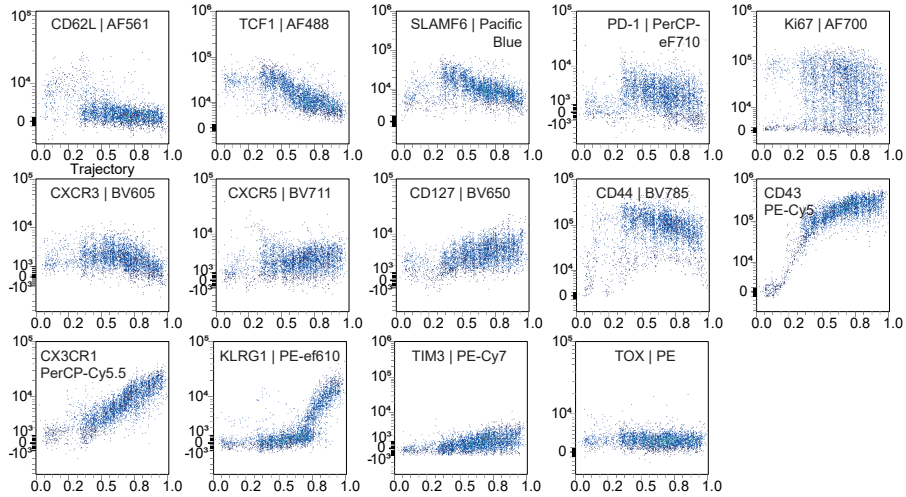

Supplementary Figure 2. Expression of marker proteins along the CTL differentiation spectrum upon vaccination. Antigen-specific E7-tetramer$^+$ CD8$^+$ T cells from blood, spleen, dLN and ndLN at day 10 after Help or No Help vaccination were analyzed by flow cytometry using the differentiation marker panel, as shown in Figure 2. FACS plots showing expression levels of each differentiation marker against the Wanderlust trajectory score. Data are from 1 experiment, representative of 2 independent experiments with n=5 mice per group.

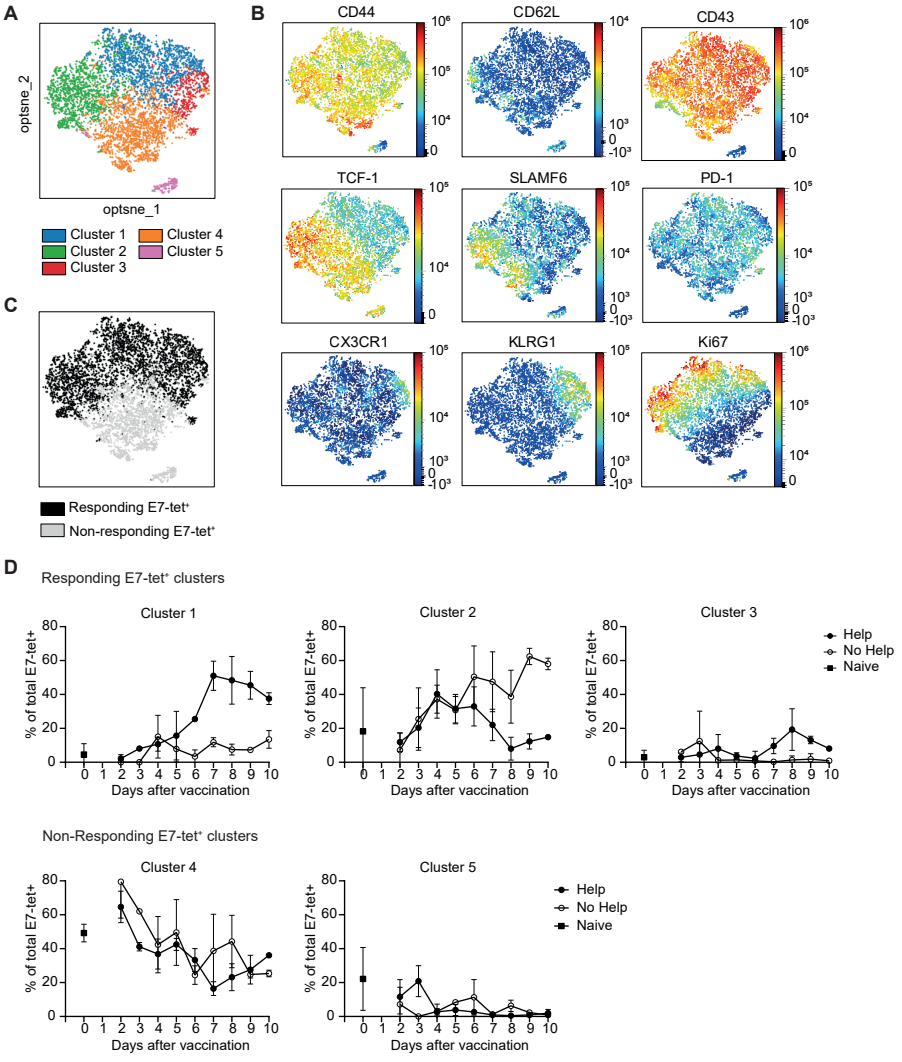

Supplementary Figure 3. Selection of responding E7-tetramer⁺ clusters for analysis over time. Experimental details related to the timecourse experiment depicted in Figure 3. Mice received Help or No Help vaccination at day 0, 3 and 6, and different cohorts of mice were sacrificed at day 2-10 after first vaccination (A) Opt-SNE dimension reduction and FlowSom clustering of E7-tetramer⁺ CD8⁺ T cells form dLN of vaccinated mice (n=3 per group per timepoint), and 3 naive LNs. (B) Expression of differentiation markers on cumulative E7-tetramer⁺ CD8⁺ T cells from all experimental settings visualized by opt-SNE. (C) Responding and non-responding E7-tetramer⁺ CD8⁺ T cells in opt-SNE. (D) Frequencies of responding E7-tetramer⁺ clusters and non-responding E7-tetramer⁺ clusters in naive LNs and at different timepoints after vaccination. Responding clusters were determined by a frequency of <20% in naive LN, and a change in frequency between different timepoints after vaccination. Responding E7-tetramer⁺ CD8⁺ T cells from vaccinated mice (day 2-10) were used for further analysis as shown in Figure 3.

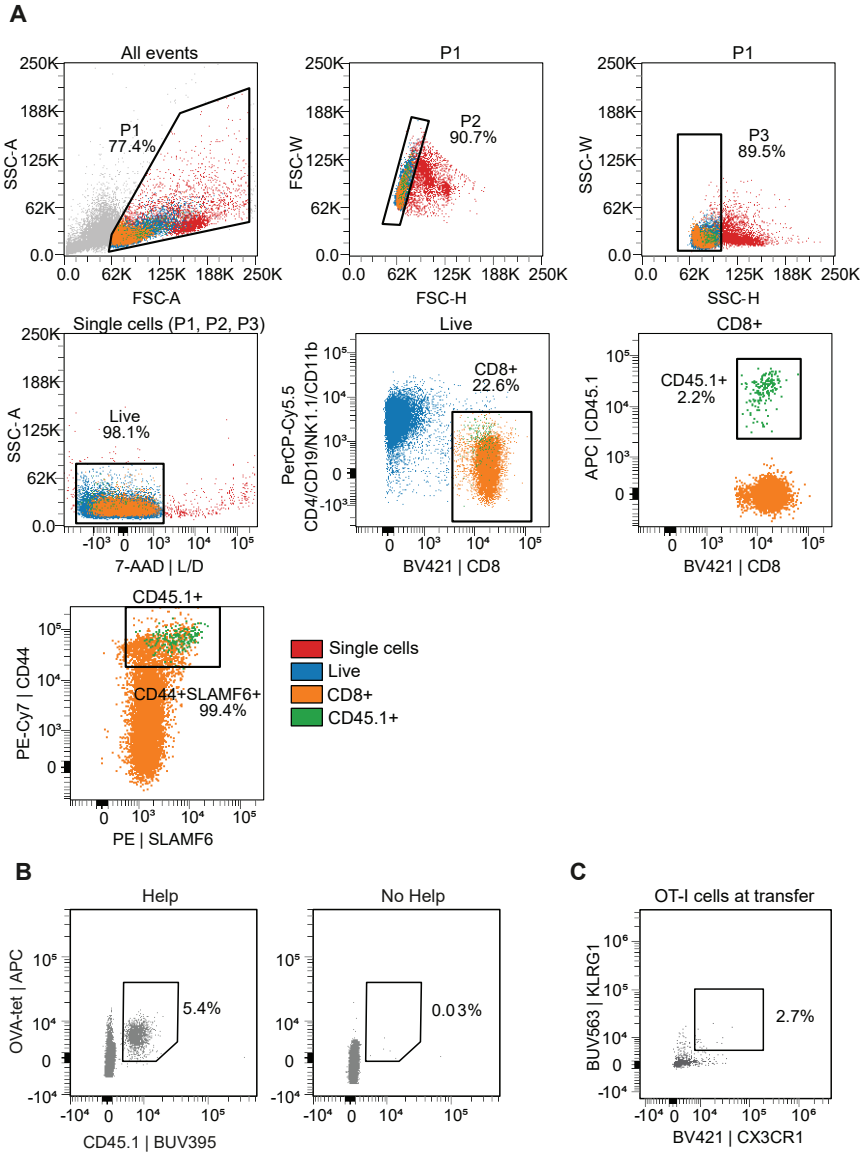

Supplementary Figure 4. Adoptive transfer of helpless OT-I cells. Naïve CD45.1$^+$ $OVA_{257/264}$/H-2K^b-specific OT-I cells were adoptively transferred to CD45.2$^+$ recipient mice, which were subsequently vaccinated with No Help vaccine encoding the $OVA_{257/264}$ epitope, as shown in Figure 3. (A) Sorting strategy of CD44$^+$SLAM-F6$^+$CD45.1$^+$CD8$^+$ (OT-I) T cells from dLN at day 10 after vaccination of the primary recipient mice. Sorting was performed on pooled dLNs from 5 mice and these cells were used for adoptive transfer into secondary CD45.2$^+$ recipient mice. (B) Representative FACS plots from one mouse per group, showing OT-I cells in blood at day 21, which is day 10 after secondary recipient vaccination. (C) Manual gating of KLRG1$^+$CX3CR1$^+$ effector cells within the pooled population of OT-I cells before transfer to secondary recipients.

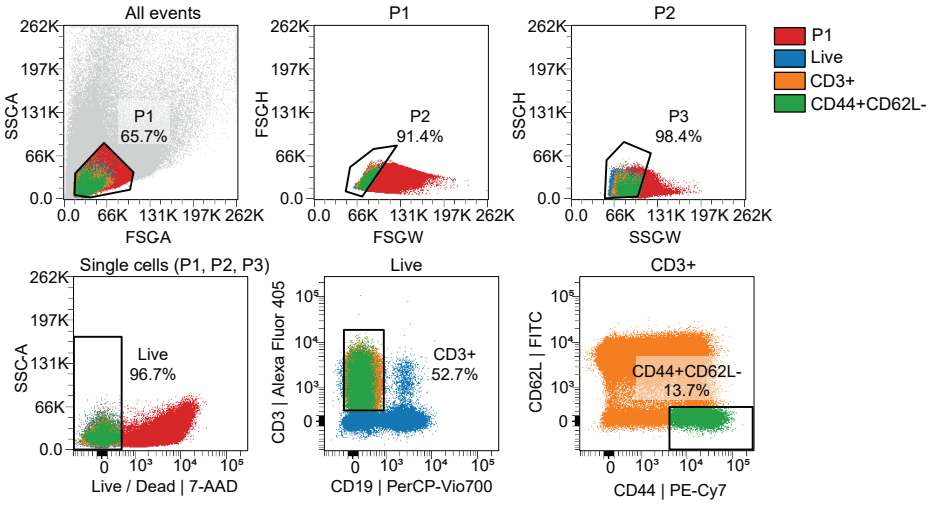

Supplementary Figure 5. Sorting strategy of activated T cells for scRNAseq. Sorting strategy for the scRNAseq experiment depicted in Figure 4. Mice were vaccinated under E7-Help or No Help conditions (n=3 per group) and activated T cells were flow cytometrically sorted per experimental group from pooled dLN or ndLN at day 5 or day 10, on a $CD3^{+}CD44^{+}CD62L^{-}$ phenotype.

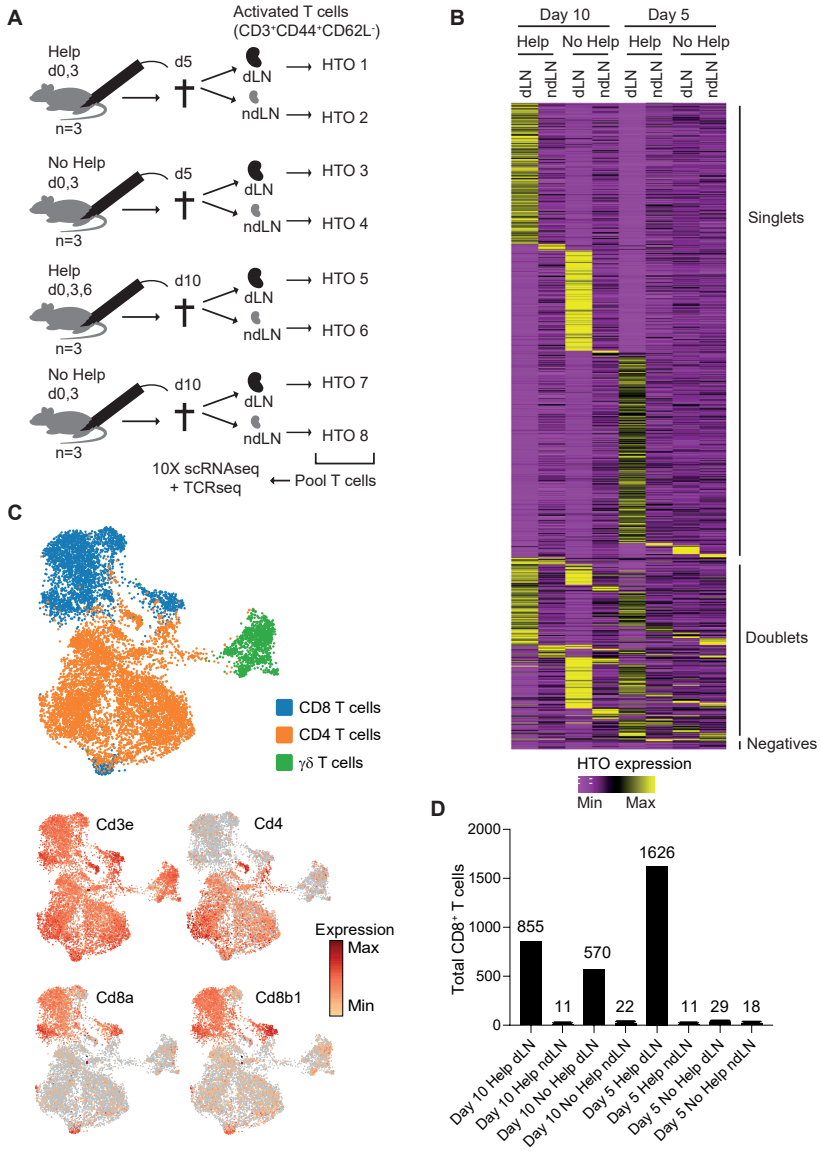

Supplementary Figure 6. Generation and processing of scRNAseq data of CD8⁺ T cells after Help or No Help vaccination. Experimental details related to the scRNAseq experiment depicted in Figure 4. (A) Experimental setup. Mice (n=3 per group) received E7-Help or No Help vaccination at the indicated days and were sacrificed at day 5 or day 10, after which dLN and ndLN were isolated and pooled per group. Activated T cells were sorted and labeled with MHC-II/CD45 antibody-coupled hashtag oligonucleotide (HTO) as indicated. T cells from all HTO groups were pooled and subjected to 10x Genomics scRNAseq, coupled to TCRseq. (B) Heatmap showing HTO demultiplexing results. The color scale indicates expression levels of HTO corresponding to each experimental condition per cell. (C) Expression of canonical T cell marker genes across UMAP of activated T cells, for identification of CD8⁺, CD4⁺ and γδT cells.(D) Number of CD8⁺ T cells per experimental condition after the entire procedure, as identified by HTO expression level.

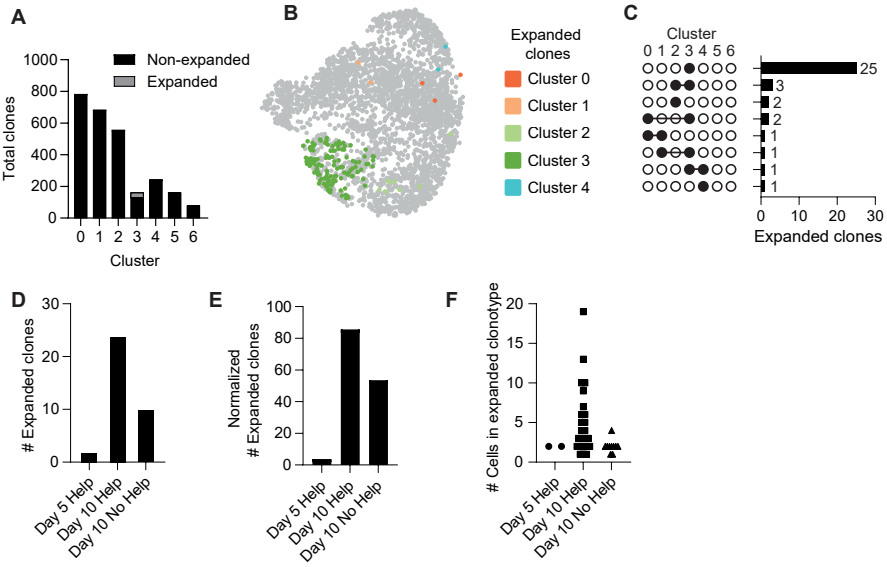

Supplementary Figure 7. Quantification and characterization of expanded TCR clones within CD8⁺ T cells after vaccination under Help or No Help conditions. Experimental details related to the TCRseq analysis depicted in Figure 4. (A) Quantification of distinct TCR clones that are non-expanded (containing 1 cell) or expanded (containing 2 or more cells) in each of the CD8⁺ T cell clusters identified in Figure 4A. (B) UMAP showing CD8⁺ T cells from expanded clones per CD8⁺ T cell cluster. (C) Number of unique expanded TCR clones, of which all cells are found within one cluster (indicated by one black circle), and shared TCR clones, containing cells that are found in multiple clusters (indicated by multiple connected black circles). (D, E) Number of expanded TCR clones per experimental condition, absolute (D) and normalized to number of cells per condition (E). (F) Number of cells belonging to each expanded clonotype per experimental condition.

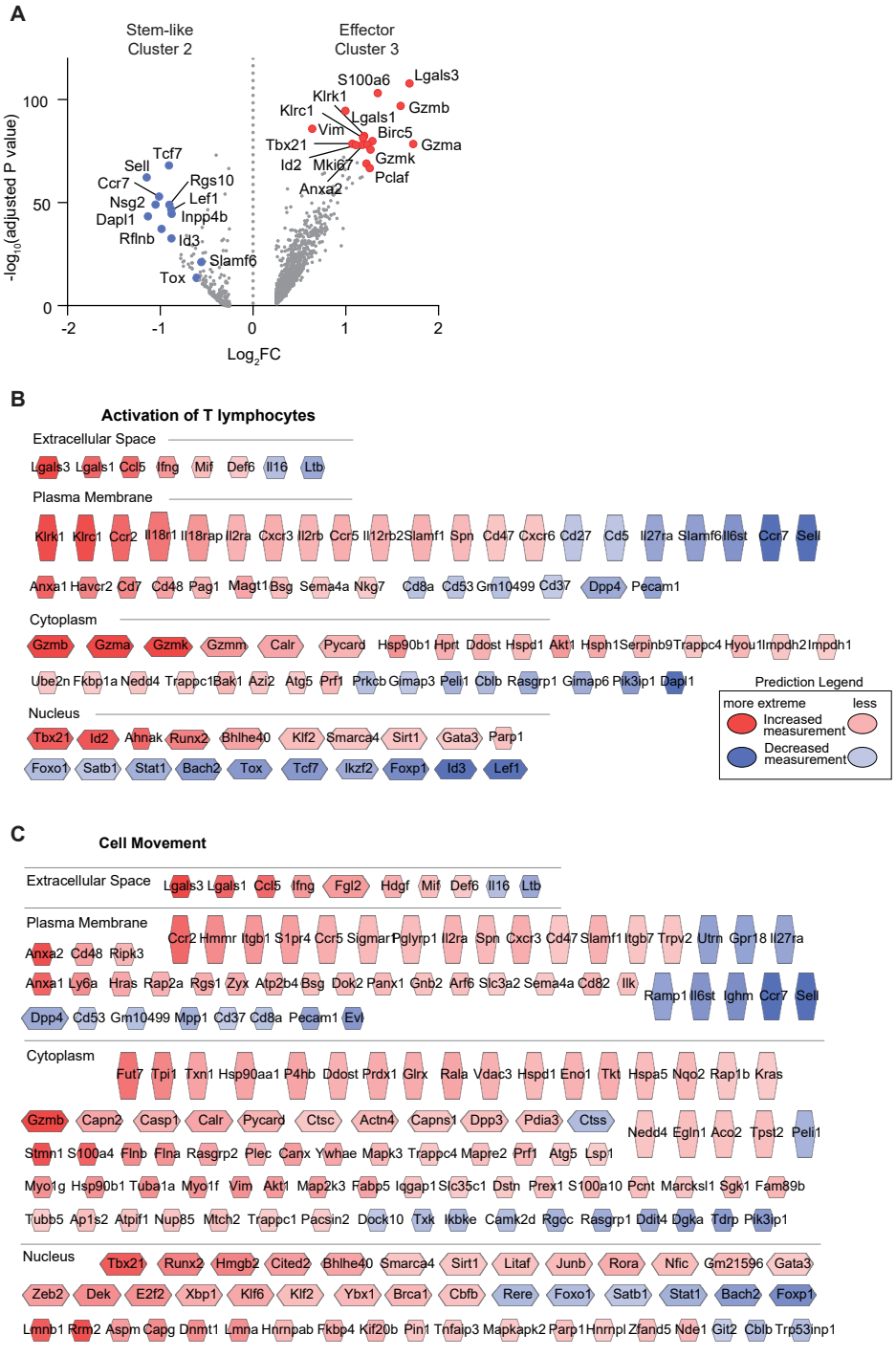
A
Stem-like
Cluster 2
Effector
Cluster 3
-log10(adjusted P value)
Log2FC
Tcf7
Sell
Ccr7
Rgs10
Nsg2
Lef1
Dapl1
Inpp4b
Rflnb
Id3
Slamf6
Tox
S100a6
Lgals3
Klrk1
Klrc1
Gzmb
Lgals1
Vim
Birc5
Tbx21
Gzma
Id2
Mki67
Gzmk
Pclaf
Anxa2
B
Activation of T lymphocytes
Extracellular Space
Lgals3 Lgals1 Ccl5 Ifng Mif Def6 Il16 Ltb
Plasma Membrane
Klrk1 Klrc1 Ccr2 Il18r1 Il18rap Il2ra Cxcr3 Il2rb Ccr5 Il12rb2 Slamf1 Spn Cd47 Cxcr6 Cd27 Cd5 Il27ra Slamf6 Il6st Ccr7 Sell
Anxa1 Havcr2 Cd7 Cd48 Pag1 Magt1 Bsg Sema4a Nkg7 Cd8a Cd53 Gm10499 Cd37 Dpp4 Pecam1
Cytoplasm
Gzmb Gzma Gzmk Gzmm Calr Pycard Hsp90b1 Hprt Ddost Hspd1 Akt1 Hsph1 Serpinb9 Trappc4 Hyou1 Impdh2 Impdh1
Ube2n Fkbp1a Nedd4 Trappc1 Bak1 Azi2 Atg5 Prf1 Prkcb Gimap3 Peli1 Cblb Rasgrp1 Gimap6 Pik3ip1 Dapl1
Nucleus
Tbx21 Id2 Ahnak Runx2 Bhlhe40 Klf2 Smarca4 Sirt1 Gata3 Parp1
Foxo1 Satb1 Stat1 Bach2 Tox Tcf7 Ikzf2 Foxp1 Id3 Lef1
Prediction Legend
more extreme
less
Increased measurement
Decreased measurement
C
Cell Movement
Extracellular Space
Lgals3 Lgals1 Ccl5 Ifng Fgl2 Hdgf Mif Def6 Il16 Ltb
Plasma Membrane
Anxa2 Cd48 Ripk3
Ccr2 Hmmr Itgb1 S1pr4 Ccr5 Sigmar1 Plgrp1 Il2ra Spn Cxcr3 Cd47 Slamf1 Itgb7 Trpv2 Utrn Gpr18 Il27ra
Anxa1 Ly6a Hras Rap2a Rgs1 Zyx Atp2b4 Bsg Dok2 Panx1 Gnb2 Arf6 Slc3a2 Sema4a Cd82 Ilk
Ramp1 Il6st Ighm Ccr7 Sell
Dpp4 Cd53 Gm10499 Mpp1 Cd37 Cd8a Pecam1 Evl
Cytoplasm
Fut7 Tpi1 Txn1 Hsp90aa1 P4hb Ddost Prdx1 Glrx Rala Vdac3 Hspd1 Eno1 Tkt Hspa5 Nqo2 Rap1b Kras
Gzmb Capn2 Casp1 Calr Pycard Ctsc Actn4 Capns1 Dpp3 Pdia3 Ctss
Nedd4 Egln1 Aco2 Tpst2 Peli1
Stmn1 S100a4 Flnb Flna Rasgrp2 Plec Canx Ywhae Mapk3 Trappc4 Mapre2 Prf1 Atg5 Lsp1
Myo1g Hsp90b1 Tuba1a Myo1f Vim Akt1 Map2k3 Fabp5 Iqgap1 Slc35c1 Dstn Prex1 S100a10 Pcnt Marcksl1 Sgk1 Fam89b
Tubb5 Ap1s2 Atpif1 Nup85 Mtch2 Trappc1 Pacsin2 Dock10 Txk Ikbke Camk2d Rgcc Rasgrp1 Ddit4 Dgka Tdrp Pik3ip1
Nucleus
Tbx21 Runx2 Hmgb2 Cited2 Bhlhe40 Smarca4 Sirt1 Litaf Junb Rora Nfic Gm21596 Gata3
Zeb2 Dek E2f2 Xbp1 Klf6 Klf2 Ybx1 Brca1 Cbfb Rere Foxo1 Satb1 Stat1 Bach2 Foxp1
Lmnb1 Rrm2 Aspm Capg Dnmt1 Lmna Hnrnpab Fkbp4 Kif20b Pin1 Tnfaip3 Mapkapk2 Parp1 Hnrnpl Zfand5 Ndel1 Git2 Cblb Trp53inp1

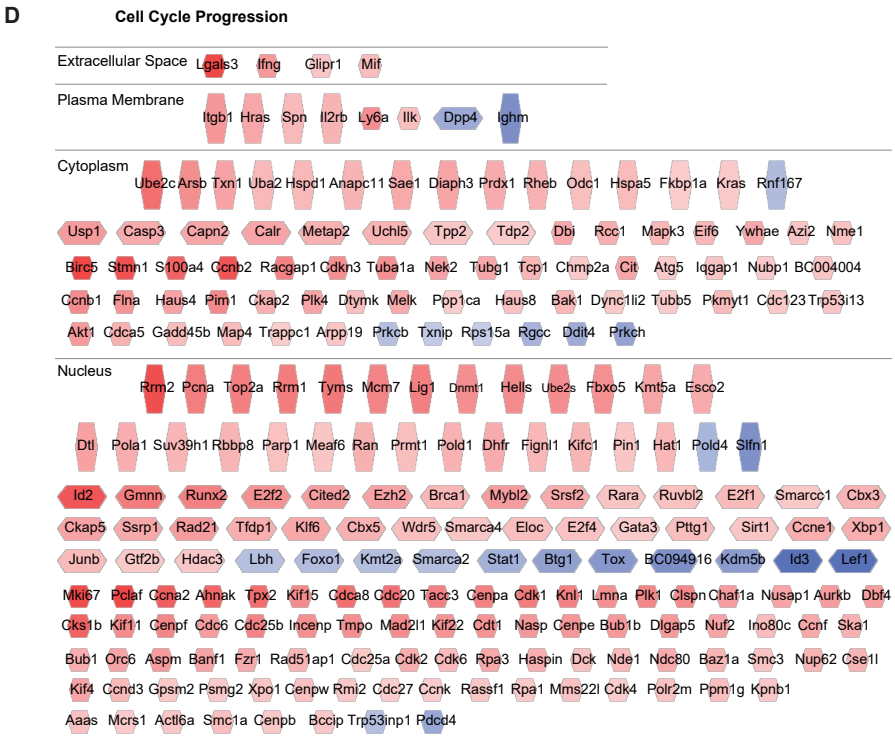

Supplementary Figure 8. Functional differences between effector and stem-like CD8⁺ T cells. (A) Volcano plot showing genes that are differentially expressed between Cluster 2 and Cluster 3. (B-D) Ingenuity Pathway Analysis (IPA) showing transcripts in the category "Activation of T lymphocytes" (B), "Cell Movement" (C) and "Cell Cycle Progression" (D), with high (red) or low (blue) expression levels in helped effector Cluster 3 as compared to stem-like Cluster 2.

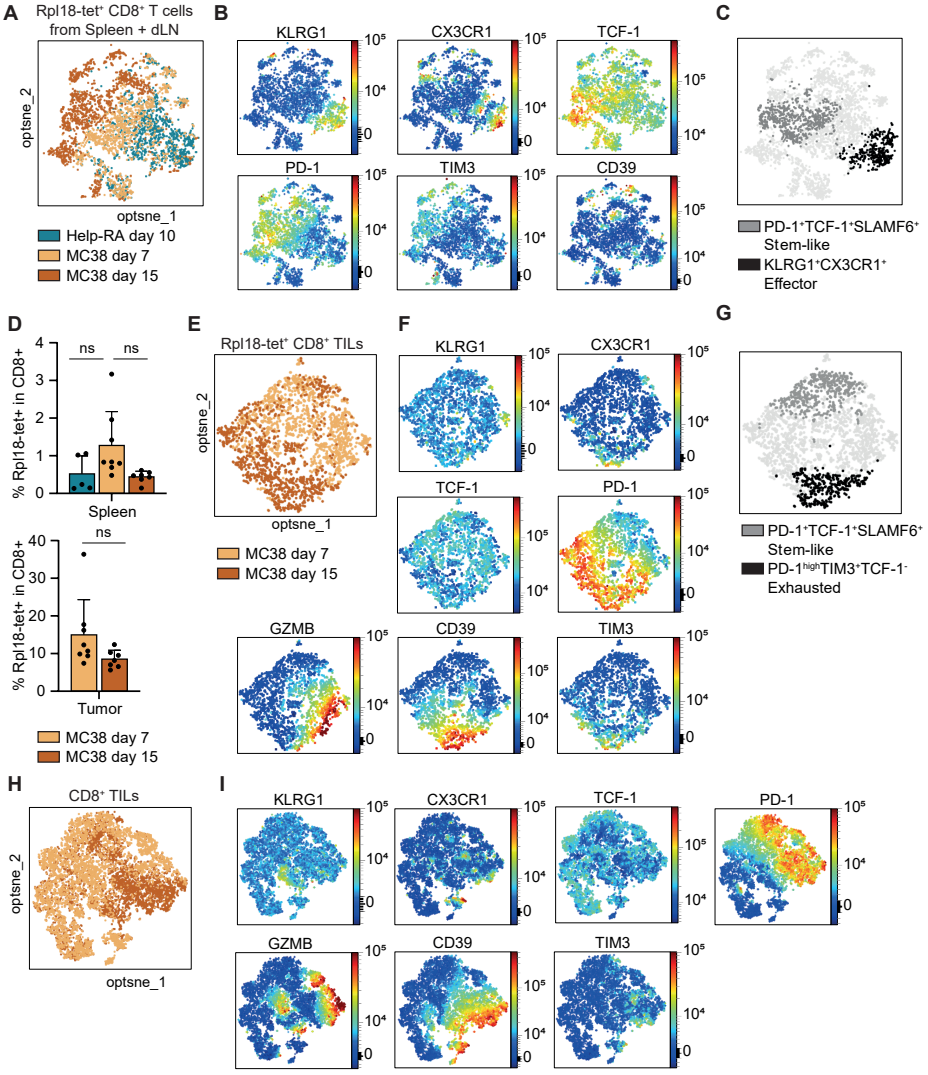

Supplementary Figure 9. Characterization of antigen-specific CD8+ T cells raised after vaccination or tumor implantation. (A) Opt-SNE visualization of Rpl18-tetramer+ CD8+ T cells from spleen and dLN after Help-RA vaccination or MC38 tumor implantation, as described in Figure 6. (B) Expression of differentiation markers on cumulative Rpl18-tetramer+ CD8+ T cells in spleen and dLN from the experimental settings visualized by opt-SNE in panel A. (C) Visualization of the PD-1+TCF-1+ stem-like and KLRG1+CX3CR1+ effector populations within opt-SNE. (D) Percentage of Rpl18-tetramer+ CD8+ T cells in spleen and the MC38 tumor, in the experiment depicted in Figure 7E-M. (E) Opt-SNE visualization of Rpl18-tetramer+ CD8+ TILs harvested from MC38 tumors at days 7 or day 15.(F) Expression of differentiation markers on cumulative Rpl18-tetramer+ CD8+ TILs visualized by opt-SNE. (G) Visualization of the PD-1hiTIM3+TCF-1- exhausted and PD-1+TCF-1+ stem-like populations within opt-SNE. (H) Opt-SNE visualization of total CD8+ TILs harvested from MC38 tumors at days 7 or day 15. (I) Expression of differentiation markers on cumulative total CD8+ TILs visualized by opt-SNE.

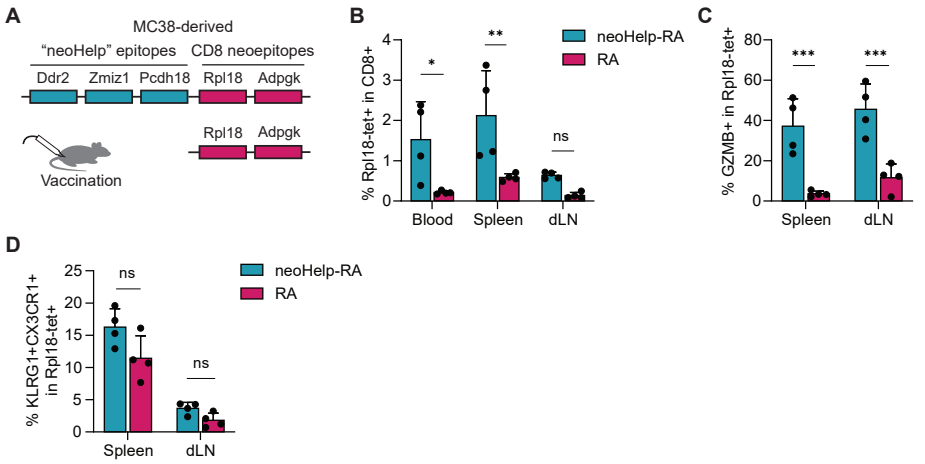

Supplementary Figure 10. Vaccination with neoHelp epitopes improves MC38-specific CTL response outside tumor context. (A) Experimental setup. Mice were vaccinated on day 0, 3 and 6 with DNA construct encoding the MC38-derived MHC-I restricted neoeptiopes mutated Rpl18 and Adpgk (RA), either alone or in conjunction with MC38-derived MHC-II restriced neoepitopes mutated Ddr2, Zmiz1 and Pcdh18 (neoHelp-RA). On day 10, mice were sacrificed and Rpl18-specifc (tet⁺) CD8⁺ T-cell responses were assessed.(B) Frequency of Rpl18-tetramer⁺ CD8⁺ T cells in indicated tissues on day 10. (C, D) Frequency of Granzyme-B (GZMB)⁺ cells (C) or KLRG1⁺CX3CR1⁺ effector cells (D) within the Rpl18-specific CD8⁺ T cell population in spleen and dLN. Data are from 1 experiment representative of 2 independent experiments, with n=4 mice per group. Error bars indicate SD. Statistical significance was calulated by two-way ANOVA and Sidak's multiple comparsions test. ns, non significant, *P < 0.05, **P < 0.005 and ***P < 0.001.

Description of Supplementary Tables

Supplementary Table 1.

Marker genes per cluster.

Supplementary Table 2.

Differentially expressed genes Cluster 2 and 3.

Supplementary Table 3.

Signature gene lists from literature.

All Supplementary Tables are available at DOI: 10.1136/jitc-2025-014041

Supplementary Methods

Vaccination

The Rpl18-Adpgk-Help vaccine was derived from the Help-E7SH plasmid[30] by replacing the E7SH sequence with codon-optimized sequences for mutated Adpgk (cacctggaactcgcgtccatgaccaacatggagctgatgtcctccatcgtgcatcag) and mutated Rpl18 (aaagcaggaggcaagattctgaccttcgacagactggcactgg-agagcccaaaa) epitopes[44], separated by an alanine linker. For both the neoHelp and neoHelp-RA vaccines, the coding sequences of the MC38 tumor-specific helper neoepitopes Pcdh18, Zmiz1, and Ddr2[45] were separated by glycine-proline linkers and preceded by a signal peptide sequence derived from the Help-E7SH vaccine. For the neoHelp-RA vaccine, the helper neoepitopes were linked to codon-optimized sequences for mutated Adpgk and mutated Rpl18, separated by an alanine linker. A 5' 27-base pair and a 3' 26-base pair flanking region with homology to KpnI- and NotI-linearized pVAX1 were added to the neoHelp and neoHelp-RA sequences. The complete DNA sequences were ordered as a gBlock from Integrated DNA Technologies (IDT), and assembled into linearized pVAX1 using NEBuilder HiFi DNA Assembly (New England Biolabs). All vaccines were verified by Sanger sequencing.

Flow cytometry staining

Cells from blood, spleen, LN and tumor were washed with FACS buffer (PBS + 2% FCS) and stained for 30 min on ice with 1:1000 LIVE/DEAD Near IR dye (Invitrogen) or 1:500 Zombie UV (Biolegend), 1:100 APC-conjugated H-2D^b/E7$_{49\text{-}57}$ tetramers, APC-conjugated H-2K^b/OVA$_{257\text{-}264}$ tetramers or APC-conjugated H-2K^b/KILTFDRL (mutated Rpl18) tetramers (produced in-house at LUMC) and combinations of the following monoclonal antibodies (mAbs) for surface staining: 1:100 CD45.1-BUV395 (clone A20, BD Bioscience); 1:100 CD45-BUV496 (clone 30-F11, BD Bioscience); 1:100 KLRG1-BUV563 (clone 2F1, BD Bioscience); 1:100 CD103-BUV661 (clone M290, BD Bioscience); 1:200 CD4-BUV805 (clone GK1.5, BD Bioscience); 1:800 CX3CR1-BV421 (clone SA011F11, Biolegend); 1:200 CD4-BV421 (clone GK1.5, Biolegend); 1:100 SLAMF6-Pacific Blue (clone 330-AJ, Biolegend); 1:100 CD8α-V500 (clone 53-6.7, BD Bioscience); 1:100 CD44-BV570 (clone IM7, Biolegend); 1:50 CXCR3-BV650 (clone CXCR3-173, Biolegend); 1:50 CD127-BV650 (clone A7R34, Biolegend); 1:50 CXCR5-BV711 (clone L138D7, Biolegend); 1:200 CD8α-BV750 (clone 53-6.7, BD Bioscience); 1:100 CD44-BV785 (clone IM7, Biolegend); 1:100 CD39-PE/Dazzle594 (clone Dua59, Biolegend); 1:200 TIM3-PE/Cy7 (clone RMT-23, eBioscience); 1:200 CD43-PE/Cy5 (clone 1B11, Biolegend); 1:100 CD3-PE/Fire700 (clone 17A2, Biolegend); 1:100 CD62L-PE/Fire810 (clone W18021D, Biolegend); 1:200 CD62L-AF561 (clone MEL-14, eBioscience); 1:200 KLRG1-PE/eF610 (clone 2F1, Invitrogen); 1:200 CX3CR1-PerCp/Cy5.5 (clone SA011F11, Biolegend); 1:200 PD-1-PerCP/eF710 (clone J43, eBioscience); 1:100 PD-1-APC/Fire810 (clone 29F.1A12, Biolgend). For intracellular staining, cells were fixed and permeabilized with the FOXP3/transcription factor staining buffer set (eBioscience), according to the manufacturer's protocol. Intracellular staining was performed for 30 min on ice in permeabilization buffer, using combinations of the following mAbs: 1:100 Helios-

BUV395 (clone 22F6, eBioscience); 1:100 TCF-1-AF488 (clone C63D9, Cell Signalling Technology); 1:200 GZMB-PE (clone GB-11, Sanquin); 1:100 TOX-PE (clone TXRX10, eBioscience); 1:100 GZMB-PE/CF594 (clone GB-11, BD Bioscience); 1:100 FOXP3-PE/Cy5 (clone FJK-16s, Invitrogen); 1:800 TOX-eF660 (clone TXRX10, eBioscience); 1:200 T-bet-eF660 (clone eBio4B10, eBioscience); 1:400 T-bet-AF660 (clone eBio4B10, eBioscience); 1:200 Ki67-AF700 (clone SolA15, eBioscience).

scRNAseq analysis

Preparation and quality control - Analysis of scRNAseq and TCRseq data was performed using CellRanger (10X Genomics, v6.0.1) and Seurat (v4.3.0) in R (v4.2.3). scRNAseq reads were aligned to the mouse reference genome mm10, and barcode counting was performed using 'cellranger count'. TCRseq reads were aligned to the mouse reference genome mm10 and consensus TCR sequences were determined using 'cellranger vdj'. From the gene expression count matrix, TCR and BCR genes were removed using the 'grep' function in R with the patterns "^Tr[abgd][cvdj]" and "Ig[hkl][cvdj]" respectively. After this, the dataset was analyzed in R using the standard Seurat pipeline. Seurat object was created using 'CreateSeuratObject', with a minimum of 200 features per cell and 3 cells expressing each gene. HTO sequencing data was added as a separate assay to the Seurat object using 'CreateAssayObject' and HTO counts were normalized by CLR method using 'NormalizeData'. HTO demultiplexing was performed using 'HTODemux' with a positive quantile of 0.99. As a result of this, each cell in the dataset was assigned to a global HTO classification (singlet, doublet, or negative), and a HTO classification (Day-5-Help-dLN, Day-5-Help-ndLN, Day-5-No-Help-dLN, Day 5-No-Help-ndLN, Day-10-Help-dLN, Day-10-Help-ndLN, Day-10-No-Help-dLN, Day 10-No-Help-ndLN, doublet or negative). Heatmap was created of HTO demultiplexing result using 'HTOHeatmap' (Supplementary Figure 6B). Singlets were selected using 'subset', and gene expression data was normalized using 'NormalizeData'. Variable features were determined using 'FindVariableFeaures' with the selection method 'mean.var.plot'. Data was scaled using 'ScaleData' on variable features. Percentage of mitochondrial gene expression per cell was determined using 'PercentageFeatureSet' with the pattern "^mt-". Singlets were filtered on number of RNA features (between 400 and 5000), number of RNA counts (<25000) and mitochondrial gene expression (<10%). Cell cycle scores for G2/M and S phase were assigned using 'CellCycleScoring', based on expression of G2/M and S phase genes. Data was normalized using 'NormalizeData' with normalization method 'LogNormalize', scale factor 25000. Top 2000 variable features were determined using 'FindVariableFeatures' with the selection method 'vst'. Data was scaled using 'ScaleData', whereby G2M scores, S scores and percentage of mitochondrial gene expression were regressed out. Principle component analysis (PCA) was run using 'RunPCA' on variable features. Clustering was performed on first 20 principle components (PCs) using 'FindNeighbors' and 'FindClusters'. Clustering resolution was set to 0.5. Uniform manifold approximation and projection (UMAP) visualization was performed using 'RunUMAP' on the first 20 PCs. Expression of known marker genes was visualized per cluster and within the UMAP projection using 'Dotplot', 'VlnPlot' and 'FeaturePlot' functions. Clusters with contaminating B cells (expression of *Cd19,*

Ms4a1), APCs (expression of *Cd40, Cd274, Cd80, Cd86*) and low quality cells (high percentage mitochondrial genes, low RNA counts) were removed. The pipeline was run again on filtered T cells, including determining variable features, data scaling, PCA, clustering and UMAP visualization. Clustering and UMAP visualization was performed on the first 50 PCs. $CD8^+$ T-cell clusters were selected by expression of *Cd8a, Cd8b1*, in absence of expression of *Cd4* (Supplementary Figure 6C). Within the $CD8^+$ T-cell subset, number of cells per HTO was determined (Supplementary Figure 6D). HTOs containing <30 $CD8^+$ T cells were excluded from further analysis.

Gene expression analysis - The pipeline was run again on $CD8^+$ T cells from selected HTOs, including determining variable features, data scaling, PCA, clustering and UMAP visualization. Clustering and UMAP visualization were performed on the first 20 PCs. UMAP embeddings, cluster annotations and HTO annotations per cell were exported from Seurat, and visualized using Loupe Browser (v6.4.1, 10X Genomics). Marker genes per cluster were calculated using 'FindAllMarkers', selecting only upregulated genes expressed in >25% of cells in the cluster, with a logFC threshold of 0.25. $CD8^+$ T-cell clusters were annotated based on expression of marker genes per cluster, as well as the expression of manually selected genes with well-known functions in T-cell differentiation according to the literature. Functional classification of differentially expressed genes between Cluster 2 and Cluster 3 was performed using Ingenuity Pathway Analysis (Qiagen).

TCRseq analysis - Sequences of CDR3 and VDJ gene annotations of paired TCRα and TCRβ chains were analyzed using Loupe VDJ Browser (v5.0.0, 10X Genomics). Expanded clones were identified as TCR clonotypes containing 2 or more cells. TCR sequences from Loupe VDJ Browser, and UMAP projection and cluster annotation from Seurat were visualized together using Loupe Browser (v6.4.1, 10X Genomics). For determining expanded clonotypes per differentiation cluster, only cells that grouped together in the UMAP with their assigned cluster were included for quantification.

Trajectory analysis was performed using Seurat and Monocle3 (v1.3.1) in R. Seurat object of $CD8^+$ T cells from selected HTOs was converted into cell data set object using 'as.cell_data_set', after which partitions, cluster annotations and UMAP embeddings were added manually. Trajectory was plotted using 'learn_graph', after which the trajectory branch of interest (from Cluster 0 to Cluster 3) was selected using 'choose_graph_segments'. Pseudotime was calculated using 'order_cells', and pseudotime values per cell were exported for visualization using GraphPad Prism and Loupe Browser.

For *comparison of our scRNAseq data to published gene signatures*, top 200 marker genes of $TCF1^+$ progenitor (cluster 9) and effector (cluster 6) $CD8^+$ T cells from chronic and acute LCMV infection were downloaded from Table S5 from Pritykin *et al.* 2021[7]. These top 200 genes were used to calculate a module score for each cell in our $CD8^+$ T cells from selected HTOs, using the function 'AddModuleScore' in R. The same method was performed using top 100 marker genes of stem-like $CD8^+$ T cells from the TdLN, (cluster 4) as published by Connolly *et al.* 2021[41], which were provided upon request.

Generation of MC38-Help cells

pCDH-EF1a-IRES-eGFP was linearized using BamHI-HF and NotI-HF (New England Biolabs, NEB). The HELP coding sequence was fused to a 3xFLAG sequence, and a 5' 20-base pair flanking region (tcaggtgtcgtgagcaattg) and a 3' 20-base pair flanking region (gctacgtaaattccgcccct) were added that are homologous to the linearized pCDH-EF1a-IRES-eGFP. The full DNA sequence was ordered as a gBlock (IDT) and NEBuilder HiFi DNA Assembly (NEB) was used to assemble pCDH-EF1a-HELP-3xFLAG-IRES-eGFP.

Third-generation lentiviruses were produced by transfecting HEK293T cells with pCMV-VSVG, pMDLg-RRE, pRSV-REV, and pCDH-EF1a-HELP-3xFLAG-IRES-eGFP. Medium was refreshed the next day and 48 hours post-transfection lentivirus-containing medium was centrifuged at 700 xg for 10 minutes to remove debris and filtered through a 0.45 µm filter (Millex Low Protein Binding Durapore, Millipore). MC38 cells were reverse transduced with lentivirus encoding EF1a-HELP-3xFLAG-IRES-eGFP in the presence of 8 µg/mL polybrene. Medium was refreshed one day after transduction and eGFP-expressing MC38 cells were sorted one week after transduction to obtain MC38-HELP cells. HELP-3xFLAG expression in MC38-HELP cells was validated by western blot.

Chapter 5

Requirements for development of T-helper1 and T-follicular helper cells from a common precursor

Douwe M. T. Bosma[1,2*], Julia Busselaar[1,2*], Mo D. Staal[1,2**], Mylene de Koning[1**], Mirna Reljić[1], Xin Lei[1,2], Tom de Wit[1,2], Yanling Xiao[1,2], Jannie Borst[1,2,3***] and Fiamma Salerno[1***]

[1]Department of Immunology;

[2]Oncode Institute, Leiden University Medical Center, 2333 ZA Leiden, The Netherlands

*Shared first authors;

**Shared second authors;

***Shared last authors

Cell Reports 2026; 45(5): 117296

DOI: 10.1016/j.celrep.2026.117296

Abstract

T-helper1 (Th1) and T-follicular helper (Tfh) cells support cellular and humoral immunity, respectively. How activated $CD4^+$ T cells commit to these fates remains unclear. Using a mouse vaccination model, we traced endogenous, polyclonal $CD4^+$ T cells during bifurcation into Th1 and Tfh lineages. We found that Th1 and Tfh cells originate from shared, highly proliferative $TCF1^+SLAMF6^+PD\text{-}1^+$ precursor clones that co-express Th1- and Tfh-related transcription factors and chemokine receptors, including T-bet, BCL6, CXCR3 and CXCR5. Generation of common Th1/Tfh precursors from naive $CD4^+$ T cells requires CD28 costimulation, but occurs independently of CD40, ICOS, and interaction with type-1 conventional dendritic cells (cDC1s) or B cells. Lineage commitment subsequently diverges: differentiation into Th1 cells relies on CD40 costimulation and cDC1s, whereas differentiation into Tfh cells requires ICOS costimulation and B cells. Activated $CD4^+$ T cells thus give rise to a common Th1/Tfh precursor whose fate depends on interactions with distinct antigen-presenting cells.

Introduction

Upon antigen encounter within secondary lymphoid organs, CD4$^+$ T cells are activated, clonally expand and initiate differentiation into T-helper (Th)1, 2 or 17 lineages to regulate cellular immunity[1]. At the same time, T-follicular helper (Tfh) cells are formed, which promote B-cell expansion and differentiation in germinal centers (GC)[2]. During a type-I immune response, Th1 and Tfh cells emerge in parallel, suggesting a bifurcation in their effector differentiation trajectories[3-5]. Tfh cells are likewise generated in parallel with Th2 or Th17 effector CD4$^+$ T cells[6,7] and acquire pathogen-tailored functional diversity[8]. Coordination of cell-mediated and humoral immunity thus depends on Th/Tfh lineage decision making in activated CD4$^+$ T cells. This process is a potential target for therapeutic intervention e.g. in vaccination, cancer and auto-immunity.

Effector CD4$^+$ T-cell differentiation relies on successive interactions with different professional antigen-presenting cells (APCs) and is initiated upon cognate contact with conventional dendritic cells (cDCs). Among these, the cDC2 lineage excels at (soluble) antigen presentation in major histocompatibility complex (MHC)-II molecules[9] and is important for initial CD4$^+$ T-cell activation[10,11]. The cDC1 lineage is much more proficient in phagocytosing cell-bound antigen and cross-presenting this in MHC-I molecules, thus playing a crucial role in CD8$^+$ T-cell activation[12-14]. cDC1s can also contribute to CD4$^+$ T-cell priming[15,16] and relay help for effector and memory differentiation of CD8$^+$ T cells[17,18]. In contrast, B cells are considered essential APCs to promote CD4$^+$ T-cell differentiation into Tfh cells[4,19].

In general, effector differentiation of CD4$^+$ T cells is guided by the activation and maturation state of cDCs and B cells, which are reflected in their costimulatory and cytokine profiles[1,7,10]. These inputs, as delivered during multiple sequential interactions between T cells and APCs, collectively regulate expression of lineage-determining transcription factors that direct Th differentiation along specific trajectories. Decision-making between Th and Tfh lineage commitment likewise depends on specific transcription factors. Whereas transient co-expression of T-bet and BCL6 has been reported in *in vitro* T-cell cultures[20], *in vivo* studies indicate that the choice between Th1 and Tfh cell differentiation depends on the ratio of T-bet versus BCL6 protein levels, which is determined by initiation of negative regulatory circuits. For example, BCL6 represses genes encoding Th1, Th2 and Th17 lineage-specific transcription factors, including *Tbx21* (encoding T-bet), *Gata3* and *Rora*[21,22]. However, when it binds to T-bet, BCL6 can no longer repress the *Prdm1* gene encoding BLIMP1. As a result, BLIMP1 starts to suppress Tfh-associated genes, thus favoring Th1 differentiation[23,24]. In contrast, transient early T-bet expression is required for upregulation of CXCR5 and generation of IFNγ-producing Tfh cells in response to infection[25,26].

CD4$^+$ T-cell differentiation to either Th1 or Tfh cell fate has largely been studied as separate processes[3], rather than interrogating how these parallel outcomes emerge within the same immune response. Also, much of our current understanding derives from experimental systems

based on T-cell receptor (TCR) transgenic CD4$^+$ T cells[4,27-29], leaving open the question of how Th1 and Tfh differentiation unfolds within endogenous, polyclonal CD4$^+$ T-cell populations. This is a relevant distinction, since TCR affinity has been proposed to impact CD4$^+$ T-cell fate decisions in some studies[28-30], but not in others[10,27], highlighting the need to examine differentiation dynamics in polyclonal contexts. In addition, deconvolution of CD4$^+$ T-cell differentiation trajectories *in vivo* can be challenged by the high plasticity of T-helper lineages[31,32] and stochastic events[33]. As a result, the temporal and mechanistic relationships between early activation states and downstream Th1 or Tfh commitment remain poorly defined in intact immune responses. Addressing these gaps is essential for understanding how immune responses are tailored toward cellular or humoral immunity and for identifying stages at which CD4$^+$ T-cell fate might be therapeutically redirected.

In this study, we used a vaccination-based mouse model to induce and longitudinally trace Th1 and Tfh cell differentiation from endogenous, polyclonal CD4$^+$ T cells. By integrating high-dimensional flow cytometry with single-cell RNA-sequencing (scRNAseq) and TCR-sequencing, we show that antigen-specific CD4$^+$ T clones pass through a common Th1/Tfh precursor state, before committing to a specific differentiation trajectory. We define the gene and protein expression profile of this precursor, demonstrate its presence across different infectious contexts in mice, and identify key costimulatory signals and antigen-presenting cell interactions that guide its formation and commitment toward either the Th1 or Tfh lineage. Together, these findings provide mechanistic insight into how CD4$^+$ T-cell fate decisions are regulated in physiologically relevant, polyclonal immune responses.

Results

Vaccination raises endogenous, functional Th1 and Tfh cells in equal measure

To study how endogenous, polyclonal CD4$^+$ T cells differentiate *in vivo*, we used a mouse vaccination model that has previously revealed the effects of CD4$^+$ T-cell help on effector and memory CD8$^+$ T-cell differentiation[34-36]. In this model, we vaccinate C57BL/6 mice with plasmid DNA encoding an immunodominant MHC-I (H-2D^b) restricted epitope $E7_{48-57}$ from human papilloma virus (HPV) either alone (Control) or linked to three MHC-II-restricted helper epitopes: p30, PADRE, and NEF (MHC-II) (Figure 1A). These MHC-II-restricted epitopes were selected for binding to human HLA-DP, -DQ and -DR, respectively[37], but p30 and PADRE can also be presented by MHC-II (I-A^b)[38,39] and prime CD4$^+$ T-cell responses in mice[34,40]. The plasmid DNA vaccine is "tattooed" on days 0, 3 and 6 into the depilated skin of the hind leg and expressed in keratinocytes, followed by antigen delivery to the draining lymph node (dLN) by cDCs and by passive drainage[41,42]. The antigen-specific CD4$^+$ T-cell response can be followed by flow cytometry using an MHC-II tetramer (tet) against the PADRE epitope (Figure 1B). PADRE tet$^+$ CD4$^+$ T cells were detected in the dLN from day 4 onwards after vaccination (Figure 1C)

and entered the circulation by day 5 (Figure S1A). In line with a type-1 immune response raised by this model, CD44$^+$ PADRE tet$^+$ cells differentiated into Th1 and Tfh cells, but not into T-regulatory (Treg), Th2 or Th17 cells (Figure S1B). PADRE tet$^+$ cells were divided into cells that retain PSGL1 (PSGL1$^+$ CXCR5$^-$) or cells that lose PSGL1 but acquire CXCR5 (PSGL1$^-$ CXCR5$^+$) (Figure 1D). Within the PSGL1$^+$ CXCR5$^-$ cell population, Th1 cells were defined as SLAM$^+$ T-bet$^+$ BCL6$^-$ PD-1^{low} FR4^{low} TCF1^{low} (Figure 1D, Figure S1C)[43-45]. Within the PSGL1$^-$ CXCR5$^+$ cell population, Tfh cells were defined as SLAM$^-$ T-bet$^-$ BCL6$^+$ PD-1^{hi} FR4$^+$ TCF1^{hi} (Figure 1D, Figure S1C)[3,7,43,46]. Th1 and Tfh populations emerged in parallel and were of similar size at day 4 after vaccination (Figure 1E). By day 5, when PADRE tet$^+$ CD4$^+$ T cells became detectable in the blood (Figure S1A), Tfh cells started accumulating in the dLN (Figure 1E). At that day, Th1 cells went from the dLN to the blood, where they represented ~50% of PADRE$^+$ CD4$^+$ T cells (Figure 1F).

To validate the helper functions of Th1 and Tfh cells, we investigated the CD8$^+$ T-cell and B-cell responses post vaccination. Mice in which CD4$^+$ T cells were activated by the MHC-II vaccine displayed an increased frequency of KLRG1$^+$ effector phenotype E7 tet$^+$ CD8$^+$ T cells at day 10 in the blood compared to mice receiving the control vaccine (Figure 1G; Figure S1D). These data confirm that Th1 cells generated by the MHC-II vaccine contributed to effector differentiation of CD8$^+$ T cells raised by the E7 epitope, as demonstrated before[34,36]. Mice that received the MHC-II vaccine also displayed increased frequencies of CD19$^+$ IgD$^-$ CD38$^-$ FAS$^+$ GL7$^+$ germinal center (GC) B cells and CD138$^+$ TACI$^+$ plasmablasts (Figure 1H; Figure S1E, F), confirming that vaccine-primed Tfh cells promoted the B-cell response. Thus, both Th1 and Tfh cells raised by the MHC-II vaccine are functionally competent. Inhibition of T-cell egress from the dLN with sphingosine 1-phosphate (S1P) receptor-targeting drug FTY720 increased the overall frequency of PADRE tet$^+$ CD4$^+$ T cells in the dLN by more than 2-fold (Figure S1G, H). At day 7 after vaccination, PADRE tet$^+$ Th1 and Tfh cell frequencies and absolute numbers were comparable in dLN of FTY720-treated mice (Figure 1I; Figure S1I). This finding indicates that the MHC-II vaccine leads in equal measure to Th1 and Tfh differentiation, making it a good model for studying the differentiation trajectories of the endogenous vaccine-specific CD4$^+$ T cells.

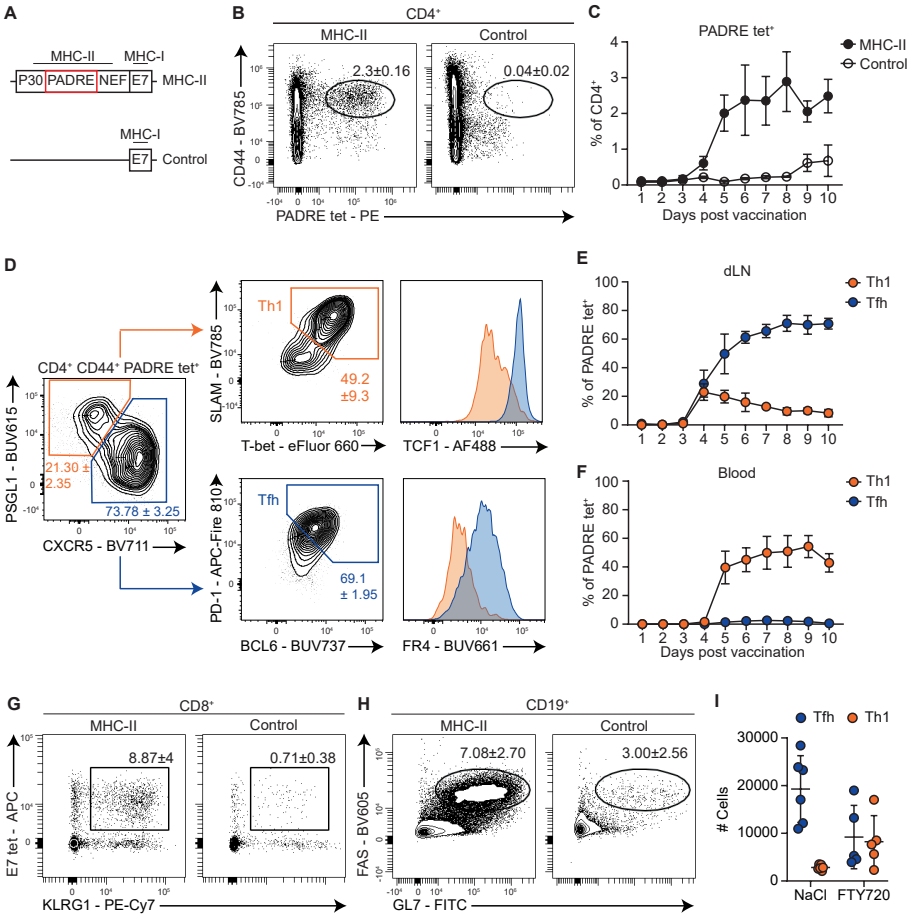

Figure 1. A vaccination model to study differentiation of endogenous, polyclonal CD4⁺ T cells into Th1 or Tfh cells. (A) Scheme of epitopes in MHC-II and control DNA vaccines. (B) Representative flow cytometry plots depicting frequency of CD44⁺ PADRE tet⁺ CD4⁺ T cells in dLN at day 5 post-vaccination (N=3, mean ± SD). (C) Frequency of PADRE tet⁺ CD4⁺ T cells in dLN over time (N=8 for MHC-II, N=3 for Control). (D) Representative flow cytometry plots depicting the phenotype of CD44⁺ PADRE tet⁺ CD4⁺ T cells in the dLN at day 8 post-vaccination, and identifying Th1 cells (orange) as PSGL1^{hi} CXCR5^{-} SLAM⁺ T-bet⁺ FR4^{low} TCF1^{low} and Tfh cells (blue) as PSGL1$^{int-low}$ CXCR5⁺ BCL6⁺ PD-1^{hi} FR4^{hi} TCF1^{hi}. (E, F) Frequency of Tfh (CXCR5⁺ PSGL1^{lo} PD-1⁺ BCL6⁺) and Th1 cells (CXCR5^{-} PSGL1^{hi} T-bet⁺ SLAM⁺) within PADRE tet⁺ CD4⁺ T cells in dLN (E) or blood (F) over time after MHC-II-vaccination (N=5). (G) Representative contour plots depicting antigen-specific effector CD8⁺ T cells (E7 tet⁺ KLRG1⁺) in blood at day 10 after MHC-II or control vaccination. (H) Representative contour plots depicting CD19⁺ IgD^{-} CD38^{-} FAS⁺ GL7⁺ GC B cells in the dLN at day 8 after MHC-II or control vaccination. (I) Absolute numbers of Th1 and Tfh PADRE tet⁺ CD4⁺ T cells in dLN at day 7 post-vaccination (N=6 mean ± SD).

Reconstruction of the Th1- and Tfh differentiation trajectories that evolve after vaccination

To gain insight into the temporal changes that $CD4^+$ T cells undergo during Th1 and Tfh differentiation, we analyzed PADRE tet^+ $CD4^+$ T cells in the dLNs of mice from day 4 to 9 after vaccination by spectral flow cytometry and dimension reduction analysis (Figure 2A; Figure S2A). To ensure that we captured the full differentiation trajectory, we gated on total $CD4^+$ PADRE tet^+ cells, which include a small proportion of $CD62L^{hi}$ $CD44^{low}$ naive cells. Indeed, PADRE tet^+ $CD4^+$ T cells were discriminated into naive $CD62L^{hi}$ $CD44^{low}$ and activated $CD44^{hi}$ cells (Figure 2B). The marker profile of the activated $PADRE^+$ $CD4^+$ T-cell pool underwent daily remodeling and displayed progressive branching towards two end points (Figure 2A; Figure S2A), which were characterized by a Th1 ($PSGL1^+$ T-bet^+ $SLAM^+$ $TCF1^-$ $SLAMF6^-$) or a Tfh ($CXCR5^+$ $PD\text{-}1^+$ $BCL6^+$ $TCF1^+$ $SLAMF6^+$ $FR4^+$) phenotype (Figure 2C-E), as we had observed before (Figure 1D, Figure S1C).

To reconstruct the temporal evolution of PADRE tet^+ $CD4^+$ T-cell differentiation towards Th1 and Tfh states, we used Wishbone, an algorithm that orders cells according to their developmental progression and infers branching trajectories into only one of two possible fates[47]. Wishbone calculates differentiation trajectories based on the rise and fall of phenotypic markers and uses nearest-neighbor graphs to capture developmental distance from a starting point, which we defined as the $CD62L^{hi}$ $CD44^{low}$ naive $CD4^+$ T-cell state. In our experimental setup, PADRE tet^+ $CD4^+$ T cells were ordered based on early activation (CD44, CD62L) and stem-like markers (TCF1, SLAMF6), as well as acquisition of the Th1 or Tfh phenotype (PSGL1, T-bet, SLAM, CXCR5, PD-1, BCL6 and FR4). PADRE tet^+ $CD4^+$ T cells were positioned along either the trunk or one of the two possible branches of the trajectory (Figure 2F; Figure S2B). Wishbone identified $PSGL1^+$ T-bet^+ $SLAM^+$ Th1 cells as branch 1 and $CXCR5^+$ $PD\text{-}1^+$ $BCL6^+$ $TCF1^+$ $FR4^+$ Tfh cells as branch 2 (Figure 2C-F). In contrast, the trunk of the Wishbone trajectory was composed of $CD62L^{hi}$ $CD44^{low}$ naive cells and $CD62L^{hi}$ $CD44^{hi}$ activated cells (Figure 2B, F). The $CD44^{hi}$ $CD62L^{hi}$ cells expressed high levels of TCF1 and SLAMF6 (Figure 2C), which are considered markers of stem-like $CD4^+$ T cells[45,48,49], thus suggesting the potential of $CD44^{hi}$ $CD62L^{hi}$ cells for further differentiation. In addition, $CD44^{hi}$ $CD62L^{hi}$ cells in the trunk of the trajectory had higher levels of CXCR5, BCL6 and PD-1 compared to naive cells, but still expressed PSGL1 (Figure 2D, E). Apart from being highly expressed by Tfh cells, PD-1 is also upregulated as a result of TCR triggering[50,51], and in line with this, all $CD44^{hi}$ cells had higher expression of PD-1 compared to $CD62L^{hi}$ $CD44^{low}$ naive cells (Figure 2E). We also show that the pseudotime calculated by Wishbone matched real-time differentiation, as visualized by the decrease in frequency of $CD62L^{hi}$ $CD44^{low}$ and $CD62L^{hi}$ $CD44^{hi}$ cells over time (Figure S2A, C). Altogether, these data suggest that, upon activation, antigen-specific $CD4^+$ T cells pass through a common $TCF1^+$ $SLAMF6^+$ $PD\text{-}1^+$ $CXCR5^+$ $BCL6^+$ $PSGL1^+$ cell state before branching into Th1 or Tfh differentiation states.

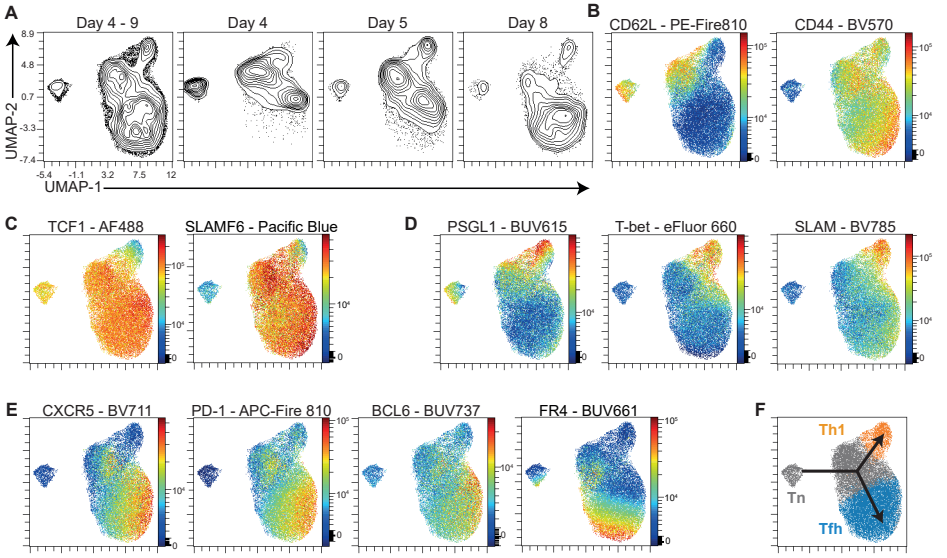

Figure 2. Temporal analysis highlights a common differentiation branchpoint for Th1 and Tfh cells. (A) UMAP projections showing concatenated PADRE tet$^+$ CD4$^+$ T cells in dLN from day 4-9 post-vaccination, or single projections at days 4, 5 or 8 (N=5 per time point). (B-E) Overlay of CD62L and CD44 (B), TCF1 and SLAMF6 (C), PSGL1, T-bet and SLAM (D) and CXCR5, PD-1, BCL6 and FR4 expression (E). (F) Overlay of Wishbone branching on UMAP from panel D. Arrows depict differentiation branches. Grey: trunk; orange: branch 1, identified as Th1 cells; blue: branch 2, identified as Tfh cells.

Th1 and Tfh cells develop from common precursor clones according to single-cell TCR sequencing

To characterize CD4$^+$ T-cell differentiation trajectories in an unbiased manner, we performed scRNAseq and paired TCRseq on activated CD3$^+$ CD44^{hi} T cells that were flow cytometrically purified from the dLN of mice at days 5 and 10 post-vaccination (Figure S3A). The MHC-II vaccine contains multiple CD4$^+$ T-cell epitopes[34], while only the responders to PADRE are detectable by MHC-II tetramer staining. We therefore analyzed the total activated T-cell population to capture the full spectrum of responding endogenous T cells, rather than restricting the analysis to a single antigen specificity. Consistent with this design, PADRE tet$^+$ cells comprised approximately 10% and 19% of the total CD44^{hi} effector population at days 5 and 10 post-vaccination, respectively (Figure S3B). After quality control filtering, selection of cells co-expressing TCRα and TCRβ sequences and exclusion of CD8$^+$ T cells and γδ T cells (Figure S3C), we obtained 4656 CD4$^+$ T cells for data analysis. Dimensionality reduction and clustering of cells based on their gene expression profiles identified 7 clusters that contained more than 20 cells (Figure 3A, B; Figure S3D, Table S1). Clusters 0 and 4 identified two Treg cell populations, characterized by expression of *Foxp3*, *Ctla4* and *Il2ra* (encoding CD25) (Figure 3C). Cluster 1 identified Tfh cells expressing *Tcf7* (encoding TCF1), *Cxcr5*, *Bcl6* and *Pdcd1* (encoding PD-1); cluster 2 identified

Th1 cells expressing *Selplg* (encoding PSGL1), *Tbx21* (encoding T-bet), *Id2*, and *Cxcr3*; cluster 3 identified naive-like cells expressing *Ccr7*, *Lef1*, *Sell* (encoding CD62L), and *Tcf7*; whereas cluster 6 was dominated by an interferon (IFN)-stimulated gene (ISG) signature (Figure 3C). Interestingly, cluster 5 contained cells expressing both Th1-related genes (*Tbx21*, *Cxcr3*) and Tfh-related genes (*Tcf7*, *Cxcr5*, *Bcl6*, *Pdcd1*) (Figure 3C), supporting the existence of a common Th1/Tfh precursor. The expression levels of these genes were intermediate between those found in Th1 cells (cl. 2) and Tfh cells (cl. 1). Cells of cluster 5 also expressed *Pdcd1* and *Cd69*, which are markers of recent TCR triggering (Figure 3C)[50-53], and were higher in frequency at day 5 after vaccination than at day 10, supporting that they represent recently activated cells (Figure 3B). The frequency of Th1 cells (cl. 2) and Tfh cells (cl. 1) on the other hand, increased over time (Figure 3B), which aligns with ongoing effector differentiation of the activated $CD4^+$ T-cell pool.

Next, to define clonal relationships between responder $CD4^+$ T cells in different states of effector differentiation, we paired the gene expression profiles per cell with TCRα and TCRβ sequence information. TCR clones were defined based on identical TCRα and TCRβ complementarity region (CDR)3 sequences, which identified a total number of 3549 clones within the $CD4^+$ T-cell compartment. We noted that Tfh cluster 1, Th1 cluster 2 and the intermediate phenotype cluster 5 had the highest frequency of expanded clones (>1 cell per clone) among all clusters (Figure 3D). Additionally, the highest number of expanded clones was observed in Tfh cluster 1, followed by Th1 cluster 2, intermediate phenotype cluster 5 and Treg cluster 0 (Figure S3E, F). Out of 352 expanded clones, 171 clones were shared between two or more clusters, while the rest was uniquely expanded within one cluster (Figure S3E). Tregs of cluster 0 comprised more unique than shared clones and sharing occurred primarily with Tregs of cluster 4 (Figure 3E, Figure S3F). The majority (72%) of expanded clones was shared between Tfh and Th1 cells (cl. 1 and 2), Tfh or Th1 cells and intermediate phenotype cells (cl. 5), or all three populations (Figure 3E), which was evident at both day 5 and day 10 after vaccination (Figure 3F). These data thus demonstrate the clonal relationship between cluster 5 cells and Th1 and Tfh cells and validate the indication from flow cytometry and associated Wishbone analysis (Figure 2) that antigen-activated $CD4^+$ T cells go through a common precursor state expressing both Th1 and Tfh-related genes, from which they can further develop into committed Th1 or Tfh cells. Cluster 5 cells thus represent the common precursors of Th1 and Tfh lineages.

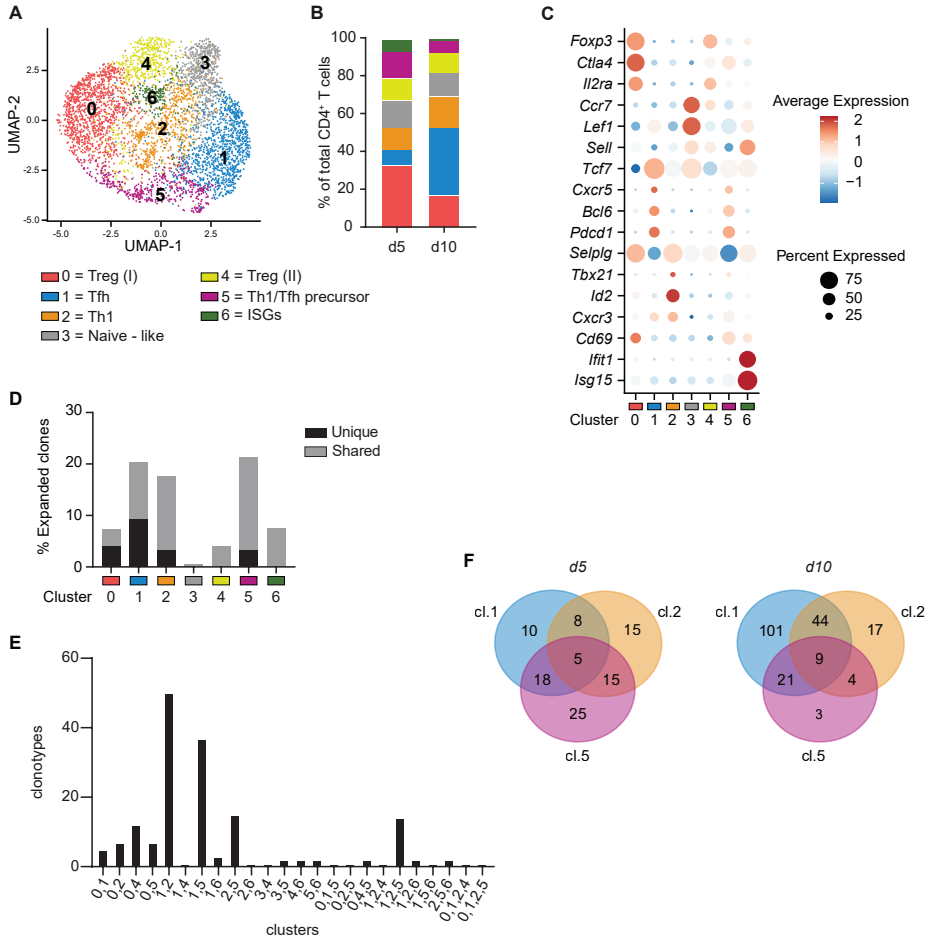

Figure 3. Identification of a common precursor for Th1 and Tfh cells in vaccinated mice. (A) UMAP projection of CD4^{+} T-cell clusters identified by scRNAseq of CD3^{+} CD44^{hi} CD62L^{low} T cells isolated from the dLN of mice at days 5 and 10 after vaccination with the MHC-II plasmid. (B) Bar plot depicting cluster distribution per time point. (C) Average mRNA expression level of indicated differentiation-associated genes and percentage of positive cells per cluster. (D) Frequency of expanded TCR clones (>1 cell per clone) per cluster. Black: TCR clones unique to one cluster; grey: TCR clones shared between two or more clusters. (E) Quantification of clonotypes shared between two or more indicated clusters. (F) Venn diagram depicting TCR sharing between Tfh cells from cluster (cl.) 1, Th1 cells from cl. 2 and Th1/Tfh precursor cells from cl. 5 derived at day 5 (left) or day 10 (right) after vaccination.

To determine whether Th1/Tfh precursor cells arise not only after vaccination, but also during infection, we analyzed previously published scRNAseq data from polyclonal GP66-tetramer$^+$ CD4$^+$ T cells isolated from spleens of mice infected with either acute LCMV-Armstrong or chronic LCMV-clone 13[54] (Figure 4A, Table S2). To identify corresponding cell states across datasets, we aligned the transcriptional profile of Tfh (cluster 1), Th1 (cluster 2) and Th1/Tfh precursor cells (cluster 5) defined in our vaccination model with the LCMV dataset using module scoring. Following LCMV infection, we detected Tfh cells and two Th1 clusters (Figure S4A-C). Th1 cells were prominent on day 8, whereas Tfh cells were more abundant on day 21 (Figure 4A). Both Th1 clusters expressed classical Th1-associated genes including *Cxcr6, Tbx21, Id2,* and *Prf1,* but were distinguished by differential expression of either *Gzma* and *Gzmb* (Th1 Gzmb$^+$ cluster) or *Prdm1, Eomes*, and *Gzmk* (Th1 Prdm1$^+$ cluster) (Figure S4A). The Tfh cluster expressed characteristic genes including *Cxcr5, Pdcd1, Il21 and Bcl6* (Figure S4A). Importantly, following both acute and chronic LCMV infection, we identified a population enriched for the transcriptional signature of the Th1/Tfh precursor cluster defined in our vaccination setting (Figure 4A, Figure S4D). This population was present under both infection conditions, but was more abundant at day 8 after acute infection (Figure 4A). Examination of the transcriptional profile revealed that approximately two-thirds of the genes differentially expressed in our vaccine-induced Th1/Tfh precursors (1,074 out of 1,576 genes) were also significantly enriched in the LCMV-induced Th1/Tfh precursor population (Figure 4B). To quantitatively assess transcriptional similarity between these two populations, we correlated average gene-expression values of their unified gene signature (Table S3) and observed a remarkably strong correlation (r = 0.94; Figure 4C). This concordance was particularly evident for transcripts that define this precursor state, including *Tcf7, Slamf6*, *Pdcd1*, *Cxcr3*, *Cxcr5*, *Tbx21* and *Bcl6*, as well as *Ldha* and *Gpr183*, which have been linked to the acquisition of stem-like properties in CD4$^+$ T cells[45].

In addition to this early Th1/Tfh precursor population, we also found the previously described *Slamf6*$^+$ *Tcf7*$^+$ *Bcl6*^{low} memory-precursor cluster[49,54] to be specifically enriched at day 21 post-chronic LCMV infection (Figure 4A, Figure S4A). A clonal relationship between this population and Th1 and Tfh cells has been documented[54]. Comparison of its gene signature (Table S3) with that of our vaccine-induced Th1/Tfh precursor revealed a more limited overlap (280 shared genes with FDR < 0.05; Figure 4D), likely reflecting differences in inflammatory context (acute vaccination versus chronic infection) and sampling time points. Nevertheless, the overall transcriptional correlation between the two populations was high (r = 0.84), particularly with respect to transcripts defining the Th1/Tfh precursor phenotype (Figure 4E). This chronic LCMV-induced memory-precursor population also shares a core gene signature with stem-like CD4$^+$ T cells in cancer that retain Th1 and Tfh differentiation potential[49]. Consistent with this relationship, the signature of stem-like CD4$^+$ T cells in cancer[49] was significantly enriched in our vaccine-induced Th1/Tfh precursor cells (Figure 4F), indicating that these cells adopt a stem-like transcriptional program.

To determine whether the Th1/Tfh precursor state was conserved across different infectious contexts, we next analyzed previously published data from *Plasmodium*-specific TCR transgenic CD4$^+$ T cells responding to malaria infection, a model in which a common activated precursor state preceding Th1 or Tfh differentiation has also been described[4]. We extracted the gene signature of malaria-induced Th1/Tfh precursors (1,626 dynamic genes; D statistic >50; Table S4) and found significant enrichment of this signature in our vaccine-induced Th1/Tfh precursor population (Figure 4G), with 1,515 of the 1,625 genes showing significantly enrichment in both datasets (FDR < 0.05). Altogether, these findings demonstrate that antigen-specific CD4$^+$ T cells transit through a conserved, uncommitted Th1/Tfh precursor state prior to differentiation into Th1 or Tfh effector lineages after vaccination or infection with acute and chronic LCMV or malaria. This precursor population further shares a core stem-like transcriptional signature with memory precursors arising specifically during chronic LCMV infection and with stem-like CD4$^+$ T cells in tumors, consistent with a shared capacity to sustain differentiation toward both Th1 and Tfh lineages across diverse immune response settings.

Th1/Tfh precursors are proliferative and co-express Th1- and Tfh-related transcription factors and chemokine receptors

To gain deeper insights into the transcriptional programs underlying Th1 and Tfh cell differentiation, we performed differential gene expression analysis between Tfh (cl.1) and Th1 (cl.2) cells generated after vaccination. Gene signatures of the two T-helper subsets were characterized by lineage-defining transcription factors, including *Tbx21*, *Id2*, *Bhlhe40* and *Prdm1* for Th1 cells, and *Bcl6*, *Tox* and *Tox2* for Tfh cells, which validated the robustness of our dataset (Figure 5A; Tables S5 and S6)[24,44,55,56]. Comparison of the transcriptional profile of the common Th1/Tfh precursor cells (cl. 5) to that of naive-like cells (cl. 3) revealed the characteristics of this population (Figure 5B). Cluster 5 cells expressed many genes associated with either Th1 or Tfh fate, including transcription factors *Tbx21*, *Bhlhe40*, *Prdm1* and *Bcl6*, as well as chemokine receptors *Cxcr3* and *Cxcr5*. These transcripts were co-expressed within the same cells and enriched in cluster 5, as shown by the positive correlation in expression of e.g. *Tbx21* and *Cxcr5*, or *Tbx21* and *Bcl6* (Figure S5A, B). In addition, cells of cluster 5 displayed upregulation of *Mki67*, indicating active cell division, and multiple costimulatory receptors including *Icos*, *Tnfrsf8* (encoding CD30), *Tnfrsf9* (encoding CD137, alias 4-1BB), *Tnfrsf18* (encoding CD357, alias GITR), and *Tnfrsf1b* (encoding CD120b, alias TNFR2) (Figure 5B).

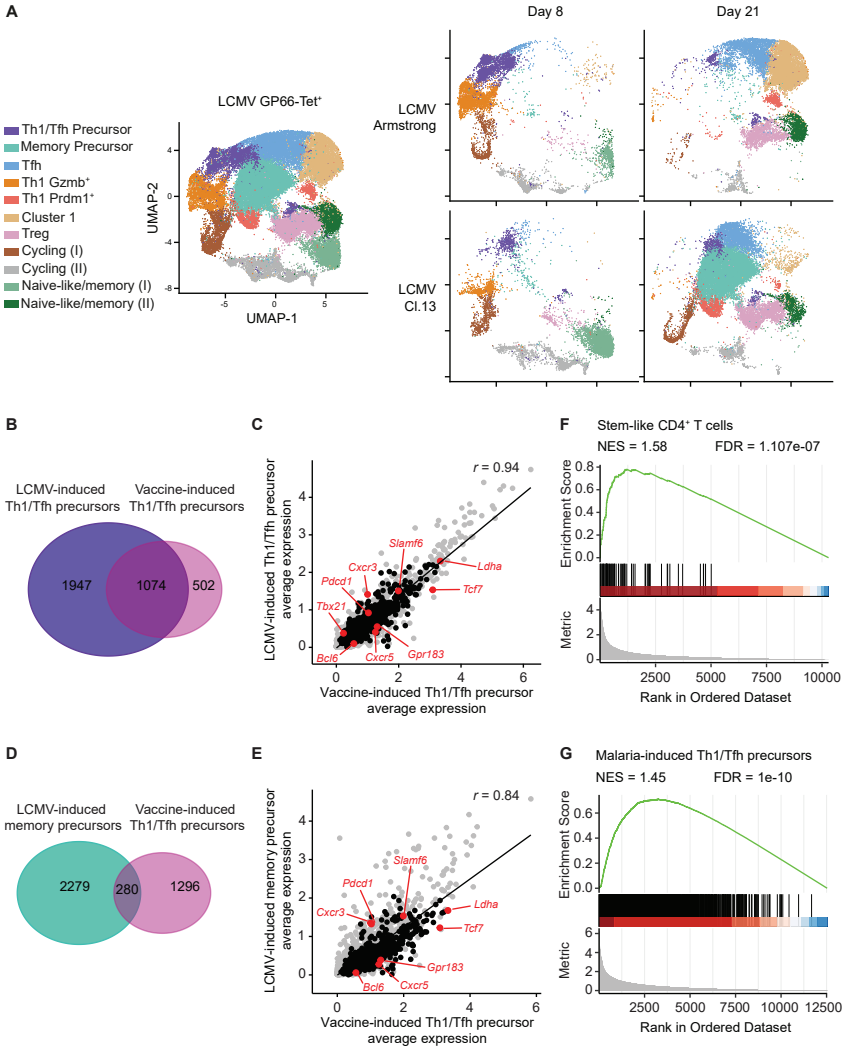

Figure 4. The Th1/Tfh precursor population is conserved across different infection models. (A) Left: UMAP projection of splenic GP-66 Tet+ CD4+ T cells derived from mice infected with LCMV-Armstrong or LCMV-clone 13 at day 8 and day 21 post-infection. Data were re-analyzed from Xia et al.[54]. Right: Deconvolution of UMAPs per infection model and time point. (B, D) Venn diagrams showing the overlap between genes significantly enriched (FDR < 0.05) in vaccine-induced Th1/Tfh precursors and either LCMV-induced Th1/Tfh precursors (B) or LCMV-induced memory precursors (D). (C, E) Scatter plots comparing the average expression of genes significantly enriched (FDR < 0.05) in vaccine-induced Th1/Tfh precursors with their expression in LCMV-induced Th1/Tfh precursors (C) or LCMV-induced memory precursors (E). Spearman's correlation coefficient (r) was calculated to quantify transcriptional similarity. Grey dots represent all genes significantly enriched (FDR < 0.05) in either population (union of enriched genes); black dots indicate genes significantly enriched in both populations (shared enriched genes); red dots highlight selected genes of interest. (F, G) Gene set enrichment analysis of gene signatures of stem-like CD4+ T cells (from Cardenas et al.[49]) (F) and malaria-induced Th1/Tfh precursor cells (from Lönnberg et al.[4]) (G) in vaccine-induced Th1/Tfh precursor cells. A total of 59/62 and 1,515/1,625 genes, respectively, overlapped with the ranked gene list.

To map the formation of common Th1/Tfh precursor cells by flow cytometry, we followed the response of TCR transgenic OTII cells that recognize $OVA_{323-339}$ peptide in the context of MHC-II. $CD45.1^+$ OTII cells were labeled with carboxyfluorescein succinimidyl ester (CFSE) to track proliferation and adoptively transferred into $CD45.2^+$ recipient mice. One day later, recipient mice received one dose of a modified MHC-II DNA vaccine encoding both PADRE and $OVA_{323-339}$ epitopes (MHC-II:OVA; Figure S5C). This vaccine simultaneously induced a transgenic OTII $CD4^+$ T-cell response to the OVA epitope and an endogenous $CD4^+$ T-cell response to the PADRE epitope (Figure S5D, E), enabling us to compare the differentiation trajectories of these two responder cell populations. Because transferred naive OTII cells are present at relatively high frequency, this system allowed us to analyze their early activation state, whereas endogenous PADRE tet^+ $CD4^+$ T cells became detectable by tetramer staining only at day 4 post-vaccination (Figure S5F, G). We therefore monitored the $CD4^+$ T-cell response in the dLNs from day 1 to 5 post-vaccination. Proliferation of OTII cells was initiated by day 3, and by day 4 the majority of OTII cells were actively dividing, with fraction having already undergone at least seven divisions (Figure 5C, Figure S5H). Accordingly, the frequencies of both OTII cells and PADRE tet^+ $CD4^+$ T cells were significantly increased by day 4 post-vaccination (Figure S5F, G). At day 3, concurrent with the start of cell division, OTII cells upregulated the activation marker CD44, as well as the chemokine receptor CXCR5 (Figure 5D, Figure S5I) that is commonly used as a marker of Tfh precursors[57-59]. Interestingly, $CD44^{hi}$ $CXCR5^+$ OTII cells also expressed high levels of CXCR3 (Figure 5E, F), a chemokine receptor that among $CD4^+$ T cells is thought to be specifically upregulated on Th1 precursors[60]. Consistent with our scRNAseq data, $CD44^{hi}$ $CXCR5^+$ $CXCR3^+$ OTII cells co-expressed T-bet and BCL6 proteins (Figure 5G, H). Within the endogenous $CD4^+$ T-cell pool, PADRE tet^+ $CD44^{hi}$ CD4 T cells also co-expressed CXCR5, CXCR3, T-bet and BCL6 at day 4 post-vaccination (Figure 5E, G; Figure S5J-L). In addition, $CD44^{hi}$ OTII cells expressed higher levels of PD-1 compared to $CD44^{low}$ cells (Figure S5M), consistent with our results for endogenous cells (Figure 2E).

TCR transgenic T cells all have the same affinity and may therefore have an intrinsic predisposition to a specific differentiation trajectory[7]. Next to low affinity OTII cells, we also used SMARTA $CD4^+$ T cells that have a transgenic, high affinity TCR recognizing the GP_{61-80} epitope of LCMV in the context of MHC-II[60], in conjunction with a modified MHC-II vaccine that encodes both the PADRE and GP_{61-80} epitopes (Figure S5N, O). SMARTA $CD4^+$ T cells also differentiated into $CD44^{hi}$ precursor cells co-expressing CXCR3, CXCR5, T-bet and BCL6, as observed at day 4 post-vaccination (Figure S5O). Obtaining the same results with low and high affinity TCR transgenic $CD4^+$ T cells, as well as PADRE-specific endogenous, polyclonal $CD4^+$ T cells indicates that the formation of the Th1/Tfh precursor cell pool is independent of TCR affinity. The collective data thus establish that activated $CD4^+$ T cells initially form a proliferative pool of common Th1/Tfh precursors with a distinct marker profile that can differentiate into either Th1 or Tfh cells, independent of TCR affinity.

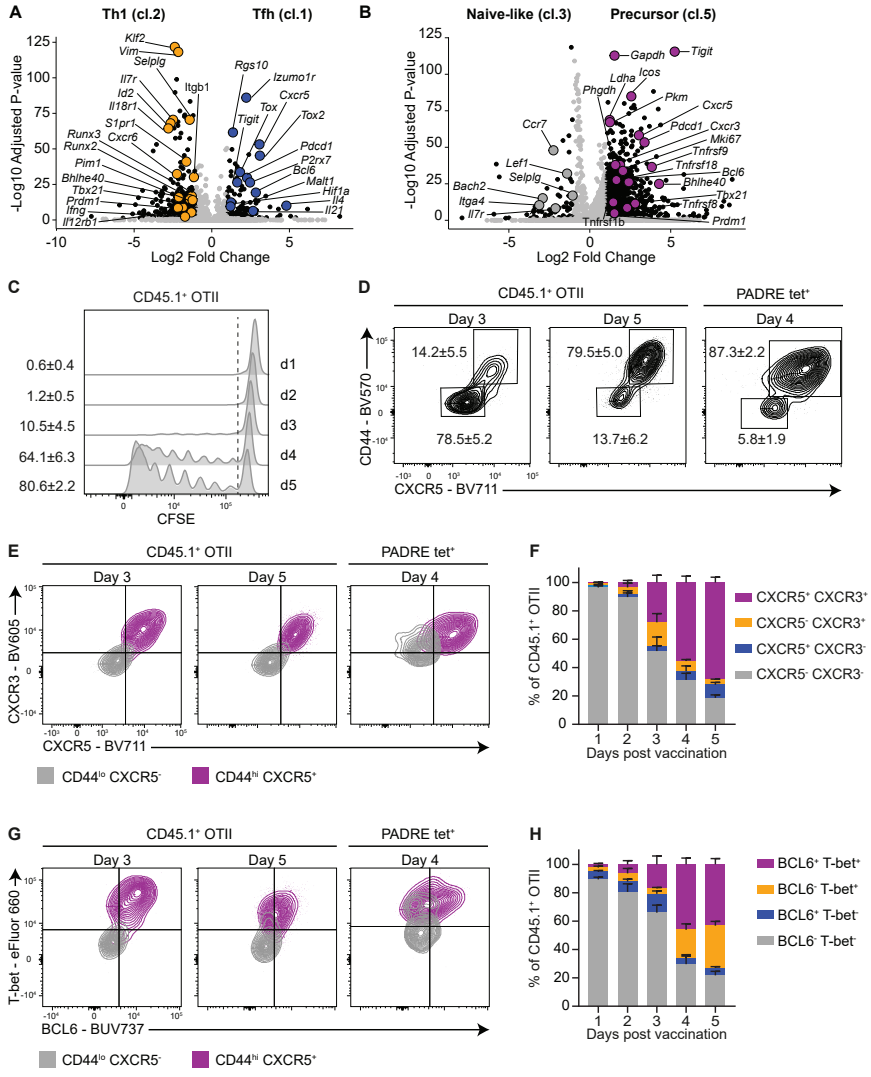

Figure 5. Common Th1/Tfh precursors co-express Th1- and Tfh markers at protein level. (A, B) Volcano plots depicting differential gene expression derived from scRNAseq data of vaccinated mice, comparing Tfh cells (cl. 1) versus Th1 cells (cl. 2) (A), or naive-like CD4$^+$ T cells (cl. 3) versus Th1/Tfh precursor cells (cl. 5) (B). Black dots depict genes with fold change < -1 or > 1 and adjusted P<0.05. (C) Mice received OTII cells, were vaccinated once with MHC-II:OVA vaccine, dLNs were harvested and cells analyzed by flow cytometry. Histograms depicting divisions of vaccine-activated, adoptively transferred OTII cells, as measured by CFSE dilution. Numbers indicate frequency of divided OTII cells (mean ± SD). (D) Representative CD44 and CXCR5 protein expression on CD45.1$^+$ OTII or PADRE tet$^+$ CD4$^+$ T cells, measured in dLNs at indicated days post-vaccination. (E, G) Representative overlays of CXCR5 and CXCR3 (E) or T-bet and BCL6 (G) protein expression in CD44^{lo} CXCR5$^-$ (gray) and CD44$^+$ CXCR5$^+$ (purple) CD45.1$^+$ OTII or PADRE tet$^+$ CD4$^+$ T cells. (F, H) Proportion of CD45.1$^+$ OTII responder cells expressing CXCR5 and CXCR3 (F) or T-bet and BCL6 (H) in the dLNs at the indicated days post-vaccination (N=3-5 per time point; representative of 3 independent experiments). Graphs depict mean ± SD.

Specific costimulatory signals drive formation of the common Th1/Tfh precursor pool and subsequent Th1 or Tfh differentiation

Having identified the common Th1/Tfh precursor, we were interested in the costimulatory signals that drive its formation and further differentiation. It is known that Th1 and Tfh differentiation rely on specific costimulatory molecules[61], but how and when these signals operate during the step-wise differentiation trajectories from the naive T cell, via the common Th1/Tfh precursor into the Th1 and Tfh lineages has not been established yet. We first examined the impact of costimulatory receptor CD28 that synergizes with the TCR/CD3 complex in initiating T-cell activation, but is also required to maintain both Th1 and Tfh cells[62]. To this end, CD28 costimulation was inhibited by infusion of blocking monoclonal antibodies (mAbs) against both CD80 and CD86 in mice that received OTII cells and MHC-II:OVA vaccination once. This intervention did not significantly affect the overall frequency of OTII cells in dLN at day 5 after vaccination (Figure S6A), but did reduce the frequency of CD44$^+$ CXCR3$^+$ CXCR5$^+$ OTII Th1/Tfh precursor cells (Figure 6A). CD80 and CD86 blockade also reduced the frequency of total PADRE tet$^+$ CD4$^+$ T cells (Figure 6B), suggesting that CD28 costimulation promotes formation of the Th1/Tfh precursor pool by supporting clonal expansion of recently activated CD4$^+$ T cells, in line with its role during initial T-cell priming[63]. Because CD80 and CD86 have different affinities for CD28[64] and distinct roles in the maturation of Tfh cells in germinal centers[65], we also investigated whether they had independent impact on the CD4$^+$ T-cell differentiation trajectory. Single blockade of either CD80 or CD86 did not affect the generation of CXCR3$^+$ CXCR5$^+$ OTII Th1/Tfh precursor cells (Figure 6C), nor the expansion and initial Th1 or Tfh bifurcation of PADRE$^+$ CD4$^+$ T cells (Figure 6D; Figure S6B-D), indicating that CD80 and CD86 are redundant in promoting formation of the Th1/Tfh precursor pool.

We next evaluated the impact of CD40 and ICOS costimulation on the CD4$^+$ T-cell differentiation trajectory towards and from the Th1/Tfh precursor state. CD40:CD40L interaction has been reported to promote both Th1 and Tfh function[66-68] and ICOS:ICOSL interaction is important for Tfh differentiation[58,66,68-70]. Blockade of CD40L or ICOSL did not affect the frequency of CD44$^+$ CXCR5$^+$ CXCR3$^+$ OTII precursor cells, total PADRE tet$^+$ CD4$^+$ T cells, or total OTII cells (Figure 6E; Figure S6E, F), indicating that CD40 and ICOS costimulation were not required for formation of the Th1/Tfh precursor pool. However, among PADRE tet$^+$ cells, CD40L blockade significantly reduced the frequency of Th1 cells, while not affecting the frequency of Tfh cells (Figure 6F, G). Conversely, blockade of ICOSL lowered the frequency of Tfh cells, while not affecting the frequency of Th1 cells (Figure 6F, G). Because early CXCR5 and BCL6 expression has been reported to depend on ICOS costimulation[57,58,71], we further validated our results for ICOS blockade using CRISPR/Cas9-mediated knockout of ICOS in OTII T cells. Mice received naive OTII cells expressing either a control gRNA (Ctrl) or a pool of three gRNAs against ICOS (ICOS^{ko}), and were subsequently vaccinated with MHCII:OVA. Whereas all activated CD44^{hi} Ctrl OTII cells upregulated ICOS, ICOS expression was abrogated in 75% of ICOS^{ko} OTII cells, confirming effective genetic disruption (Figure S6G). We restricted our analysis to bona fide

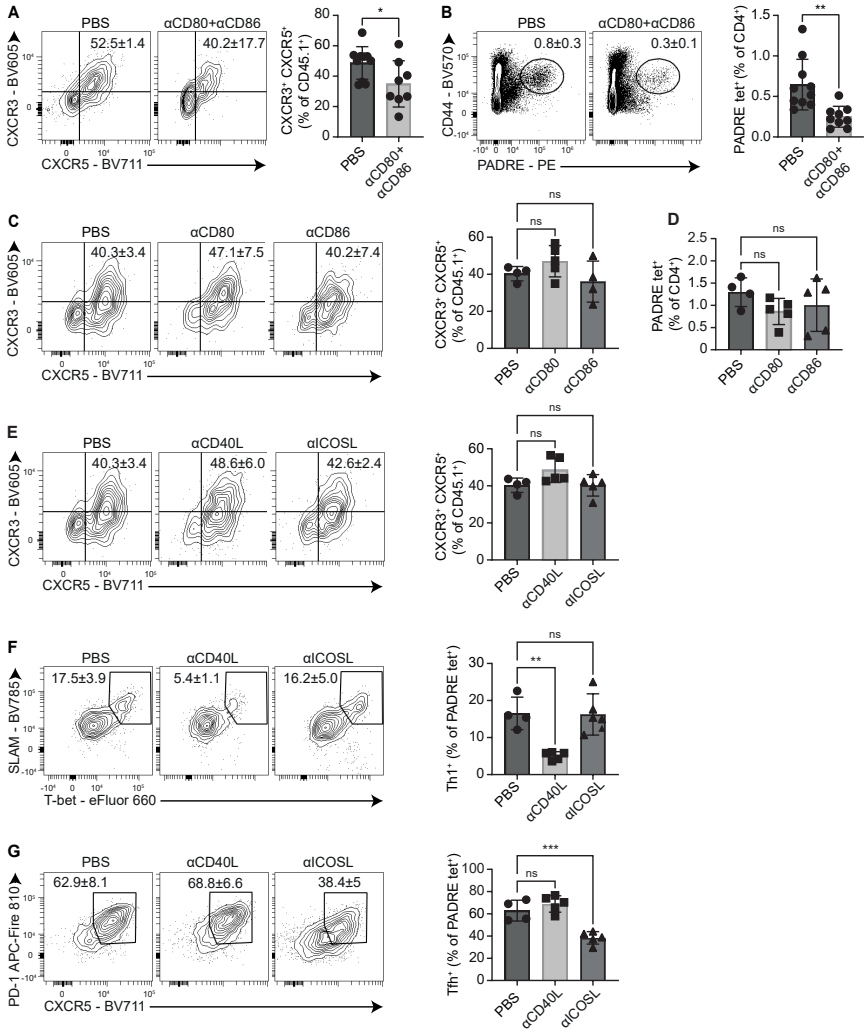

Figure 6. CD28 costimulation promotes formation of the Th1/Tfh precursor pool, from which CD40 or ICOS drive Th1 or Tfh differentiation, respectively. OTII cells were adoptively transferred in recipient mice, which were vaccinated one day later with a single dose of MHC-II:OVA vaccine and treated with blocking monoclonal antibodies (mAbs) against the indicated costimulatory ligands or PBS (control). dLNs were harvested at day 5 after vaccination and analyzed by flow cytometry. Representative plots and quantification of frequencies of cells expressing indicated markers are shown. (A, B) Frequencies of CXCR3$^+$ CXCR5$^+$ CD45.1$^+$ OTII cells (A) and CD45.2$^+$ PADRE tet$^+$ CD4$^+$ T cells in mice treated with a combination of blocking mAbs to CD80 and CD86 (B) (N=9-10 per group; data pooled from 2 independent experiments). Unpaired Student's t-test. (C, D) Frequencies of CXCR3$^+$ CXCR5$^+$ CD45.1$^+$ OTII cells (C) and CD45.2$^+$ PADRE tet$^+$ CD4$^+$ T cells (D) in mice treated with blocking mAbs to either CD80 or CD86. (E, F, G) Frequencies of CXCR3$^+$ CXCR5$^+$ precursor CD45.1$^+$ OTII T cells (E), CD45.2$^+$ PADRE$^+$ SLAM$^+$ T-bet$^+$ Th1 (F) and CD45.2$^+$ PADRE$^+$ CXCR5$^+$ PD-1$^+$ Tfh (G) cells in mice treated with blocking mAb to either CD40L or ICOSL. (C-G) N=4-5 per group; data are representative of at least two independent experiments. One-Way ANOVA with Dunnett's post hoc test was used to correct for multiple testing when comparing inhibitory conditions to control. All graphs show mean ± SD.

ICOS-deficient cells within the ICOS^{ko} OTII population and found that activated CD44^{hi} ICOS-deleted OTII cells effectively upregulated CXCR5 and BCL6 expression compared to their naive CD44^{low} counterpart, although their expression levels were slightly lower than in CD44^{hi} Ctrl OTII cells (Figure S6H, I). Consistent with this, the frequency of CXCR3^{+} CXCR5^{+} cells was comparable between ICOS-deleted and Ctrl OTII cells (Figure S6J), confirming that early CXCR5 and BCL6 upregulation, and the resulting formation of the Th1/Tfh precursor pool, occur independently of ICOS signaling. In line with our results using ICOSL antibody blockade, CRISPR/Cas9-mediated deletion of ICOS in OTII cells impaired Tfh differentiation (Figure S6K), without affecting Th1 cells (Figure S6L). Altogether, these data provide a scenario wherein CD28 costimulation driven by either CD80 or CD86 promotes formation of the Th1/Tfh precursor cell pool, whereafter the precursors are driven into Th1 cells with the aid of CD40-CD40L interactions and into Tfh cells with the aid of ICOS-ICOSL interactions.

Th1/Tfh precursors differentiate into either Th1 or Tfh cells in a second priming step on cDC1s or B cells, respectively

We next examined the role of cDC1s and B cells in guiding the differentiation of Th1 and Tfh cells from the Th1/Tfh precursor. The role of cDC1s was determined by using *Batf3*$^{-/-}$ mice on a C57BL6/J background[13,72], which display complete loss of migratory cDC1s (MHCII^{hi} CD11c^{int} CD103^{+} XCR1^{+}) and partial loss of resident cDC1s (MHCII^{int} CD11c^{hi} XCR1^{+}) (Figure S7A-F). The role of B cells was determined by effective B-cell depletion using a mAb to CD20 prior to vaccination (Figure S7G). In both experimental set-ups, OTII cells were adoptively transferred, the MHC-II:OVA vaccine was administered once, and responses were read out in the dLNs by flow cytometry at day 5 after vaccination. Neither *Batf3*-deficiency (Figure S7H, I), nor B cell depletion (Figure S7L, M) affected the clonal expansion of endogenous PADRE tet^{+} CD4^{+} T cells or OTII cells. Formation of CD44^{+} CXCR3^{+} CXCR5^{+} Th1/Tfh precursor cells was also unaffected in mice lacking these APCs (Figure 7A, B). However, *Batf3*$^{-/-}$ mice showed a decrease in the generation of Th1, but not Tfh cells, while B-cell depleted mice showed a decrease in the generation of Tfh, but not Th1 cells. This was the case for both endogenous PADRE tet^{+} CD4^{+} T cells (Figure 7C-F) and for exogenous OTII cells (Figure S7J-K, N-O). Altogether, these data indicate that CD28-dependent formation of the Th1/Tfh precursor pool is instructed by APCs other than cDC1s and B cells, most likely cDC2s. Thereafter, in a second step of priming, the precursor cells are instructed for Th1 differentiation on cDC1, as driven by CD40 costimulation, or for Tfh differentiation on B cells, as driven by ICOS costimulation.

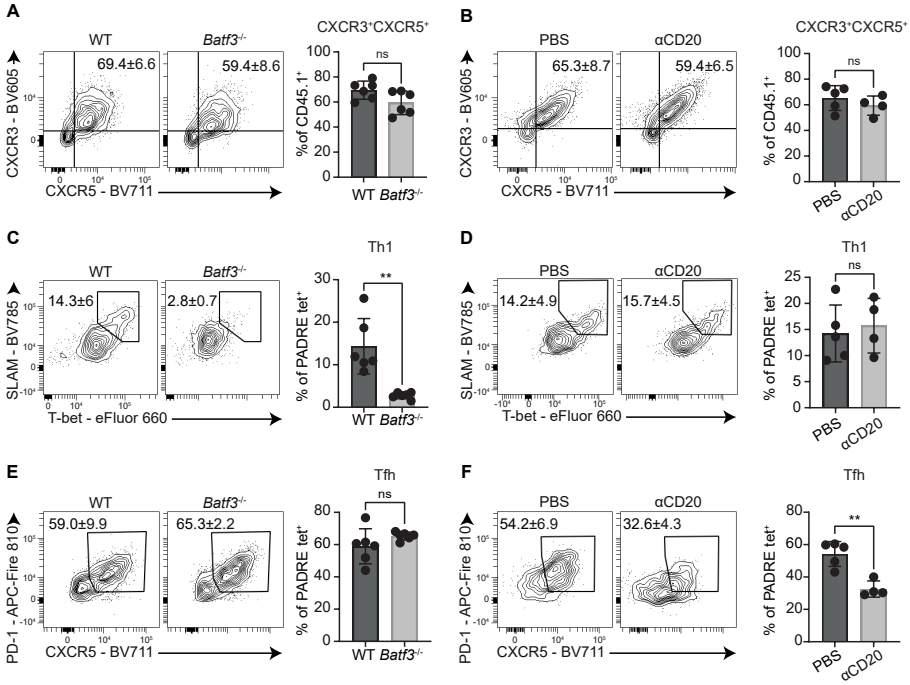

Figure 7. Th1 or Tfh differentiation from the common Th1/Tfh precursor is driven by interactions with cDC1s or B cells, respectively. Wild-type (WT) or Batf3$^{-/-}$ mice received OTII cells, were vaccinated once with MHC-II:OVA vaccine and were treated with depleting mAb to CD20 or PBS (control) as indicated. At day 5 after vaccination, cells from dLN were analyzed by flow cytometry. Representative plots and quantification of frequencies of cells with indicated markers are shown. (A, B) Flow cytometry plots and quantification of CXCR3^{+} CXCR5^{+} CD45.1^{+} OTII cells in the dLN of WT versus Batf3$^{-/-}$ mice (A), or WT mice that were treated with B-cell depleting anti-CD20 mAb or PBS (control), two days before vaccination (B). (C-F) Flow cytometry plots and quantification of SLAM^{+} T-bet^{+} Th1 (C, D) or CXCR5^{+} PD-1^{+} Tfh (E, F) PADRE tet^{+} CD4^{+} T cells in WT versus Batf3$^{-/-}$ mice (C, E), or WT mice treated with anti-CD20 mAb or PBS (D, F). All graphs depict mean ± SD (N=6 per group in A, C, E; N=4-5 per group in B, D, F). A-F, Unpaired Student's t-test.

Discussion

In this study, we characterize a mouse vaccination model that enables longitudinal tracing of Th1 and Tfh differentiation from endogenous, polyclonal CD4$^+$ T cells. By integrating single-cell transcriptomics, TCR sequencing, and high-dimensional flow cytometry, we demonstrate that individual antigen-specific CD4$^+$ T cell clones transiently pass through a common, highly proliferative Th1/Tfh precursor state before committing to either Th1 or Tfh effector phenotypes. This precursor population exhibits features of recent activation and stem-like potential, marked by expression of CD69, PD-1, TCF1 and SLAMF6, while simultaneously co-expressing key Th1- and Tfh-associated molecules at both the mRNA and protein levels, including CXCR3, T-bet, CXCR5, and BCL6. The vaccine-induced Th1/Tfh precursor state aligns transcriptionally with analogous populations identified during malaria[4] and both acute and chronic LCMV infection[55]. In addition, it shares a core gene signature with memory precursors and stem-like CD4$^+$ T cells described in chronic LCMV infection and tumors, respectively[49,54]. Interestingly, its transcriptional program also resembles that of stem-like LCMV-specific CD8$^+$ T cells[73-75], suggesting that CD4$^+$ and CD8$^+$ T cell lineages can transiently form similar intermediate states during immune responses.

During priming in secondary lymphoid organs, CD4$^+$ T cells have multiple contacts with different APCs. This is most explicit for Tfh formation in which both cDCs and B cells play a role. Initial priming typically occurs in the T-cell zone by cDC2s[76-78], giving rise to activated CD4$^+$ T cells that upregulate CXCR5 and are commonly referred to as pre-Tfh cells. These cells migrate along a CXCL13 gradient towards the border between the T- and B-cell zone or the interfollicular region (IFR)[19,79], where they receive additional stimulation that promote entry into the B-cell follicle and completion of Tfh differentiation[79-81]. Although early expression of CXCR5 and PD-1 on activated CD4$^+$ T cells is often considered indicative of Tfh commitment, not all CXCR5$^+$ PD-1$^+$ CD4$^+$ T cells ultimately become Tfh cells[79,81]. In contrast to CXCR5, CXCR3, a chemokine receptor responsive to IFN-induced CXCL9 and CXCL10, has classically been associated with Th1 differentiation[82]. This chemokine receptor also guides activated CD4$^+$ T cells towards the IFR[82]. At this site, CD4$^+$ T cells can provide help to CD8$^+$ T cells through cognate interactions with the same cDC1[5,83,84], but they can also interact with B cells[79]. Consistent with co-expression of CXCR3 and CXCR5 on the common Th1/Tfh precursor as documented here, CXCR3 expression has previously been detected on cells with a Tfh-like phenotype[7,26]. CXCR3$^+$ CXCR5$^+$ PD-1^{low} cells, as well as Tfh-like cells that share chemokine receptor and transcription factor expression with Th2 or Th17 cells, have also been detected in human peripheral blood[85]. CXCR3$^+$ Tfh-like cells have been associated with improved responses to influenza vaccination and correlate with neutralizing antibodies in HIV controllers[86-88]. These circulating Tfh-like cells express CD62L and CCR7, suggesting that they are in a less differentiated or memory-like state[85] and remain responsive to antigenic stimulation. Our definition of a CXCR3$^+$ CXCR5$^+$ Th1/Tfh precursor state thus provides a mechanistic explanation for these dual phenotypes, revealing a flexible intermediate state

that can give rise to both Th1 and Tfh lineages and likely corresponds to previously described pre-Tfh cells. We postulate that the differentiation fate of these Th1/Tfh precursors is guided by the relative dominance of chemokine cues, with CXCR5 directing cells toward B cells for Tfh differentiation and CXCR3 guiding them to cDC1s for Th1 differentiation.

Our data also clarify the step-wise differentiation process in which responder CD4$^+$ T cells rely on interactions with different antigen presenting cells and the costimulatory signals they provide. Formation of Th1/Tfh precursors depends on CD28-signalling via either CD80 or CD86, likely reflecting the essential role of CD28 in driving clonal expansion of responder T cells[63]. Consistent with a chemokine- and costimulation-guided model, we found that cDC1 and CD40:CD40L interaction are required for Th1 differentiation from the common precursor, whereas B cells and ICOS costimulation are required for Tfh differentiation. CD40 signaling in cDC1 is associated with upregulation of costimulatory molecules such as CD70, expression of IL-12 and apoptosis resistance[18,89,90]. CD40 is also critical in the maintenance of Tfh and GC responses[66], and it was somewhat surprising that blockade did not affect Tfh cell differentiation in our model. Similarly, CD86 is known to promote Tfh differentiation[65], but we did not find any effects of single CD86 blockade. This may be explained by the fact that we focused on early differentiation stages, prior to the establishment of germinal centers, when CD40 and CD86 signals may be trivial or compensated for. In addition to cDC1, CD40 signals and CXCR3-attracting chemokines can also be delivered by monocyte-derived (Mo)DCs present within the IFR[91]. This aligns with our recent data showing that CD4$^+$ T cells and MoDCs communicate in a CD40-dependent feed-forward loop to enforce Th1 effector differentiation[40], which can be mediated by IL-12[92,93].

The formation of a Th1/Tfh precursor thus allows immune system flexibility in tailoring host protection to ongoing infections. Different viral infections can result in different Th1/Tfh ratios, which are reinforced through regulatory feedback loops that modulate the expression of T-bet or BCL6[5,10,21,94]. For example, acute LCMV and influenza infections differentially depend on T-bet expression[95], whereas vesicular stomatitis virus (VSV) induces a higher Tfh/Th1 ratio than LCMV[10]. Given that Th1/Tfh precursors arise across diverse infection models, their subsequent differentiation is likely context-dependent, with the relative balance of T-bet and BCL6 expression determining commitment to either the Th1 or Tfh lineage[24].

Our data further demonstrate that Th1/Tfh precursors are not restricted to vaccination or acute infection, but share a core gene signature with stem-like CD4$^+$ T cells, including *Tcf7*, *Pdcd1*, *Slamf6*, *Ldha*, and *Gpr183*, underscoring their conserved and flexible nature. Stem-like CD4$^+$ T cells, previously identified in transplantation rejection and cancer, have been shown to act as key intermediates that can re-establish Th1 effector differentiation[45,49]. Interestingly, a pan-cancer analysis across 21 tumor types identifies a tumor-enriched CD4$^+$ T-cell population predicted to be tumor-specific and characterized by both Th1- and Tfh-associated gene expression[96], which

qualifies as Th1/Tfh precursor cells. Together, these findings underscore the need to generally acknowledge the Th1/Tfh precursor cell state and to fully define the developmental cues for either Th1 or Tfh differentiation from this state.

Limitations of the study

A limitation of our study is that we did not directly test whether individual precursors are truly bipotent, which would require tracking of single $CXCR3^{+}CXCR5^{+}$ Th1/Tfh cells after adoptive transfer into recipient mice. In addition, given the transcriptional similarity between the Th1/Tfh precursor population, stem-like $CD4^{+}$ T cells, and memory-precursors arising during chronic LCMV-infection, future studies should determine whether Th1/Tfh precursor cells possess self-renewal and memory potential, and can therefore be functionally classified as stem-like.

Methods

Animal models

Mice were housed in individually ventilated cages (IVC) under specific pathogen free (SPF) conditions in groups of 2-4 mice per cage for males or 2-5 mice per cage for females. Mice received *ad libitum* access to water and standard laboratory chow diet. Ambient temperature was ~19-21°C and humidity 30-70%. Lighting was provided on a 12 h light/dark cycle. Eight-week-old male and female C57BL/6JRj mice were purchased from Janvier laboratories (Le Genest Saint Isle, France). OTII*CD45.1 (B6.SJL-PtprcaPepcbTg(TcraTcrb)425Cbn/CrlLumc) on a C57BL/6JRj background were bred in-house, and genotype was verified by flow cytometry. $Batf3^{-/-}$ (B6.129S(C)-Batf3tm1Kmm/J) on a C57BL/6J background and wild-type C57BL/6J control mice were obtained from The Jackson Laboratory. Mice were habituated for 1 week prior to the start of an experiment and only one sex was used per experiment. All mouse experiments were performed in accordance with institutional and national guidelines under license number AVD16497, and were approved by the Animal Welfare Body at Leiden University Medical Center.

DNA tattoo vaccination

The cDNAs encoding the MHC-II, MHC-II:OVA, MHC-IIGP(61-80) and control sequences used for DNA vaccination were expressed in a pVAX1 plasmid vector. MHC-II and control vaccines have previously been described[34,37]. MHC-II:OVA and MHC-II-GP(61-80) vaccines were generated by excising the cassette encoding the MHC-II epitopes (p30, PADRE, HIV $Nef_{56\text{-}68}$) from the MHC-II vaccine cDNA with HindIII and XhoI restriction enzymes, and replacing it with a gBlock containing the MHC-II cassette linked to nucleotide sequences encoding $OVA_{323\text{-}339}$ (ISQAVHAAHAEINEAGR) or LCMV-Armstrong derived $GP_{61\text{-}80}$ (GLKGPDIYKGVYQFKSVEFD) and a GPGPGPG linker on both ends as for the original MHC-II vaccine.

For intraepidermal DNA tattoo vaccination[34,41], mice were anesthetized using isoflurane (Alvira Isoflutek 1000mg/g, induction phase: 4% isoflurane, airflow 0.8 l/min; maintenance phase: 2% isoflurane, airflow 0.4 l/min) and the right hind leg of mice was depilated using Veet containing limonene (Reckitt Benckiser). Subsequently, 15 µl of a 2 mg/ml plasmid DNA in H_2O was tattooed into the skin with a Permanent Make Up tattoo machine (Cheyenne, MT Derm GmbH) using a sterile disposable needle with a needle depth of 1 mm. Tattooing was performed for 45 sec, oscillating at a frequency of 100 Hertz. Mice were vaccinated on day 0, 3, and 6 unless otherwise indicated in the relevant figure legend or Results section, and alternating between the internal or external upper part of the right hind leg.

Adoptive T-cell transfer

For adoptive transfer, spleens were isolated from 8- to 12-week-old, sex matched OTII*CD45.1 mice after euthanasia. Spleens were mechanically disrupted and passed through a 70 µM Falcon strainer (Corning). Subsequently, single cell suspensions were incubated in red blood cell (RBC) lysis buffer (Santa Cruz) for 5 min at room temperature. $CD4^+$ T cells were isolated by negative selection using a $CD4^+$ T-cell isolation kit (Miltenyi) according to the manufacturer's protocol. If indicated, purified OTII*CD45.1 $CD4^+$ T cells were labelled with 2.5 µM CFSE (Invitrogen) for 10 min at 37°C. Free CFSE was then quenched by adding at least five times excess of Iscove's modified Dulbecco's medium (IMDM) with L-glutamine (Capricorn) and 10% fetal bovine serum (FBS), 100 units/ml penicillin and 100 mg/ml streptomycin (Gibco), and resting cells for 5 min at room temperature. Cell purity (>90%) and CFSE-labelling were checked for each experiment by flow cytometry using the following monoclonal antibodies (mAbs) against mouse molecules: 1:100 CD45.1 BUV395 (clone A20, BD Biosciences), 1:200 CD4 BUV805 (clone GK1.5, BD Biosciences), 1:200 TCRvα2 BV421 (clone B20.1),TCRvβ5.1/5.2 PE-Cy7 (clone MR9-4), 1:100 CD44 BV570 (clone IM7), and 1:100 CD62L PE-Fire 810 (clone W18021D; all BioLegend). C57BL/6JRj mice received 0.1 x 10^6 or 0.5 x 10^6 or 1 x 10^6 OTII*CD45.1 cells in 100 µl Hank's Balanced Salt Solution (HBSS) depending on the day of read out, or 5 x 10^5 purified SMARTA*GFP (B6.Cg-Ptprca Pepcb Tg(TcrLCMV)1Aox/PpmJx) cells in 100 µl HBSS, kindly provided by Dr. K. Jobin and Prof. W. Kastenmüller (University of Würzburg, Germany), by retro-orbital i.v. injection under isoflurane anesthesia.

When indicated, purified OTII*CD45.1 $CD4^+$ T cells were genetically modified using Cas9 RNPs (protocol adapted from refs.[97,98]). Briefly, purified cells were electroporated with complexes of *S. pyogenes* Cas9 nuclease V3 (Integrated DNA Technologies) and control or ICOS targeting gRNAs in P4 Primary Cell solution (Lonza) using a 4D Nucleofector X-16 Strip unit (Lonza) with DN100 settings. A combination of three guide sequences were used to target the genomic sequence of the *Icos* gene: #1 ACAATCGCATTTTTAACTGC; #2 TGGTCTTGGTGAGTTCGCAG; #3 GAGGTGGGTCAAAAATGGAC; whereas the following sequence was used as non-targeting control: GCACTACCAGAGCTAACTCA[97] (all from Integrated DNA Technologies). After electroporation cells were cultured for 24h in IMDM medium (Gibco) containing 10% FCS and

10 ng/mL recombinant IL-7 (Peprotech; 217-17), before transfer into recipient mice. Knockout efficiency was determined on day 5 or day 8 post-vaccination by flow cytometry. Only cells that lacked ICOS expression were analyzed for the $ICOS^{ko}$ group.

Antibody and reagent treatment of mice

All antibodies or reagents were injected intraperitoneally (i.p.). Mice received 250 µg depleting anti-CD20 mAb (MB20-11, BioXcell) at day -2. Mice with incomplete B-cell depletion were excluded from analysis. For blocking costimulatory ligands, mice received injections on days 0 and 3 post vaccination with 150 µg anti-CD40L mAb (MR-1, BioXcell), 200 µg anti-CD80 mAb (1G10, BioXcell), 200 µg anti-CD86 mAb (GL-1, BioXcell) or 200 µg anti-ICOSL mAb (HK5.3, BioXcell). FTY720 (Fingolimod, Cayman Chemicals) was dissolved in 96% ethanol at 20 mg/ml and prior to injection diluted in 0.9% NaCl. Mice received 25 µg FTY720 in 200 µl 0.9% NaCl at days 0, 3 and 6.

Cell isolation

On the day of readout, mice were euthanized and organs collected. Blood was collected by tail vein puncture or cardiac puncture. Erythrocytes were lysed by incubation in RBC lysis buffer (Santa Cruz) for 5 min at room temperature. Inguinal dLNs of the vaccination site were punched repeatedly with a 25G needle and incubated for 30 min at 37°C while shaking in 100 µg/ml Liberase TL (Roche) prepared in 500 ml DMEM. Enzymatic digestion was quenched by adding FBS-supplemented IMDM, and single cell suspensions prepared by mechanical disruption of dLNs through 70 µm Falcon strainers (Corning).

Flow cytometry

For cell surface staining, mAbs were diluted in FACS buffer (PBS + 2% FBS). Single cell suspensions were first incubated for 1 h at room temperature with 1:200 PE-conjugated PADRE tetramer (AKFVAAWTLKAA in I-A(b), NIH tetramer facility), and then for 30 min on ice with the following mAbs: 1:200 CD4 BUV805 (clone GK1.5), 1:200 PSGL1 BUV661 (clone 2PH1), 1:200 CD8a BV750 (clone 53-6.7), 1:100 CD8a V500 (clone 53-6.7), 1:400 CD95 BV605 (clone Jo2), 1:100 FR4 BUV661 (clone 12A5), 1:100 CD45.1 BUV395 (clone A20, all BD Biosciences), 1:200 CD138 BV421 (clone 281-2), 1:400 GL7 FITC (clone GL-7), 1:600 IgD PerCP-Cy5.5 (clone 11-26c2a), 1:100 CD44 BV570 (clone IM7), 1:100 CD44 BV785 (clone IM7), 1:100 CD62L PE-Fire 810 (clone W18021D), 1:100 PD-1 APC-Fire 810 (29F.1A12), 1:100 SLAM BV785 (clone TC15-12F12.2), 1:100 SLAMF6 Pacific Blue (clone 330-AJ), 1:100 CD3 PE-Fire 700 (17A2), 1:50 CXCR5 BV711 (clone L138D7), 1:50 CXCR3 BV605 (clone CXCR3-173), 1:200 ICOS PE-Cy7 (clone C398.4A, all BioLegend), 1:200 TACI APC (clone ebio8F10-3, eBioscience), 1:800 CD19 BUV661 (clone ebio1D3, Invitrogen), and APC-conjugated E7 tetramer (E7(49-57) RAHYNIVTF in $H\text{-}2D^{b}$, produced in house). Dead cells were excluded using 1:500 Zombie UV fixable viability dye (BioLegend) or 1:1000 LIVE/DEAD NIR fixable viability dye (Invitrogen).

For intracellular staining of T cell-related markers, cells were fixed with the Foxp3/Transcription factor staining kit (eBioscience). For intracellular staining of B cell-related markers, cells were

fixed with BD Cytofix/Cytoperm (BD Biosciences). In both cases, fixation was performed for 30 min on ice. After fixation, cells were either permeabilized and intracellularly stained directly or washed with FACS buffer and frozen gradually at -80°C in 10% DMSO and 90% FBS. Upon thawing, cells were washed with FACS buffer and re-fixed for 5 min at room temperature prior to permeabilization and intracellular antibody staining. The following mAbs were used: 1:50 BCL6 BUV737 (clone K112-91), 1:50 GATA3 BUV395 (clone L50-823), 1:100 RORγt BV480 (clone Q31-378, all BD Biosciences), 1:100 TCF1 Alexa fluor 488 (clone C63D9, Cell Signalling Technology), 1:200 T-bet eFluor 660 (clone ebio4B10, eBioscience) and 1:100 FOXP3 PE-Cy5 (clone FJK16s, Invitrogen). Data were acquired using a Cytek Aurora Spectral Flow Cytometer equipped with 355 nm, 405 nm, 488 nm, 561 nm and 640 nm lasers (Cytek Biosciences), and analysed with OMIQ (Dotmatics version 2024.07) or FlowJo software (TreeStar, version 10.8.1).

UMAP analysis and Wishbone trajectory analysis were performed using OMIQ on a maximum of 1000 PADRE^{+} CD4^{+} T cells per mouse (N=5/time point, total 27867 cells). For dimension reduction and Wishbone analysis, the following markers were included: PSGL1, FR4, BCL6, SLAMF6, CD44, CXCR5, SLAM, TCF1, CD62L, T-bet and PD-1. For Wishbone analysis, diffusion maps were generated first and then Wishbone was performed from diffusion components, with naive (CD62L^{low} CD44^{hi} PD-1^{-} SLAMF6^{-}) cells selected as starting point.

Preparations for transcriptome analysis

Mice received MHC-II vaccine and cells were harvested at day 5 or 10 after the first vaccination. Single cell suspensions of dLNs from 3 mice per time point were pooled to reduce biological variability. Samples were incubated with 1:50 anti-mouse CD16/32 mAb (Fc Block™, clone 2.4G2, BD Biosciences) in BD Stain buffer (with FBS, BD Biosciences) for 5 min on ice and subsequently stained with the following mAbs in BD stain buffer: 1:100 CD3 BV421 (clone 17A2, Biolegend), 1:100 CD19 PerCP-Vio700 (clone REA749, Miltenyi Biotech), 1:100 CD44 PE-Cy7 (clone IM7, eBioscience), 1:100 CD62L FITC (clone Mel-14, eBioscience) and 1:1000 LIVE/DEAD Fixable Near-IR dye (Invitrogen). CD3^{+} CD44^{hi} CD62L^{low} cells were FACS-sorted on a FACSAria II (BD Biosciences). Subsequently, samples were stained with unique hashtag oligonucleotide (HTO)-conjugated antibodies to CD45/MHC-I (TotalSeq C hashtags, C0301 to C0307 and C0309, BioLegend). Staining was performed according to the manufacturer's instructions. Briefly, FACS-sorted T cells were stained with 0.5 µg TotalSeq hashtag per sample for 30 min on ice and washed 5 times with PBS + 0.04% BSA. Prior to last wash, cells were passed through a 40 µm Flowmi Cell Strainer (Sigma-Aldrich) and samples were pooled. scRNAseq libraries were created according to the manufacturer's protocol, using a 10X Chromium single cell 5'v2 chemistry kit (10X Genomics). TCRseq library was prepared using a 10X Chromium single cell V(D)J enrichment kit for mouse T cells (10X Genomics). Nucleotide sequencing was performed on a NovaSeq6000 system (Illumina). In total, 25132 cells were analyzed for sequencing with a median sequencing-depth of 11196 reads per cell.

Processing, integration and clustering of transcriptome data

Analysis of scRNAseq and TCRseq data was performed using CellRanger (10X Genomics, v6.0.1) and Seurat (v4.3.0) in R (v4.2.3). scRNAseq reads were aligned to the mouse reference genome mm10, and barcode counting was performed using 'cellranger count'. TCRseq reads were aligned to the mouse reference genome mm10 and consensus TCR sequences were determined using 'cellranger vdj'. From the gene expression count matrix, TCR and BCR genes were removed using the 'grep' function in R with the patterns "^Tr[abgd][cvdj]" and "Ig[hkl][cvdj]" respectively. After this, the dataset was analyzed in R using the standard Seurat pipeline. Seurat object was created using 'CreateSeuratObject,' with a minimum of 200 features per cell and 3 cells expressing each gene. HTO sequencing data was added as a separate assay to the Seurat object using 'CreateAssayObject' and HTO counts were normalized by CLR method using 'NormalizeData.' HTO demultiplexing was performed using 'HTODemux' with a positive quantile of 0.99. As a result of this, each cell in the dataset was assigned to a global (singlet, doublet, or negative) and a sample-related HTO classification. Heatmap was created of HTO demultiplexing result using 'HTOHeatmap.' Singlets were selected using 'subset', and gene expression data was normalized using 'NormalizeData'. Variable features were determined using 'FindVariableFeatures' with the selection method 'mean.var.plot'. Data was scaled using 'ScaleData' on variable features. Percentage of mitochondrial gene expression per cell was determined using 'PercentageFeatureSet' with the pattern "^mt-". Singlets were filtered on number of RNA features (between 400 and 5000), number of RNA counts (<25000) and mitochondrial gene expression (<10%). Cell cycle scores for G2/M and S phase were assigned using 'CellCycleScoring', based on expression of G2/M and S phase genes. Data was normalized using 'NormalizeData' with normalization method 'LogNormalize', scale factor 25000. Top 2000 variable features were determined using 'FindVariableFeatures' with the selection method 'vst'. Data was scaled using 'ScaleData', whereby G2M scores, S scores and percentage of mitochondrial gene expression were regressed out. Principal component analysis (PCA) was run using 'RunPCA' on variable features. Clustering was performed on first 20 principal components (PCs) using 'FindNeighbors' and 'FindClusters'. Clustering resolution was set to 0.5. Uniform manifold approximation and projection (UMAP) visualization was performed using 'RunUMAP' on the first 20 PCs. Expression of known marker genes was visualized per cluster and within the UMAP projection using 'Dotplot', 'VlnPlot' and 'FeaturePlot' functions. Clusters with contaminating B cells (expression of *Cd19*, *Ms4a1*), APCs (expression of *Cd40*, *Cd274*, *Cd80*, *Cd86*) and low-quality cells (high percentage mitochondrial genes, low RNA counts) were removed. The pipeline was run again on filtered T cells, including determining variable features, data scaling, PCA, clustering and UMAP visualization. $CD4^+$ T-cell clusters were selected by expression of *Cd4*, in absence of expression of *Cd8a* and *Cd8b1* or TCRg/d. Within $CD4^+$ T-cell subsets, Help d5 and Help d10 were selected for further analysis. Clusters were annotated based on differentially expressed genes (Table S1). Venn Diagrams were created with http://bioinformatics.psb.ugent.be/webtools/Venn/.

Previously generated scRNAseq datasets from I-A^b-LCMV-gp66 tetramer-sorted CD4$^+$ T cells from LCMV-Armstrong or LCMV-Clone 13 derived at day 8 and day 21 post infection were obtained from Xia *et al.*[54]. Feature barcode matrices derived from 10x scRNA expression libraries reads aligned to mouse genome assembly GRCm38 were imported into R (version 4.4.0). A Seurat-based (version 5.2.1) quality control on the scRNA-seq samples was performed individually. TCR and BCR counts were removed from the raw gene expression count matrix (UMI) to prevent TCR/BCR chain driven clustering bias. A per-sample Seurat object was created by selecting cells on the criterium of containing a minimum of 200 genes and genes on being expressed in a minimum of 3 cells. Cells (~30%) were excluded from the subsequent analysis based on the mitochondrial content (>5%), RNA count (<1000 and >25000) and genetic content (<400 and >4000). The top 2000 highly variable genes were selected using 'FindVariableFeatures' for subsequent analysis. Cells of all 19 samples were first normalized using Seurat's 'NormalizeData' function and then scaled individually while regressing out mitochondrial gene expression and cell cycle scores for G2/M and S phase genes assigned using 'CellCycleScoring' as described above. Clustering was done on the first 30 principal components (PCs) with the default cluster resolution. Doublets were removed using 'DoubletFinder' based on the first 40 principal components (PCs).

Singlets of each sample were integrated by identifying anchors between datasets, using the top 2000 variable genes, 30 reciprocal PCA dimensions and an integration strength of 5. Clusters with contaminating B cells (expression of Cd19 Ms4a1), CD8 T cells (expression of Cd8a, Cd8b), APCs (expression of Cd40, Cd80, Cd86) or low-quality cells were removed. Data scaling and PCA was done once more on the integrated and filtered object. A k-nearest neighbors' graph was generated with the first 20 PCs and community detection for cluster identification was performed using the Louvain algorithm with a resolution of 0.4. The integrated matrix visualized as an UMAP was subsequently divided based on the day of infection (Day 8 or Day 21) and the viral strain (LCMV-Arm and LCMV-cl.13) as annotated in the metadata of the Seurat object.

Clusters were annotated based on differentially expressed genes (Table S2). To facilitate cluster identification, we compared each cluster to CD4$^+$ T-cell-specific signatures derived from vaccine-induced Th1, Tfh, and Th1/Tfh precursor populations characterized in this study. Module scores for each gene signature were calculated per cell using Seurat's 'AddModuleScore' function, based on normalized expression values from the 'data' slot of the integrated object, which were not corrected for cell cycle gene expression. Cluster-defining markers were then selected and their relative normalized expression values represented in z-scores were visualized in a heatmap using Seurat's 'pheatmap'.

The correlation plots were generated by extraction of the upregulated differentially expressed (DE) genes (only.pos = TRUE) of the concerning clusters compared to all other clusters present in the UMAP using 'FindAllMarkers' on the integrated Seurat object. Only significant DE genes (FDR < 0.05) were then used to determine the intersected (intersect) and unified (union) gene

collection when comparing the LCMV with the vaccination model. List of differentially expressed genes of LCMV-specific Th1/Tfh precursor and LCMV-specific memory-precursor cell cluster are provided in Table S3. The DE gene collection was then projected (filter and select) onto the ranked normalized expression list of all genes present in the concerning clusters. The extracted expression values of DE markers for both the LCMV and the vaccination model were correlated using the stats::cor() function and the "spearman" method for correlation. Plots were generated using ggplot() and the linear model ("lm") method to create a regression line for visualization.

The stem-like $CD4^+$ T-cell signature was derived from Cardenas *et al.*[49] (62 genes). The Th1/Tfh precursor gene signature for malaria-specific $CD4^+$ T cells was obtained from Lönnberg *et al.*[4] and comprised 1,625 dynamic genes [D statistic >50; kindly analyzed by Dr. Valentine Svensson (Tahoe Therapeutics)]. These genes were selected based on peak expression between pseudotime values of 0.5 and 1.6, corresponding to the period immediately before and after the Th1/Tfh bifurcation, which was inferred at a pseudotime value of 1.27. Gene signatures of malaria-induced Th1/Tfh precursor is provided in Table S4. A ranked list of genes and normalized expression values (ranking metric) of the vaccine-induced Th1/Tfh precursor cluster was extracted from the integrated Seurat object. The running-sum statistic was then calculated using the clusterProfiler::GSEA() function and the results were plotted with enrichplot::gseaplot2().

Statistics

For mouse experiments, statistical analysis was performed with GraphPad Prism 9.3.1 (Dotmatics) using two-tailed unpaired Student's *t*-test when comparing two groups, One-Way ANOVA with Dunnett's *post hoc* test to correct for multiple testing when comparing multiple groups at one timepoint or Two-Way ANOVA with Šidák *post hoc* test to correct for multiple testing when comparing multiple groups at multiple time points. Explanation of statistical parameters such as mean, SD and n are mentioned in figure legends. P values < 0.05 were considered statistically significant. Statistics were denoted as follows: * P≤0.05, ** P≤0.01, *** P≤0.001, and **** P≤0.0001. Plots were generated with ggplot2 (3.3.3) and GraphPad Prism 9.3.1.

Data availability

All data generated and analyzed in this study are included in this article, its supplementary information, or have been made available in public repositories. ScRNAseq and TCRseq data generated in this study are available from the NCBI Gene Expression Omnibus (GEO) repository under the accession code GSE249046. scRNAseq data of GP66 tet^+ $CD4^+$ T cells following LCMV-Armstrong or LCMV-Clone 13 infections were extracted and re-analysed from GSE181474[54]. scRNAseq data of *Plasmodium*-specific TCR transgenic $CD4^+$ T (PbTII) cells post *Plasmodium chabaudi chabaudi* AS (PcAS) infection were extracted and re-analysed from Lönnberg et al.

2017[4]. Gene signature of stem-like CD4$^+$ T cells was extracted from Cardenas et al. 2024[50]. Flow cytometry data from this study are available upon request.

Acknowledgements

We thank the Animal facility, Flow Cytometry Facility and Leiden Genome Technology Center from the LUMC for technical assistance. We also thank Dr. Vincent van Unen (LUMC) for his support with scRNAseq data analysis, and Dr. Tapio Lönnberg (University of Turku) and Dr. Valentine Svensson (Tahoe Therapeutics) for providing us with the malaria-induced Th1/Tfh gene signature. This work was supported by grants 11079 (to J.Bo and Y.X) and 10894 (to J.Bo) from the Dutch Cancer Society (KWF); a grant from Oncode to J.Bo; a VENI grant (ZonMw project n. 09150162010046) from the Dutch Science Foundation (NWO) and a Gisela Thier fellowship from Leiden University Medical Center to F.S.

Author contributions

Conceptualization: D.M.T.B, J.Bo, F.S. Methodology and investigation: D.M.T.B, J.Bu, M.D.S, M.R, X.L, T.d.W, Y.X, F.S. Formal analysis, visualization and data curation: D.M.T.B, J.Bu, M.d.K, F.S. Writing - original draft: D.M.T.B, J.Bo, F.S. Writing - review and editing: D.M.T.B, J.Bu, M.D.S, M.R, M.d.K, X.L, T.d.W, Y.X, J.Bo, F.S. Project administration, funding acquisition and supervision: J.Bo. and F.S.

Competing Interests

The authors declare no competing interests.

References

1. Yin, X., Chen, S., and Eisenbarth, S.C. (2021). Dendritic Cell Regulation of T Helper Cells. Annual review of immunology *39*, 759-790. 10.1146/ANNUREV-IMMUNOL-101819-025146.
2. Vinuesa, C.G., Linterman, M.A., Yu, D., and Maclennan, I.C.M. (2016). Follicular Helper T Cells. Annual review of immunology *34*, 335-368. 10.1146/ANNUREV-IMMUNOL-041015-055605.
3. Osum, K.C., and Jenkins, M.K. (2023). Toward a general model of CD4+ T cell subset specification and memory cell formation. Immunity *56*, 475-484. 10.1016/J.IMMUNI.2023.02.010.
4. Lönnberg, T., Svensson, V., James, K.R., Fernandez-Ruiz, D., Sebina, I., Montandon, R., Soon, M.S.F., Fogg, L.G., Nair, A.S., Liligeto, U.N., et al. (2017). Single-cell RNA-seq and computational analysis using temporal mixture modelling resolves Th1/Tfh fate bifurcation in malaria. Science immunology *2*. 10.1126/SCIIMMUNOL.AAL2192.
5. Duckworth, B.C., and Groom, J.R. (2021). Conversations that count: Cellular interactions that drive T cell fate. Immunological reviews *300*, 203-219. 10.1111/IMR.12945.
6. Eisenbarth, S.C., Baumjohann, D., Craft, J., Fazilleau, N., Ma, C.S., Tangye, S.G., Vinuesa, C.G., and Linterman, M.A. (2021). CD4+ T cells that help B cells - a proposal for uniform nomenclature. Trends in immunology *42*, 658-669. 10.1016/J.IT.2021.06.003.
7. Künzli, M., and Masopust, D. (2023). CD4+ T cell memory. Nature Immunology 2023 *24*, 1-12. 10.1038/s41590-023-01510-4.
8. Dalit, L., Tan, C.W., Sheikh, A.A., Munnings, R., Howson, L.J., Alvarado, C., Hussain, T., Zaini, A., Cooper, L., Kirn, A., et al. (2025). Divergent cytokine and transcriptional signatures control functional T follicular helper cell heterogeneity. Nature immunology *26*, 1821-1835. 10.1038/S41590-025-02258-9.
9. Dudziak, D., Kamphorst, A.O., Heidkamp, G.F., Buchholz, V.R., Trumpfheller, C., Yamazaki, S., Cheong, C., Liu, K., Lee, H.W., Chae, G.P., et al. (2007). Differential antigen processing by dendritic cell subsets in vivo. Science *315*, 107-111. 10.1126/science.1136080
10. De Giovanni, M., Cutillo, V., Giladi, A., Sala, E., Maganuco, C.G., Medaglia, C., Di Lucia, P., Bono, E., Cristofani, C., Consolo, E., et al. (2020). Spatiotemporal regulation of type I interferon expression determines the antiviral polarization of CD4+ T cells. Nature Immunology *21*, 321-330. 10.1038/s41590-020-0596-6.
11. Hilligan, K.L., and Ronchese, F. (2020). Antigen presentation by dendritic cells and their instruction of CD4+ T helper cell responses. Cellular & Molecular Immunology 2020 17:6 *17*, 587-599. 10.1038/s41423-020-0465-0.
12. Den Haan, J.M.M., Lehar, S.M., and Bevan, M.J. (2000). CD8(+) but not CD8(-) dendritic cells cross-prime cytotoxic T cells in vivo. The Journal of experimental medicine *192*, 1685-1695. 10.1084/JEM.192.12.1685.
13. Hildner, K., Edelson, B.T., Purtha, W.E., Diamond, M., Matsushita, H., Kohyama, M., Calderon, B., Schraml, B.U., Unanue, E.R., Diamond, M.S., et al. (2008). Batf3 deficiency reveals a critical role for CD8alpha+ dendritic cells in cytotoxic T cell immunity. Science (New York, N.Y.) *322*, 1097-1100. 10.1126/SCIENCE.1164206.
14. Martínez-López, M., Iborra, S., Conde-Garrosa, R., and Sancho, D. (2015). Batf3-dependent CD103+ dendritic cells are major producers of IL-12 that drive local Th1 immunity against Leishmania major infection in mice. European journal of immunology *45*, 119-129. 10.1002/EJI.201444651.
15. Ferris, S.T., Durai, V., Wu, R., Theisen, D.J., Ward, J.P., Bern, M.D., Davidson, J.T., Bagadia, P., Liu, T., Briseño, C.G., et al. (2020). cDC1 prime and are licensed by CD4+ T cells to induce anti-tumour immunity. Nature *584*, 624-629. 10.1038/S41586-020-2611-3.

16. Wu, R., and Murphy, K.M. (2022). DCs at the center of help: Origins and evolution of the three-cell-type hypothesis. The Journal of experimental medicine *219*. 10.1084/JEM.20211519.

17. Borst, J., Ahrends, T., Bąbała, N., Melief, C.J.M., and Kastenmüller, W. (2018). CD4+ T cell help in cancer immunology and immunotherapy. Nature Reviews Immunology. 18(10):635-647.

18. Lei, X., de Groot, D.C., Welters, M.J.P., de Wit, T., Schrama, E., van Eenennaam, H., Santegoets, S.J., Oosenbrug, T., van der Veen, A., Vos, J.L., et al. (2024). CD4+ T cells produce IFN-I to license cDC1s for induction of cytotoxic T-cell activity in human tumors. Cellular & molecular immunology *21*, 374-392. 10.1038/S41423-024-01133-1.

19. Crotty, S. (2014). T follicular helper cell differentiation, function, and roles in disease. Immunity *41*, 529-542. 10.1016/J.IMMUNI.2014.10.004.

20. Nakayamada, S., Kanno, Y., Takahashi, H., Jankovic, D., Lu, K.T., Johnson, T.A., Sun, H.w., Vahedi, G., Hakim, O., Handon, R., et al. (2011). Early Th1 Cell Differentiation Is Marked by a Tfh Cell-like Transition. Immunity *35*, 919-931. 10.1016/J.IMMUNI.2011.11.012.

21. Choi, J., Diao, H., Faliti, C.E., Truong, J., Rossi, M., Bélanger, S., Yu, B., Goldrath, A.W., Pipkin, M.E., and Crotty, S. (2020). Bcl-6 is the nexus transcription factor of T follicular helper cells via repressor-of-repressor circuits. Nature immunology *21*, 777-789. 10.1038/S41590-020-0706-5.

22. Nurieva, R.I., Chung, Y., Martinez, G.J., Yang, X.O., Tanaka, S., Matskevitch, T.D., Wang, Y.H., and Dong, C. (2009). Bcl6 mediates the development of T follicular helper cells. Science (New York, N.Y.) *325*, 1001-1005. 10.1126/SCIENCE.1176676.

23. Johnston, R.J., Poholek, A.C., DiToro, D., Yusuf, I., Eto, D., Barnett, B., Dent, A.L., Craft, J., and Crotty, S. (2009). Bcl6 and Blimp-1 are reciprocal and antagonistic regulators of T follicular helper cell differentiation. Science (New York, N.Y.) *325*, 1006-1010. 10.1126/SCIENCE.1175870.

24. Oestreich, K.J., Mohn, S.E., and Weinmann, A.S. (2012). Molecular mechanisms that control the expression and activity of Bcl-6 in TH1 cells to regulate flexibility with a TFH-like gene profile. Nature Immunology 2012 13:4 *13*, 405-411. 10.1038/ni.2242.

25. Fang, D., Cui, K., Mao, K., Hu, G., Li, R., Zheng, M., Riteau, N., Reiner, S.L., Sher, A., Zhao, K., and Zhu, J. (2018). Transient T-bet expression functionally specifies a distinct T follicular helper subset. Journal of Experimental Medicine *215*, 2705-2714. 10.1084/JEM.20180927.

26. Weinstein, J.S., Laidlaw, B.J., Lu, Y., Wang, J.K., Schulz, V.P., Li, N., Herman, E.I., Kaech, S.M., Gallagher, P.G., and Craft, J. (2018). STAT4 and T-bet control follicular helper T cell development in viral infections. Journal of Experimental Medicine *215*, 337-355. 10.1084/JEM.20170457.

27. Cho, Y.L., Flossdorf, M., Kretschmer, L., Höfer, T., Busch, D.H., and Buchholz, V.R. (2017). TCR Signal Quality Modulates Fate Decisions of Single CD4+ T Cells in a Probabilistic Manner. Cell Reports *20*, 806-818. 10.1016/J.CELREP.2017.07.005.

28. Fazilleau, N., McHeyzer-Williams, L.J., Rosen, H., and McHeyzer-Williams, M.G. (2009). The function of follicular helper T cells is regulated by the strength of T cell antigen receptor binding. Nature immunology *10*, 375-384. 10.1038/NI.1704.

29. Tubo, N.J., Pagán, A.J., Taylor, J.J., Nelson, R.W., Linehan, J.L., Ertelt, J.M., Huseby, E.S., Way, S.S., and Jenkins, M.K. (2013). Single Naive CD4+ T Cells from a Diverse Repertoire Produce Different Effector Cell Types during Infection. Cell *153*, 785-796. 10.1016/J.CELL.2013.04.007.

30. Künzli, M., Reuther, P., Pinschewer, D.D., and King, C.G. (2021). Opposing effects of T cell receptor signal strength on CD4 T cells responding to acute versus chronic viral infection. eLife *10*. 10.7554/ELIFE.61869.

31. Alterauge, D., Bagnoli, J.W., Dahlström, F., Bradford, B.M., Mabbott, N.A., Buch, T., Enard, W., and Baumjohann, D. (2020). Continued Bcl6 Expression Prevents the Transdifferentiation of Established Tfh Cells into Th1 Cells during Acute Viral Infection. Cell Reports *33*, 108232-108232. 10.1016/J.CELREP.2020.108232.

32. O'Shea, J., and Paul, W.E. (2010). Mechanisms underlying lineage commitment and plasticity of helper CD4+ T cells. Science (New York, N.Y.) *327*, 1098-1102. 10.1126/SCIENCE.1178334.

33. Kiner, E., Willie, E., Vijaykumar, B., Chowdhary, K., Schmutz, H., Chandler, J., Schnell, A., Thakore, P.I., LeGros, G., Mostafavi, S., et al. (2021). Gut CD4+ T cell phenotypes are a continuum molded by microbes, not by TH archetypes. Nature immunology *22*, 216-228. 10.1038/S41590-020-00836-7.

34. Ahrends, T., Babała, N., Xiao, Y., Yagita, H., Van Eenennaam, H., and Borst, J. (2016). CD27 Agonism Plus PD-1 Blockade Recapitulates CD4 + T-cell Help in Therapeutic Anticancer Vaccination. Cancer Research *76*, 2921-2931. 10.1158/0008-5472.CAN-15-3130.

35. Ahrends, T., Busselaar, J., Severson, T.M., Bąbała, N., de Vries, E., Bovens, A., Wessels, L., van Leeuwen, F., and Borst, J. (2019). CD4+ T cell help creates memory CD8+ T cells with innate and help-independent recall capacities. Nature communications *10*. 10.1038/S41467-019-13438-1.

36. **3**Ahrends, T., Spanjaard, A., Pilzecker, B., Bąbała, N., Bovens, A., Xiao, Y., Jacobs, H., and Borst, J. (2017). CD4+ T Cell Help Confers a Cytotoxic T Cell Effector Program Including Coinhibitory Receptor Downregulation and Increased Tissue Invasiveness. Immunity *47*, 848-861.e845. 10.1016/J.IMMUNI.2017.10.009.

37. Oosterhuis, K., Aleyd, E., Vrijland, K., Schumacher, T.N., and Haanen, J.B. (2012). Rational Design of DNA Vaccines for the Induction of Human Papillomavirus Type 16 E6- and E7-Specific Cytotoxic T-Cell Responses. Human Gene Therapy *23*, 1301-1312. 10.1089/hum.2012.101.

38. Alexander, J., Sidney, J., Southwood, S., Ruppert, J., Oseroff, C., Maewal, A., Snoke, K., Serra, H.M., Kubo, R.T., Sette, A., and Grey, H.M. (1994). Development of high potency universal DR-restricted helper epitopes by modification of high affinity DR-blocking peptides. Immunity *1*, 751-761. 10.1016/S1074-7613(94)80017-0.

39. Rice, J., Elliott, T., Buchan, S., and Stevenson, F.K. (2001). DNA fusion vaccine designed to induce cytotoxic T cell responses against defined peptide motifs: implications for cancer vaccines. Journal of immunology (Baltimore, Md. : 1950) *167*, 1558-1565. 10.4049/JIMMUNOL.167.3.1558.

40. Bosma, D.M.T., Busselaar, J., Staal, M.D., Frijlink, E., Mack, M., Salerno, F., and Borst, J. (2025). CD4+ T-cell help delivery to monocyte-derived dendritic cells promotes effector differentiation of helper and cytotoxic T cells. Immunology letters *275*. 10.1016/J.IMLET.2025.107022.

41. Babała, N., Bovens, A., De Vries, E., Iglesias-Guimarais, V., Ahrends, T., Krummel, M.F., Borst, J., and Bins, A.D. (2018). Subcellular localization of antigen in keratinocytes dictates delivery of CD4 þ T-cell Help for the CTL response upon therapeutic DNA vaccination into the Skin. Cancer Immunology Research *6*, 835-847. 10.1158/2326-6066.CIR-17-0408.

42. Bins, A.D., Jorritsma, A., Wolkers, M.C., Hung, C.F., Wu, T.C., Schumacher, T.N.M., and Haanen, J.B.A.G. (2005). A rapid and potent DNA vaccination strategy defined by in vivo monitoring of antigen expression. Nature medicine *11*, 899-904. 10.1038/NM1264.

43. Marshall, H.D., Chandele, A., Jung, Y.W., Meng, H., Poholek, A.C., Parish, I.A., Rutishauser, R., Cui, W., Kleinstein, S.H., Craft, J., and Kaech, S.M. (2011). Differential Expression of Ly6C and T-bet Distinguish Effector and Memory Th1 CD4+ Cell Properties during Viral Infection. Immunity *35*, 633-646. 10.1016/J.IMMUNI.2011.08.016.

44. Shaw, L.A., Bélanger, S., Omilusik, K.D., Cho, S., Scott-Browne, J.P., Nance, J.P., Goulding, J., Lasorella, A., Lu, L.F., Crotty, S., and Goldrath, A.W. (2016). Id2 reinforces TH1 differentiation and inhibits E2A to repress TFH differentiation. Nature immunology *17*, 834-843. 10.1038/NI.3461.

45. Zou, D., Yin, Z., Yi, S.G., Wang, G., Guo, Y., Xiao, X., Li, S., Zhang, X., Gonzalez, N.M., Minze, L.J., et al. (2024). CD4+ T cell immunity is dependent on an intrinsic stem-like program. Nature immunology *25*, 66-76. 10.1038/S41590-023-01682-Z.

46. Choi, Y.S., Gullicksrud, J.A., Xing, S., Zeng, Z., Shan, Q., Li, F., Love, P.E., Peng, W., Xue, H.H., and Crotty, S. (2015). LEF-1 and TCF-1 orchestrate TFH differentiation by regulating differentiation circuits upstream of the transcriptional repressor Bcl6. Nature Immunology 2015 16:9 *16*, 980-990. 10.1038/ni.3226.

47. Setty, M., Tadmor, M.D., Reich-Zeliger, S., Angel, O., Salame, T.M., Kathail, P., Choi, K., Bendall, S., Friedman, N., and Pe'Er, D. (2016). Wishbone identifies bifurcating developmental trajectories from single-cell data. Nature biotechnology *34*, 637-645. 10.1038/NBT.3569.

48. Busselaar, J., Tian, S., van Eenennaam, H., and Borst, J. (2020). Helpless Priming Sends CD8+ T Cells on the Road to Exhaustion. Frontiers in Immunology *11*, 2637-2637. 10.3389/fimmu.2020.592569.

49. Cardenas, M.A., Prokhnevska, N., Sobierajska, E., Gregorova, P., Medina, C.B., Valanparambil, R.M., Greenwald, R., DelBalzo, L., Bilen, M.A., Joshi, S.S., et al. (2024). Differentiation fate of a stem-like CD4 T cell controls immunity to cancer. Nature 2024 636:8041 *636*, 224-232. 10.1038/s41586-024-08076-7.

50. Agata, Y., Kawasaki, A., Nishimura, H., Ishida, Y., Tsubata, T., Yagita, H., and Honjo, T. (1996). Expression of the PD-1 antigen on the surface of stimulated mouse T and B lymphocytes. International immunology *8*, 765-772. 10.1093/INTIMM/8.5.765.

51. Baumeister, S.H., Freeman, G.J., Dranoff, G., and Sharpe, A.H. (2016). Coinhibitory Pathways in Immunotherapy for Cancer. Annual review of immunology *34*, 539-573. 10.1146/ANNUREV-IMMUNOL-032414-112049.

52. Cibrián, D., and Sánchez-Madrid, F. (2017). CD69: from activation marker to metabolic gatekeeper. European journal of immunology *47*, 946-953. 10.1002/EJI.201646837.

53. Simms, P.E., and Ellis, T.M. (1996). Utility of flow cytometric detection of CD69 expression as a rapid method for determining poly- and oligoclonal lymphocyte activation. Clinical and diagnostic laboratory immunology *3*, 301-304. 10.1128/CDLI.3.3.301-304.1996.

54. Xia, Y., Sandor, K., Pai, J.A., Daniel, B., Raju, S., Wu, R., Hsiung, S., Qi, Y., Yangdon, T., Okamoto, M., et al. (2022). BCL6-dependent TCF-1+ progenitor cells maintain effector and helper CD4+ T cell responses to persistent antigen. Immunity *55*, 1200-1215.e1206. 10.1016/J.IMMUNI.2022.05.003.

55. Nguyen, C., Kudek, M., Zander, R., Niu, H., Shen, J., Bauer, A., Alson, D., Khatun, A., Chen, Y., Sun, J., et al. (2024). Bhlhe40 Promotes CD4+ T Helper 1 Cell and Suppresses T Follicular Helper Cell Differentiation during Viral Infection. Journal of immunology (Baltimore, Md. : 1950) *212*, 1829-1842. 10.4049/JIMMUNOL.2300355.

56. Xu, W., Zhao, X., Wang, X., Feng, H., Gou, M., Jin, W., Wang, X., Liu, X., and Dong, C. (2019). The Transcription Factor Tox2 Drives T Follicular Helper Cell Development via Regulating Chromatin Accessibility. Immunity *51*, 826-839.e825. 10.1016/J.IMMUNI.2019.10.006.

57. Baumjohann, D., Okada, T., and Ansel, K.M. (2011). Cutting Edge: Distinct Waves of BCL6 Expression during T Follicular Helper Cell Development. The Journal of Immunology *187*, 2089-2092. 10.4049/JIMMUNOL.1101393.

58. Choi, Y.S., Kageyama, R., Eto, D., Escobar, T.C., Johnston, R.J., Monticelli, L., Lao, C., and Crotty, S. (2011). ICOS Receptor Instructs T Follicular Helper Cell versus Effector Cell Differentiation via Induction of the Transcriptional Repressor Bcl6. Immunity *34*, 932-946. 10.1016/J.IMMUNI.2011.03.023.

59. Ma, C.S., Deenick, E.K., Batten, M., and Tangye, S.G. (2012). The origins, function, and regulation of T follicular helper cells. The Journal of Experimental Medicine *209*, 1241-1241. 10.1084/JEM.20120994.

60. Ditoro, D., Winstead, C., Pham, D., Witte, S., Andargachew, R., Singer, J.R., Wilson, C.G., Zindl, C.L., Luther, R.J., Silberger, D.J., et al. (2018). Differential IL-2 expression defines developmental fates of follicular versus nonfollicular helper T cells. Science *361*. 10.1126/SCIENCE.AAO2933.

61. Schorer, M., Kuchroo, V.K., and Joller, N. (2019). Role of co-stimulatory molecules in T helper cell differentiation. Advances in Experimental Medicine and Biology *1189*, 153-177. 10.1007/978-981-32-9717-3_6.

62. Linterman, M.A., Denton, A.E., Divekar, D.P., Zvetkova, I., Kane, L., Ferreira, C., Veldhoen, M., Clare, S., Dougan, G., Espéli, M., and Smith, K.G.C. (2014). CD28 expression is required after T cell priming for helper T cell responses and protective immunity to infection. eLife *3*, 1-21. 10.7554/ELIFE.03180.

63. Acuto, O., and Michel, F. (2003). CD28-mediated co-stimulation: a quantitative support for TCR signalling. Nature reviews. Immunology *3*, 939-951. 10.1038/NRI1248.

64. Collins, A.V., Brodie, D.W., Gilbert, R.J.C., Iaboni, A., Manso-Sancho, R., Walse, B., Stuart, D.I., Van Der Merwe, P.A., and Davis, S.J. (2002). The interaction properties of costimulatory molecules revisited. Immunity *17*, 201-210. 10.1016/S1074-7613(02)00362-X.

65. Wang, C.J., Heuts, F., Ovcinnikovs, V., Wardzinski, L., Bowers, C., Schmidt, E.M., Kogimtzis, A., Kenefeck, R., Sansom, D.M., Walker, L.S.K., and Weiss, A. (2015). CTLA-4 controls follicular helper T-cell differentiation by regulating the strength of CD28 engagement. Proceedings of the National Academy of Sciences of the United States of America *112*, 524-529. 10.1073/PNAS.1414576112.

66. Baumjohann, D., Preite, S., Reboldi, A., Ronchi, F., Ansel, K.M., Lanzavecchia, A., and Sallusto, F. (2013). Persistent Antigen and Germinal Center B Cells Sustain T Follicular Helper Cell Responses and Phenotype. Immunity *38*, 596-605. 10.1016/J.IMMUNI.2012.11.020.

67. Grewal, I.S., Xu, J., and Flavell, R.A. (1995). Impairment of antigen-specific T-cell priming in mice lacking CD40 ligand. Nature *378*, 617-620. 10.1038/378617A0.

68. Liu, D., Xu, H., Shih, C., Wan, Z., Ma, X., Ma, W., Luo, D., and Qi, H. (2014). T–B-cell entanglement and ICOSL-driven feed-forward regulation of germinal centre reaction. Nature 2014 517:7533 *517*, 214-218. 10.1038/nature13803.

69. Shin, C., Han, J.A., Koh, H., Choi, B., Cho, Y., Jeong, H., Ra, J.S., Sung, P.S., Shin, E.C., Ryu, S., and Do, Y. (2015). CD8α– Dendritic Cells Induce Antigen-Specific T Follicular Helper Cells Generating Efficient Humoral Immune Responses. Cell Reports *11*, 1929-1940. 10.1016/J.CELREP.2015.05.042.

70. Xu, H., Li, X., Liu, D., Li, J., Zhang, X., Chen, X., Hou, S., Peng, L., Xu, C., Liu, W., et al. (2013). Follicular T-helper cell recruitment governed by bystander B cells and ICOS-driven motility. Nature *496*, 523-527. 10.1038/NATURE12058.

71. Chen, X., Ma, W., Zhang, T., Wu, L., and Qi, H. (2015). Phenotypic Tfh development promoted by CXCR5-controlled re-localization and IL-6 from radiation-resistant cells. Protein & cell *6*, 825-832. 10.1007/S13238-015-0210-0.

72. Edelson, B.T., Bradstreet, T.R., Kc, W., Hildner, K., Herzog, J.W., Sim, J., Russell, J.H., Murphy, T.L., Unanue, E.R., and Murphy, K.M. (2011). Batf3-dependent CD11b(low/-) peripheral dendritic cells are GM-CSF-independent and are not required for Th cell priming after subcutaneous immunization. PloS one *6*. 10.1371/JOURNAL.PONE.0025660.

73. McManus, D.T., Valanparambil, R.M., Medina, C.B., Scharer, C.D., McGuire, D.J., Sobierajska, E., Hu, Y., Chang, D.Y., Wieland, A., Lee, J., et al. (2025). An early precursor CD8+ T cell that adapts to acute or chronic viral infection. Nature *640*, 772-781. 10.1038/S41586-024-08562-Y.

74. Pritykin, Y., van der Veeken, J., Pine, A.R., Zhong, Y., Sahin, M., Mazutis, L., Pe'er, D., Rudensky, A.Y., and Leslie, C.S. (2021). A unified atlas of CD8 T cell dysfunctional states in cancer and infection. Molecular cell *81*, 2477-2493.e2410. 10.1016/J.MOLCEL.2021.03.045.

75. Prokhnevska, N., Cardenas, M.A., Valanparambil, R.M., Sobierajska, E., Barwick, B.G., Jansen, C., Reyes Moon, A., Gregorova, P., delBalzo, L., Greenwald, R., et al. (2023). CD8+ T cell activation in cancer comprises an initial activation phase in lymph nodes followed by effector differentiation within the tumor. Immunity *56*, 107-124.e105. 10.1016/J.IMMUNI.2022.12.002.

76. Gerner, M.Y., Casey, K.A., Kastenmuller, W., and Germain, R.N. (2017). Dendritic cell and antigen dispersal landscapes regulate T cell immunity. The Journal of experimental medicine *214*, 3105-3122. 10.1084/JEM.20170335.

77. Krishnaswamy, J.K., Gowthaman, U., Zhang, B., Mattsson, J., Szeponik, L., Liu, D., Wu, R., White, T., Calabro, S., Xu, L., et al. (2017). Migratory CD11b+ conventional dendritic cells induce T follicular helper cell-dependent antibody responses. Science immunology *2*. 10.1126/SCIIMMUNOL.AAM9169.

78. Li, J., Lu, E., Yi, T., and Cyster, J.G. (2016). EBI2 augments Tfh cell fate by promoting interaction with IL-2-quenching dendritic cells. Nature 2016 533:7601 *533*, 110-114. 10.1038/nature17947.

79. Kerfoot, S.M., Yaari, G., Patel, J.R., Johnson, K.L., Gonzalez, D.G., Kleinstein, S.H., and Haberman, A.M. (2011). Germinal center B cell and T follicular helper cell development initiates in the interfollicular zone. Immunity *34*, 947-960. 10.1016/J.IMMUNI.2011.03.024.

80. Kim, Y.J., Choi, J., and Choi, Y.S. (2024). Transcriptional regulation of Tfh dynamics and the formation of immunological synapses. Experimental & Molecular Medicine 2024 56:6 *56*, 1365-1372. 10.1038/s12276-024-01254-7.

81. Song, W., and Craft, J. (2024). T Follicular Helper Cell Heterogeneity. Annual review of immunology *42*, 127-152. 10.1146/ANNUREV-IMMUNOL-090222-102834.

82. Groom, J.R., Richmond, J., Murooka, T.T., Sorensen, E.W., Sung, J.H., Bankert, K., von Andrian, U.H., Moon, J.J., Mempel, T.R., and Luster, A.D. (2012). CXCR3 chemokine receptor-ligand interactions in the lymph node optimize CD4+ T helper 1 cell differentiation. Immunity *37*, 1091-1103. 10.1016/J.IMMUNI.2012.08.016.

83. Eickhoff, S., Brewitz, A., Gerner, M.Y., Klauschen, F., Komander, K., Hemmi, H., Garbi, N., Kaisho, T., Germain, R.N., and Kastenmüller, W. (2015). Robust Anti-viral Immunity Requires Multiple Distinct T Cell-Dendritic Cell Interactions. Cell *162*, 1322-1337. 10.1016/J.CELL.2015.08.004.

84. Hor, J.L., Whitney, P.G., Zaid, A., Brooks, A.G., Heath, W.R., and Mueller, S.N. (2015). Spatiotemporally Distinct Interactions with Dendritic Cell Subsets Facilitates CD4+ and CD8+ T Cell Activation to Localized Viral Infection. Immunity *43*, 554-565. 10.1016/J.IMMUNI.2015.07.020.

85. Morita, R., Schmitt, N., Bentebibel, S.E., Ranganathan, R., Bourdery, L., Zurawski, G., Foucat, E., Dullaers, M., Oh, S.K., Sabzghabaei, N., et al. (2011). Human Blood CXCR5+CD4+ T Cells Are Counterparts of T Follicular Cells and Contain Specific Subsets that Differentially Support Antibody Secretion. Immunity *34*, 108-121. 10.1016/J.IMMUNI.2010.12.012.

86. Bentebibel, S.E., Khurana, S., Schmitt, N., Kurup, P., Mueller, C., Obermoser, G., Palucka, A.K., Albrecht, R.A., Garcia-Sastre, A., Golding, H., and Ueno, H. (2016). ICOS+PD-1+CXCR3+ T follicular helper cells contribute to the generation of high-avidity antibodies following influenza vaccination. Scientific Reports 2016 6:1 *6*, 1-8. 10.1038/srep26494.

87. Bentebibel, S.E., Lopez, S., Obermoser, G., Schmitt, N., Mueller, C., Harrod, C., Flano, E., Mejias, A., Albrecht, R.A., Blankenship, D., et al. (2013). Induction of ICOS+CXCR3+CXCR5+ T H cells correlates with antibody responses to influenza vaccination. Science Translational Medicine *5*. 10.1126/scitranslmed.3005191

88. Martin-Gayo, E., Cronin, J., Hickman, T., Ouyang, Z., Lindqvist, M., Kolb, K.E., Schulze zur Wiesch, J., Cubas, R., Porichis, F., Shalek, A.K., et al. (2017). Circulating CXCR5+CXCR3+PD-1lo Tfh-like cells in HIV-1 controllers with neutralizing antibody breadth. JCI Insight *2*, e89574-e89574. 10.1172/JCI.INSIGHT.89574.

89. Schulz, O., Edwards, A.D., Schito, M., Aliberti, J., Manickasingham, S., Sher, A., and Reis e Sousa, C. (2000). CD40 triggering of heterodimeric IL-12 p70 production by dendritic cells in vivo requires a microbial priming signal. Immunity *13*, 453-462. 10.1016/S1074-7613(00)00045-5.

90. Wu, R., Ohara, R.A., Jo, S., Liu, T.T., Ferris, S.T., Ou, F., Kim, S., Theisen, D.J., Anderson, D.A., Wong, B.W., et al. (2022). Mechanisms of CD40-dependent cDC1 licensing beyond costimulation. Nature immunology *23*, 1536-1550. 10.1038/S41590-022-01324-W.

91. Duckworth, B.C., Lafouresse, F., Wimmer, V.C., Broomfield, B.J., Dalit, L., Alexandre, Y.O., Sheikh, A.A., Qin, R.Z., Alvarado, C., Mielke, L.A., et al. (2021). Effector and stem-like memory cell fates are imprinted in distinct lymph node niches directed by CXCR3 ligands. Nature immunology *22*, 434-448. 10.1038/S41590-021-00878-5.

92. De Koker, S., Van Hoecke, L., De Beuckelaer, A., Roose, K., Deswarte, K., Willart, M.A., Bogaert, P., Naessens, T., De Geest, B.G., Saelens, X., et al. (2017). Inflammatory monocytes regulate Th1 oriented immunity to CpG adjuvanted protein vaccines through production of IL-12. Scientific reports *7*. 10.1038/S41598-017-06236-6.

93. Leal, J.M., Huang, J.Y., Kohli, K., Stoltzfus, C., Lyons-Cohen, M.R., Olin, B.E., Gale, M., and Gerner, M.Y. (2021). Innate cell microenvironments in lymph nodes shape the generation of T cell responses during type I inflammation. Science Immunology *6*, eabb9435-eabb9435. 10.1126/sciimmunol.abb9435.

94. Sheikh, A.A., and Groom, J.R. (2021). Transcription tipping points for T follicular helper cell and T-helper 1 cell fate commitment. Cellular & molecular immunology *18*, 528-538. 10.1038/S41423-020-00554-Y.

95. Sheikh, A.A., Cooper, L., Feng, M., Souza-Fonseca-Guimaraes, F., Lafouresse, F., Duckworth, B.C., Huntington, N.D., Moon, J.J., Pellegrini, M., Nutt, S.L., et al. (2019). Context-Dependent Role for T-bet in T Follicular Helper Differentiation and Germinal Center Function following Viral Infection. Cell reports *28*, 1758-1772.e1754. 10.1016/J.CELREP.2019.07.034.

96. Zheng, L., Qin, S., Si, W., Wang, A., Xing, B., Gao, R., Ren, X., Wang, L., Wu, X., Zhang, J., et al. (2021). Pan-cancer single-cell landscape of tumor-infiltrating T cells. Science (New York, N.Y.) *374*. 10.1126/SCIENCE.ABE6474.

97. Nüssing, S., House, I.G., Kearney, C.J., Chen, A.X.Y., Vervoort, S.J., Beavis, P.A., Oliaro, J., Johnstone, R.W., Trapani, J.A., and Parish, I.A. (2020). Efficient CRISPR/Cas9 Gene Editing in Uncultured Naive Mouse T Cells for In Vivo Studies. J Immunol *204*, 2308-2315. 10.4049/jimmunol.1901396.

98. Seki, A., and Rutz, S. (2018). Optimized RNP transfection for highly efficient CRISPR/Cas9-mediated gene knockout in primary T cells. J Exp Med *215*, 985-997. 10.1084/jem.20171626.

Supplementary Figures

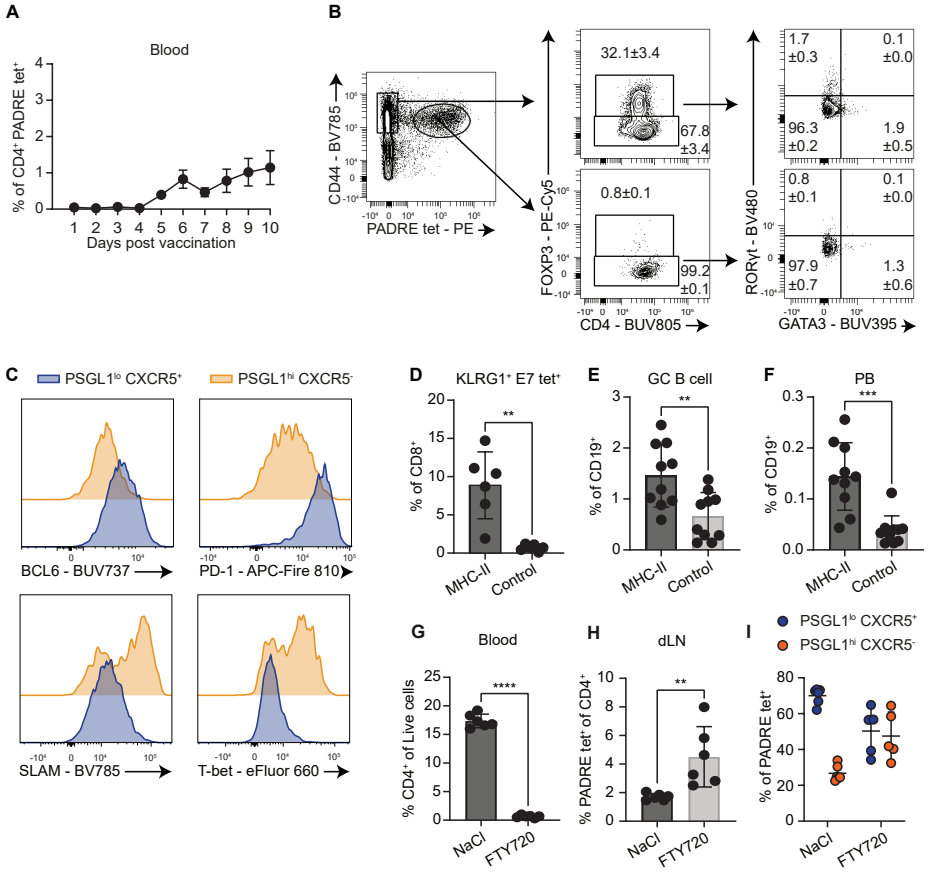

Figure S1 (related to Figure 1): A vaccination model to study differentiation of endogenous, polyclonal CD4⁺ T cells into Th1 or Tfh cells. (A) Frequency of PADRE tet⁺ CD4⁺ T cells in blood over time after vaccination (N=5 mice per group). (B) Representative contour plots depicting FOXP3, GATA3 and RORγt expression in CD44⁺ PADRE tet⁻ (top) and CD44⁺ PADRE tet⁺ (bottom) CD4⁺ T cells. (C) Representative histograms of BCL6, PD-1, SLAM, and T-bet expression in PSGL1^{lo} CXCR5⁺ (blue) and PSGL1^{hi} CXCR5⁻ (orange) CD44⁺ PADRE tet⁺ CD4⁺ T cells in dLNs at day 8 post-vaccination. (D) Frequency of antigen-specific effector CD8⁺ T cells (E7 tet⁺ KLRG1⁺) in blood at day 10 after MHC-II or control vaccination (N=6 mice per group). (E) Frequency of GL7⁺ FAS⁺ GC B cells in dLNs at day 8 post-vaccination (N=10 mice per group). Cells were pre-gated as CD19⁺ IgD⁻ live cells. (F) Frequency of plasmablasts (PB; CD19$^{int/lo}$ IgD⁻ CD138⁺ TACI⁺) at day 8 days after vaccination in dLNs (N=10 mice per group). (G-I) Mice were vaccinated on day 0 and day 3 and treated with FTY720 or NaCl vehicle at day 0, 3 and 6 after vaccination and analyzed at day 7 (N=6 mice per group). (G) Frequency of total CD4⁺ T cells in blood. (H) PADRE tet⁺ CD4⁺ T cells in dLNs. (I) Frequency of PSGL1^{lo} CXCR5⁺ and PSGL1^{hi} CXCR5⁻ PADRE tet⁺ CD4⁺ T cells in dLNs. All graphs show mean ± SD; (D-H) Unpaired Student's t-test.

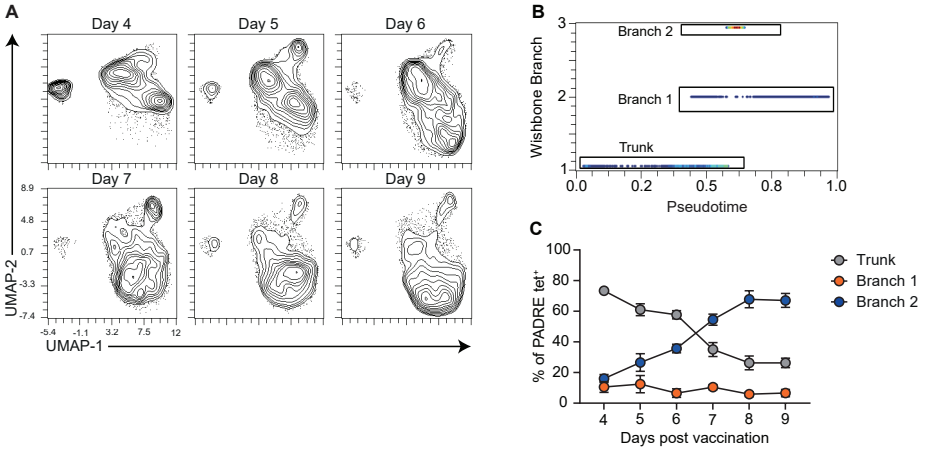

Figure S2 (related to Figure 2): Temporal analysis highlights a common differentiation branchpoint for Th1 and Tfh cells. (A) UMAP projections showing PADRE tet$^+$ CD4$^+$ T cells in the dLN of mice from day 4-9 post-vaccination (N=5 per time point). (B) Wishbone trajectory and branching of concatenated PADRE tet$^+$ CD4$^+$ T cells. (C) Frequency of PADRE tet$^+$CD4$^+$ T cells within trunk, branch 1 and branch 2 in the dLN as calculated by Wishbone. All graphs show mean ± SD.

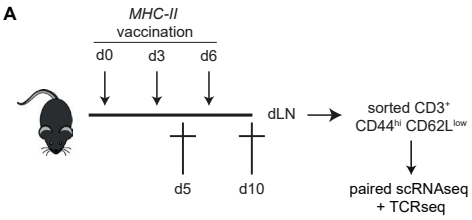

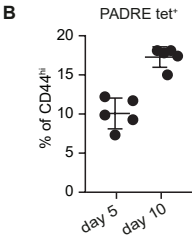

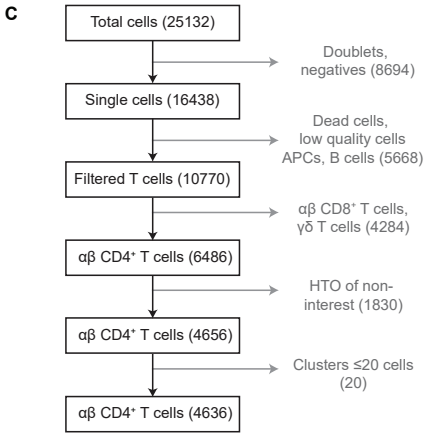

D

	Cell number per cluster		
	d5	*d10*	*total*
cl.0	721	412	1133
cl.1	182	881	1063
cl.2	258	413	671
cl.3	315	299	614
cl.4	254	259	513
cl.5	310	156	466
cl.6	176	35	176

E

	Expanded TCR clones per cluster		
	unique	*shared*	*total*
cl.0	45	37	82
cl.1	99	117	216
cl.2	22	95	117
cl.3	0	3	3
cl.4	0	20	20
cl.5	15	85	100
cl.6	0	13	13

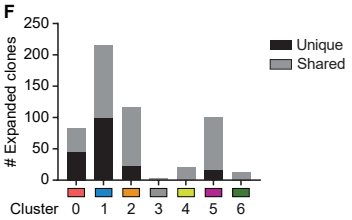

Figure S3 (related to Figure 3): scRNAseq and TCRseq of dLN-derived CD4⁺ T cells after vaccination. (A, C) Schematic overview of mouse treatment, sample preparation (A) and pipeline for quality control and filtering steps of scRNAseq data analysis (C). (B) Frequency of PADRE tet⁺ cells among CD4⁺ CD44^{hi} cells at days 5 and 10 post-vaccination (N=5 mice per timepoint). Data are representative of 2 independent experiments, graphs depict mean ± SD. (D, E) Tables report numbers of cells identified per cluster (cl.) at days 5 and 10 (D), or numbers of expanded TCR clones per cluster, which identify clones that were uniquely found in one cluster, or were shared between at least two clusters (E). (F) Number of expanded TCR clones (>1 cell per clone) per cluster. Black: TCR clones unique to one cluster; grey: TCR clones shared between two or more clusters.

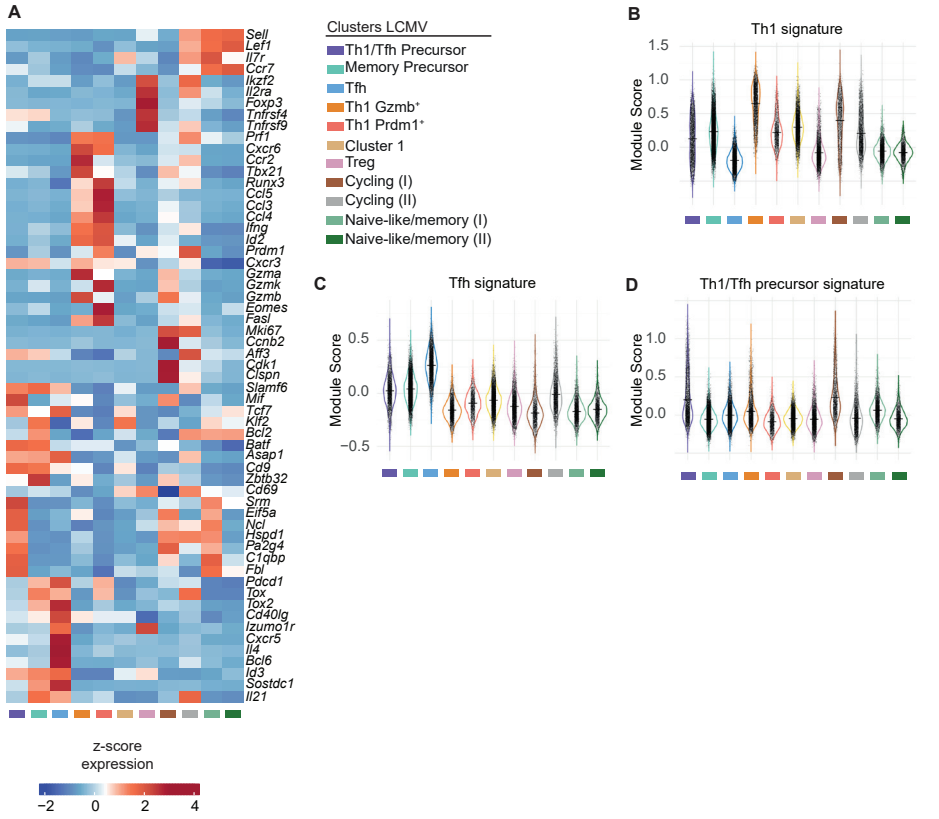

Figure S4 (related to Figure 4): Gene profile of the LCMV-specific CD4⁺ T cells. (A) Heatmap showing selected differentially expressed genes across clusters of LCMV-specific CD4⁺ T cells. Colors indicate normalized (z-scored) gene-expression levels within each cluster. (B-D) Violin plots displaying module scores for vaccine-induced Th1 (B), Tfh (C), and Th1/Tfh precursor (D) gene signatures across clusters of GP66 tet⁺ LCMV-specific CD4⁺ T cells isolated from mice infected with LCMV-Armstrong or LCMV-Clone 13 at days 8 and 21 post-infection. Module scores indicate per-cell expression levels of genes within each signature, based on normalized expression value.

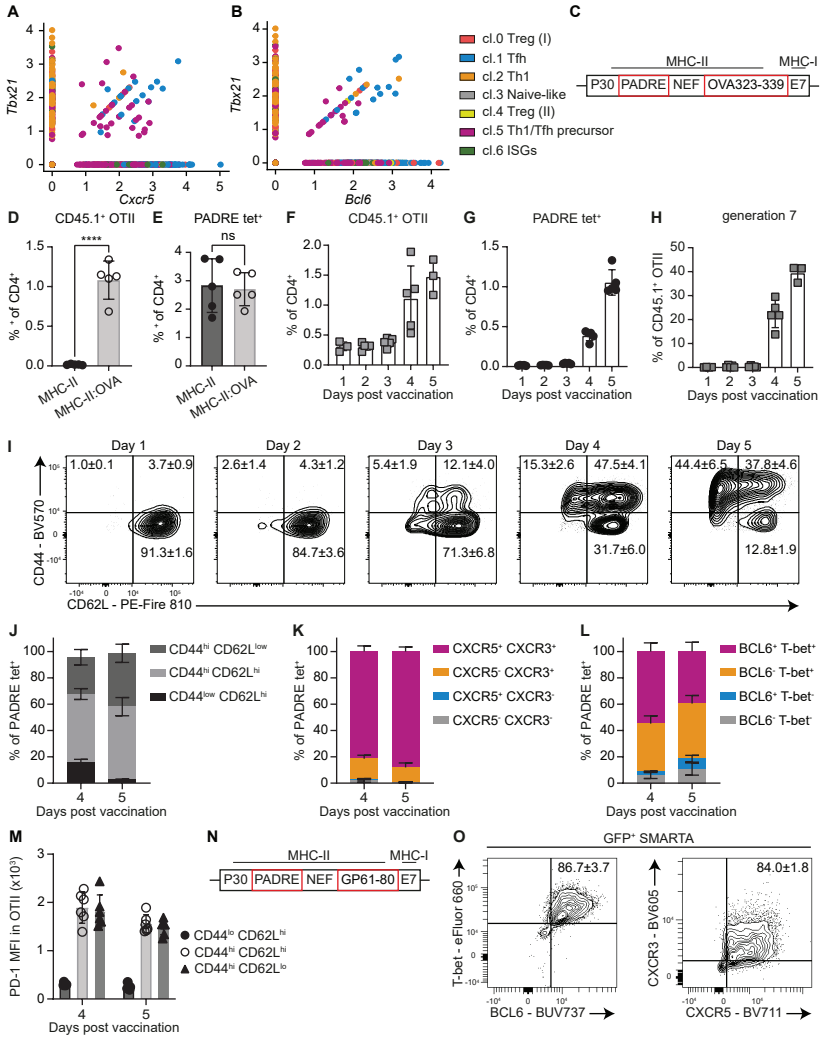

Figure S5 (related to Figure 5): Phenotypic analysis of the common Th1/Tfh precursor pool. (A-B) Expression levels per cell of Tbx21 and Cxcr5 (A) or Tbx21 and Bcl6 (B) mRNA. CD4⁺ T cell clusters from scRNAseq of vaccinated mice are color-coded as in Figure 3. (C) Schematic overview of epitopes in MHC-II:OVA vaccine. (D, E) Frequency of CD45.1⁺ OTII (D) or PADRE tet⁺ (E) CD4⁺ T cells in the dLN of mice at day 8 after vaccination with MHC-II or MHC-II:OVA plasmid (N=5 mice per group), as determined by flow cytometry. Unpaired Student's t-test. (F-M) Mice were vaccinated once with MHC-II:OVA vaccine. (F, G) Frequency of CD45.1⁺ OTII (F) or CD45.2⁺ PADRE tet⁺ (G) CD4⁺ T cells at indicated times after vaccination, as determined by flow cytometry. (H) Frequency of CD45.1⁺ OTII that underwent 7 cell divisions at indicated time points post-vaccination (N=3-5 per timepoint), as determined by CFSE dilution. I) Flow cytometric detection of CD44 and CD62L on CD45.1⁺ OTII cells in the dLN at indicated time points. (J-L) Graphs displaying mean ± SD of CD44 and CD62L (K), CXCR5 and CXCR3 (L), or BCL6 and T-bet (M) protein levels as detected by flow cytometry in PADRE tet⁺ CD4+ T cells at days 4 and 5 post-vaccination (N=5 per time point). (M) Median fluorescence intensity (MFI) for PD-1 on CD44^{lo} CD62L^{hi}, CD44^{hi} CD62L^{hi}, and CD44^{hi} CD62L^{lo} CD45.1⁺ OTII cells at days 4 or 5 after vaccination. (N) Schematic overview of epitopes in the LCMV-GP$_{61-80}$ modified MHC-II vaccine. (O) Mice were vaccinated once with MHCII:LCMV-GP$_{61-80}$ vaccine. Representative contour plots depicting T-bet and BCL6 or CXCR3 and CXCR5 protein levels in GFP⁺ SMARTA cells at day 4 post-vaccination (N=6 mice per group). All graphs show mean ± SD.

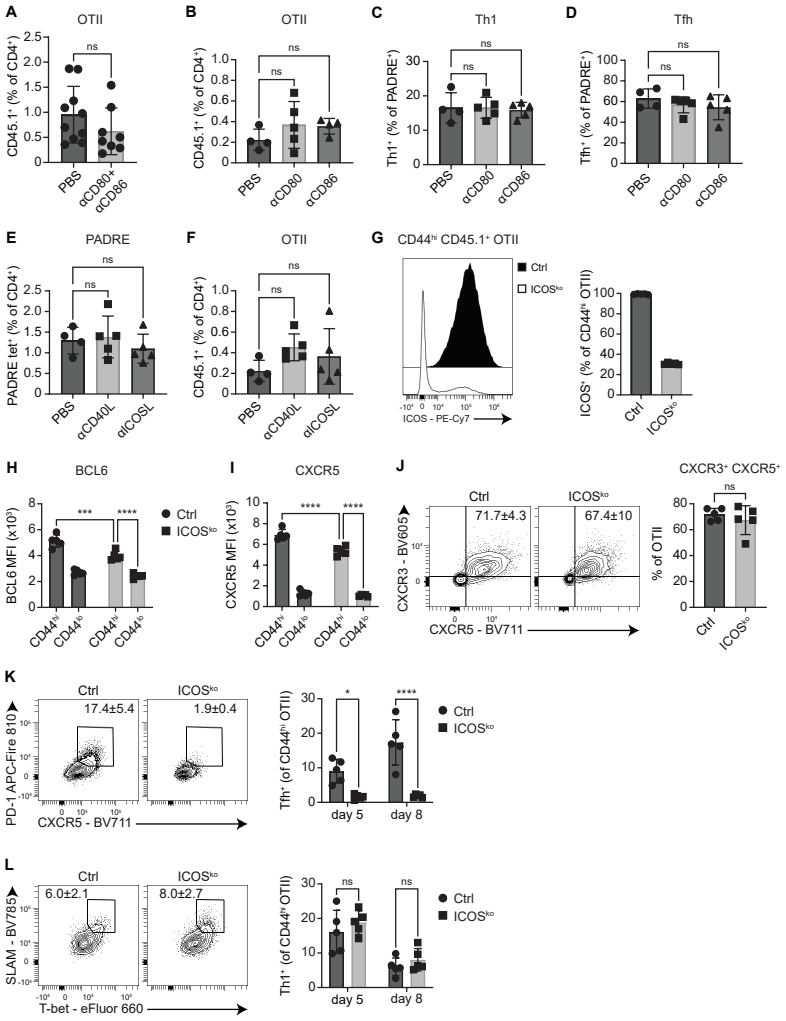

Figure S6 (related to Figure 6): Costimulatory molecules driving CD4⁺ T-cell differentiation. Mice received OTII cells and MHC-II:OVA vaccine and were treated with blocking mAbs to the indicated molecules or PBS (control). At day 5 after vaccination, dLNs were harvested and cells were analyzed by flow cytometry. (A) Mice received one vaccination. Quantification of CD45.1⁺ OTII cells in dLNs after blocking CD80 and CD86 or control (N=9-10 mice per group pooled from two experiments). (B-D) Quantification of CD45.1⁺ OTII cells (B), CD45.2⁺ PADRE tet⁺ SLAM⁺ Tbet+ Th1 cells (C) and CD45.2⁺ PADRE tet⁺CXCR5⁺ PD-1⁺ Tfh cells (D) in dLN after blocking either CD80, or CD86, or control. (E-F) Quantification of CD45.2⁺ PADRE tet⁺ (E) and CD45.1⁺ OT-II (F) cells in dLN after blocking CD40L or ICOSL, or control (N=4-5 mice per group). (G-L) Mice received OTII cells after CRISPR/Cas9-gene editing for ICOS (ICOSko) or with a non-targeting gRNA (Ctrl) . Mice were subsequently vaccinated with MHC-II:OVA, and dLNs were isolated at day 5 (G-L) or day 8 (K,L) (N=5 mice per group per timepoint). G) Concatenated histograms and frequency depicting ICOS expression (left) and the frequency of ICOS⁺ cells (right) in CD44^{hi} CD45.1⁺ OTII cells. (H-L) For the ICOSko group, only ICOS⁻ cells were assessed. (H, I) MFI of BCL6 (H) and CXCR5 (I) in activated CD44^{hi} and naive CD44^{lo} OTII cells. (J-L) Representative contour plots and graphs depicting frequency of CXCR3⁺ CXCR5⁺ Th1/Tfh precursor cells (J), CXCR5⁺ PD-1⁺ Tfh (K), and SLAM⁺ T-bet⁺ Th1 (L) CD44^{hi} OTII cells. (A, J) Unpaired Student's t-test. (B-F) One-Way ANOVA with Dunnett's post hoc test was used to correct for multiple testing when comparing inhibitory conditions to control. Data are representative of at least two independent experiments. (H, I, K, L) Two-way ANOVA with Šidák post hoc test was used. (A-L). All graphs show mean ± SD.

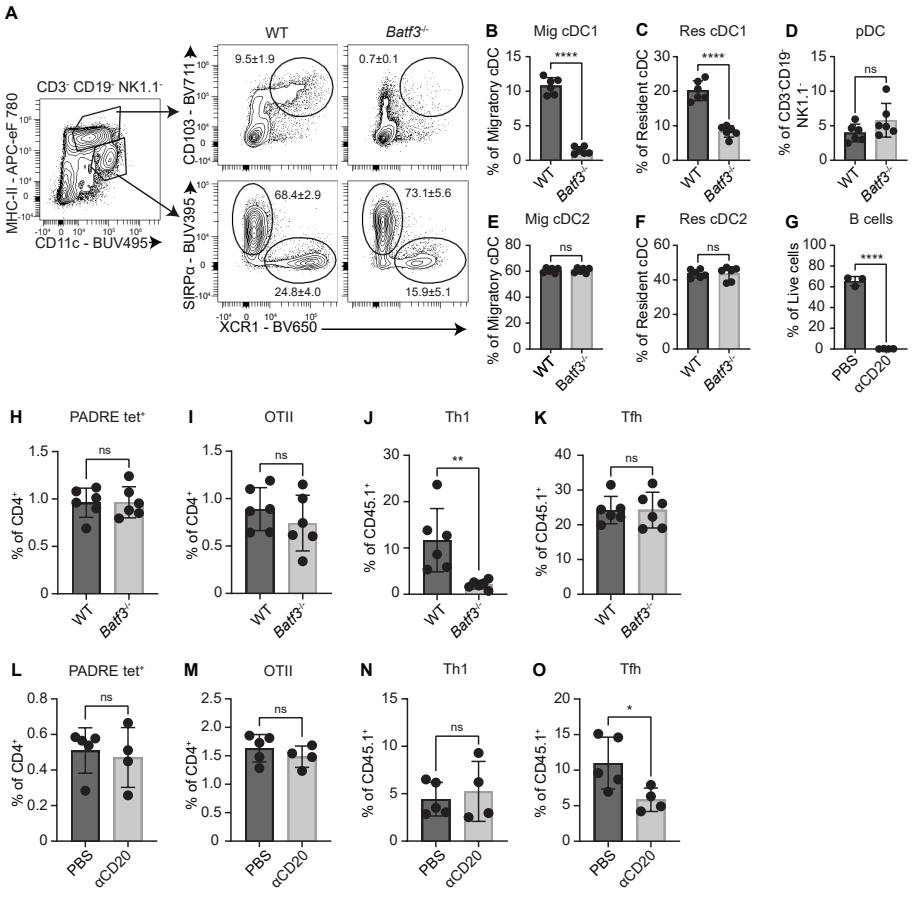

Figure S7 (related to Figure 7): Antigen presenting cells driving CD4⁺ T-cell differentiation. WT or Batf3-/- mice received OTII cells, were vaccinated once with MHC-II:OVA vaccine and were treated with depleting anti-CD20 mAb or PBS (control) as indicated. At day 5 after vaccination, dLNs were harvested and cells were analyzed by flow cytometry. (A) Gating strategy to identify migratory cDC1s (MHC-II^{hi} CD11c^{int} CD103^{+} XCR1^{+}), resident cDC1s (MHC-II^{int} CD11c^{hi} XCR1^{+}SIRPα^{-}) and resident cDC2s (MHC-II^{int} CD11c^{hi} XCR1^{-} SIRPα^{+}) in the dLN at day 3 post-vaccination. (B-F) Quantification of migratory (B) and resident (C) cDC1, pDCs (Ly6C^{+} Siglec H^{+}; D), migratory (MHC-II^{hi} CD11c^{int} XCR1^{-} SIRPα^{+}; E) and resident cDC2 (F) in WT and Batf3-/- mice (N=6 mice per group). (G) Quantification of CD19^{+} B cells in peripheral blood two days after treatment with anti-CD20 mAb (N=3-4 mice per group). (H, L) Frequency of PADRE tet^{+} among CD4^{+} T cells in dLNs of indicated test groups. (I, M) Frequency of CD45.1^{+} OTII cells in dLN of indicated test groups. (J-K, N-O) Frequency of CD45.1^{+} OTII cells with SLAM^{+} T-bet^{+} Th1 phenotype (J, N) or CXCR5^{+} PD-1^{+} Tfh phenotype (K, O) CD45.1^{+} OTII cells in dLNs of indicated test groups. All graphs depict mean ± SD (N=6 mice per group in A-K; N=4-5 mice per group in L-O). Unpaired Student's t-test.

Description of Supplementary Tables

Supplementary Table 1:

List of differentially expressed genes by $CD4^+$ T cell clusters generated by scRNAseq after DNA tattoo vaccination.

Supplementary Table 2:

List of differentially expressed genes by $CD4^+$ T cell clusters derived from Xia *et al.*, 2022 (ref. 54).

Supplementary Table 3:

List of differentially expressed genes in LCMV-specific Th1/Tfh precursor and LCMV-specific memory-precursor cell clusters derived from Xia *et al.*, 2022 (ref. 54).

Supplementary Table 4:

Gene signature of malaria-induced Th1/Tfh precursor cells derived from Lönnberg *et al.*, 2017 (ref. 4).

Supplementary Table 5:

List of differentially expressed genes between clusters 1 (Tfh) and cluster 2 (Th1) $CD4^+$ T cells identified by scRNAseq after DNA tattoo vaccination.

Supplementary Table 6:

List of differentially expressed genes between clusters 5 (Th1/Tfh precursors) and cluster 3 (naive-like) $CD4^+$ T cells identified by scRNAseq after DNA tattoo vaccination.

Key Resource Table

Details of used reagents and resources

All Supplementary Tables are available at DOI: 10.1016/j.celrep.2026.117296

Chapter 6

The importance of type I interferon in orchestrating the cytotoxic T-cell response to cancer

Julia Busselaar*, Merel Sijbranda* and Jannie Borst

Leiden University Medical Center, 2333 ZA Leiden, The Netherlands

* These two authors contributed equally to this work

Immunology Letters 2024; 270:106938

DOI: 10.1016/j.imlet.2024.106938

Abstract

Both type I interferon (IFN-I) and $CD4^+$ T-cell help are required to generate effective $CD8^+$ T-cell responses to cancer. We here outline based on existing literature how IFN-I signaling and $CD4^+$ T-cell help are connected. Both impact on the functional state of dendritic cells (DCs), particularly conventional (c)DC1. The cDC1s are critical for crosspresentation of cell-associated antigens and for delivery of $CD4^+$ T-cell help for cytotoxic T-lymphocyte (CTL) effector and memory differentiation. In infection, production of IFN-I is prompted by pathogen-associated molecular patterns (PAMPs), while in cancer it relies on danger-associated molecular patterns (DAMPs). IFN-I production by tumor cells and pDCs in the tumor micro-environment (TME) is often limited. IFN-I signals increase the ability of migratory cDC1 and cDC2 to transport tumor antigens to tumor-draining lymph nodes (tdLNs). IFN-I also enables cDC1 to form and sustain the platform for help delivery by stimulating the production of chemokines that attract $CD4^+$ and $CD8^+$ T cells. IFN-I promotes delivery of help in concert with CD40 signals by additive and synergistic impact on cross-presentation and provision of critical costimulatory and cytokine signals for CTL effector and memory differentiation. The scenario of $CD4^+$ T-cell help therefore depends on IFN-I signaling. This scenario can play out in tdLNs as well as in the TME, thereby contributing to the cancer immunity cycle. The collective observations may explain why both IFN-I and $CD4^+$ T-cell help signatures in the TME correlate with good prognosis and response to PD-1 targeting immunotherapy in human cancer. They also may explain why a variety of tumor types in which IFN-I signaling is attenuated, remain devoid of functional CTLs.

Introduction

Early studies in mice identified that type I and -II interferon (IFN) contribute to tumor rejection[1,2]. In agreement, the "inflamed" or "hot" tumor micro-environment (TME) in mouse melanoma, qualified by presence of $CD8^+$ T cells in the tumor core, had an IFN-associated transcriptional profile[3]. In human, histology identified the inflamed TME with presence of $CD8^+$ T cells in many cancer types associated with better prognosis[4]. $CD8^+$ T cells play a central role in anti-tumor immunity because they can recognize and kill virtually all cell types upon recognition of antigens in the context of major histocompatibility complex I (MHC-I) molecules. Immunogenic tumors can spontaneously raise tumor-specific cytotoxic T lymphocyte (CTL) responses that are initiated by migratory dendritic cells (DCs) that bring tumor antigens to tumor-draining lymph nodes (tdLNs). $CD4^+$ helper T cells recognize antigens in context of MHC-II primarily on professional antigen-presenting cells (APCs) and have immunomodulatory roles. While $CD4^+$ T cells therefore generally do not play a direct role in elimination of tumor cells, they are critical for optimal differentiation of $CD8^+$ T cells into primary effector and effector memory CTLs.

Until recently, the conventional (c)DC1 was thought to be essential for anti-tumor immunity mainly due to its optimal capacity to process and cross-present tumor antigens. However, the cDC1 also performs a unique function among other DC types in relaying $CD4^+$ T-cell help for the CTL response[5,6]. For optimal activation and maturation of cDC1s, both IFN-I and help signals from $CD4^+$ T cells are essential. Early studies have demonstrated that IFN-I production by host hematopoietic cells[1] and IFN-I signaling into cDC1s[7,8] are critical for spontaneous CTL priming against immunogenic tumors. IFN-I signaling optimizes cDC1s to support tumor-specific CTL responses by multiple mechanisms (reviewed in[9,10]). Since these mechanisms are also activated by $CD4^+$ T-cell help, help was originally proposed as an amplification signal of the innate IFN-I stimulus[11]. In this review, we provide an update on the mechanisms that connect IFN-I signaling with $CD4^+$ T-cell help, and propose a model explaining how lack of IFN-I signals in tumors may contribute to failed CTL-based tumor control.

CTL priming, role of cDCs and $CD4^+$ T-cell help

CTL priming in LNs

The cDCs comprise two lineages, namely cDC1 ($XCR1^+$/$CD103^+$) and cDC2 ($CD11b^+$/$SIRP\alpha^+$)[12]. In both mouse and human, cDC1 are discerned from cDC2 by cell surface markers XCR1 and Clec9A. In the mouse, cDC2 are commonly defined by cell surface markers CD11b/SIRPα and in human by CD11c/CD1c[13,14]. Each lineage is subdivided into migratory and lymph-node resident populations. After collection of antigens and activation in the TME, cDCs rely on chemokine receptor CCR7 for migration to tdLN[15]. Early *in vivo* experiments showed that cDC1s are more

efficient than cDC2s in antigen cross-presentation, i.e. loading exogenous antigens into MHC-I molecules and presenting them to CD8$^+$ T cells[16]. In agreement with this unique function of cDC1s, they proved to be critical for tumor control in mouse models[17,18]. cDC2s are reportedly more prone to stimulate CD4$^+$ T cells[19,20].

When cDCs encounter infected or damaged cells in peripheral tissues, they can be activated via multiple types of pathogen- or "danger" associated molecular patterns (PAMPs or DAMPs) that can bind to a variety of plasma membrane, endosomal and cytoplasmic sensors, that we collectively call pattern recognition receptors (PRRs). Activated migratory cDC have optimized antigen presentation, as well as expression of costimulatory ligands including CD80/86 and CD70 and make specific cytokines including IL-12 or IL-15 that collectively induce initial T-cell activation and effector differentiation. According to intravital imaging of the murine immune response to virus infection, the first step of CD8$^+$ and CD4$^+$ T-cell priming occurs in spatially segregated regions of the lymph node (LN) by migratory cDCs[21–23]. In this initial activation step, CD4$^+$ T cells recognize with their T-cell receptor (TCR) antigen presented in MHC-II on cDC2s, while CD8$^+$ T cells recognize antigen in the context of MHC-I on cDC1s.

CD4$^+$ T-cell help for the CTL response

In what we have termed the second step of T-cell priming, CD4$^+$ T cells help CD8$^+$ T cells to become competent cytotoxic effector- and effector-memory cells[24]. The capacity of cDC1s to present antigens in both MHC-I and MHC-II enables them to act as a bridge between CD8$^+$ and CD4$^+$ T cells[6,21,22]. In mice, help delivery has been shown to be performed by migratory cDC1s[5], or by LN-resident (CD8a$^+$) cDC1s that can receive antigen from migratory DCs via synaptic transfer[22,25]. Using mice lacking MHC-II on cDC1s, it was proven that help delivery relies on cDC1s and contributes to optimal priming of CD8$^+$ and CD4$^+$ T cells[5]. In this second step of priming, not PRRs, but CD4$^+$ T cells activate the cDC1. Earlier, CD4$^+$ T cells were shown to activate cDCs via CD40 ligand (L) that is expressed on upon TCR stimulation and engages CD40 on the cDC[26–28]. CD40 signaling into DCs induces the production of cytokines IL-12 and IL-15[29,30], which both promote CTL differentiation [31,32]. CD40 signaling also upregulates co-stimulatory molecules CD80, CD86 and CD70 on cDC, which engage costimulatory receptors CD28 and CD27 on the CD8$^+$ T-cell[33,34]. Recently, the cDC1 in both mouse and human was shown to be the specific responder to these CD40 signals downstream of CD4$^+$ T-cell help[6,35] (Figure 1). The collective input of CD4$^+$ T-cell help into the cDC1, also termed "licensing", induces gene expression programs in cDC1s[6,35,36] that promote CTL effector and memory differentiation by multiple mechanisms[37,38]. In addition, IL-21 produced by CD4$^+$ T cells plays a role in sustaining CD8$^+$ T-cell effector functions in mouse models of chronic infection [39–41], but this mechanism likely takes place after initial priming. Without "help" signals, clonal expansion of primed T cells is limited and effector and memory differentiation of CD8$^+$ T cells is incomplete[37,38]. Helpless CD8$^+$ T cells have limited cytotoxicity and express diverse coinhibitory receptors such as PD-1 and BTLA that impede their function[37,42].

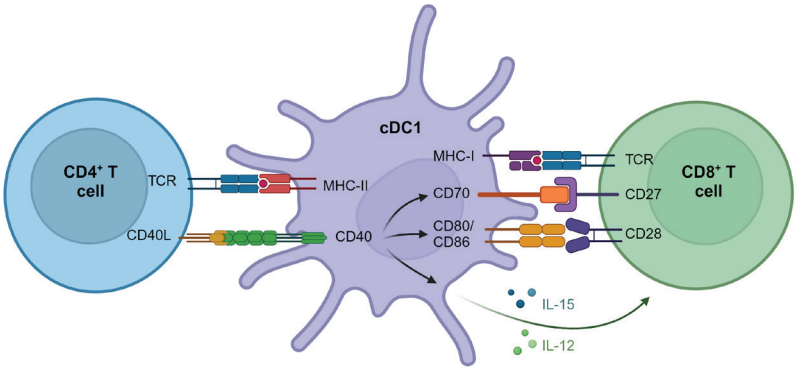

Figure 1. Pathways underlying CD4⁺ T-cell help delivery to CD8⁺ T cells during priming. Upon antigen recognition via the TCR, CD40L is upregulated on the activated CD4⁺ T-cell and binds the CD40 on the cDC1.These interactions promote antigen cross-presentation on cDC1 and production of cytokines such as IL-12 and IL-15, which support the differentiation of CD8⁺ T cells into effector CTLs. Additionally, cDC1s upregulate co-stimulatory ligands CD80/86 and CD70, which bind to respectively CD28 and CD27 on the CD8⁺ T cell. The combined signals delivered during CD4⁺ T- cell help result in the priming of optimally differentiated, 'helped' CTLs [24]. cDC1: conventional dendritic cell type I; CTL: cytotoxic T lymphocyte; MHC: major histocompatibility complex; TCR: T-cell receptor.

Spatial aspects of T-cell priming

Optimal signal exchange between players in CD4⁺ T-cell help delivery requires their proximal localization in the LN, which is regulated by chemokines. In settings where DCs are not infected, such as in cancer, initial activation of murine CD8⁺ T cells depends on cross-presentation by migratory or resident cDC1s, which are located in the LN paracortex[22,23,25,43]. In vaccination and infection mouse models, CCR5 and CXCR3 chemokine gradients were shown to attract initially activated CD8⁺ T cells from the paracortex into the interfollicular region (IFR) of the LN, which likely represents the secondary priming site[44]. The CXCR3-dependent migration of CD4⁺ T cells into the IFR was also shown to be essential for T helper (h)1 differentiation in response to viral infection and vaccination[45], indicating that interactions at the secondary priming site contribute to CD4⁺ T-cell priming and effector differentiation as well.

CTL priming in cancer

Stem-like and exhausted CD8⁺ T cells

The generation of an effective CTL response against cancer is often impaired, resulting in tumor progression. It may be that no CTL response to the cancer is initiated, or that the CTL response is ineffective. Regularly, dysfunctional or exhausted CD8⁺ T cells are found within the TME, characterized by high expression of inhibitory receptors and impaired proliferation and effector function[46]. Initially, it was thought that exhausted CD8⁺ T cells stem from previously active effector cells that become exhausted due to chronic antigen stimulation. However, various studies

both in mouse and human have shown that exhausted CD8$^+$ T cells instead derive from PD-1$^+$ TCF-1$^+$ progenitor exhausted (Tpex) or 'stem-like' CD8$^+$ T cells, which are poorly differentiated, 'predysfunctional' cells that arise early after tumorigenesis. While some stem-like cells can be maintained in the tdLN or specific intratumoral niches, chronic antigen stimulation in the TME drives the progression of stem-like cells into exhausted T cells[47,48]. In both mouse and human, the CD8$^+$ T-cell differentiation trajectory from stem-like to terminally exhausted is described as a spectrum which consists of different subpopulations of exhausted cells, including early effector-like and intermediate or transitional exhausted populations which still have some cytolytic capacity[49–52]. In mouse tumor models, stem-like CD8$^+$ T cells in the tdLN display a more memory-like functional state than those in the TME[53,54], and are suggested to be bona-fide memory cells, which could maintain a memory phenotype when shielded from antigen exposure[50,54].

Help delivery in cancer

Fewer studies have focused on the process of CD4$^+$ T-cell help delivery in the context of a tumor compared to viral infection, but it is clear that the cDC1 is responsible for help delivery to tumor-specific CD8$^+$ T cells[5,6]. In a mouse tumor model, it has been suggested that the initial priming of both CD4$^+$ and CD8$^+$ T cells takes place on cDC1[5]. This indicates the importance of cDC1-CD4$^+$ T-cell interactions for the CD4$^+$ T-cell response, but this study did not rule out initial CD4$^+$ T-cell activation by cDC2s.

While initial priming of tumor-specific CD8$^+$ T cells depends on their activation in the tdLN, increasing evidence supports the idea that help delivery may also occur in the TME. In a pan-cancer analysis of 16 human carcinoma types, co-localization of CD8$^+$ T cells, CD4$^+$ T cells and cDC1s within the TME was observed in a subset of tumor samples[55]. In such tumors, local help delivery may take place, according to the identification of the "helped" cDC1 signature in these tumors[6]. Additionally, intratumoral so-called 'triads' of DC, CD4$^+$ Th cells, and CD8$^+$ T cells, which likely represent CD4$^+$ T-cell help delivery, were associated with better response to ICB treatment in hepatocellular carcinoma patients[56]. Also larger, more complex immune structures in close localization to the tumor, so-called tertiary lymphoid structures (TLS), where DCs and T cells colocalize, have been associated with better prognosis and response to ICB therapy (reviewed by[57,58]).

Based on transcriptomic analyses of the predysfunctional / stem-like CD8$^+$ T-cell population in cancer and supported by literature, our group proposed a new model arguing that stem-like cells equal 'helpless' cells, generated as a result of priming in the absence of CD4$^+$ T-cell help[59]. Helpless CD8$^+$ T cells have not received all the required signals to complete their CTL effector differentiation, but instead are arrested in the PD-1$^+$TCF-1$^+$ stem-like state. Our model proposes that in the absence of 'helped' effector CTLs, cellular sources of antigen are insufficiently removed, leading to continuous antigen stimulation of the stem-like population which eventually drives their conversion into exhausted cells. Thus, helpless priming may be an important underlying mechanism for the occurrence of stem-like and exhausted CD8$^+$ T cells in cancer.

Help and IFN-I signals

Not only in cancer, but also in virus infection, IFN-I has been identified as key signal for CTL responses, which impinges on the functional state of cDC1s[60]. IFN-I signaling into cDC1s, as well as delivery of $CD4^+$ T-cell help signals to cDC1 are decisive for the CTL response to cancer. In virus infection models, $CD4^+$ T-cell help signals were suggested to amplify IFN-I signals in cDC1 licensing[11], but recently gene expression studies have led to an alternative model of signal integration[36]. Recently, human $CD4^+$ T cells were shown to deliver IFNb to the cDC1 during the "licensing" process, which acted in a partially non-redundant manner with CD40 ligand to optimize CTL priming *in vitro*[61]. These data explain the unique role of the $CD4^+$ T-cell help process in optimization of CTL responses. Below, we will describe that IFN-I plays a key role in CTL priming to cancer, not only for initial DC activation but also via orchestrating the platform for $CD4^+$ T-cell help delivery and making additive and synergistic contributions to cDC1 licensing.

Type I IFN production and signaling

IFN-I induction

The IFN-I family comprises as major species one IFNb protein produced by many cell types and multiple homologous IFNα proteins produced primarily by hematopoietic cells[62]. While most cell types can produce IFNβ, hematopoietic cells and in particular pDCs produce also IFNα. A primary role of IFN-I signaling is to provoke antiviral states in infected and neighboring cells and to limit their proliferation. However, IFN-I also has a multitude of immunomodulatory roles[63], of which specific ones will be addressed here. The key stimuli that lead to IFN-I production are RNA or DNA derived from pathogens upon infection or from endogenous sources after cell damage or death. These PAMPs or DAMPs are recognized by a number of PRRs that induce IFN-I gene expression. Toll-like receptor family members TLR3, 7, 8 and 9 can recognize specific DNA or RNA patterns in endosomes. TLR4 that recognizes bacterial lipopolysaccharide at the cell surface can also induce IFN-I. Furthermore, the cytosolic RIG-I family of RNA sensors can do so, as well as several cytosolic DNA sensors, among which cGAS. This enzyme produces the cyclic dinucleotide cGAMP that activates Stimulator of Interferon Genes (STING) at the endoplastic reticulum (Figure 2). In the context of cancer, where PAMPs are lacking, IFN-I production can be induced in tumor cells themselves by self-derived DNA, such as endogenous retroviral elements, mitochondrial DNA and micronuclei that reach the cytosol upon upon cellular damage or stress[64]. Tumor cell-derived DNA or RNA released into the extracellular environment may also be sensed in particular by phagocytic immune cells such as DCs via TLRs, or by cytoplasmic sensors upon transfer from endosomes to cytosol[65]. The different PRRs mentioned activate kinases that phosphorylate IFN regulatory factor 3 (IRF3) or IRF7. These factors then locate to the nucleus and activate IFNA and IFNB gene transcription[63].

IFN-I signaling

IFNα and IFNβ both signal via the IFNα/β receptor (IFNAR) that is composed of IFNAR1 and -2 subunits. IFNAR activates the tyrosine kinases JAK1 and TYK2 are that phosphorylate and activate STAT1, -2 in the cytosol. Upon dimerization and nuclear translocation, these transcription factors form a trimeric complex with IRF9, called ISGF3. This complex binds to cognate IFN-stimulated response elements (ISREs) in the DNA, resulting in the transcription hundreds of interferon-stimulated genes (ISGs)[66]. These ISGs restrict pathogen replication and spread by diverse mechanisms[67]. In addition, STAT1 homodimers bind to gamma-activated sequences (GAS), which leads to expression of pro-inflammatory genes. IFNAR signaling is subject to positive and negative regulation and crosstalk with signaling components activated by other membrane receptors. E.g. STAT1 levels and activity can be amplified by diverse cytokine- and chemokine signaling pathways and ISGF3 complex formation is regulated by Tumor Necrosis Factor (TNF) receptor signaling[66].

IFN-I production in cancer

IFN-I production by tumor cells

In tumor cells, DNA damage and genomic instability lead to DNA leakage into the cytosol and activation of the cGAS-STING pathway. Therefore, tumor cells are potential IFN-I producers. However, in a variety of human cancers, the STING pathway is suppressed or defective due to epigenetic silencing, loss-of-function mutations or overexpression of inhibitory factors[68–71]. As a result, spontaneous IFN-I production by tumor cells is rare, and has been mainly reported to occur after treatment with STING- or TLR agonists[10]. In a recent study, murine metastatic breast cancer cells showed active cGAS-STING signaling and IFN-I production *in vitro*, but this response was dampened when these cells formed a tumor *in vivo*[72]. Overexpression of the MYC oncogene in mouse breast cancer models downregulated various STING pathway-related genes and ISGs, resulting in immune cell exclusion[71]. In breast cancer and melanoma patients, lower IFN-I or ISG expression signatures in the tumor correlated with reduced T-cell infiltration and worse prognosis[8,72,73]. These results suggest that in the TME, tumor cells suppress their own IFN-I production in order to evade antitumor immune responses. In a spontaneously regressing fibrosarcoma mouse model, constitutive IFN-I production by tumor cells induced an intratumoral ISG^+ DC population, which was required for tumor control[74]. Interestingly, this ISG^+ DC population consisted not of cross-presenting cDC1s, but of $CD11b^+$ cDC2s that gained the capacity to prime $CD8^+$ T cells via MHC-I cross-dressing, the presentation of intact tumor-derived peptide-MHC-I complexes. The ISG^+ DC state has not been widely described in the context of progressing tumors, consistent with tumor-intrinsic IFN-I production being a rather rare phenotype[74].

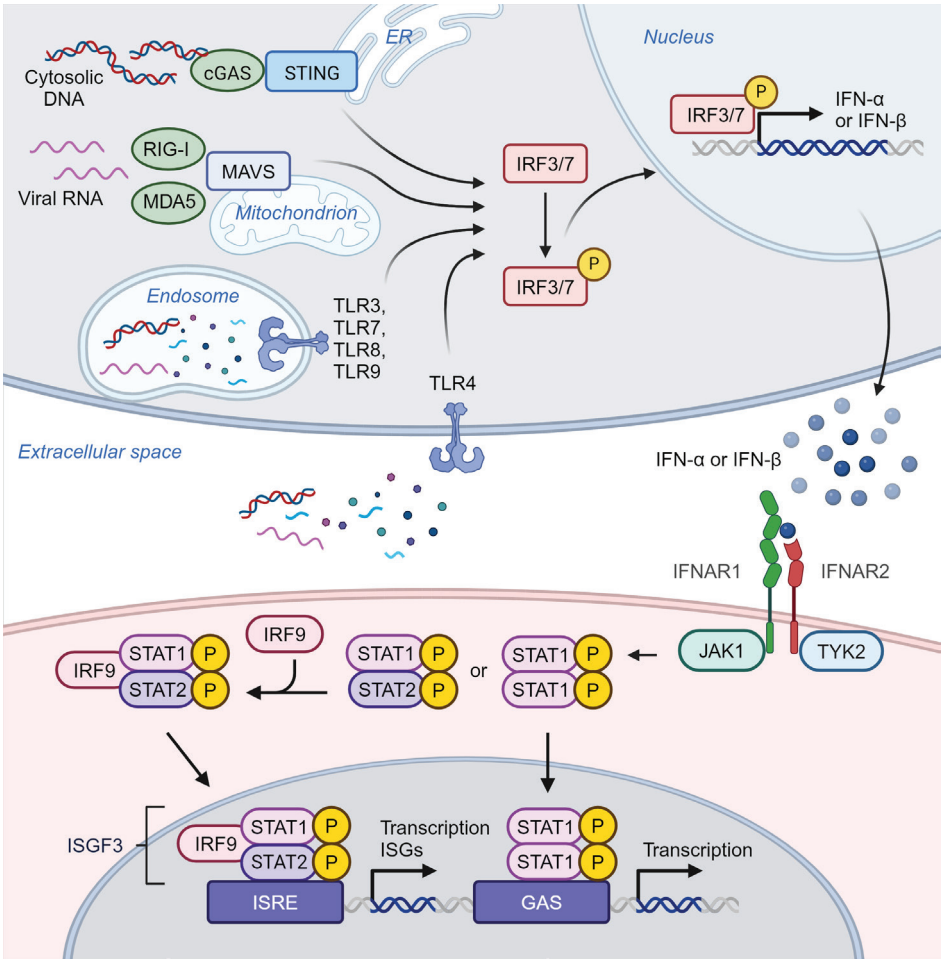

Figure 2. IFN-I production and signaling pathway. Extracellular and endosomal DNA, RNA and microbial molecules are sensed by TLRs on immune cells. Cytosolic DNA is sensed by the cGAS-STING pathway in immune cells and tumor cells. Viral RNA is sensed by cytosolic RIG-I-like sensors, which signal via MAVS. This causes the phosphorylation of IRF3/7, which subsequently translocates to the nucleus and induces the transcription of IFN-α and IFN-β. IFN-I binds to IFNAR, resulting in activation of JAK1 and TYK2. Consequently, STAT1 and STAT2 are phosphorylated and bind IRF9, which together form a heterodimer ISGF3. ISGF3 translocates to the nucleus where it can induce the transcription of a wide range of ISGs by binding to ISRE. In addition, STAT1 homodimers can bind to GAS to induce transcription of pro-inflammatory genes [66]. GAS: gamma-activated sequences; IFN: interferon; IFNAR; interferon α receptor; IRF: interferon regulatory factor; ISG: interferon-stimulated gene; ISGF3: interferon-stimulated gene factor 3; ISRE: interferon-stimulated response element; JAK1; Janus kinase 1; MAVS: mitochondrial antiviral-signaling protein; MDA5: melanoma differentiation-associated protein 5; RIG: retinoic acid-inducible gene; STAT: signal transducer and activator of transcription; STING stimulator of interferon genes; TLR: Toll-like receptor; TYK2: tyrosine kinase 2.

IFN-I production by DCs

In immunogenic fibrosarcoma, IFNAR signaling into hematopoietic cells rather than the cancer cells themselves proved important for immunosurveillance[1]. Pioneering studies demonstrated that IFN-I signaling into cDC1s is critical for antigen crosspresentation and CTL-mediated rejection of spontanously immunogenic tumors in mice[7,8]. In these models, cGAS/STING rather than TLR- of RIG-I-like receptors were decisive for spontaneous CTL priming by the tumor cells[65,75]. Reporter mice identified in the key model of immunogenic fibrosarcoma $CD11c^+$ cDCs and more specifically $CD11b^+$ DCs, likely cDC2, as the main source of IFN-I (IFNβ) in the TME[75], in agreement with earlier findings[8]. Both studies argue that cDC-derived rather than tumor-derived IFN-I was the decisive factor for tumor rejection.

During steady state, tonic IFN-I produced by pDCs instructs a basal cDC state permissive for $CD8^+$ T-cell priming[76]. In infection, when PAMPs are abundant, PRR stimulation evokes robust IFN-I production by pDCs. In cancer, however, PAMPs are generally lacking and the TME is often highly infiltrated by dysfunctional pDCs. Such pDCs display impaired IFNα production and are associated with tumor progression (reviewed by[77]). For example, pDCs in the TME of breast- and ovarian cancer patients did not produce IFNα, unlike circulating pDCs[78,79]. Inhibition of IFN-I production by intratumoral pDCs has been mainly attributed to TGF-β produced by tumor cells, both in mouse and in human[80,81]. In breast cancer patients, dysfunctional pDCs co-localized with regulatory T cells (Tregs) and were shown to promote Treg proliferation *ex vivo*[78]. This effect could be reversed by administration of IFN-I, suggesting that the lack of IFN-I production by pDCs is an important underlying mechanism for Treg maintenance and the establishment of an all-over immunosuppressive environment in the TME. Taken together, impaired IFN-I production both by tumor cells and by tumor-infiltrating pDCs contribute to the IFN-I poor environment of the TME that impedes initial cDC activation for the initiation of antitumor T-cell responses. In mouse models where immune-mediated tumor rejection takes place, the necessary IFN-I to drive CTL priming by cDC1s is most likely produced by cDC2s in the TME.

While the tdLN likely embodies a less immunosuppressive environment than the TME, often without the constant presence of (derivates of) tumor cells, the environment of the tdLN may also lack sufficient IFN-I signals for cDC1 activation. In a mouse model of viral infection, functional pDCs provide the cDC1 with IFN-I within the LN, which optimizes cDC1 functionality and establishment of the $CD4^+$ T-cell help delivery platform[82]. However, in a mouse melanoma model a subset of pDCs in the tdLN adopted a suppressive phenotype via expression of indoleamine 2,3-dioxygenase (IDO), which inhibited T-cell responses via activation of mature Tregs[83,84]. Until now, limited literature has touched upon the activation mechanisms and IFN-I production of non-suppressive pDCs in the tdLN. Therefore, it remains unclear whether pDCs in the tdLN are typically capable of producing sufficient IFN-I for cDC1 optimization and delivery of $CD4^+$ T-cell help.

IFN-I production by CD4$^+$ T cells

In this context, it is of interest that activated CD4$^+$ T cells can be a source of IFN-I that contributes to cDC1 functionality, as we have recently documented[61]. Unlike myeloid cells, T cells are generally not considered major producers of IFN-I due to a more strictly regulated cGAS-STING pathway[85]. However, upon stimulation via CD3 and CD28, mimicking initial T-cell activation, human CD4$^+$ T cells produced IFNβ via the cGAS-STING pathway and delivered it to cDC1 in a human *in vitro* model of CTL priming, which optimized cDC1 for CTL crosspriming to tumor antigens[61]. IFN-I production was also observed in human CD4$^+$ T cells with a tumor antigen-specific phenotype in the TME[61]. Thus, in the TME where IFN-I inducing signals and IFN-I production by pDCs are scarce, IFN-I production by tumor-specific CD4$^+$ T cells may play a role in cDC stimulation.

Effects of IFN-I on cDC1s

Given the convergence of IFN-I signals into the CD4$^+$ T-cell help scenario, we focus on how IFN-I has been described to impact on cDC1s, CD4$^+$ and CD8$^+$ T-cell functions and may shape their mutual interactions (Figure 3). Between the cell types that make up the help delivery platform, most effects of IFN-I signaling have been described for cDC1s. As shown in various studies in mouse and human, IFN-I improves the survival of cDC1s, as well as all three T-cell activating signals: 1) antigen presentation by MHC, 2) co-stimulation, and 3) specific cytokine production. In addition, IFN-I induces specific chemokine expression in cDC1, which is important for T-cell recruitment, as will be further discussed later.

Antigen presentation

Several studies in both mouse and human have shown that IFN-I promotes antigen cross-presentation by cDC1s (reviewed in[86]). In a murine thymoma model, IFN-I promoted survival of CD8α$^+$ DCs, MHC-I expression and cross-presentation of tumor cell-associated antigens by prolonging antigen persistence within the DCs[87]. Antigen presentation on MHC-II in murine DCs was also upregulated by IFN-I, improving the interaction with CD4$^+$ T cells[88]. In a viral infection model, IFN-I optimized cross-presentation of antigens by cDC1 to CD8$^+$ T cells in the context of CD4$^+$ T-cell help delivery in the LN[82]. In another study, upregulation of MHC-II on CD8α$^+$ cDC1s upon viral infection relied on IFNAR signaling[36]. Recently, our group showed that IFN-I stimulation of human cDC1s increased their expression of both MHC-I and MHC-II, as well as proteosome subunits and TAP1 and -2 that transport antigen into the ER for MHC-I loading[61]. Furthermore, IFN-I upregulated CD83 that promotes cell surface expression of MHC-II[89]. Taken together, IFN-I signaling in cDC1s enhances antigen processing and presentation on both MHC-I and MHC-II. In this way, it contributes to cognate interactions and synaptic communication with both CD4$^+$ and CD8$^+$ T cells.

Costimulation

IFN-I also promotes T-cell costimulatory capacity of cDC1s. Early *in vitro* experiments showed that IFN-I stimulation upregulated CD86 on mouse CD8α⁺ DCs and CD80 and CD86 on primary human DCs [87,88,90]. Selective deletion of IFNAR on cDCs led to reduced expression of CD80 and CD86 on non-infected cDC1s in a viral infection mouse model, where pDCs delivered IFN-I[82]. In human cDC1, IFN-I signaling enhanced expression of CD80, CD86 and CD70[61], of which the latter was shown to be important for CTL differentiation in both mouse and human[6,35,37]. IFN-I signaling also upregulated PD-L1 [61] that can form a costimulatory heterodimer with CD80[91–93]. Interestingly, IFN-I stimulation of murine and human cDC1s also results in upregulation of CD40 [61,87]. In a viral infection model, mice that specifically lacked IFNAR1 on cDCs showed a striking reduction in CD40 expression on cDC1s [82]. These results indicate that IFN-I signaling *in vivo* leads to upregulation of CD40 on cDC1s, which promotes their ability to receive help signals from CD4⁺ T cells via CD40L.

Integration of IFN-I and CD40 signals

Many effects of IFN-I on cDC1s are comparable to those of CD40 signaling and it has been questioned whether these signals are additive or synergistic[11]. Similar to IFN-I signaling[87], CD40 signaling into cDC1 increases survival, MHC-I expression and cross-presentation of antigens[35,94]. In a mouse tumor model, adenoviral delivery of membrane-stable CD40L and IFNβ increased the expression of CD80 and CD86 on migratory cDC1s, while this effect was diminished upon delivery of either stimulus alone[95]. Treatment of mice with IFN-I and CD40 agonist, but not either of these strategies alone, resulted in upregulation of CD70 on CD8α⁺ cDC1s, and a CD70-dependent enhanced CTL response[96].

Gressier *et al*. have recently illuminated how cDC1s integrate IFN-I and CD40 signals by transcriptomics. Treating murine bone-marrow-derived cDC1-like cells with CD40 agonist and/or IFNα/β indicated that CD40 signaling can amplify IFN-I induced signals, but also that the combined signals activate specific transcriptional programs, by integration of transcription factor activity[36]. By comparing different stimulation regimens, the authors demonstrated that cDC1s first need to be exposed to IFN-I in order to become receptive to CD40 signals. Thus, IFN-I signaling conditions the cDC1 to become receptive to CD4⁺ T-cell help mediated through CD40L-CD40 interactions and shapes the transcriptional response to CD40 stimulation.

Cytokines

IFN-I stimulation also induces the expression of specific cytokines by cDC1s, improving their function as mediator of CD4⁺ T-cell help. Stimulation with either agonistic anti-CD40 or IFN-I alone was not sufficient to induce production of IL-15 or IL-6 by *in vitro* generated murine cDCs, but upon dual stimulation their expression was amplified[60]. The same paper also demonstrated that CD8α⁺ cDC1 relied on IFNAR expression for IL-15 production that was required for HSV-specific CD8⁺ T-cell priming[60]. IL-15, produced by cDC1, is known to be required for CTL

differentiation and long-lived memory T-cell maintenance[30,97]. In mice, IL-6 has been reported for its anti-apoptotic functions in activated CD8$^+$ T cells, even in the presence of IL-15[97]. Thus, both cytokines exhibit distinct roles in improving CD8$^+$ T-cell survival and CTL differentiation, and they are produced by DCs only when both CD40 and IFN-I signals are present.

Direct effects of IFN-I on T cells

Effects of IFN-I *in vivo* can be indirect, but direct effects of IFN-I on T cells have been identified in mice with T-cell specific deletion of IFNAR. In this way, IFNAR signaling into antigen-specific CD8$^+$ T cells was found to dictate their survival during clonal expansion and formation of a memory pool after infection with *lymphocytic choriomeningitis virus* (LCMV)[98]. This agrees with earlier *in vitro* data showing that IFN-I promotes survival of activated T cells[99]. However, this effect may depend on the *in vivo* context, since IFNAR-proficient and deficient CD4$^+$ and CD8$^+$ T cells were found expand equally upon *vaccina virus* or *vesicular stomatitis virus* (VSV) infection in mice[82,100].

CD8$^+$ T cells

Recently, IFN-I was found to promote survival and activation potential of naïve CD8$^+$ T cells in mice. IFNα signals induced and sustained a Ly6C$^+$ subpopulation of naïve CD8$^+$ T cells via MHC-I upregulation and induction of tonic TCR signaling. IFN-I-induced Ly6C$^+$ naïve CD8$^+$ T cells responded more rapidly upon specific interaction with cognate antigen *in vivo*, and expressed higher levels of effector molecules such as IFNγ[101]. Earlier data also show that murine CD8$^+$ T-cell differentiation into effector cells depends greatly on IFN-I signaling directly to CD8$^+$ T cells[98,102]. IFN-I signals promote the production of effector molecules such as IFNγ and Granzyme-B by CD8$^+$ T cells and increase their cytolytic activity[102,103]. Moreover, IFN-I can prevent the elimination of antigen-activated CTLs by natural killer cells[104,105]. Thus, IFN-I signaling directly to CD8$^+$ T cells contributes to their survival, clonal expansion and effector differentiation upon activation (Figure 3).

CD4$^+$ T cells

Early research showed that direct stimulation of human CD4$^+$ T cells with IFNα, in the context of TCR triggering, drives an IFNγ$^+$ Th1 phenotype[106] (Figure 3). In a mouse infection model, IFN-I and IL-12 signaling on CD4$^+$ T cells showed synergistic effects for the promotion of Th1 differentiation[107]. Direct IFN-I signaling into CD4$^+$ T cells has also been demonstrated to support CD4$^+$ T-cell expansion and survival in a mouse model of acute viral infection[108]. A rapid IFN-I response promoted T follicular helper (Tfh) differentiation of CD4$^+$ T cells after VSV infection, while a later, prolonged IFN-I response resulted in more Th1 differentiation after LCMV infection. However, these effects did not result from direct IFN-I signaling into CD4$^+$ T cells, since Tfh and Th1 polarization was comparable in wild-type and IFNAR$^{-/-}$ CD4$^+$ T cells[100].

Tregs

IFN-I also affects CD4⁺ Treg differentiation and function. In a human *in vitro* setting, addition of IFNα to a co-culture of APCs and CD4⁺ T cells prevented IL-2-driven Treg proliferation and suppressive capacity, and this effect was dependent on IFNAR expression on both on APCs and Tregs[109]. Mice that specifically lacked IFNAR expression in Tregs showed increased Treg activity and decreased CD8⁺ and CD4⁺ T-cell responses upon viral infection, indicating that IFN-I signaling in Tregs dampens their suppressive capacity[110]. It has been described that IFN-I can inactivate the suppressive function of human Tregs through activation of phosphodiesterase 4 and the consequent depletion of cyclic AMP[111]. Thus, apart from acting via cDC, IFN-I can also promote effector T-cell responses by direct effects on conventional CD4⁺ T cells, CD8⁺ T cells and Tregs.

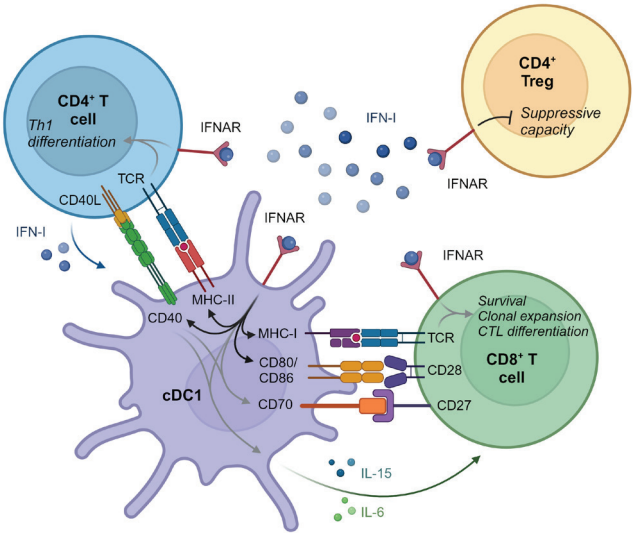

Figure 3. Effects of IFN-I on cells in the help delivery platform. On cDC1, direct IFN-I signaling (black arrows) induces upregulation of both MHC-II and MHC-I, thereby promoting interactions with both CD8⁺ and CD4⁺ T cells[36,61,82,87,88]. Also, IFN-I upregulates co-stimulatory molecules CD80/86 and CD40 on cDC1[61,82,87,88]. Combined stimulation of cDC1 with IFN-I and CD40L (grey arrows) results in a synergistic upregulation of CD70 and production of IL-6 and IL-15, which all contribute to optimal CD8⁺ T-cell functionality[60,96]. On CD4⁺ T cells, IFN-I stimulation during activation contributes to Th1 differentiation[106,107]. On CD8⁺ T cells, direct stimulation with IFN-I in the context of TCR stimulation contributes to clonal expansion and optimal CTL differentiation[98,102,103,112]. On Tregs, IFNAR signaling dampens their suppressive capacity[109–111]. cDC1: conventional dendritic cell type I; CTL: cytotoxic T lymphocyte; MHC: major histocompatibility complex; pDC: plasmacytoid dendritic cell; IFNAR: interferon α receptor; IFN-I: type I interferon; Treg: regulatory T cell.

Effects of IFN-I on cDC and T-cell migration and localization in LNs

Chemokines play a crucial role in cell migration and localization of cDCs and T cells towards and within LNs and tumor and between these compartments. In this section, we will describe the role of IFN-I in inducing chemokine gradients that contribute to the communication between T cells and cDCs and organization of the help delivery platform (Figure 4).

CCR7

In human cDC1s, *in vitro* stimulation with IFN-I resulted in upregulation of CCR7[61], which is the key chemokine receptor that enables trafficking of cDCs to LNs[113]. Expression of CCR7 ligands CCL19 and CCL21 in the LN recruites mature CCR7$^+$ cDCs to the LN, a process which is essential for anti-tumor CTL priming[23,114]. Under steady-state conditions, immature cDCs also express CCR7, allowing them to migrate to the LN and activate Tregs for the maintenance of immunological tolerance[114]. In a melanoma mouse model, intratumoral delivery of IFNβ contributed to CCR7 upregulation on migratory cDC1s[95]. cDCs from IFNAR$^{-/-}$ mice failed to upregulate CCR7 upon infection and showed impaired migration to the LN upon adoptive transfer[115]. Localization to the T-cell zone within the LN was also impaired in IFNAR$^{-/-}$ cDCs[115], which suggests an additional role of IFN-I, possibly via CCR7, for intranodal migration[15]. Thus, IFN-I signals in the TME are important for CCR7 upregulation on cDCs and their migration to the TdLN, thus allowing T-cell priming.

CCR5 ligands

IFN-I alone or in combination with CD40 signaling induced in murine cDCs the production of CCL3, CCL4 and CCL5, ligands for chemokine receptor CCR5[36,60]. CCL3 and CCL4 have been reported to orchestrate CD4$^+$ T-cell help delivery[97,116]. After vaccination, CCL3/4 was produced at sites of CD4$^+$ T cell-DC interactions in the IFR of the LN, which attracted CCR5$^+$ CD8$^+$ T cells and was crucial for CTL differentiation. In a mouse infection model, the gradient of CCL3 and CCL4 produced at the DC-CD8$^+$ T-cell interface was crucial for the migration of CCR5$^+$ pDCs to the CD8$^+$ T-cell priming site in the IFR. IFN-I produced by the pDCs optimized CD8$^+$ T-cell priming by improving cDC1 function[82]. Taken together, CCR5 ligands are likely important to spatially orchestrate the second step of T-cell priming. CCL4 and CCL5 have also been shown to enable DC migration into the TME[117] .

CXCR3 ligands

CXCR3 ligands CXCL9, -10 and -11 are differentially regulated and display individual binding characteristics which may result in distinct signal transduction upon CXCR3 engagement[118]. Humans express CXCL9, -10 and -11, of which the latter is suggested to induce a tolerizing state. C57BL/6 mice lack CXCL11 expression due to several mutations, but restoration of CXCL11 in these animals resulted in similar responses to viral infection as compared to wildtype mice[119]. Addition of IFN-I to human cDC1s led to increased expression of CXCL9, -10 and -11. Furthermore, human cDC1s produced CXCL9/10 in an IFNAR-dependent manner upon stimulation with CD4$^+$ T cells[61].

CXCL10 was also upregulated at the mRNA level in murine cDC1-like cells upon combined IFN-I and CD40 stimulation[36]. The common receptor for these chemokines is CXCR3 that enables T cells to migrate into non-lymphoid tissues, but also regulates their positioning within LNs during priming (reviewed by[120]).

In a viral infection model, IFN-I signaling proved crucial to induce CXCL10 expression within the LN[121]. After LCMV infection, cDC1s and stromal cells in the LN center predominantly expressed CXCL9, while CXCL9 and CXCL10 were produced by cDC2s, inflammatory monocytes and stromal cells in the periphery of the LN, including the IFR where "help" has been localized in vaccination models[44]. IFN-I-induced CXCL10 but not CXCL9 was required for $CD8^+$ T cells to migrate to the IFR in a CXCR3-dependent manner in order to undergo full effector differentiation[122]. $CXCR3^{-/-}$ $CD8^+$ T cells were retained in the LN paracortex and showed impaired effector functions, in line with earlier observations[122,123]. A recent study showed that early IFNAR blockade during acute viral infection in mice increased the stem-like phenotype of $CD8^+$ T cells and their localization in the LN paracortex[124]. Taken together, IFN-I signaling in the LN likely plays an important role in the induction of CXCR3 ligands for the intranodal localization and differentiation of CTLs. Also the CXCL10/CXCR3-dependent migration of $CD4^+$ T cells into the IFR was shown to be essential for Th1 differentiation in response to viral infection and vaccination[45]. Thus, IFN-I-induced CXCL10 expression in the IFR of the LN results in optimized priming, likely by facilitating optimal positioning of $CD4^+$ and $CD8^+$ T cells for help delivery. Upon CD70/CD27 co-stimulation, which is an important signal in help delivery, $CD8^+$ T cells produced CXCL10 themselves, acting as a chemoattractant for other activated $CD8^+$ T cells[125]. Thus, the accumulation of CXCR3 ligands locally surrounding the $CD4^+$ T-cell help platform may additionally attract other activated $CD4^+$ and $CD8^+$ T cells for help delivery.

Summary and proposed model

In the TME, IFN-I is required for the activation of migratory cDC1s and their localization to the LN to initiate the first step of T-cell priming. In addition, IFN-I also acts during the second step of T-cell priming, where delivery of $CD4^+$ T-cell help to $CD8^+$ T cells takes place. While it is commonly accepted both $CD4^+$ T-cell help and innate signals such as IFN-I are crucial for raising an effective anti-tumor $CD8^+$ T-cell response (reviewed in[9,10,24], thus far it has remained unclear how IFN-I affects all players deemed important for help delivery. In the sections above, we have provided an integrated view of the effects of IFN-I on all participants in help delivery, as well as on their spatial organization within the LN. In summary, IFN-I optimizes the cDC1 as mediator to transduce $CD4^+$ T-cell signals to $CD8^+$ T cells in various ways: 1) enhancing survival of the cDC1, 2) improving antigen presentation on both MHC-I and MHC-II, 3) upregulating co-stimulatory molecules, such as CD70 and CD80/86, 4) inducing the production of cytokines, such as IL-15 and IL-6, and 5) inducing the secretion of chemokines, such as CCR5 and CXCR3 ligands. Thus, IFN-I facilitates initial

cDC1 activation and direct interactions between cells in the help delivery platform, via antigen presentation, co-stimulatory molecules and cytokines, as well as their proximal localization in the IFR of the LN, via chemokines. This creates an optimal communication platform for the cDC1 to interact with $CD4^+$ and $CD8^+$ T cells, which ultimately results in the generation of optimally differentiated effector and memory CTLs. While presumably many effects of IFN-I on T cells are indirect because of the interaction with the optimized cDC, IFN-I has also been shown to act directly on T cells. It promotes $CD8^+$ T-cell survival and effector differentiation, and $CD4^+$ T-cell differentiation into the Th1 phenotype. Thus, the scenario of $CD4^+$ T-cell help depends on IFN-I for raising optimally differentiated effector CTLs against tumor antigens.

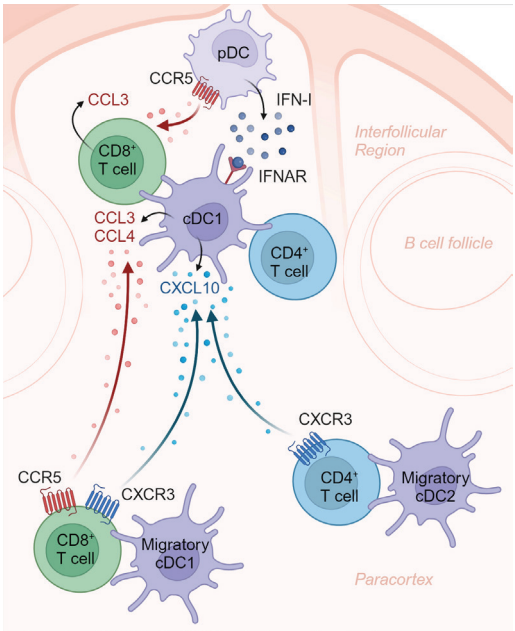

Figure 4: IFN-I induced chemokines in the LN involved in spatial organization of the help delivery platform. IFN-I promotes the production of CCR5 ligands (CCL3 and CCL4) and CXCR3 ligand (CXCL10) by the cDC1[36,60,121,122]. As a result, $CD4^+$ and $CD8^+$ T cells, initially activated in the paracortex, are attracted to the IFR via CXCR3 ligands, and $CD8^+$ T cells are additionally attracted via CCR5 ligands[45,116,122]. This facilitates the proximal localization of all participating cell types in $CD4^+$ T-cell help delivery. In virus infection, IFN-I producing pDCs are attracted to the secondary priming site by cDC1-derived and/or $CD8^+$ T cell-derived CCR5 ligands, leading to locally increased levels of IFN-I [82]. CCL3/4: CC-chemokine ligand 3/4; CCR5: CC-chemokine receptor 5; CXCL10: CXC-motif chemokine ligand 10; CXCR3: CXC-motif chemokine receptor 3; cDC1: conventional dendritic cell type 1; IFN-I: type I interferon; IFNAR: interferon α receptor; IFR: interfollicular region; LN: lymh node; pDC: plasmacytoid dendritic cell.

However, tumors often represent an IFN-I-poor environment. The strong induction of IFN-I by PAMPs as seen in viral infection is lacking in non-viral tumor settings, instead IFN-I induction relies on sensing of DAMPs. The main pathway driving IFN-I production in tumor settings is the cGAS-STING pathway, which can sense cytosolic DNA as a result of DNA damage, mitochondrial stress and

genomic instability in tumor cells. This pathway is defective or downregulated in many tumor cells. Also pDCs, which are the most important IFN-I producers in viral infections, are often dysfunctional in the TME. In parallel, T-cell infiltrated tumors often accommodate exhausted, or predysfunctional / stem-like $CD8^+$ T cells, with impaired effector function. Previous work from our group postulated that these stem-like T cells equal helpless $CD8^+$ T cells, generated after priming in absence of $CD4^+$ T-cell help[59]. Combining these observations, we propose that the IFN-I-poor environment of the TME is an important underlying mechanism for impaired $CD4^+$ T-cell help delivery to tumor-specific $CD8^+$ T cells. We argue that by removing IFN-I from the TME, tumors prevent the proper priming of CTLs not only by impaired DC activation, but also by impaired delivery of $CD4^+$ T-cell help, thereby impacting all steps in the cancer-immunity cycle[126,127] (Figure 5). This explains why tumors in which IFN-I signaling is attenuated, remain devoid of functional CTLs.

Clinical data support the importance of IFN-I in anticancer immunity. In breast cancer and melanoma patients, higher expression of IFN-I-related genes or ISGs in the tumor correlated with increased T-cell infiltration and better prognosis [8,72,73,128]. An increased IFN-I gene signature in intratumoral myeloid cells predicted better response to PD-1 blockade therapy in basal cell carcinoma patients [129]. Also, the presence of functional pDCs in the TME, considered the main producers of IFN-I, correlated with increased survival of patients with colon cancer and follicular lymphoma [130,131]. In a pan-cancer analysis of 16 solid tumor types, carcinoma ecotypes showing co-localization of $CD8^+$ T cells, $CD4^+$ T cells and cDC1s were associated with the highest overall survival and response to PD-1 blockade therapy [55]. In these tumors help delivery likely takes place, as testified by the helped cDC1 gene expression signature in the TME [6]. Since effective anti-tumor CTL priming requires IFN-I signaling to cDC1s [1,7,8], in these types of tumors there must be cell types in the TME or tdLN that can produce IFN-I. The most likely candidates for this are cDC2s in the TME, which can produce IFNβ in mouse tumor models, possibly via STING-mediated sensing of tumor-derived DNA in their cytosol [65,75]. Also DCs in the tdLN have been described to produce IFNβ in immunogenic mouse models [8], however the type of DCs or the precise role of IFN-I signaling within the tdLN has not been further elucidated. pDCs in the tdLN have been suggested to produce IFN-I and contribute to spontaneous CTL priming, but this hypothesis has not yet been formally addressed [132]. Another outstanding question remains if in cancer, cDC1s are capable of producing IFN-I in an autocrine manner, whether as a first signal or as an amplifying response to IFN-I derived from other sources. Our recent findings suggest that once $CD4^+$ T cells have been primed, they may also provide IFN-I to cDC1s to further optimize help delivery [61]. Taken together, understanding the role of IFN-I signaling, $CD4^+$ T-cell help and how these mechanisms are connected, will contribute to better insights into the conditions required for effective CTL priming in cancer.

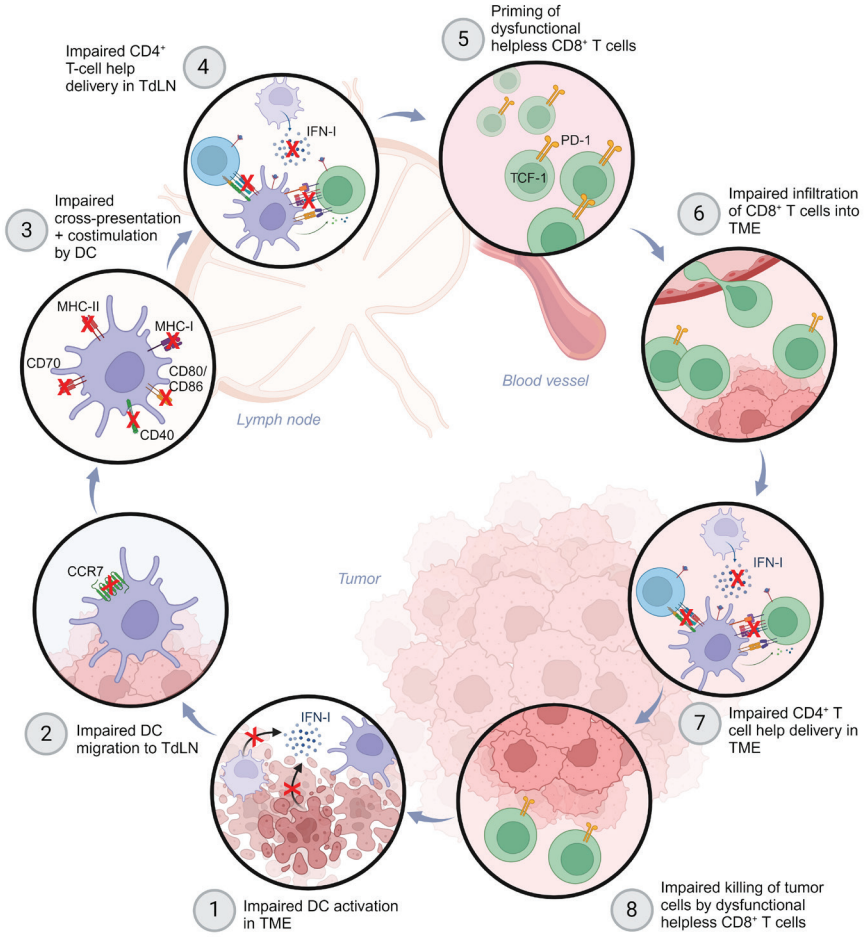

Figure 5. The effects of lack of IFN-I on the cancer-immunity cycle[126,127]. Step 1) Lack of IFN-I production by tumor cells and intratumoral pDCs leads to impaired cDC activation in the TME, and potentially impaired cDC infiltration into the TME. Step 2) Lack of IFN-I signaling in cDC results in lower expression of CCR7, which leads to impaired LN homing of the DC. Step 3) Cross-presentation of tumor antigens and expression of MHC-I, MHC-II and co-stimulatory ligands is decreased as a result of insufficient IFN-I-mediated activation of cDCs. Step 4) $CD4^+$ T-cell help delivery is hindered by the impaired initial cDC activation in the TME. pDCs in the TdLN may also be partly dysfunctional, potentially leading to a decrease in local IFN-I production within the TdLN. Step 5) As a result of impaired $CD4^+$ T-cell help delivery, helpless $CD8^+$ T cells are primed. Step 6) Helpless $CD8^+$ T cells display impaired migratory capacities and tumor infiltration. The absence of IFN-I in the TME may also result in a lack of chemokines, such as CXCR3 and CCR5 ligands, which are responsible for T-cell infiltration into the TME. Consequently, T cells are hindered to infiltrate the tumor. Step 7) $CD4^+$ T-cell help cannot be delivered as a result of the lack of IFN-I in the TME. The close localization of the participating cells, as well as their maturation, cannot be established. Step 8) Dysfunctional helpless $CD8^+$ T cells exhibit impaired effector potential, which results in decreased tumor killing. CCR5: CC-chemokine receptor 5; CCR7: CC-chemokine receptor 7; cDC: conventional dendritic cell; CXCR3: CXC-motif chemokine receptor 3; IFN-I: type I interferon; LN: lymph node; MHC: major histocompatibility complex; pDC: plasmacytoid dendritic cell; TdLN: tumor-draining lymph node; TME: tumor-microenvironment.

Competing Interests

The authors declare no competing interests.

Funding

This research was supported by Oncode and grant 2017-11079 of the Dutch Cancer Society (KWF) to J. Borst.

References

1. Dunn, G. P. *et al.* A critical function for type I interferons in cancer immunoediting. *Nature Immunology* **6**, 722–729 (2005).
2. Shankaran, V. *et al.* IFNγ and lymphocytes prevent primary tumour development and shape tumour immunogenicity. *Nature* **410**, 1107–1111 (2001).
3. Gajewski, T. F. The Next Hurdle in Cancer Immunotherapy: Overcoming the Non–T-Cell–Inflamed Tumor Microenvironment. *Seminars in Oncology* **42**, 663–671 (2015).
4. Fridman, W. H., Pagès, F., Sautès-Fridman, C. & Galon, J. The immune contexture in human tumours: impact on clinical outcome. *Nature Reviews Cancer* **12**, 298–306 (2012).
5. Ferris, S. T. *et al.* cDC1 prime and are licensed by CD4+ T cells to induce anti-tumour immunity. *Nature* **584**, 624–629 (2020).
6. Lei, X. *et al.* CD4+ helper T cells endow cDC1 with cancer-impeding functions in the human tumor micro-environment. *Nat Commun* **14**, 217 (2023).
7. Diamond, M. S. *et al.* Type I interferon is selectively required by dendritic cells for immune rejection of tumors. *Journal of Experimental Medicine* **208**, 1989–2003 (2011).
8. Fuertes, M. B. *et al.* Host type I IFN signals are required for antitumor CD8+ T cell responses through CD8α+ dendritic cells. *Journal of Experimental Medicine* **208**, 2005–2016 (2011).
9. Liang, Y., Hannan, R. & Fu, Y.-X. Type I IFN Activating Type I Dendritic Cells for Antitumor Immunity. *Clinical Cancer Research* **27**, 3818–3824 (2021).
10. Yu, R., Zhu, B. & Chen, D. Type I interferon-mediated tumor immunity and its role in immunotherapy. *Cellular and Molecular Life Sciences* **79**, 191 (2022).
11. Bedoui, S., Heath, W. R. & Mueller, S. N. CD4+ T-cell help amplifies innate signals for primary CD8+ T-cell immunity. *Immunol Rev* **272**, 52–64 (2016).
12. Murphy, T. L. & Murphy, K. M. Dendritic cells in cancer immunology. *Cellular & Molecular Immunology* **19**, 3–13 (2022).
13. Wculek, S. K. *et al.* Dendritic cells in cancer immunology and immunotherapy. *Nat Rev Immunol* **20**, 7–24 (2020).
14. Segura, E. Human dendritic cell subsets: An updated view of their ontogeny and functional specialization. *European Journal of Immunology* **52**, 1759–1767 (2022).

15. Braun, A. *et al.* Afferent lymph–derived T cells and DCs use different chemokine receptor CCR7–dependent routes for entry into the lymph node and intranodal migration. *Nature Immunology* **12**, 879–887 (2011).

16. den Haan, J. M. M., Lehar, S. M. & Bevan, M. J. Cd8+ but Not Cd8− Dendritic Cells Cross-Prime Cytotoxic T Cells in Vivo. *The Journal of Experimental Medicine* **192**, 1685–1696 (2000).

17. Broz, M. L. *et al.* Dissecting the Tumor Myeloid Compartment Reveals Rare Activating Antigen-Presenting Cells Critical for T Cell Immunity. *Cancer Cell* **26**, 638–652 (2014).

18. Hildner, K. *et al.* Batf3 Deficiency Reveals a Critical Role for CD8α + Dendritic Cells in Cytotoxic T Cell Immunity. *Science* **322**, 1097–1100 (2008).

19. Dudziak, D. *et al.* Differential antigen processing by dendritic cell subsets in vivo. *Science* **315**, 107–111 (2007).

20. Binnewies, M. *et al.* Unleashing Type-2 Dendritic Cells to Drive Protective Antitumor CD4+ T Cell Immunity. *Cell* **177**, 556–571 (2019).

21. Eickhoff, S. *et al.* Robust anti-viral immunity requires multiple distinct T cell-dendritic cell interactions. *Cell* **162**, 1322–1337 (2015).

22. Hor, J. L. *et al.* Spatiotemporally distinct interactions with dendritic cell subsets facilitates CD4+and CD8+T cell activation to localized viral infection. *Immunity* **43**, 554–565 (2015).

23. Roberts, E. W. *et al.* Critical Role for CD103+/CD141+ Dendritic Cells Bearing CCR7 for Tumor Antigen Trafficking and Priming of T Cell Immunity in Melanoma. *Cancer Cell* **30**, 324–336 (2016).

24. Borst, J., Ahrends, T., Bąbała, N., Melief, C. J. M. & Kastenmüller, W. CD4+ T cell help in cancer immunology and immunotherapy. *Nat Rev Immunol* **18**, 635–647 (2018).

25. Ruhland, M. K. *et al.* Visualizing Synaptic Transfer of Tumor Antigens among Dendritic Cells. *Cancer Cell* **37**, 786-799.e5 (2020).

26. Schoenberger, S. P., Toes, R. E. M., van der Voort, E. I. H., Offringa, R. & Melief, C. J. M. T-cell help for cytotoxic T lymphocytes is mediated by CD40–CD40L interactions. *Nature* **393**, 480–483 (1998).

27. Bennett, S. R. M. *et al.* Help for cytotoxic-T-cell responses is mediated by CD40 signalling. *Nature* **393**, 478–480 (1998).

28. Ridge, J. P., Di Rosa, F. & Matzinger, P. A conditioned dendritic cell can be a temporal bridge between a CD4+ T-helper and a T-killer cell. *Nature* **393**, 474–478 (1998).

29. Schulz, O. *et al.* CD40 Triggering of Heterodimeric IL-12 p70 Production by Dendritic Cells In Vivo Requires a Microbial Priming Signal. *Immunity* **13**, 453–462 (2000).

30. Oh, S. *et al.* IL-15 as a mediator of CD4+ help for CD8+ T cell longevity and avoidance of TRAIL-mediated apoptosis. *Proc Natl Acad Sci U S A* **105**, 5201–5206 (2008).

31. Agarwal, P. *et al.* Gene Regulation and Chromatin Remodeling by IL-12 and Type I IFN in Programming for CD8 T Cell Effector Function and Memory. *The Journal of Immunology* **183**, 1695–1704 (2009).

32. Schluns, K. S., Williams, K., Ma, A., Zheng, X. X. & Lefrançois, L. Cutting Edge: Requirement for IL-15 in the Generation of Primary and Memory Antigen-Specific CD8 T Cells. *The Journal of Immunology* **168**, 4827–4831 (2002).

33. Prilliman, K. R. *et al.* Cutting Edge: A Crucial Role for B7-CD28 in Transmitting T Help from APC to CTL. *The Journal of Immunology* **169**, 4094–4097 (2002).

34. Bullock, T. N. J. & Yagita, H. Induction of CD70 on dendritic cells through CD40 or TLR stimulation contributes to the development of CD8 + T cell responses in the absence of CD4 + T cells. *The Journal of Immunology* **174**, 710–717 (2005).

35. Wu, R. *et al.* Mechanisms of CD40-dependent cDC1 licensing beyond costimulation. *Nature Immunology* **23**, 1536–1550 (2022).

36. Gressier, E. *et al.* CD4+ T cell calibration of antigen-presenting cells optimizes antiviral CD8+ T cell immunity. *Nat Immunol* **24**, (2023).

37. Ahrends, T. *et al.* CD4+T cell help confers a cytotoxic T cell effector program including coinhibitory receptor downregulation and increased tissue invasiveness. *Immunity* **47**, 848–861 (2017).

38. Ahrends, T. *et al.* CD4+ T cell help creates memory CD8+ T cells with innate and help-independent recall capacities. *Nat Commun* **10**, 5531 (2019).

39. Elsaesser, H., Sauer, K. & Brooks, D. G. IL-21 Is Required to Control Chronic Viral Infection. *Science (1979)* **324**, 1569–1572 (2009).

40. Fröhlich, A. *et al.* IL-21R on T Cells Is Critical for Sustained Functionality and Control of Chronic Viral Infection. *Science (1979)* **324**, 1576–1580 (2009).

41. Yi, J. S., Du, M. & Zajac, A. J. A Vital Role for Interleukin-21 in the Control of a Chronic Viral Infection. *Science (1979)* **324**, 1572–1576 (2009).

42. Provine, N. M. *et al.* Immediate dysfunction of vaccine-elicited CD8 + T cells primed in the absence of CD4 + T cells. *The Journal of Immunology* **197**, 1809–1822 (2016).

43. Gerner, M., Casey, K. A., Kastenmuller, W. & Germain, R. N. Dendritic cell and antigen dispersal landscapes regulate T cell immunity. *Journal of Experimental Medicine* **214**, 3105–3122 (2017).

44. Castellino, F. *et al.* Chemokines enhance immunity by guiding naive CD8+ T cells to sites of CD4+ T cell-dendritic cell interaction. *Nature* **440**, 890–895 (2006).

45. Groom, J. R. *et al.* CXCR3 Chemokine Receptor-Ligand Interactions in the Lymph Node Optimize CD4+T Helper 1 Cell Differentiation. *Immunity* **37**, 1091–1103 (2012).

46. Blank, C. U. *et al.* Defining 'T cell exhaustion'. *Nature Reviews Immunology* **19**, 665–674 (2019).

47. Philip, M. & Schietinger, A. CD8+ T cell differentiation and dysfunction in cancer. *Nat Rev Immunol* **22**, 209–223 (2022).

48. van der Leun, A. M., Thommen, D. S. & Schumacher, T. N. CD8+ T cell states in human cancer: insights from single-cell analysis. *Nat Rev Cancer* **20**, 218–232 (2020).

49. Beltra, J.-C. *et al.* Developmental relationships of four exhausted CD8+ T Cell subsets reveals underlying transcriptional and epigenetic landscape control mechanisms. *Immunity* **52**, 825–841 (2020).

50. Gebhardt, T., Park, S. L. & Parish, I. A. Stem-like exhausted and memory CD8+ T cells in cancer. *Nature Reviews Cancer* **23**, 780–798 (2023).

51. Daniel, B. *et al.* Divergent clonal differentiation trajectories of T cell exhaustion. *Nature Immunology* **23**, 1614–1627 (2022).

52. Li, H. *et al.* Dysfunctional CD8 T cells form a proliferative, dynamically regulated compartment within human melanoma. *Cell* **176**, 775–789 (2019).

53. Prokhnevska, N. *et al.* CD8+ T cell activation in cancer comprises an initial activation phase in lymph nodes followed by effector differentiation within the tumor. *Immunity* **56**, 107–124 (2023).

54. Huang, Q. *et al.* The primordial differentiation of tumor-specific memory CD8+ T cells as bona fide responders to PD-1/PD-L1 blockade in draining lymph nodes. *Cell* **185**, 4049–4066 (2022).

55. Luca, B. A. *et al.* Atlas of clinically distinct cell states and ecosystems across human solid tumors. *Cell* **184**, 5482–5496 (2021).

56. Magen, A. *et al.* Intratumoral dendritic cell–CD4+ T helper cell niches enable CD8+ T cell differentiation following PD-1 blockade in hepatocellular carcinoma. *Nat Med* **29**, 1389–1399 (2023).

57. Schenkel, J. M. & Pauken, K. E. Localization, tissue biology and T cell state — implications for cancer immunotherapy. *Nat Rev Immunol* **23**, 807–823 (2023).

58. Schumacher, T. N. & Thommen, D. S. Tertiary lymphoid structures in cancer. *Science (1979)* **375**, eabf9419 (2022).

59. Busselaar, J., Tian, S., van Eenennaam, H. & Borst, J. Helpless Priming Sends CD8+ T Cells on the Road to Exhaustion. *Front Immunol* **11**, 592569 (2020).

60. Greyer, M. *et al.* T Cell Help Amplifies Innate Signals in CD8+DCs for Optimal CD8+T Cell Priming. *Cell Rep* **14**, 586–597 (2016).

61. Lei, X. *et al.* CD4+ T cells produce IFN-I to license cDC1s for induction of cytotoxic T-cell activity in human tumors. *Cell Mol Immunol* 1–19 (2024) doi:10.1038/s41423-024-01133-1.

62. Pestka, S., Krause, C. D. & Walter, M. R. Interferons, interferon-like cytokines, and their receptors. *Immunological Reviews* **202**, 8–32 (2004).

63. McNab, F., Mayer-Barber, K., Sher, A., Wack, A. & O'Garra, A. Type I interferons in infectious disease. *Nature Reviews Immunology* **15**, 87–103 (2015).

64. Dhanwani, R., Takahashi, M. & Sharma, S. Cytosolic sensing of immuno-stimulatory DNA, the enemy within. *Current Opinion in Immunology* **50**, 82–87 (2018).

65. Woo, S.-R. *et al.* STING-Dependent Cytosolic DNA Sensing Mediates Innate Immune Recognition of Immunogenic Tumors. *Immunity* **41**, 830–842 (2014).

66. Ivashkiv, L. B. & Donlin, L. T. Regulation of type I interferon responses. *Nature Reviews Immunology* **14**, 36–49 (2014).

67. Schneider, W. M., Chevillotte, M. D. & Rice, C. M. Interferon-Stimulated Genes: A Complex Web of Host Defenses. *Annual Review of Immunology* **32**, 513–545 (2014).

68. Konno, H. *et al.* Suppression of STING signaling through epigenetic silencing and missense mutation impedes DNA damage mediated cytokine production. *Oncogene* **37**, 2037–2051 (2018).

69. Kitajima, S. *et al.* Suppression of STING Associated with LKB1 Loss in KRAS-Driven Lung Cancer. *Cancer Discovery* **9**, 34–45 (2019).

70. Wu, S. *et al.* HER2 recruits AKT1 to disrupt STING signalling and suppress antiviral defence and antitumour immunity. *Nature cell biology* **21**, 1027–1040 (2019).

71. Zimmerli, D. *et al.* MYC promotes immune-suppression in triple-negative breast cancer via inhibition of interferon signaling. *Nature Communications* **13**, 6579 (2022).

72. Lamsal, A. *et al.* Opposite and dynamic regulation of the interferon response in metastatic and non-metastatic breast cancer. *Cell Communication and Signaling* **21**, 50 (2023).

73. Linsley, P. S., Speake, C., Whalen, E. & Chaussabel, D. Copy Number Loss of the Interferon Gene Cluster in Melanomas Is Linked to Reduced T Cell Infiltrate and Poor Patient Prognosis. *PLOS ONE* **9**, e109760 (2014).

74. Duong, E. *et al.* Type I interferon activates MHC class I-dressed CD11b+ conventional dendritic cells to promote protective anti-tumor CD8+ T cell immunity. *Immunity* **55**, 308–323 (2022).

75. Andzinski, L. *et al.* Growing tumors induce a local STING dependent Type I IFN response in dendritic cells. *International Journal of Cancer* **139**, 1350–1357 (2016).

76. Schaupp, L. *et al.* Microbiota-Induced Type I Interferons Instruct a Poised Basal State of Dendritic Cells. *Cell* **181**, 1080–1096 (2020).

77. Zhou, B., Lawrence, T. & Liang, Y. The Role of Plasmacytoid Dendritic Cells in Cancers. *Frontiers in Immunology* **12**, 749190 (2021).

78. Sisirak, V. *et al.* Impaired IFN-α production by plasmacytoid dendritic cells favors regulatory T-cell expansion that may contribute to breast cancer progression. *Cancer Research* **72**, 5188–97 (2012).

79. Labidi-Galy, S. I. *et al.* Quantitative and functional alterations of plasmacytoid dendritic cells contribute to immune tolerance in ovarian cancer. *Cancer Research* **71**, 5423–5434 (2011).

80. Sisirak, V. *et al.* Breast cancer-derived transforming growth factor-β and tumor necrosis factor-α compromise interferon-α production by tumor-associated plasmacytoid dendritic cells. *International journal of cancer* **133**, 771–778 (2013).

81. Terra, M. *et al.* Tumor-Derived TGFβ Alters the Ability of Plasmacytoid Dendritic Cells to Respond to Innate Immune Signaling. *Cancer Research* **78**, 3014–3026 (2018).

82. Brewitz, A. *et al.* CD8+T cells orchestrate pDC-XCR1+dendritic cell spatial and functional cooperativity to optimize priming. *Immunity* **46**, 205–219 (2017).

83. Munn, D. H. *et al.* Expression of indoleamine 2,3-dioxygenase by plasmacytoid dendritic cells in tumor-draining lymph nodes. *Journal of Clinical Investigation* **114**, 280–290 (2004).

84. Sharma, M. D. *et al.* Plasmacytoid dendritic cells from mouse tumor-draining lymph nodes directly activate mature Tregs via indoleamine 2,3-dioxygenase. *Journal of Clinical Investigation* **117**, 2570–2582 (2007).

85. Jeremiah, N. *et al.* RELA tunes innate-like interferon I/III responses in human T cells. *The Journal of experimental medicine* **220**, (2023).

86. Schiavoni, G., Mattei, F. & Gabriele, L. Type I Interferons as Stimulators of DC-Mediated Cross-Priming: Impact on Anti-Tumor Response. *Frontiers in Immunology* **4**, (2013).

87. Lorenzi, S. *et al.* Type I IFNs Control Antigen Retention and Survival of CD8α+ Dendritic Cells after Uptake of Tumor Apoptotic Cells Leading to Cross-Priming. *The Journal of Immunology* **186**, 5142–5150 (2011).

88. Simmons, D. P. *et al.* Type I IFN Drives a Distinctive Dendritic Cell Maturation Phenotype That Allows Continued Class II MHC Synthesis and Antigen Processing. *The Journal of Immunology* **188**, 3116–3126 (2012).

89. Grosche, L. *et al.* The CD83 Molecule - An Important Immune Checkpoint. *Frontiers in immunology* **11**, 721 (2020).

90. Ito, T. *et al.* Differential Regulation of Human Blood Dendritic Cell Subsets by IFNs. *The Journal of Immunology* **166**, 2961–2969 (2001).

91. Zhao, Y. *et al.* PD-L1:CD80 Cis-Heterodimer Triggers the Co-stimulatory Receptor CD28 While Repressing the Inhibitory PD-1 and CTLA-4 Pathways. *Immunity* **51**, 1059–1073 (2019).

92. Hui, E. *et al.* T cell costimulatory receptor CD28 is a primary target for PD-1-mediated inhibition. *Science* **355**, 1428–1433 (2017).

93. Oh, S. A. *et al.* PD-L1 expression by dendritic cells is a key regulator of T-cell immunity in cancer. *Nature Cancer* **1**, 681–691 (2020).

94. Bullock, T. N. J. CD40 stimulation as a molecular adjuvant for cancer vaccines and other immunotherapies. *Cellular & Molecular Immunology* **19**, 14–22 (2022).

95. Zheng, H. *et al.* Combination IFNβ and Membrane-Stable CD40L Maximize Tumor Dendritic Cell Activation and Lymph Node Trafficking to Elicit Systemic T-cell Immunity. *Cancer Immunology Research* **11**, 466–485 (2023).

96. McWilliams, J. A., Sanchez, P. J., Haluszczak, C., Gapin, L. & Kedl, R. M. Multiple innate signaling pathways cooperate with CD40 to induce potent, CD70-dependent cellular immunity. *Vaccine* **28**, 1468–1476 (2010).

97. Castellino, F. & Germain, R. N. Chemokine-Guided CD4+ T Cell Help Enhances Generation of IL-6RαhighIL-7Rαhigh Prememory CD8+ T Cells. *The Journal of Immunology* **178**, 778–787 (2007).

98. Kolumam, G. A., Thomas, S., Thompson, L. J., Sprent, J. & Murali-Krishna, K. Type I interferons act directly on CD8 T cells to allow clonal expansion and memory formation in response to viral infection. *The Journal of Experimental Medicine* **202**, 637–650 (2005).

99. Marrack, P., Kappler, J. & Mitchell, T. Type I interferons keep activated T cells alive. *The Journal of experimental medicine* **189**, 521–529 (1999).

100. De Giovanni, M. *et al.* Spatiotemporal regulation of type I interferon expression determines the antiviral polarization of CD4+ T cells. *Nature Immunology* **21**, 321–330 (2020).

101. Jergović, M. *et al.* Infection-induced type I interferons critically modulate the homeostasis and function of CD8+ naïve T cells. *Nature Communications* **12**, 5303 (2021).

102. Curtsinger, J. M., Valenzuela, J. O., Agarwal, P., Lins, D. & Mescher, M. F. Cutting Edge: Type I IFNs Provide a Third Signal to CD8 T Cells to Stimulate Clonal Expansion and Differentiation. *The Journal of Immunology* **174**, 4465–4469 (2005).

103. Lu, C. *et al.* Type I interferon suppresses tumor growth through activating the STAT3-granzyme B pathway in tumor-infiltrating cytotoxic T lymphocytes. *Journal for ImmunoTherapy of Cancer* **7**, 157 (2019).

104. Crouse, J. *et al.* Type I Interferons Protect T Cells against NK Cell Attack Mediated by the Activating Receptor NCR1. *Immunity* **40**, 961–973 (2014).

105. Xu, H. C. *et al.* Type I Interferon Protects Antiviral CD8+ T Cells from NK Cell Cytotoxicity. *Immunity* **40**, 949–960 (2014).

106. Brinkmann, V., Geiger, T., Alkan, S. & Heusser, C. H. Interferon alpha increases the frequency of interferon gamma-producing human CD4+ T cells. *The Journal of experimental medicine* **178**, 1655–1663 (1993).

107. Way, S. S., Havenar-Daughton, C., Kolumam, G. A., Orgun, N. N. & Murali-Krishna, K. IL-12 and Type-I IFN Synergize for IFN-γ Production by CD4 T Cells, Whereas Neither Are Required for IFN-γ Production by CD8 T Cells after Listeria monocytogenes Infection. *The Journal of Immunology* **178**, 4498–4505 (2007).

108. Havenar-Daughton, C., Kolumam, G. A. & Murali-Krishna, K. Cutting Edge: The Direct Action of Type I IFN on CD4 T Cells Is Critical for Sustaining Clonal Expansion in Response to a Viral but Not a Bacterial Infection. *The Journal of Immunology* **176**, 3315–3319 (2006).

109. Pace, L. *et al.* APC Activation by IFN-α Decreases Regulatory T Cell and Enhances Th Cell Functions. *The Journal of Immunology* **184**, 5969–5979 (2010).

110. Gangaplara, A. *et al.* Type I interferon signaling attenuates regulatory T cell function in viral infection and in the tumor microenvironment. *PLOS Pathogens* **14**, e1006985 (2018).

111. Bacher, N. *et al.* Interferon-a suppresses cAMP to disarm human regulatory T cells. *Cancer Research* **73**, 5647–5656 (2013).

112. Nguyen, K. B. *et al.* Critical role for STAT4 activation by type 1 interferons in the interferon-gamma response to viral infection. *Science (New York, N.Y.)* **297**, 2063–2066 (2002).

113. Martín-Fontecha, A. *et al.* Regulation of Dendritic Cell Migration to the Draining Lymph Node: Impact on T Lymphocyte Traffic and Priming. *The Journal of Experimental Medicine* **198**, 615 (2003).

114. Liu, J., Zhang, X., Cheng, Y. & Cao, X. Dendritic cell migration in inflammation and immunity. *Cellular & Molecular Immunology* **18**, 2461–2471 (2021).

115. Webb, L. M. *et al.* Type I interferon is required for T helper (Th) 2 induction by dendritic cells. *The EMBO Journal* **36**, 2404 (2017).

116. Castellino, F. & Germain, R. N. Cooperation between CD4 + and CD8 + T cells: when, where, and how. *Annual Review of Immunology* **24**, 519–540 (2006).

117. Kohli, K., Pillarisetty, V. G. & Kim, T. S. Key chemokines direct migration of immune cells in solid tumors. *Cancer Gene Therapy* **29**, 10–21 (2022).

118. Groom, J. R. & Luster, A. D. CXCR3 ligands: redundant, collaborative and antagonistic functions. *Immunology & Cell Biology* **89**, 207–215 (2011).

119. Dalit, L. *et al.* CXCL11 expressing C57BL/6 mice have intact adaptive immune responses to viral infection. *Immunology & Cell Biology* **100**, 312–322 (2022).

120. Groom, J. R. Regulators of T-cell fate: Integration of cell migration, differentiation and function. *Immunological Reviews* **289**, 101–114 (2019).

121. Sung, J. H. *et al.* Chemokine Guidance of Central Memory T Cells Is Critical for Antiviral Recall Responses in Lymph Nodes. *Cell* **150**, 1249–1263 (2012).

122. Duckworth, B. C. *et al.* Effector and stem-like memory cell fates are imprinted in distinct lymph node niches directed by CXCR3 ligands. *Nature Immunology* **22**, 434–448 (2021).

123. Hickman, H. D. *et al.* CXCR3 Chemokine Receptor Enables Local CD8+ T Cell Migration for the Destruction of Virus-Infected Cells. *Immunity* **42**, 524–537 (2015).

124. Broomfield, B. J. *et al.* (Preprint) Transient inhibition of type I interferon enhances CD8+ T cell stemness and vaccine protection. *bioRxiv* 2024.06.26.600763 (2024) doi:10.1101/2024.06.26.600763.

125. Peperzak, V. *et al.* CD8+ T Cells Produce the Chemokine CXCL10 in Response to CD27/CD70 Costimulation To Promote Generation of the CD8+ Effector T Cell Pool. *The Journal of Immunology* **191**, 3025–3036 (2013).

126. Chen, D. S. & Mellman, I. Oncology meets immunology: the cancer-immunity cycle. *Immunity* **39**, 1–10 (2013).

127. Mellman, I., Chen, D. S., Powles, T. & Turley, S. J. The cancer-immunity cycle: Indication, genotype, and immunotype. *Immunity* **56**, 2188–2205 (2023).

128. Harlin, H. *et al.* Chemokine expression in melanoma metastases associated with CD8 + T-Cell recruitment. *Cancer Research* **69**, 3077–3085 (2009).

129. Klement, J. D. *et al.* Tumor PD-L1 engages myeloid PD-1 to suppress type I interferon to impair cytotoxic T lymphocyte recruitment. *Cancer Cell* **41**, 620–636 (2023).

130. Butsch, R. *et al.* Intratumoral plasmacytoid dendritic cells associate with increased survival in patients with follicular lymphoma. *Leukemia & Lymphoma* **52**, 1230–1238 (2011).

131. Kießler, M. *et al.* Tumor-infiltrating plasmacytoid dendritic cells are associated with survival in human colon cancer. *Journal for ImmunoTherapy of Cancer* **9**, e001813 (2021).

132. Zitvogel, L., Galluzzi, L., Kepp, O., Smyth, M. J. & Kroemer, G. Type I interferons in anticancer immunity. *Nature Reviews Immunology* **15**, 405–414 (2015)

Chapter 7

Mechanism of action of PD-1 receptor/ligand targeted cancer immunotherapy

Jannie Borst[1,2], Julia Busselaar[1,2], Douwe M. T. Bosma[1,2] and Ferry Ossendorp[1]

[1]Department of Immunology;
[2]Oncode Institute, Leiden University Medical Center, Leiden, The Netherlands.

European Journal of Immunology 2021; 51(8): 1911-1920
DOI: 10.1002/eji.202048994

Abstract

Immunotherapy targeting the Programmed Death (PD-1) receptor/ligand (L) "checkpoint" rapidly gains ground in the treatment of many cancer types. To increase treatment scope and efficacy, predictive biomarkers and rational selection of co-treatments is required. To meet these demands, we must understand PD-1 function in detail. We here outline recent insights into the regulation of the $CD8^+$ T cell response by PD-1. The prevailing view has been that PD-(L)1 blockade "reinvigorates" cytotoxic T cells (CTL) that were rendered dysfunctional in the tumor microenvironment (TME). However, this review stresses that tumors continuously communicate with adjacent draining lymph nodes (LNs) and that the PD-1 checkpoint also operates during T cell priming. We clarify the role of the PD-1/ligand system at the T cell/dendritic cell (DC) interface, where it regulates T cell receptor (TCR) signaling and CD28 costimulation and thus controls activation of tumor-specific T cells. We also highlight the importance of $CD4^+$ T-cell help during priming, which allows DCs to provide other costimulatory and cytokine signals required for optimal CTL differentiation and likely avoidance of a dysfunctional state. Therefore, we pose that PD-(L)1 blockade should exploit LN function and be combined with "help" signals to optimize CTL efficacy.

Introduction

Immunotherapy is becoming the fourth pillar in cancer treatment next to surgery, chemotherapy and radiotherapy. Its aim is to activate a tumor-specific CTL response that eradicates all tumor mass, regardless of metastatic spread. CTL responses generally are polyclonal, harboring T cells with different antigenic specificities. Therefore, immunotherapy can be effective against genetically heterogeneous, disseminated tumors, where (targeted) chemotherapies fail. Nevertheless, tumors can display inherent or acquired resistance to immunotherapy[1].

This review focuses on the current mainstay of cancer immunotherapy in the clinic: monoclonal antibodies (mAbs) that block the coinhibitory receptor PD-1 or its ligand PD-L1[1,2]. This therapy proved to evoke durable responses in a proportion of patients with stage IV melanoma, non-small cell lung cancer (NSCLC) and mismatch repair-deficient colon cancer[2]. These cancer types all have a high tumor mutational burden (TMB) and consequently express neoantigens[3]. Such cancers potentially evoke a T cell response and then present as "T cell inflamed" or "hot" tumors with a T cell-rich TME with an interferon (IFN)-driven signature[4]. The dramatic and long-lasting responses observed in previously untreatable cancer patients has led to application of PD-(L)1-targeted therapy in earlier disease stages. In recent years, neo-adjuvant immunotherapy, prior to surgical resection of the primary tumor has produced remarkable responses, also in cancers that were previously not recognized as antigenic[5]. In neo-adjuvant treatment, the untouched tumor serves as a reservoir of tumor antigens, that can apparently be tapped into to generate systemic, anti-tumor CTL responses by PD-(L)1 blockade.

Since PD-(L)1 targeted immunotherapy is successful in only a fraction of patients, and moreover is costly and may be accompanied by immune-related adverse events[6], predictive biomarkers are urgently needed. At present, key potential biomarkers are neoantigen load, T cell infiltrate, PD-L1 expression and/or an IFNg signature in the TME[3,7]. A recent meta-analysis indicates that high TMB only predicts responsiveness to PD-(L)1 blockade in about 25% of all cancers types where high TMB correlates with $CD8^+$ T cell infiltration of the tumor. In a wide variety of other cancer types including triple negative breast cancer and prostate cancer, high TMB did not correlate with $CD8^+$ T cell infiltration and overall response rates to PD-(L)1 blockade[8]. These data clearly indicate that presence of recognizable antigens in the tumor does not equate immunogenicity and point to important additional requirements for evoking an effective anti-tumor $CD8^+$ T cell response, such as dendritic cell (DC) activation and CTL functionality in terms of tumor penetration, as well as undefined requirements for $CD8^+$ T cells to respond to PD-(L)1-targeted therapy.

In addition, PD-(L)1 targeting needs to be combined with other approaches to increase efficacy. There are hundreds of clinical trials ongoing that test combinations with radiotherapy, conventional or targeted anti-cancer drugs, or antibodies to other coinhibitory or costimulatory

receptors. To select the most promising combination therapies, we need maximal information on the mechanism of action of PD-(L)1 targeted therapy. Recently, several discoveries have been made regarding molecular and cellular mechanisms underlying the response to PD-(L)1 checkpoint blockade, which are very important for research into biomarkers and candidate targets for combination therapy. We will present this new information and combine it with new data on the mechanism of CTL priming into a comprehensive model of anti-PD-(L)1 action that can help guide further translational research and clinical decision making.

The CD8$^+$ T cell population that is targeted by PD-(L)1 inhibition

In chronic infection and cancer, CD8$^+$ T cell populations have been defined that express PD-1 and other coinhibitory receptors and display impaired proliferative and cytotoxic capacities. Classically, cells with this phenotype have been termed "exhausted" and PD-(L)1 targeted immunotherapy was thought to help "reinvigorate" these exhausted cells[9,10]. However, the view on T cell exhaustion has dramatically changed in recent years, based on transcriptome data and lineage tracing that makes use of TCR sequences as clonal marker. It is now established that exhausted CD8$^+$ T cells are not derived from previously active effector cells. Rather, CD8$^+$ T cells can attain a reversible, "predysfunctional" state early after infection or tumorigenesis that may progress into an irreversible, terminally exhausted state[10,11] (Figure 1). There are different types of nomenclature for the predysfunctional state of CD8$^+$ T cells and different markers, as outlined in, e.g.[12]. The common features of this state are deficient effector functionality, expression of PD-1 and other coinhibitory receptors and, as recently recognized, expression of the transcription factor TCF-1[11,12].

In chronic infection with lymphocytic choriomeningitis virus (LCMV), the predysfunctional pool of virus-specific CD8$^+$ T cells proved to rely on TCF-1 and to coexpress PD-1, CXCR5 and SLAMF6[13,14]. This population proliferates and constantly replenishes a short-lived pool of CD8$^+$ T cells that are truly exhausted, i.e. irreversibly, epigenetically fixed in a non-functional state[15-17]. Also in mouse models of cancer, predysfunctional CD8$^+$ T cells were found in the TME that could become irreversibly exhausted[16,18,19]. Likewise, in the TME of various human cancers, TCR tracing argues for progressive differentiation of predysfunctional into terminally exhausted CD8$^+$ T cells[20-25]. In human kidney, prostate and bladder tumors, TCF-1$^+$ predysfunctional CD8$^+$ T cells were found in proximity of MHC class II$^+$, CD11c$^+$ cells, most likely DCs, denoting cellular niches that resembled T cell zones in secondary lymphoid organs. The presence of such niches in the TME positively correlated with long term patient survival after surgery[24].

Importantly, PD-(L)1 blockade was recently found to reinvigorate predysfunctional, but not terminally exhausted CD8$^+$ T cells. Predysfunctional cells respond to PD-(L)1 blockade by proliferation. This was demonstrated in mouse models of chronic LCMV infection[13,26,27] and

cancer[16,28,29]. Moreover, in melanoma patients, an increased fraction of TCF-1$^+$ predysfunctional CD8$^+$ tumor-infiltrating lymphocytes is a positive predictor for a clinical response to PD-1 targeted therapy[16,30]. It is now clear that predysfunctional CD8$^+$ T cells are in an early stage of CTL effector differentiation and still have the opportunity to proliferate and further differentiate. They do this to a certain extent upon PD-1 blockade[11,12].

PD-L1 on DCs is important for the response to PD-(L)1 targeted therapy

Initially, a reductionist model was prevalent in the cancer immunotherapy field, in which PD-1 on the CTL finds its ligand on tumor cells and thus imposes a brake on tumor cell killing in the TME (**Figure 1**). This view was likely inspired by the landmark study of Iwai *et al.* who discovered that deliberate PD-L1 expression in tumor cells inhibits anti-tumor immunity[31]. PD-1 has two ligands, PD-L1 and PD-L2, with distinct expression patterns. PD-L1 is expressed on lymphocytes and myeloid cells and is upregulated under conditions of immune activation, e.g. by type I and type II IFN. In addition, PD-L1 is expressed on non-hematopoietic cells, such as vascular endothelium and pancreatic islands. PD-L2 expression is more restricted and found on activated DCs, macrophages, mast cells and peritoneal B1 cells[32]. Furthermore, both PD-L1 and PD-L2 are expressed on placental trophoblasts, indicating an important role in fetal tolerance[33]. PD-1 sets signaling thresholds during T cell selection in the thymus and plays a role in peripheral tolerance, as judged by the auto-immune phenotypes of genetically deficient mice[32].

Due to the reductionist model, clinical studies initially focused on PD-L1 expression on tumor cells as biomarker for PD-(L)1 targeted therapy. However, in early phase I studies with anti-PD-L1 mAb Atezolizumab (MPDL3280A), it was already noted that clinical responses in multiple cancer types correlated with expression of PD-L1 on either tumor cells, or tumor-infiltrating immune cells[34]. Immunohistochemistry identified three typical expression patterns of PD-L1 in human cancer with expression on either tumor cells or immune cells, or both[35]. Mechanistic studies were performed in mouse models to assess the relative importance of PD-L1 expression on either cell type. For this purpose, predominant tumor models are s.c. implanted MC38 or CT26 colon carcinoma cells that have a high mutational load, are “hot” and responsive to PD-(L)1 targeted therapy. Genetic deletion of PD-L1 in tumor cells and/or in the background of the host proved that spontaneous tumor rejection was suppressed by PD-L1 in both compartments[35]. Strikingly, the response to PD-L1 targeted therapy was not affected by genetic deletion of PD-L1 in MC38 tumor cells, while it was abolished by PD-L1 deletion in the hematopoietic compartment of the host[36,37]. In agreement, another group found that effective anti-PD-L1 therapy required PD-L1 expression by the host in MC38, 1D8 and B16-F10 tumor models[38]. Genetic deletion identified PD-L1 on DCs (CD11c$^+$ cells) as critical for the response of MC38 to anti-PD-L1 therapy[39]. These findings were refined by comparing the therapeutic response to PD-

L1-deficient MC38 cells in mice that were PD-L1 deficient in either conventional (c)DCs (Clec9a$^+$ cells) or macrophages (LysM$^+$ cells). PD-L1 on cDCs proved most important for the response to anti-PD-L1 therapy, even though MC38 tumors harbor large amounts of PD-L1$^+$ macrophages[40]. In human melanoma, a correlation was suggested between PD-L1 expression on DCs and the response to PD-L1 targeted therapy[38].

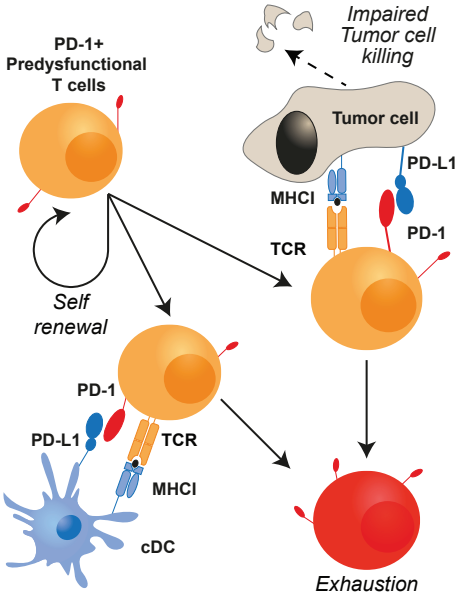

Figure 1. Predysfunctional PD-1$^+$ CD8$^+$ T cells in the TME. In the TME, a pool of PD-1$^+$ predysfunctional CD8$^+$ T cells exists that undergoes self-renewal. PD-1 on the predysfunctional CD8$^+$ T cells can interact with PD-L1 on tumor cells or on cDCs. These interactions impair tumor cell killing, limiting tumor clearance and antigen availability. Furthermore, these interactions help drive the cells into an irreversibly exhausted state. Color codes: grey = tumor cell; blue = cDC; orange = predysfunctional CD8$^+$ T cell; red = exhausted CD8$^+$ T cell.

The importance of cDCs, particularly cDC1s, in the response to PD-(L)1 targeting therapy is supported by distinct lines of investigation. In B16 mouse melanoma, the modest therapeutic effect of anti-PD-L1 mAb was lost upon genetic elimination of cDC1s, i.e. in a *Batf3*$^{-/-}$ background. In the MC38 tumor model, response to anti-PD-1 treatment was upon genetic elimination of cDC1s, i.e., in a *Batf3*$^{-/-}$ background[41]. In B16 mouse melanoma, the modest therapeutic effect of anti-PD-L1 mAB also depended on *Batf3* proficiency. Promoting the generation of DCs from progenitors by Flt3 ligand together with DC-activating compound poly-IC, synergized with anti-PD-L1 therapy[42]. Moreover, anti-PD-1 treatment was found to induce IL-12b production by tumor-resident cDC1s, which proved important for tumor regression. The cDC1s made IL-12b in response to IFNg that was produced by other cells in the TME upon anti-PD-1 therapy. Direct application of IL-12 into the tumor increased IFNg production, suggesting effector T cell and/or

NK cell activation. The authors also present data from melanoma patients that were treated with ImmunoPulse tavokinogene telseplasmid, an IL-12 encoding plasmid that was electroporated into melanoma lesions on the skin. IL-12 delivery upregulated multiple genes encoding CTL effector molecules, supporting the idea that this important DC-derived cytokine can promote CTL function in the TME[43]. CXCL9 production by intratumoral cDC1s has also been implicated in the response to anti-PD-1 therapy in the MC38 model, with the data supporting a model in which CXCL9 facilitates communication of these cDC1s with $CD8^+$ T cells in the tumor. CXCL9 levels in blood positively correlated with the response to anti-PD-1 in a small cohort of melanoma patients[44]. In renal cell carcinoma and NSCLC patients treated with Atezolizumab, a cumulative expression score based on cDC1 signature genes *XCR1, BATF3, IRF8, FLT3* in the tumor was associated with improved survival, also arguing in favor of a role for cDC1s in the response to PD-(L)1 targeted therapy[45]. The cumulative data change the reductionist model, highlighting that the response to PD-(L)1 targeted therapy primarily depends on altered T cell/cDC) communication (Figure 1). The special role of the cDC1 in invigorating the anti-tumor $CD8^+$ T cell response upon anti-PD-(L)1 treatment ties in with its well-documented specialization in antigen cross-presentation and cross-priming of $CD8^+$ T cells, which is key for anti-tumor immunity[46].

PD-(L)1 targeted therapy impacts T cell priming

In the cancer immunotherapy field, the prevailing view has been that PD-(L)1 blockade acts within the TME. However, it has long been known that PD-1 controls $CD8^+$ T cell priming[47]. Earlier studies showed that PD-1 is upregulated on T cells within 24 hours after initial activation[48] and that PD-1 ligands are expressed on activated DCs[32]. In fact, the original study that defined PD-1 function already demonstrated that PD-L1 is expressed on APCs and that PD-1 inhibits both TCR- and CD28 signals[49]. PD-1 signaling was shown to limit the TCR-driven motility arrest of $CD4^+$ T cells on cognate DC[50], which can be attributed to a later demonstrated negative impact on the formation of stable synaptic contacts needed for effector T-cell differentiation[51]. In agreement, in a mouse model of acute virus infection PD-1 constrained effector differentiation of $CD8^+$ T cells during priming[52]. Clinical data pointed out that PD-(L)1 targeted immunotherapy can also be effective in patients that do not express PD-L1 in the TME[53]. Collectively, these data illuminate that PD-(L)1 blockade may facilitate *de novo* priming of (tumor-specific) CTLs in tumor-draining lymph nodes (tdLNs).

Indeed, in the MC38 tumor model, newly primed $CD8^+$ T cells were found to contribute to the treatment response. Tang *et al*. established that s.c. implantation of MC38 cells raises an IFNg-producing T cell response in the tdLNs. Entrapment of newly primed T cells in the tdLN with the drug FTY720 prohibited the response to anti-PD-L1 therapy[36]. Extending these findings, Fransen et al. showed that s.c. implantation of MC38 cells leads to increased PD-L1 expression on myeloid cells in tdLNs, but not in non-tdLNs. It also leads to $CD8^+$ T cell priming in the tdLNs, which is

increased by PD-1 blockade. Either FTY720 treatment, or surgical resection of the tdLNs abrogated tumor infiltration by newly primed CD8$^+$ T cells and anti-PD-1 mediated tumor control[54]. These studies clarify that T-cell inflamed tumors communicate with their tdLNs to invite new T cell priming, which is constrained by the PD-(L)1 checkpoint. The link between these compartments is formed by migratory cDCs that deliver tumor antigen and signals that dictate the T cell response (Figure 2). Participation of the tdLNs in the response to PD-L1 blockade was also demonstrated in a mouse model with mesothelioma tumor cell lines that were implanted intrapleurally. This tumor type was shown to raise predysfunctional ("progenitor exhausted") PD-1$^+$ CD4$^+$ and CD8$^+$ T cells in mediastinal tdLNs. Selective inhibition of PD-L1 in tdLNs by low dose, intrapleural injection of the mAb increased the frequency and proliferation of intratumoral CD8$^+$ T cells and mediated tumor control, which relied on PD-L1 expression in the tdLN by cDC1s and cDC2s, but not macrophages. Thereby, this study supports the concept that PD-(L)1 blockade promotes T cell priming. The authors furthermore suggest that in human stage II melanoma, PD-1/PD-L1 proximity in tdLNs, rather than in the tumor, is a prognosticator for early distant recurrence following surgery[55].

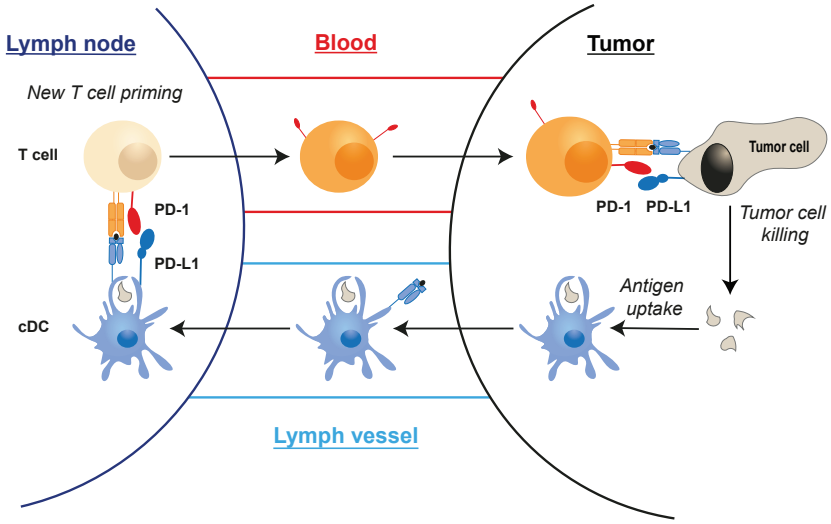

Figure 2. The PD-1 checkpoint in T cell priming and effector stages. Upon killing of tumor cells, antigen can be taken up by cDCs, and subsequently be transported via the lymph to tdLNs. Here, the cDCs prime new T cells, which leave the tdLN via the blood and enter the tumor. If these cells are properly differentiated into effector CTLs, they can kill more tumor cells, increasing antigen availability. However, interactions between PD-1 and its ligands may limit efficacy of CTLs by limiting their priming and activity in the TME. Color codes: beige = naïve CD8$^+$ T cell; blue = cDC; orange = predysfunctional CD8$^+$ T cell; grey = tumor cell.

These findings imply that the clinical response to PD-(L)1 targeted therapy may be visualized in the peripheral blood, where after therapy certain newly primed T cell clones should be expanded. Indeed, in a cohort of 29 advanced stage NSCLC patients, 70% responded by an increase in dividing (Ki-67$^+$) PD-1$^+$ CD8$^+$ T cells in the blood upon PD-1-targeted therapy[56]. More detailed information

has recently come from TCR-based tracing of T cell clones. In a neo-adjuvant trial with anti-PD-1 treatment of stage II NSCLC patients, TCR sequencing was performed on serial samples of peripheral blood, as well on tumor and normal lung samples at the endpoint. Interestingly, high intratumoral TCR clonality was associated with reduced residual tumor mass at time of surgery and tumor responsiveness was correlated to high TCR clonality, with clonotypes shared between tumor and peripheral blood[57]. In basal cell carcinoma, single cell transcriptomics coupled to TCR sequencing revealed that particularly in the intratumoral $CD8^+$ T cell population, changes in TCR repertoire took place upon PD-1 targeted therapy. T cell clones that were present in the TME pre-treatment and displayed a terminally exhausted phenotype did not contribute to the response. Also, the main responders were not $TCF\text{-}1^+$ predysfunctional $CD8^+$ T cells that were present pre-treatment, but new clonotypes with an exhausted phenotype that were found in the tumor post-treatment. These data suggest that upon PD-1 targeted therapy, newly primed $CD8^+$ T cells entered into the tumor and turned into exhausted cells in the TME[58]. An independent analysis of the same data lent support to this conclusion and emphasized the sharing of T cell clones between tumor and blood [59]. Together, these data change the view on the mode of action of PD-(L)1 targeted therapy: Rather than acting exclusively in the TME by "reinvigorating" tumor-resident predysfunctional $CD8^+$ T cells, it can instead or in addition, promote $CD8^+$ T cell priming in tdLNs[60].

PD-1 checkpoint controls TCR and CD28 signaling during T cell-DC communication

CTLA-4 and PD-1 are both termed "checkpoints" for T cell activation and considered coinhibitory receptors, but their mechanisms of action are distinct. CTLA-4's exclusive function is to inhibit CD28 costimulation of conventional T cells (Tconvs). CTLA-4 is constitutively expressed on regulatory $CD4^+$ T cells (Tregs) and inducibly expressed on activated $CD4^+$ and $CD8^+$ Tconvs. CTLA-4 inhibits CD28 costimulation of Tconvs by binding and downregulating the CD28 ligands CD80 and/or CD86 from the plasma membrane of DCs by transendocytosis[61]. Tregs attenuate in this way the costimulatory state of migratory DCs that present autoantigens. CTLA-4-deficient mice develop dramatic auto-immune symptoms, even under germ-free conditions, supporting that CTLA-4 is essential to maintain peripheral tolerance to self-antigen. Deletion of CTLA-4 from Tregs likewise precipitates autoimmunity[62]. Autoimmune symptoms resulting from PD-1 deficiency are much milder, alluding to the distinct functions of CTLA-4 and PD-1[32,33].

In terms of signal transduction, CTLA-4 and PD-1 are very different. CTLA-4 has tyrosines in its cytoplasmic tail that were long thought to represent immunoreceptor tyrosine-based inhibitory motifs (ITIMs). However, CTLA-4 does not have bona fide ITIMs, but internalization motifs that allow rapid endocytosis from the plasma membrane. CTLA-4 is constitutively recycled from the plasma membrane, befitting its role in transendocytosis of CD80 and CD86[61]. The cytoplasmic tail

of PD-1 on the other hand, contains two well-defined ITIMs that upon tyrosine phosphorylation by Src family kinases recruit the tyrosine phosphatase SHP-2[51,63-66]. Both the TCR/CD3 complex and CD28 activate the T cell by virtue of tyrosine kinases that phosphorylate many signal transduction molecules. By bringing the SHP-2 tyrosine phosphatase in proximity, PD-1 negates these signals[51]. In the cancer immunotherapy field, PD-1 was largely viewed as an inhibitor of the TCR/CD3 signal, but reinvigoration of dysfunctional $CD8^+$ T cells by PD-1 blockade proved to be critically dependent on CD28[67]. In the same year, a biochemical study using reconstituted lipid vesicles revealed that the PD-1/SHP-2 complex dephosphorylates CD28 with preference over CD3 components[63]. Subsequently, the picture was completed by mass spectrometry studies showing that in the cellular context, PD-1 prefers SHP-2 over SHP-1 but can function with either and dephosphorylates CD28, and the LAT and SLP72 signaling adaptors[64]. In conclusion, CTLA-4 exclusively inhibits CD28 costimulation, while PD-1 inhibits both TCR/CD3 signaling and CD28 costimulation (Figure 3A). It follows from these findings that both "checkpoints" can act in priming and effector phases of the T cell response, particularly at the T cell/DC interface. It still needs to be resolved how combined inhibition of both "checkpoints" can synergize in stimulating the T cell response[68].

Recent data add another layer of complexity on the mode of action of PD-(L)1 inhibition. It turns out that PD-L1 can bind CD80 on the membrane of the same cell (*in cis*)[69]. This ability to heterodimerize is unique to the CD80;PD-L1 pair and not shared with CD86 and/or PD-L2[70,71]. The CD80;PD-L1 dimer cannot bind to PD-1, nor can it be downregulated by CTLA-4[70,71]. Strikingly, the CD80;PD-L1 heterodimer can bind to CD28 and as a consequence, it induces T cell costimulation while negating coinhibition (Figure 3B). Primary $CD4^+$ and $CD8^+$ T cells were shown to escape from PD-1-mediated inhibition by virtue of CD80;PD-L1 interactions in a study comparing wild-type DCs and those with mutations disrupting the CD80;PD-L1 interaction. Accordingly, mice with the same mutations had an attenuated anti-tumor response upon therapeutic vaccination[71]. Reportedly, activated cDC1s and cDC2s express PD-L1[39,45,71]. At first glance, this contradicts the role of activated cDCs in T cell priming, but coexpression of PD-L1 with CD80 will allow their heterodimerization, which favors CD28 costimulation. These new insights emphasize that we need to pay more attention to the expression patterns of CD80, CD86, PD-L1 and PD-L2 on cDC1s and cDC2s, since these dictate the ability of cDCs to costimulate Tconvs via CD28 and to relieve CTLA-4-based suppression by Tregs. We also need to reconsider the potential mechanisms underlying synergistic effects of combined CTLA-4 and PD-(L)1 blockade in the clinic[68] and be aware that clinical targeting of PD-1 or PD-L1 may not have the same effects on the T cell response.

It is also very important to consider the effects of checkpoint inhibition on Treg responses. It is well established that PD-1 engagement on Tconvs can drive their conversion into peripherally induced (p)Tregs[72] and in this context, PD-1 blockade is expected to promote Tconv responses. However, it has recently been established in mice genetically deficient for PD-1 in Foxp3-expressing cells,

that PD-1 constrains Treg activation, proliferation and suppressive activity, at least in part via the PKB / AKT pathway[73]. This finding indicates that clinical PD-1 blockade may lead to increased Treg-mediated suppression of Tconv responses. Accordingly, a pioneering study in human NSCLC and gastric cancer combined with work in the MC38 mouse model confirms these findings and provides evidence that it is the ratio of PD-1$^+$ Tconvs versus PD-1$^+$ Tregs in the TME that predicts responsiveness to PD-(L)1 blockade rather than the frequency of PD-1$^+$ Tconvs as such[74].

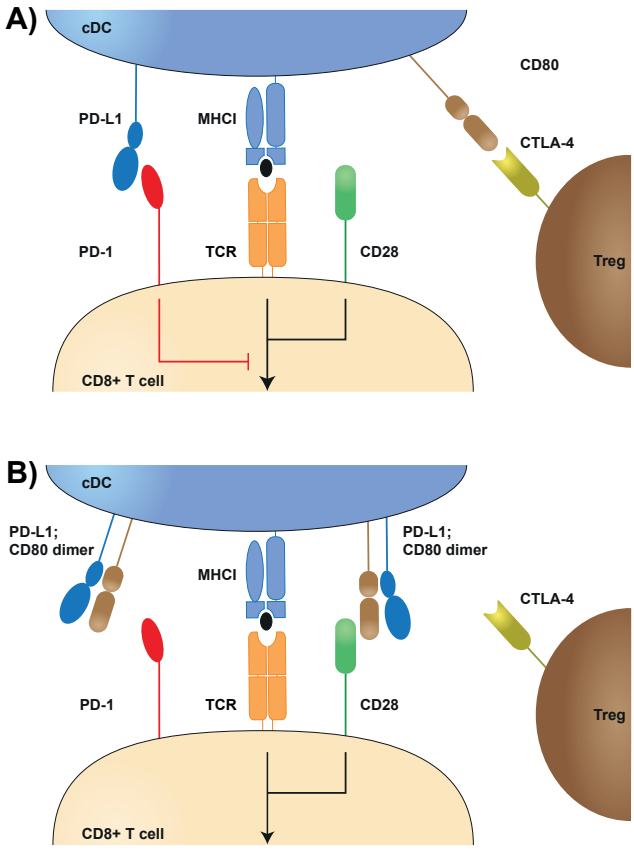

Figure 3. Impact of PD-L1 on TCR/CD28 signaling at the T cell/DC interface. A) PD-L1 expressed on activated DCs binds to PD-1 on CD8$^+$ T cells, thereby inhibiting the TCR/CD28 signal during priming. Costimulation via CD28 is also impaired by the CTLA-4 mediated downregulation of its ligand CD80. B) When PD-L1 forms a heterodimer with CD80 on the DC cell surface, signaling through PD-1 is abrogated, but signaling through CD28 can still take place. Moreover, the CD80;PD-L1 dimer can no longer be downregulated by CTLA-4, resulting in an increase of CD28 costimulation.

The PD-1 checkpoint in two-step priming

In this section, we would like to present a model that clarifies how reinvigoration of predysfunctional tumor-specific CD8$^+$ T cells by PD-(L)1 blockade links to PD-(L)1 checkpoint function in T cell priming. We have recently provided evidence that predysfunctional CD8$^+$ T cells likely have been primed in absence of CD4$^+$ T-cell help[12]. CD4$^+$ T-cell help is essential for full differentiation of CD8$^+$ T cells into short-lived effector and effector/memory cells[75-77]. We discovered that predysfunctional CD8$^+$ T cells in mouse models of chronic LCMV infection and cancer have a "helpless" gene expression signature[12], as we defined in CD8$^+$ T cells that were primed by vaccination in absence of CD4$^+$ T-cell help[75]. An independent study supports this notion[78]. In our vaccination model, helpless CD8$^+$ T cells displayed the typical predysfunctional phenotype and had limited efficacy against a s.c. implanted tumor, due to reduced cytotoxic and migratory potential and expression of PD-1, BTLA and other coinhibitory receptors. Our hypothesis based on these data is that CD8$^+$ T cells primed in absence of CD4$^+$ T-cell help have not yet completed their effector differentiation pathway and therefore present as "predysfunctional". However, they are not exhausted and can still complete their effector differentiation pathway, provided that they receive the stimuli that equate "help"[12] (Figure 4).

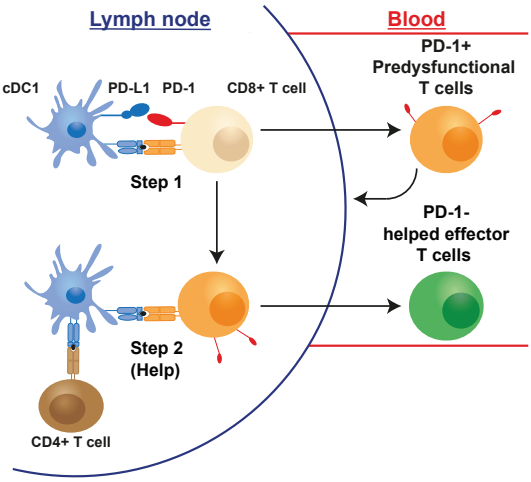

Figure 4. Proposed connection between help, optimal CTL priming and the PD-1 checkpoint. Naïve CD8$^+$ T cells are activated by (migratory) cDC1s during the first step of priming. The PD-1 axis inhibits TCR/CD28 signaling and thereby prevents clonal expansion. CD8$^+$ T cells may leave the LN at this point, but are in an early stage of effector differentiation with limited cytotoxic and migratory abilities and expression of PD-1 and other coinhibitory receptors. We propose that this "helpless" state equals the "predysfunctional" state identified in many studies. When appropriate activating signals are available, such as type I IFN, the CD8$^+$ T cells undergo a second step of priming wherein help is delivered by CD4$^+$ T cells via LN-resident cDC1s. This leads to optimal effector differentiation of CD8$^+$ T cells into potent CTLs that lack PD-1 expression. Color codes: beige = naïve CD8$^+$ T cell; blue = cDC; orange = unhelped/predysfunctional CD8$^+$ T cell; brown = CD4$^+$ T helper cell; green = optimally primed/helped CTL.

To explain how helpless/predysfunctional CD8$^+$ T cells may emerge from the priming process in LNs, we refer to recent insights from intravital imaging. In secondary lymphoid organs, individual T cells move from one DC to the other, until they are arrested by a TCR-mediated "stop" signal on the DC that presents their cognate antigen. Among DC subsets, migratory cDCs deliver self-antigens at steady state and may deliver foreign antigen from infected or transformed tissue, while LN-resident cDCs pick up antigen locally. Data argue that CD4$^+$ and CD8$^+$ T cells are initially activated independent from each other by migratory cDC1 and cDC2 subsets. After this first step of priming, a second step of priming takes place on LN-resident cDC1s[79-81]. In this interaction, CD4$^+$ T-cell help for CD8$^+$ T cells is delivered[77]. Upon cognate contact with the CD4$^+$ T cell, the LN-resident cDC1 gains the ability to optimize the CD8$^+$ T cell response, in terms of clonal expansion, effector and effector/memory differentiation. Key signals include interaction between CD40 ligand on the CD4$^+$ T cell and CD40 on the cDC1, which promotes its expression of IL-12, CD80/CD86 and CD70. CD27 costimulation of CD8$^+$ T cells via CD70 is a very important effector pathway of CD4$^+$ T-cell help[75,77]. Whether CD4$^+$ T-cell help is delivered depends on chemokines such as XCL-1 that bring the cells together and on type I IFN, that is likely delivered by plasmacytoid DCs[82]. Type I IFN has long been known to promote CTL responses and optimizes the cross-presentation and costimulatory ability of cDC1s[83].

We have found that CD8$^+$ T cells primed in absence of CD4$^+$ T-cell help can go from the LN into the circulation, but then display the helpless/dysfunctional phenotype that includes PD-1 cell surface expression. In contrast, cells that have received help have downregulated PD-1[75]. Thus, we propose a model in which the PD-1 axis operates transiently during T cell priming to inhibit CD28 costimulation and resulting T cell clonal expansion, likely at the first step of priming. It is intuitive that clonal expansion should only take place optimally after the second step of priming, since in this way, only a limited number of lymph node resident cDC1s are needed to relay CD4$^+$ T-cell help. In tumor settings, PD-1 expression on CD8$^+$ T cells in the blood enriches for tumor-specificity [84], in line with the idea that tumors likely prime helpless CTLs, because essential signals such as activated CD4$^+$ T cells and/or type I IFN may be lacking[83].

Several preclinical studies in chronic LCMV infection and tumor models have shown that helpless/predysfunctional PD1$^+$ CD8 T cells are the population that is reinvigorated by PD-(L)1 blockade[13,16,26]. In line with the idea that they receive CD28 costimulation, reinvigorated cells undergo proliferation and transiently gain effector functions that can contribute to tumor control, but they do not undergo full CTL effector differentiation. Instead, they retain expression of inhibitory receptors and eventually turn into terminally exhausted cells[16,85]. At present, there is no data that argue in favor of a transition of predysfunctional CD8$^+$ T cells into terminally differentiated, short-lived effector CTL upon PD-(L)1 targeting therapy[11]. Reinvigoration likely takes place on migratory cDC1s that present antigen from the tumor. The interaction can take place within the TME, and/or in the tdLN (Figure 5).

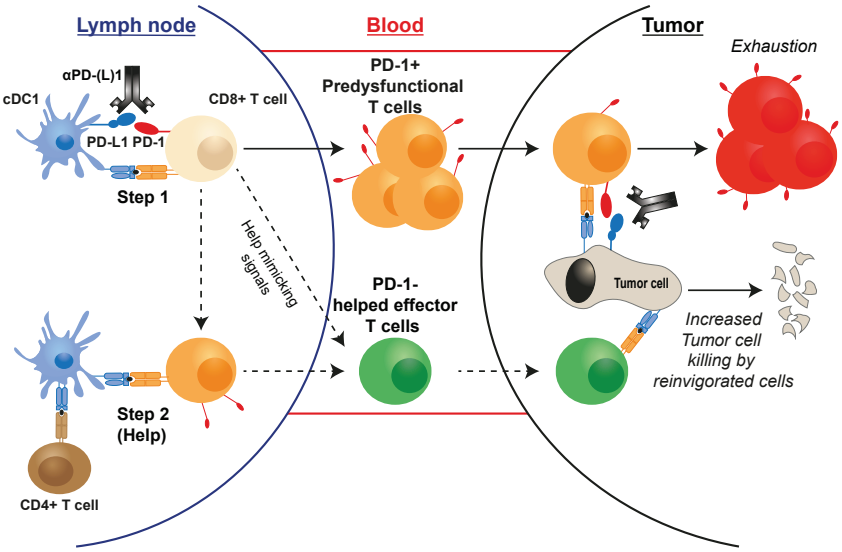

Figure 5. Proposed effects of PD-(L)1 targeted therapy in tdLNs and tumor. The effects of PD-(L)1 blockade are threefold: 1) They enable CD28 signaling during priming of naïve (tumor-specific) T cells, inducing proliferation of these cells. However, PD-(L)1 blockade alone is not sufficient to allow the second step of priming in which help signals are delivered (dotted lines). Therefore, 2) PD-(L)1 blockade in the tdLN increases the pool of (tumor-specific) predysfunctional T cells. These cells will exit the tdLN and potentially reach the tumor, even though they have limited migratory ability. 3) In the TME, PD-(L)1 blockade will also allow predysfunctional T cells to proliferate and transiently improve their cytotoxic capacities. However, ultimately these "reinvigorated" T cells will become exhausted. When "help mimicking" signals such as CD40 or CD27 agonism are added to PD-(L)1 blockade, the second step of priming will be recapitulated and helped effector CTLs will be generated that lack PD-1 expression and can more effectively kill the tumor cells. $CD4^+$ T-cell help (or its replacing signals) also allow for generation of CTL memory. Color codes: beige = naïve $CD8^+$ T cell; blue = cDC; orange = unhelped/predysfunctional $CD8^+$ T cell; brown = $CD4^+$ T helper cell; green = optimally primed/helped CTL; red = exhausted $CD8^+$ T cell; grey = tumor cell.

Conclusions and future perspectives

The remarkable effects of PD-(L)1 checkpoint blockade have put immunotherapy firmly on the map as a treatment modality for cancers that cannot be controlled by surgery or radiotherapy alone. As we reviewed here, PD-(L)1 blockade transiently activates predysfunctional $CD8^+$ T cells by enabling TCR signaling and CD28 costimulation at the interface with cDCs, either in the tumor or in the tdLNs. These new insights argue that sparing tdLNs during surgery is important in adjuvant immunotherapy. The recent finding that PD-(L)1 blockade can likewise promote Treg responses, brings Tregs into the equation when considering effects of PD-1 blockade on T cell priming and effector stages. Furthermore, we propose that the restoration of CTL function by PD-(L)1 blockade is temporary and incomplete, because other essential costimulatory and cytokine signals are still lacking. For adequate display of CTL effector function and generation of memory, the full spectrum

of $CD4^+$ T-cell help signals should be provided to predysfunctional $CD8^+$ T cells (Figure 5). $CD4^+$ T-cell help signals can be replaced by combining PD-(L)1 blockade with CD27 agonism[77,86-88]. Alternatively, CD40 agonism will instruct cDCs to provide all required costimulatory signals and cytokines[77]. In addition, enlarging the pool of cDC1s by the differentiation factor Flt3L, in combination with DC activation signals can be a powerful approach to break anti-PD-1 resistance[89]. A constraint in all of these approaches may be that tumors prime strong Treg responses, which reduce the ability of tdLN to prime tumor-specific conventional T cells[90,91]. Detailed knowledge on the division of labor between CD80, CD86, PD-L1 and PD-L2 and their impact on Treg versus Tconv priming should help to allow for new interventions that do not break tolerance to self-antigen but do overrule Treg activity and promote responses to tumor antigens.

Acknowledgements

We thank Elselien Frijlink for helpful discussions. This work was financially supported by grant 11079 from the Dutch Cancer Society (KWF) to Jannie Borst.

Author contributions

Jannie Borst (ORCID iD 0000-0002-8043-5009) wrote the paper, Julia Busselaar (ORCID iD 0000-0003-2402-4245) provided insights for text and figures and edited the paper, Douwe M. T. Bosma (ORCID iD 0000-0002-3500-8649) made the figures and edited the paper, Ferry Ossendorp (ORCID iD 0000-0001-9730-7954) provided insights and edited the paper.

Competing Interests

The authors declare no conflicts of interest.

References

1. Sharma, P., Hu-Lieskovan, S., Wargo, J. A. & Ribas, A. Primary, Adaptive, and Acquired Resistance to Cancer Immunotherapy. *Cell* **168**, 707–723 (2017).
2. Ribas, A. & Wolchok, J. D. Cancer immunotherapy using checkpoint blockade. *Science* **359**, 1350–1355 (2018).
3. Schumacher, T. N. & Schreiber, R. D. Neoantigens in cancer immunotherapy. *Science* **348**, 69–74 (2015).
4. Palucka, A. K. & Coussens, L. M. The Basis of Oncoimmunology. *Cell* **164**, 1233–1247 (2016).
5. Topalian, S. L., Taube, J. M. & Pardoll, D. M. Neoadjuvant checkpoint blockade for cancer immunotherapy. *Science* **367**, eaax0182 (2020).
6. Wang, Y. *et al.* A Systematic Review and Meta-Analysis of Immune-Related Adverse Events of Anti-PD-1 Drugs in Randomized Controlled Trials. *Technol. Cancer Res. Treat.* **19**, 1–12 (2020).
7. Gibney, G. T., Weiner, L. M. & Atkins, M. B. Predictive biomarkers for checkpoint inhibitor-based immunotherapy. *Lancet Oncol.* **17**, e542–e551 (2016).
8. McGrail, D. J. *et al.* High tumor mutation burden fails to predict immune checkpoint blockade response across all cancer types. *Ann. Oncol.* Advance online publication (2021). doi:10.1016/j.annonc.2021.02.006
9. Wherry, E. J. & Kurachi, M. Molecular and cellular insights into T cell exhaustion. *Nat. Rev. Immunol.* **15**, 486–499 (2015).
10. Blank, C. U. *et al.* Defining 'T cell exhaustion'. *Nat. Rev. Immunol.* **19**, 665–674 (2019).
11. van der Leun, A. M., Thommen, D. S. & Schumacher, T. N. CD8+ T cell states in human cancer: insights from single-cell analysis. *Nat. Rev. Cancer* **20**, 218–232 (2020).
12. Busselaar, J., Tian, S., van Eenennaam, H. & Borst, J. Helpless Priming Sends CD8+ T Cells on the Road to Exhaustion. *Front. Immunol.* **11**, 592569 (2020).
13. Utzschneider, D. T. *et al.* T Cell Factor 1-expressing memory-like CD8+T cells sustain the immune response to chronic viral infections. *Immunity* **45**, 415–427 (2016).
14. Wu, T. *et al.* The TCF1-Bcl6 axis counteracts type I interferon to repress exhaustion and maintain T cell stemness. *Sci. Immunol.* **1**, eaai8593 (2016).
15. Chen, Z. *et al.* TCF-1-Centered Transcriptional Network Drives an Effector versus Exhausted CD8 T Cell-Fate Decision. *Immunity* **51**, 840–855 (2019).
16. Miller, B. C. *et al.* Subsets of exhausted CD8+ T cells differentially mediate tumor control and respond to checkpoint blockade. *Nat. Immunol.* **20**, 326–336 (2019).
17. Beltra, J.-C. *et al.* Developmental relationships of four exhausted CD8+ T Cell subsets reveals underlying transcriptional and epigenetic landscape control mechanisms. *Immunity* **52**, 825–841 (2020).
18. Schietinger, A. *et al.* Tumor-specific T cell dysfunction is a dynamic antigen-driven differentiation program initiated early during tumorigenesis. *Immunity* **45**, 389–401 (2016).
19. Philip, M. *et al.* Chromatin states define tumour-specific T cell dysfunction and reprogramming. *Nature* **545**, 452–456 (2017).
20. Zheng, C. *et al.* Landscape of infiltrating T cells in liver cancer revealed by single-cell sequencing. *Cell* **169**, 1342–1356 (2017).
21. Brummelman, J. *et al.* High-dimensional single cell analysis identifies stem-like cytotoxic CD8+ T cells infiltrating human tumors. *J. Exp. Med.* **215**, 2520–2535 (2018).

22. Guo, X. *et al.* Global characterization of T cells in non-small-cell lung cancer by single-cell sequencing. *Nat. Med.* **24**, 978–985 (2018).

23. Zhang, L. *et al.* Lineage tracking reveals dynamic relationships of T cells in colorectal cancer. *Nature* **564**, 268–272 (2018).

24. Jansen, C. S. *et al.* An intra-tumoral niche maintains and differentiates stem-like CD8 T cells. *Nature* **576**, 465–470 (2019).

25. Li, H. *et al.* Dysfunctional CD8 T cells form a proliferative, dynamically regulated compartment within human melanoma. *Cell* **176**, 775–789 (2019).

26. Im, S. J. *et al.* Defining CD8+ T cells that provide the proliferative burst after PD-1 therapy. *Nature* **537**, 417–421 (2016).

27. He, R. *et al.* Follicular CXCR5-expressing CD8+ T cells curtail chronic viral infection. *Nature* **537**, 412–416 (2016).

28. Siddiqui, I. *et al.* Intratumoral Tcf1+PD-1+CD8+ T cells with stem-like properties promote tumor control in response to vaccination and checkpoint blockade immunotherapy. *Immunity* **50**, 195–211 (2019).

29. Kurtulus, S. *et al.* Checkpoint blockade immunotherapy induces dynamic changes in PD-1 – CD8 + tumor-infiltrating T cells. *Immunity* **50**, 181–194 (2019).

30. Sade-Feldman, M. *et al.* Defining T cell states associated with response to checkpoint immunotherapy in melanoma. *Cell* **175**, 998–1013 (2018).

31. Iwai, Y. *et al.* Involvement of PD-L1 on tumor cells in the escape from host immune system and tumor immunotherapy by PD-L1 blockade. *PNAS* **99**, 12293–12297 (2002).

32. Keir, M. E., Butte, M. J., Freeman, G. J. & Sharpe, A. H. PD-1 and Its Ligands in Tolerance and Immunity. *Annu. Rev. Immunol.* **26**, 677–704 (2008).

33. Philips, E. A. *et al.* The structural features that distinguish PD-L2 from PD-L1 emerged in placental mammals. *J. Biol. Chem.* **295**, 4372–4380 (2020).

34. Herbst, R. S. *et al.* Predictive correlates of response to the anti-PD-L1 antibody MPDL3280A in cancer patients. *Nature* **515**, 563–567 (2014).

35. Lau, J. *et al.* Tumour and host cell PD-L1 is required to mediate suppression of anti-tumour immunity in mice. *Nat. Commun.* **8**, 14572 (2017).

36. Tang, H. *et al.* PD-L1 on host cells is essential for PD-L1 blockade–mediated tumor regression. *J. Clin. Invest.* **128**, 580–588 (2018).

37. Kleinovink, J. W. *et al.* PD-L1 expression on malignant cells is no prerequisite for checkpoint therapy. *Oncoimmunology* **6**, e1294299 (2017).

38. Lin, H. *et al.* Host expression of PD-L1 determines efficacy of PD-L1 pathway blockade–mediated tumor regression. *J. Clin. Invest.* **128**, 805–815 (2018).

39. Peng, Q. *et al.* PD-L1 on dendritic cells attenuates T cell activation and regulates response to immune checkpoint blockade. *Nat. Commun.* **11**, 4835 (2020).

40. Oh, S. A. *et al.* PD-L1 expression by dendritic cells is a key regulator of T-cell immunity in cancer. *Nat. Cancer* **1**, 681–691 (2020).

41. Sánchez-Paulete, A. R. *et al.* Cancer immunotherapy with immunomodulatory anti-CD137 and anti–PD-1 monoclonal antibodies requires BATF3-dependent dendritic cells. *Cancer Discov.* **6**, 71–79 (2016).

42. Salmon, H. *et al.* Expansion and Activation of CD103+ Dendritic Cell Progenitors at the Tumor Site Enhances Tumor Responses to Therapeutic PD-L1 and BRAF Inhibition. *Immunity* **44**, 924–938 (2016).

43. Garris, C. S. *et al.* Successful Anti-PD-1 Cancer Immunotherapy Requires T Cell-Dendritic Cell Crosstalk Involving the Cytokines IFN-g and IL-12. *Immunity* **49**, 1148–1161 (2018).

44. Chow, M. T. *et al.* Intratumoral Activity of the CXCR3 Chemokine System Is Required for the Efficacy of Anti-PD-1 Therapy. *Immunity* **50**, 1498–1512 (2019).

45. Mayoux, M. *et al.* Dendritic cells dictate responses to PD-L1 blockade cancer immunotherapy. *Sci. Transl. Med.* **12**, eaav7431 (2020).

46. Gajewski, T. F. & Cron, K. R. CDC1 dysregulation in cancer: An opportunity for intervention. *J. Exp. Med.* **217**, e20200816 (2020).

47. Probst, H. C., McCoy, K., Okazaki, T., Honjo, T. & Van Den Broek, M. Resting dendritic cells induce peripheral CD8+ T cell tolerance through PD-1 and CTLA-4. *Nat. Immunol.* **6**, 280–286 (2005).

48. Baumeister, S. H., Freeman, G. J., Dranoff, G. & Sharpe, A. H. Coinhibitory Pathways in Immunotherapy for Cancer. *Annu. Rev. Immunol.* **34**, 539–573 (2016).

49. Freeman, G. J. *et al.* Engagement of the PD-1 immunoinhibitory receptor by a novel B7 family member leads to negative regulation of lymphocyte activation. *J. Exp. Med.* **192**, 1027–1034 (2000).

50. Fife, B. T. *et al.* Interactions between PD-1 and PD-L1 promote tolerance by blocking the TCR-induced stop signal. *Nat. Immunol.* **10**, 1185–1192 (2009).

51. Yokosuka, T. *et al.* Programmed cell death 1 forms negative costimulatory microclusters that directly inhibit T cell receptor signaling by recruiting phosphatase SHP2. *J. Exp. Med.* **209**, 1201–1217 (2012).

52. Ahn, E. *et al.* Role of PD-1 during effector CD8 T cell differentiation. *PNAS* **115**, 4749–4754 (2018).

53. Chen, D. S. & Mellman, I. Elements of cancer immunity and the cancer-immune set point. *Nature* **541**, 321–330 (2017).

54. Fransen, M. F. *et al.* Tumor-draining lymph nodes are pivotal in PD-1/PD-L1 checkpoint therapy. *JCI Insight* **3**, e124507 (2018).

55. Dammeijer, F. *et al.* The PD-1/PD-L1-Checkpoint Restrains T cell Immunity in Tumor-Draining Lymph Nodes. *Cancer Cell* **38**, 1–16 (2020).

56. Kamphorst, A. O. *et al.* Proliferation of PD-1+ CD8 T cells in peripheral blood after PD-1-targeted therapy in lung cancer patients. *PNAS* **114**, 4993–4998 (2017).

57. Zhang, J. *et al.* Compartmental analysis of T-Cell clonal dynamics as a function of pathologic response to neoadjuvant PD-1 blockade in resectable non-small cell lung cancer. *Clin. Cancer Res.* **26**, 1327–1337 (2020).

58. Yost, K. E. *et al.* Clonal replacement of tumor-specific T cells following PD-1 blockade. *Nat. Med.* **25**, 1251–1259 (2019).

59. Wu, T. D. *et al.* Peripheral T cell expansion predicts tumour infiltration and clinical response. *Nature* **579**, 274–278 (2020).

60. Callahan, M. K. & Wolchok, J. D. Recruit or Reboot? How Does Anti-PD-1 Therapy Change Tumor-Infiltrating Lymphocytes? *Cancer Cell* **36**, 215–217 (2019).

61. Walker, L. S. K. & Sansom, D. M. Confusing signals: Recent progress in CTLA-4 biology. *Trends Immunol.* **36**, 63–70 (2015).

62. Wing, K., Yamaguchi, T. & Sakaguchi, S. Cell-autonomous and -non-autonomous roles of CTLA-4 in immune regulation. *Trends Immunol.* **32**, 428–433 (2011).

63. Hui, E. *et al.* T cell costimulatory receptor CD28 is a primary target for PD-1-mediated inhibition. *Science* **355**, 1428–1433 (2017).

64. Celis-Gutierrez, J. *et al.* Quantitative Interactomics in Primary T Cells Provides a Rationale for Concomitant PD-1 and BTLA Coinhibitor Blockade in Cancer Immunotherapy. *Cell Rep.* **27**, 3315–3330 (2019).

65. Patsoukis, N. *et al.* Interaction of SHP-2 SH2 domains with PD-1 ITSM induces PD-1 dimerization and SHP-2 activation. *Commun. Biol.* **3**, 128 (2020).

66. Okazaki, T., Maeda, A., Nishimura, H., Kurosaki, T. & Honjo, T. PD-1 immunoreceptor inhibits B cell receptor-mediated signaling by recruiting src homology 2-domain-containing tyrosine phosphatase 2 to phosphotyrosine. *PNAS* **98**, 13866–13871 (2001).

67. Kamphorst, A. O. *et al.* Rescue of exhausted CD8 T cells by PD-1–targeted therapies is CD28-dependent. *Science* **355**, 1423–1427 (2017).

68. Wei, S. C. *et al.* Distinct Cellular Mechanisms Underlie Anti-CTLA-4 and Anti-PD-1 Checkpoint Blockade. *Cell* **170**, 1120–1133 (2017).

69. Chaudhri, A. *et al.* PD-L1 Binds to B7-1 only in cis on the same cell surface. *Cancer Immunol. Res.* **6**, 921–929 (2018).

70. Zhao, Y. *et al.* PD-L1:CD80 Cis-Heterodimer Triggers the Co-stimulatory Receptor CD28 While Repressing the Inhibitory PD-1 and CTLA-4 Pathways. *Immunity* **51**, 1059–1073 (2019).

71. Sugiura, D. *et al.* Restriction of PD-1 function by cis-PD-L1/CD80 interactions is required for optimal T cell responses. *Science* **364**, 558–566 (2019).

72. Wang, L. *et al.* Programmed death 1 ligand signaling regulates the generation of adaptive Foxp3+CD4+ regulatory T cells. *PNAS* **105**, 9331–9336 (2008).

73. Tan, C. L. *et al.* PD-1 restraint of regulatory T cell suppressive activity is critical for immune tolerance. *J. Exp. Med.* **218**, e20182232 (2021).

74. Kumagai, S. *et al.* The PD-1 expression balance between effector and regulatory T cells predicts the clinical efficacy of PD-1 blockade therapies. *Nat. Immunol.* **21**, 1346–1358 (2020).

75. Ahrends, T. *et al.* CD4+T cell help confers a cytotoxic T cell effector program including coinhibitory receptor downregulation and increased tissue invasiveness. *Immunity* **47**, 848–861 (2017).

76. Ahrends, T. *et al.* CD4+ T cell help creates memory CD8+ T cells with innate and help-independent recall capacities. *Nat. Commun.* **10**, 5531 (2019).

77. Borst, J., Ahrends, T., Bąbała, N., Melief, C. J. M. & Kastenmüller, W. CD4+ T cell help in cancer immunology and immunotherapy. *Nat. Rev. Immunol.* **18**, 635–647 (2018).

78. Provine, N. M. *et al.* Immediate dysfunction of vaccine-elicited CD8 + T cells primed in the absence of CD4 + T cells. *J. Immunol.* **197**, 1809–1822 (2016).

79. Eickhoff, S. *et al.* Robust Anti-viral Immunity Requires Multiple Distinct T Cell- Dendritic Cell Interactions. *Cell* **162**, 1322–1337 (2015).

80. Hor, J. L. *et al.* Spatiotemporally distinct interactions with dendritic cell subsets facilitates CD4+and CD8+T cell activation to localized viral infection. *Immunity* **43**, 554–565 (2015).

81. Kitano, M. *et al.* Imaging of the cross-presenting dendritic cell subsets in the skin-draining lymph node. *PNAS* **113**, 1044–1049 (2016).

82. Brewitz, A. *et al.* CD8+T cells orchestrate pDC-XCR1+dendritic cell spatial and functional cooperativity to optimize priming. *Immunity* **46**, 205–219 (2017).

83. Flood, B. A., Higgs, E. F., Li, S., Luke, J. J. & Gajewski, T. F. STING pathway agonism as a cancer therapeutic. *Immunol. Rev.* **290**, 24–38 (2019).

84. Gros, A. *et al.* Prospective identification of neoantigen-specific lymphocytes in the peripheral blood of melanoma patients. *Nat. Med.* **22**, 433–438 (2016).

85. Hudson, W. H. *et al.* Proliferating Transitory T Cells with an Effector-like Transcriptional Signature Emerge from PD-1+ Stem-like CD8+ T Cells during Chronic Infection. *Immunity* **51**, 1043–1058 (2019).

86. Ahrends, T. *et al.* CD27 Agonism Plus PD-1 Blockade Recapitulates CD4+ T-cell Help in Therapeutic Anticancer Vaccination. *Cancer Res.* **76**, 2921–2931 (2016).

87. Buchan, S. L. *et al.* PD-1 Blockade and CD27 Stimulation Activate Distinct Transcriptional Programs That Synergize for CD8 + T-Cell–Driven Antitumor Immunity. *Clin. Cancer Res.* **24**, 2383–2394 (2018).

88. Vitale, L. A. *et al.* Development of CDX-527: a bispecific antibody combining PD-1 blockade and CD27 costimulation for cancer immunotherapy. *Cancer Immunol. Immunother.* **69**, 2125–2137 (2020).

89. Oba, T. *et al.* Overcoming primary and acquired resistance to anti-PD-L1 therapy by induction and activation of tumor-residing cDC1s. *Nat. Commun.* **11**, 5415 (2020).

90. Bauer, C. A. *et al.* Dynamic Treg interactions with intratumoral APCs promote local CTL dysfunction. *J. Clin. Invest.* **124**, 2425–2440 (2014).

91. Heeren, A. M. *et al.* High and Interrelated Rates of PD-L1 + CD14 + Antigen-Presenting Cells and Regulatory T Cells Mark the Microenvironment of Metastatic Lymph Nodes from Patients with Cervical Cancer. *Cancer Immunol. Res.* **3**, 48–58 (2015).

Chapter 8

General Discussion

Cancer immunotherapy is used as a strategy to boost the anti-tumor immune response, by raising new or improving existing tumor-specific T-cell responses. $CD8^+$ T-cell exhaustion, characterized by loss of cytotoxic function and high expression of inhibitory receptors, limits anti-tumor responses. Since the late 1990s, it was believed that exhausted cells derive from eroded effector CTLs[1,2], but this has been disproven in the last 10 years. It was discovered that exhausted cells are derived from PD-1^+TCF-1^+ stem-like cells[3–6]. More recent data have further attenuated this model by showing that also functional effector cells derive from stem-like cells, and therefore stem-like $CD8^+$ T cells form the branchpoint between effector and exhausted trajectories[7–10]. An important outstanding question remains which signals during priming decide the differentiation at this branchpoint, and how to steer stem-like cells away from exhaustion and towards the effector state. To answer these questions we need to investigate the cellular and molecular mechanisms of $CD8^+$ T-cell differentiation upon priming.

Effects of $CD4^+$ T-cell help on linear CTL differentiation

It has long been known that during priming, $CD4^+$ T helper cells can deliver 'help' for the CTL response via DCs[11]. Our research group previously identified molecular mechanisms of $CD4^+$ T-cell help using a vaccination model in which mice are vaccinated with DNA constructs encoding an immunodominant tumor-associated MHC-I epitope with or without tumor unrelated MHC-II helper epitopes. In this reductionistic approach, vaccine antigen-specific $CD4^+$ T cells are engaged during the priming of tumor-specific $CD8^+$ T cells or not. This method showed that helped CTLs, primed in the presence of $CD4^+$ T-cell help, display superior effector and migratory functions, and are more effective in tumor killing compared to their 'helpless' counterparts[12,13].

In Chapter 2, we show in the same system the effects of $CD4^+$ T-cell help on $CD8^+$ T-cell memory differentiation. Memory T cells are cells that persist long-term after clearance of their cognate antigen, following an immunogenic challenge such as vaccination or acute infection. Based on functional capacities, localization and marker expression, circulating memory cells are classically divided into central memory (T_{CM}) and effector memory (T_{EM}) subsets. T_{CM} cells, usually identified by a $CD44^+CD62L^+$ phenotype, circulate via the blood through the T-cell zone of secondary lymphoid organs (lymph nodes and spleen). T_{CM} cells are characterized by high self-renewal capacities and robust clonal expansion upon antigen encounter. T_{EM} cells, usually identified by a $CD44^+CD62L^-$ phenotype, circulate through blood, the red pulp of the spleen and non-lymphoid organs, and can rapidly respond to antigen by expressing cytolytic and pro-inflammatory proteins[14]. We show that $CD4^+$ T-cell help improves mostly the formation, maintenance and gene expression profile of T_{EM} cells. T_{CM} cells can still be formed in absence of help, although their long-term maintenance is impaired. Within the T_{EM} population, helped cells display a more effector-like phenotype, which is maintained upon help-independent secondary activation.

Models of CD8$^+$ T-cell differentiation

Memory and effector differentiation in T cells is driven by the expression of transcription factors, wherein the balance between pairs of opposing transcription factors, including T-bet/Eomes, Blimp1/Bcl6 or ID2/ID3, determines if a T cell will differentiate towards an effector or memory cell fate. These transcription factors are strictly regulated by epigenetic mechanisms, such as DNA methylation and histone modification[15,16]. Since we observed that CD4$^+$ T-cell help delivered during priming promotes both effector and memory CD8$^+$ T-cell formation, we aimed to find an overarching explanation for the effects of CD4$^+$ T-cell help on CD8$^+$ T-cell differentiation as a whole. For this purpose, one needs to consider the different models of effector and memory T-cell differentiation that are used in the field. According to the effector-first model[2,17], antigen-specific naïve CD8$^+$ T cells all become effector cells upon activation, during the expansion phase of the response. Effector cells can be subdivided into a population of short-lived effector cells (SLECs) and memory precursor effector cells (MPECs)[18,19]. Following antigen clearance, SLECs die during the contraction phase, while MPECs persist and de-differentiate to form steady-state T_{EM} and T_{CM} memory cells. Upon re-encounter with antigen, memory cells can differentiate again into effector cells during the secondary response (Figure 1A). This model implies that a division between SLEC and MPEC differentiation occurs upon priming, and that MPEC cells can differentiate in a circular manner, or back-and-forth between the memory and the effector state.

In contrast, the linear or progressive differentiation model[20] proposes that CD8$^+$ T-cell differentiation is unidirectional. During priming, a spectrum of T-cell differentiation states is formed, ranging from stem-cell memory (T_{SCM}) cells, T_{CM} cells, T_{EM} cells, to short-lived effector cells[21]. Cells in the highest differentiation state, which as proposed received the most TCR input during priming, will become short-lived effector cells and die during the contraction phase of the response. Cells that have attained a lower differentiation state after priming persist after antigen clearance and form the memory populations (Figure 1B). Upon antigen re-encounter, the entire spectrum is formed again from the lowly differentiated memory cells. This model implies that upon priming, all CD8$^+$ T cells follow the same differentiation path, just to different extents.

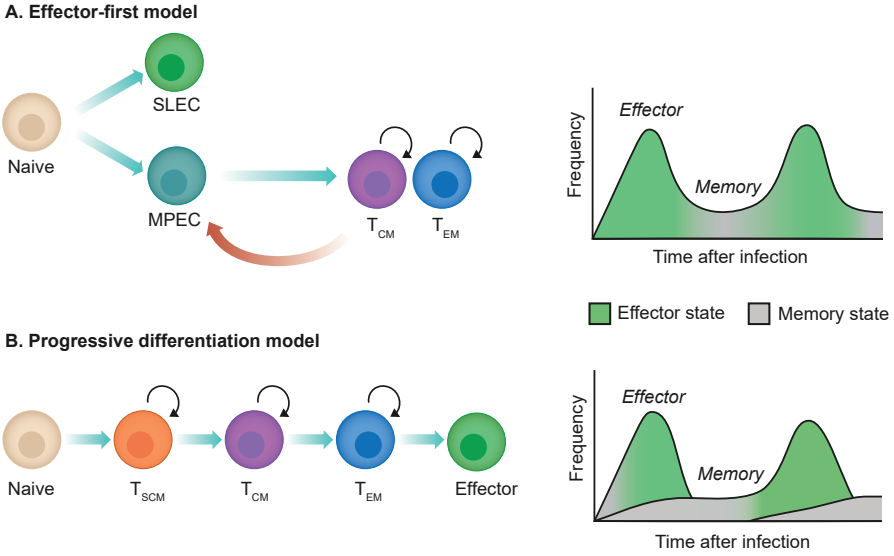

Figure 1. Effector-first vs progressive differentiation model.

While the effector-first model was originally thought to be true, more and more evidence from epigenetic, transcriptomic and TCR tracing studies argues that the progressive differentiation model is the correct one to describe T-cell differentiation[16,22–25]. Instead of the black-and-white subset division of effector and memory populations based on the expression of limited markers such as CD62L or CD44, a further refinement of T-cell differentiation states has been proposed based on proliferative state[26] and expression of additional differentiation markers such as CX3CR1 or KLRG1[27–29]. These studies also point towards a continuum of T-cell differentiation states. TCR input during priming, which is determined both by TCR affinity and antigen abundance at the time of priming, is a key determinant of the differentiation fate of a $CD8^+$ T cell[30–32].

Nowadays the progressive differentiation model is well-established in the $CD8^+$ T-cell differentiation field and supported by many studies. However, the question remains whether this model rules out the possibility of T cell de-differentiation, as suggested by the effector-first model[25]. Early studies describing de-differentiation of $CD8^+$ T cells mainly investigated this by comparing transcriptional and epigenetic properties of phenotypically defined total effector versus memory $CD8^+$ T-cell populations isolated at various stages of the response[33–37]. However, these type of analyses do not prove de-differentiation on a per-cell level, because changes in the total pool can also be explained by differences in outgrowth or maintenance of populations. A more convincing approach is by permanent fluorescent labeling of individual $CD8^+$ T cells that express effector molecules, in order to trace their differentiation fate over time. Using this system, it was shown that a subset of $KLRG1^+$ effector $CD8^+$ T cells could lose their KLRG1 expression and turn into long-lived “ex-KLRG1” memory cells[29]. While these

results can indeed be interpreted as de-differentiation of effector cells into memory cells, they may also reflect the formation of an intermediate population of $CD8^+$ T cells that transiently expresses effector marker molecules but are not stably committed to the effector fate after priming. These cells could still be part of a linear trajectory, highlighting the continuity of the differentiation spectrum. The same principle has been recently shown for the transient downregulation of memory-related genes, such as TCF-1, in a subset of $CD8^+$ T cells[38]. Earlier studies also demonstrated that a subset of $CD62L^-$ effector/T_{EM} $CD8^+$ T cells can re-express $CD62L^+$ upon adoptive transfer into a naïve host[28,39,40]. Taken together, there is evidence for some level of plasticity or "de-differentiation" of $CD8^+$ T cells via transient expression of effector (marker) genes or transient downregulation of memory genes. However, this is likely occurring in intermediate populations within the progressive differentiation spectrum, and does not imply an effector-first fate for all $CD8^+$ T cells.

$CD4^+$ T-cell help during priming shifts the CTL differentiation spectrum

Our results indicate that $CD4^+$ T-cell help during priming improves both effector and memory formation of $CD8^+$ T cells. How does this observation fit within the paradigm of progressive $CD8^+$ T-cell differentiation? We see that $CD4^+$ T-cell help delivered during priming promotes formation of more and better CTL effectors as revealed in the primary response, and formation of more T_{EM} with a more explicit effector-like phenotype, as revealed in the steady-state memory phase. These results are in line with the progressive differentiation model, wherein $CD4^+$ T-cell help shifts the differentiation spectrum towards more effector-like states (Figure 2). This hypothesis is laid out in Chapter 3. In Chapter 4, we provide the experimental evidence for this shift in differentiation as a result of $CD4^+$ T-cell help during priming. We demonstrate that help is required for $CD8^+$ T cells to differentiate past the PD-1^+TCF-1^+ stem-like state towards the KLRG1^+CX3CR1^+ cytotoxic effector state. If $CD4^+$ T-cell help is absent during priming, the so-called ‘helpless’ $CD8^+$ T-cell population displays lower levels of differentiation and cells accumulate mostly in the stem-like state. We also show that even after initial priming, stem-like $CD8^+$ T cells are still able to complete their CTL differentiation when they are provided with antigen and help signals. This indicates that stem-like cells lie within the progressive differentiation spectrum, but need $CD4^+$ T-cell help to progress further along this spectrum.

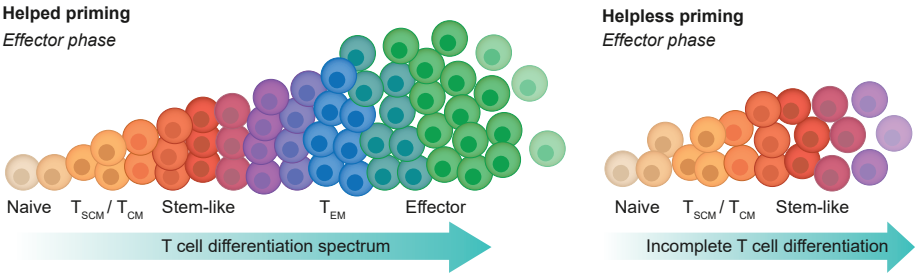

Figure 2. CD4⁺ T-cell help shifts the CTL differentiation spectrum.

Thus, not only TCR input but also costimulatory and cytokine input, including all signals resulting from CD4⁺ T-cell help determine how far CD8⁺ T cells progress along the differentiation spectrum upon priming. Potentially, the total input that determines how far a CD8⁺ T cell progresses on the spectrum, equals the cumulative TCR/costimulatory/cytokine signals from both the first and second priming steps (Figure 3). It is important to consider that even if CD4⁺ T cells are engaged in the response, it does not automatically mean that each CD8⁺ T cell will receive CD4⁺ T-cell help. This depends on the likelihood that a "help" platform on cDC1 is formed, engaging all three cell types. In the Help vaccination setting, we do not see all antigen-specific CD8⁺ T cells becoming terminally differentiated effectors, but rather formation of the entire differentiation spectrum, including low differentiation states as also seen in the No Help setting (Chapter 4). In fact, the effector cells are the only population of which we can safely conclude that have received CD4⁺ T-cell help, because these cells are lacking in the No Help setting. For the other states formed upon vaccination under the Help condition, such as the stem-like cells, we cannot determine whether these cells have actually received CD4⁺ T-cell help during priming or not. Since stem-like cells from Help and No Help are transcriptionally identical (Chapter 4), we propose that these cells have received similar input during priming. This means that stem-like cells generated in the Help vaccination condition are cells that have not (yet) received help. Alternatively, if the eventual differentiation state of a CD8⁺ T cell is determined by the sum of TCR/costimulatory/cytokine signals from both the first and the second priming steps, the relative contribution of these signals may be different between individual cells in the same differentiation state.

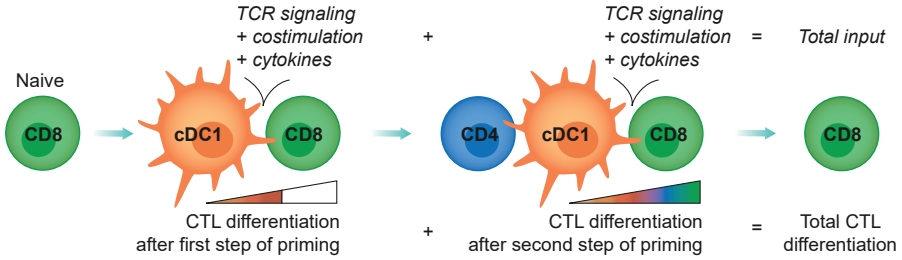

Figure 3. Total CTL differentiation state is determined by input during first + second priming step.

Requirement of CD4⁺ T-cell help for effector and memory CTL responses

Historically, it has been debated whether CD4⁺ T-cell help is always necessary for raising an effective CTL response to pathogens, with the suggestion that helpless priming may also be sufficient in some settings[41]. Early studies showed that primary infections such as by vaccinia virus or acute LCMV can be cleared independently of CD4⁺ T-cell help[42–44], but even in those circumstances there is a difference in helped versus helpless memory formation[43–47]. Of note, the effects of CD4⁺ T-cell help in infection models are typically studied by antibody-based or genetic depletion of the total CD4⁺ T-cell population, including Tregs. Co-depletion of Tregs removes a constraint on CD8⁺ T-cell priming, and thereby likely masks the effects of CD4⁺ T-cell help on the frequency and effector phenotype of primary CD8⁺ T cells, as recently shown in a vaccinia virus infection model[48].

It has been proposed that CD4⁺ T-cell help via CD40 signaling amplifies innate signals to DCs[49], suggesting that in settings with high innate signaling CD4⁺ T-cell help may not be necessary. However, the authors more recently attenuated this model, demonstrating that CD40 signaling can amplify innate signals to DCs, but can in addition induce specific transcriptional programs upon integration of innate signaling by IFN-I[50]. In light of the CTL differentiation trajectory, it can be envisaged that in settings with high levels of antigen and innate signals for DC activation (such as acute infection), the combined TCR/costimulatory/cytokine input CD8⁺ T cells receive during the first step of priming can drive their differentiation along the trajectory. As a consequence, the shift in differentiation between helped and helpless priming may be less pronounced in these circumstances (Figure 4). Thus, the model in which CD4⁺ T-cell help shifts the CD8⁺ T-cell differentiation spectrum further actually fits well with the differential dependence on CD4⁺ T-cell help for effector and/or memory responses in different infection, tumor or vaccination settings, in which the amount of antigen and inflammatory signals that initially drive the differentiation spectrum vary.

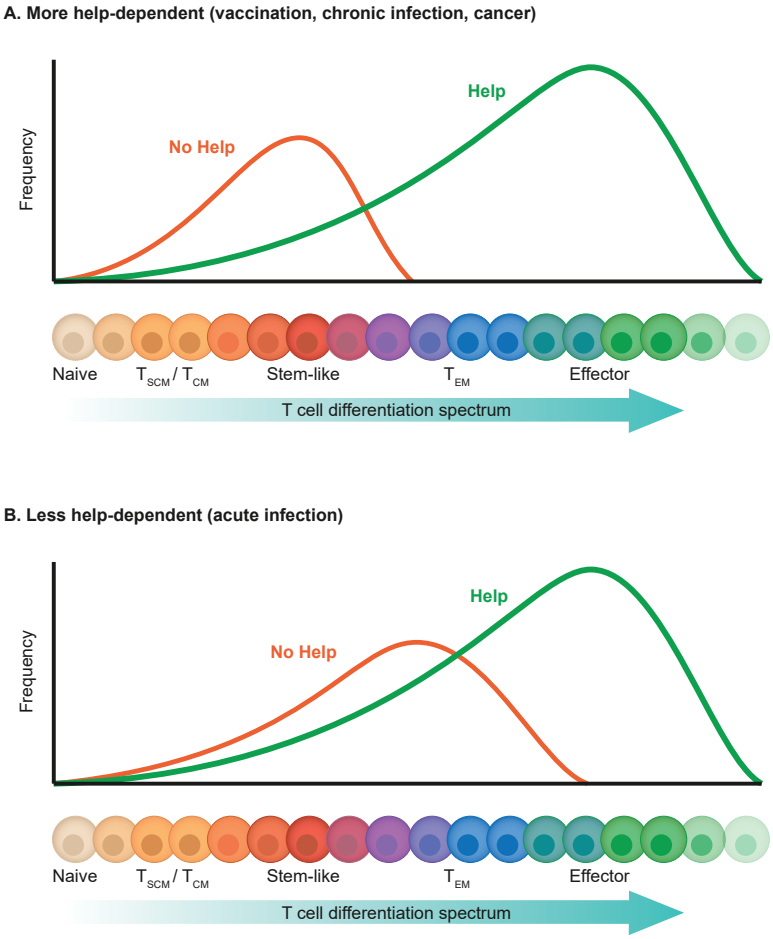

Figure 4. High or low dependence on $CD4^+$ T-cell help is determined by $CD8^+$ T-cell differentiation input during first priming step.

$CD4^+$ T-cell differentiation

In Chapter 5, we focus on $CD4^+$ T-cell differentiation. In type-1 immunity directed against intracellular antigens, such as virus infection or cancer, $CD4^+$ Th1 and Tfh responses are raised in parallel. Th1 cells can deliver help to $CD8^+$ T cells, while Tfh cells can help B cells by promoting isotype class switching and somatic hypermutation. Thus, $CD4^+$ T-cell differentiation coordinates both cellular and humoral immunity. Using our vaccination system, we show that Th1 and Tfh cells are clonally related and are generated from the same uncommitted Th1/Tfh population. Uncommitted Th1/Tfh cells are formed early in the response and express chemokine receptors and transcription factors characteristic for both Th1 and Tfh cells. Interactions with cDC1s or B cells are critical for differentiation of Th1 cells or Tfh cells respectively, but not for initial $CD4^+$ T-cell activation and the generation of the uncommitted Th1/Tfh population. We demonstrate that terminal Th1 differentiation also depends on CD40L-CD40

signaling, which is the main pathway in help delivery from CD4+ T cells to cDC1[51–53]. Thus, in line with earlier observations [54], our data indicate that cDC1-mediated help delivery during the second step of priming is not only crucial for stem-like CD8+ T cells to differentiate into effector CTLs, but also for uncommitted Th1/Tfh CD4+ T cells to differentiate into Th1 cells.

Direct versus indirect effects of CD4+ T-cell help on CTL differentiation

To understand the impact of CD4+ T-cell help on CD8+ T-cell differentiation, it is important to discriminate between direct and indirect effects of responder CD4+ T cells on the total antigen-specific CD8+ T-cell population. In Chapter 2, we demonstrated an increased frequency of T_{EM} cells after helped versus helpless priming. This seems to contrast with results from studies in mouse models of acute infection, where CD4+ T-cell depletion impaired T_{CM} formation and increased T_{EM} formation[46,47,55]. To reconcile these data, it is important to consider that antigen must be cleared to permit the formation of a stable T_{CM} cell population after priming. Accordingly, limiting exposure to cognate antigen improved generation of a CD8+ T_{CM} cell pool under helpless conditions in an allogeneic transplantation model[56]. This principle was also demonstrated in acute infection[47,57]. For example, it was shown that 7-9 weeks after acute LCMV infection under conditions of CD4+ T-cell depletion, the formation of a T_{CM} population was impaired, which was driven by the prolonged presence of antigen[47]. In the same study, the increased frequency of T_{EM} cells within the total memory pool after helpless priming was due to continued presence of antigen for at least 8 weeks. Thus, helpless priming likely resulted in lack of antigen clearance, which impacted T_{EM} formation and/or maintenance. In CD4+ T-cell depleted mice, CTLs are not helped and can therefore less efficiently clear antigen, but help for B cells is also lacking, which will add to antigen persistence driven by impaired antibody-mediated clearance. Due to these effects, CD4+ T-cell depletion in chronic or acute infection models does not allow for a distinction between the direct effects of CD4+ T-cell help during priming on CD8+ T-cell-intrinsic capabilities and the indirect effects of CD4+ T-cell help on CD8+ T-cell differentiation via antigen persistence[9,57]. In our vaccination model, the indirect effect of antigen persistence on memory CD8+ T-cell differentiation does not play a role, because antigen produced in transfected keratinocytes is rapidly lost regardless of the immune response[58,59].

Besides the effect of CD4+ T-cell help on cDC1 licensing, CD4+ T cells may additionally play a direct role in CD8+ T-cell memory maintenance. It has been shown that CD4+ T cells can support CD8+ T-cell responses via the production of IL-21 that acts directly on CD8+ T cells and sustains effector functions during chronic infection[60–62]. During acute infection, IL-21 signaling to CD8+ T cells was dispensable for effector and memory differentiation[63], indicating that the importance of this 'direct' IL-21-mediated help pathway is context-dependent. In our reductionistic Help / No Help vaccination system, vaccine-specific CD4+ T cells are not engaged during steady-state memory. Therefore, improved maintenance of memory CD8+ T cells after Help vaccination results from CD8+ T cell-intrinsic alterations resulting from help during priming.

Tissue-resident memory T cells

Tissue-resident memory T cells (T_{RM}) constitute another T-cell memory population that is not traditionally described as part of the differentiation spectrum, but has recently caught more attention in the cancer immunology field. After antigen clearance, T_{RM} cells differentiate from precursors upon entry in non-lymphoid tissue and exposure to local cues. T_{RM} cells are characterized by expression of the sphingosine-1 receptor inhibitor CD69, and the αEβ7 integrin CD103, which both play a role in tissue retention. They are long-lived, retain high proliferative capacity and exert rapid cytotoxicity upon antigen re-encounter[64]. Epigenetically, T_{RM} cells resemble T_{CM} cells, they have a high plasticity and can give rise to effector cells as well as circulating T_{CM} and T_{EM} cells after restimulation[65–67]. Within the linear $CD8^+$ T-cell differentiation spectrum, T_{RM} cells could therefore be considered as tissue-resident T_{CM} cells. In our vaccination system, we did not specifically investigate the role of $CD4^+$ T-cell help on the priming of T_{RM} $CD8^+$ T cells. However, $CD4^+$ T-cell depletion studies by others showed that $CD4^+$ T-cell help was required for the formation of a lung-resident T_{RM} $CD8^+$ T-cell population after influenza virus infection, and for brain-resident T_{RM} $CD8^+$ T-cell populations after VSV or mouse polyoma virus infections[68,69]. The rate of antigen clearance or quality of priming did not play a role in formation of the T_{RM} $CD8^+$ T-cell pool, but rather, tissue-resident antigen-specific $CD4^+$ T cells produced IL-21 to promote long-term maintenance of $CD8^+$ T_{RM} cells[70,71]. Thus, $CD4^+$ T-cell help for T_{RM} cells seems to be delivered during the steady-state memory phase rather than during priming.

Effects of $CD4^+$ T-cell help on dysfunctional $CD8^+$ T-cell differentiation in cancer

Helpless cells are characterized by impaired functionality and expression of inhibitory receptors such as PD-1, LAG3 and BTLA, but also by expression of the transcription factor TCF-1[12]. This phenotype resembles that of $CD8^+$ T cells found in mouse models of cancer and chronic infection, where they are termed TCF-1^+ stem-like cells, and identified as the precursors of exhausted cells[72]. In Chapter 3, we show the similarity in the transcriptomes of helpless $CD8^+$ T cells raised in our vaccination model and 'predysfunctional' or stem-like $CD8^+$ T cells identified in mouse models of cancer and chronic infection. We propose that stem-like, and eventually also exhausted $CD8^+$ T cells, as found in chronic infection and cancer result from helpless priming. This hypothesis is named the helpless dysfunction model (Figure 5). According to this model, $CD4^+$ T-cell help is needed for formation of the complete $CD8^+$ T-cell differentiation spectrum, including the optimal effector CTL state. These optimal effector CTLs are mainly responsible for antigen clearance, after which $CD8^+$ T cells with lower differentiation states establish memory pools that persist long-term. However, in the case of helpless priming, optimal effector CTLs are lacking, resulting in impaired antigen clearance. The resulting persistent antigen prevents the formation of proper memory pools, but instead drives the formation of exhausted cells from the stem-like population.

In Chapter 4 we provide experimental evidence for the helpless dysfunction model. We show, in line with two-step priming, that under conditions of CD4⁺ T-cell help initially stem-like CD8⁺ T cells are primed, but that these develop in time into effector cells that disseminate systemically. On the other hand, in absence of help, stem-like cells accumulate in the priming lymph node and do not reach the effector state. Moreover, we show that immunogenic MC38 tumors can prime neoantigen-specific stem-like CD8⁺ T cells, but fail to prime neoantigen-specific CD8⁺ T cells with a helped effector phenotype. Instead, stem-like cells in the TME increasingly adopt an exhausted phenotype over time during tumor progression.

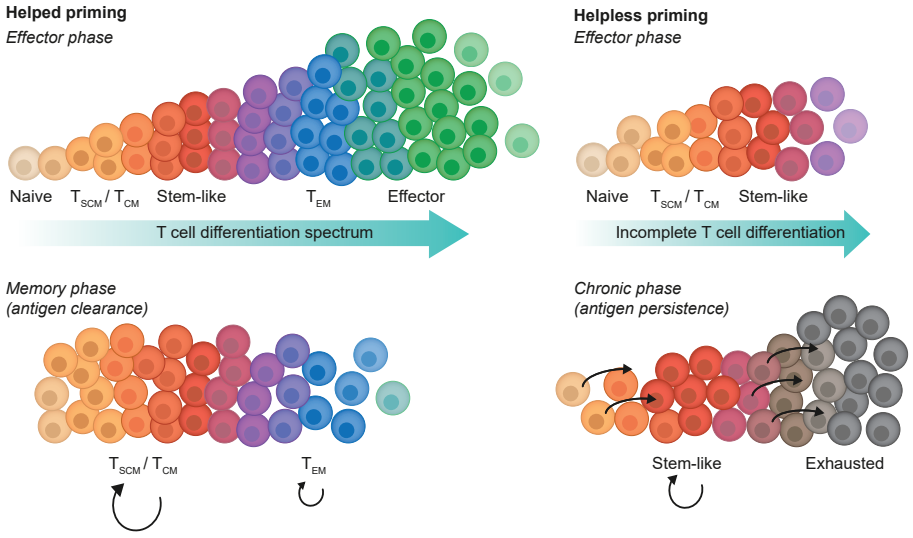

Figure 5. Helpless dysfunction model.

Chronic antigenic stimulation to drive exhaustion

Both aspects that are reportedly needed for CD8⁺ T-cell exhaustion, namely the formation of stem-like cells as well as driving their exhaustion by constant antigen exposure can be explained by helpless priming, according to the helpless dysfunction model. In mouse tumor models, CD8⁺ T cells that do not recognize tumor-specific antigen do not become exhausted, even if they are exposed to the same suppressive TME[73]. Also in human cancer, virus-specific bystander CD8⁺ T cells do not have an exhausted phenotype[74–76]. Thus, chronic antigen exposure is crucial for exhaustion of tumor-specific CD8⁺ T cells, rather than the effects of the suppressive TME. Exhaustion of tumor-specific CD8⁺ T cells can therefore be seen as a reflection of insufficient reduction of tumor antigen burden[77]. In line with this, we do not observe exhaustion of the helpless population in our vaccination model where antigen is quickly removed, but we do see exhaustion in a tumor model where antigen is constantly expressed (Chapter 4).

As discussed above, helpless priming can lead to chronic antigen persistence via lack of help for $CD8^+$ T cells, but probably also via lack of help for B cells. Although they are not as extensively studied as CTL responses, tumor-specific antibodies produced by B cells may contribute to tumor control via various mechanisms, such as antibody-dependent cell-mediated cytotoxicity (ADCC) or signaling interference on tumor cells[78]. In a mouse lung cancer model, CTL-mediated tumor control was decreased upon depletion of $CD4^+$ Tfh cells or B cells, indicating that these cell types can contribute to anti-tumor effector $CD8^+$ T-cell responses[79]. If tumors are unable to prime $CD4^+$ T helper cells, insufficient $CD4^+$ T-cell help to B cells may impair antibody-mediated antigen clearance, and thereby contribute to chronic antigen persistence that further drives exhaustion of helpless $CD8^+$ T cells. In our tumor model, we did not address this hypothesis, but it would be of interest for further investigation.

$CD8^+$ T-cell exhaustion as a spectrum

In chronic infection models, the $CD8^+$ T-cell differentiation trajectory from stem-like to terminally exhausted has also been described as a continuous spectrum (Figure 6). In early studies, the terms 'stem-like' and 'progenitor exhausted (T_{PEX})' were often used interchangeably, but more recent literature preferably uses stem-like for all TCF-1^+ $CD8^+$ T cells that have self-renewing capacity (including memory cells), while T_{PEX} refers specifically to TCF-1^+ $CD8^+$ T cells that are already on the trajectory towards exhaustion[80,81]. The differentiation spectrum towards terminal exhaustion also includes 'intermediate' or 'transitory' exhausted populations with an effector-like phenotype including expression of T-bet and CX3CR1[82–86]. In chronic LCMV infection, it was shown that transitory cells have cytolytic function and can contribute to viral control[82]. Transitory $CD8^+$ T cells have also been identified in human lung cancer and head and neck cancer patients, where they showed TCR sharing with stem-like and exhausted TIL populations[87,88]. Thus, while they express effector-related gene programs, transitory cells are distinct from bona-fide effector CTLs, and lie on the trajectory resulting in terminal exhaustion. Studies in chronic LCMV infection demonstrated that CX3CR1$^+$ transitory $CD8^+$ T cells raised under $CD4^+$ T-cell-depleted conditions became exhausted upon continuous antigen exposure[82], while CX3CR1$^+$ functional effector CTLs capable of clearing the virus followed a separate differentiation path and could only be raised in presence of $CD4^+$ T cells[9]. These results fit with our helpless dysfunction model (Chapter 3, 4), in which the presence of $CD4^+$ T-cell help during priming is required for stem-like cells to further differentiate into proper effector CTLs, but not for their differentiation towards exhausted cells (Figure 6).

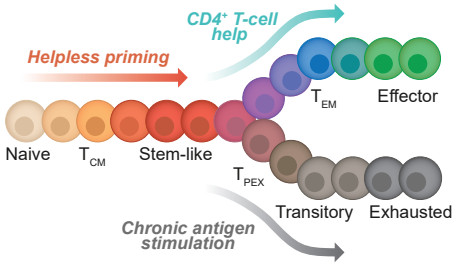

Figure 6. Stem-like CD8⁺ T cells at the branchpoint of CD8⁺ T-cell differentiation trajectories towards the functional effector (dependent on CD4⁺ T-cell help) or terminally exhausted state (driven by chronic antigen stimulation).

Localization of stem-like and exhausted populations

Stem-like CD8⁺ T cells in cancer were first identified as a small subset in the TME, but have later been discovered to mainly reside in TdLN, from where they travel to the tumor to sustain the short-lived exhausted population[89–91]. In accordance with this, we found that in our vaccination setting stem-like/helpless cells preferentially localized to the dLN (Chapter 4). While helped effector CD8⁺ T cells were able to leave the dLN into the circulation, stem-like cells were found to be mainly retained at the priming site. This is in line with a recent study showing that Notch signaling as part of the CD4⁺ T-cell help program is required for LN egress of CD8⁺ T cells after priming (Laurent *et al.*, manuscript in preparation). In mouse tumor models, stem-like and T_{PEX} cells present in the TdLN displayed a less exhausted phenotype than T_{PEX} cells in the TME[92,93], which agrees with the proposed spectrum of exhausted T-cell states. Stem-like cells in the TdLN, but not in the TME, have been suggested to be bona-fide memory cells, which maintained a memory phenotype when shielded from antigen exposure[92]. The same has been suggested for stem-like cells in chronic LCMV infection[10]. These views are in line with our data from the vaccination setting, where stem-like cells are mapped within the linear differentiation spectrum (Chapter 4).

In our tumor experiments using MC38 implantation in mice, we also observed a higher expression of PD-1 and TOX in stem-like cells from the TME compared to stem-like cells from the TdLN. In agreement with literature data, exhausted CD8⁺ T cells were found only in the TME, and not in the TdLN (Chapter 4). We also observed a higher frequency of stem-like cells in TME at an early timepoint and more exhausted cells at a later timepoint, in line with stem-like cells becoming progressively exhausted over time.

Impaired CD4⁺ T-cell help in cancer

In mouse tumor models, CD4⁺ T-cell help is often assumed to be in place unless CD4⁺ T cells are depleted. Recently, it was shown that CD4⁺ T-cell depletion in models of pancreatic cancer did not affect the frequency or phenotype of tumor-specific CD8⁺ T cells[94]. While the authors concluded that the anti-tumor CTL response occurred independently of CD4⁺ T-cell help, this data also supports the alternative hypothesis that tumor-specific CD8⁺ T cells raised in these models were

the result of helpless priming, regardless of whether CD4$^+$ T cells were depleted. In a squamous cell carcinoma model, providing help by adoptive transfer of tumor-specific CD4$^+$ T cells improved anti-tumor CTL responses[95], supporting that spontaneously raised tumor-specific CD8$^+$ T cells in this model lacked sufficient help. Taken together, these findings suggest that raising anti-tumor CD8$^+$ T-cell responses in mice with an intact CD4$^+$ T-cell population does not automatically result in helped CTLs. Our experimental results confirm this hypothesis and show that even in mice that are not depleted of CD4$^+$ T cells, immunogenic MC38 tumors fail to induce priming of helped effector CTLs (Chapter 4). We propose that the occurrence of stem-like, and eventually exhausted CD8$^+$ T cells in cancer can be explained by these tumors inducing helpless priming. With this model, the most important question that comes up is: Why would help be lacking in cancer settings?

There are probably two main reasons for this. Firstly, tumors may lack the expression of immunogenic MHC-II restricted epitopes necessary to raise tumor-specific CD4$^+$ T-cell responses. Potential neoantigens presented by a tumor can be predicted *in silico*, based on genetic profiling of the tumor and the calculated ability of mutated peptides to bind to MHC-I or MHC-II. Since most tumors types do not express MHC-II, testing the presence or immunogenicity of predicted neoantigens is often focused on MHC-I epitopes. As a result, less is known about the immunogenicity of MHC-II-restricted neoantigens, and the contribution of spontaneously raised CD4$^+$ T helper cells in anti-tumor immunity[96,97].

Secondly, the immunotolerant or suppressive TME may lead to impaired DC activation for the priming of helper CD4$^+$ T-cell responses, or impaired cDC1-mediated delivery of CD4$^+$ T-cell help to tumor-specific CD8$^+$ T cells[98]. In Chapter 4 we show that expression of strong helper epitopes by MC38 cells raised a tumor-specific CD4$^+$ T-cell response, but could not rescue the formation of tumor-specific CD8$^+$ T cells with a helped effector phenotype. Our results suggest that help for CD8$^+$ T cells is impaired in the MC38 model regardless of the formation of a tumor-specific CD4$^+$ T cell pool, which is in line with a previous study where MC38 tumors raised an antigen-specific, but dysfunctional CD4$^+$ T-cell response[99]. The absence of inflammatory signals and insufficient DC activation at early stages of tumorigenesis can induce priming of thymus-derived (t)Tregs, or steer differentiation of neoantigen-specific CD4$^+$ T cells towards peripherally induced (p)Tregs, which in turn contribute to the suppressive environment as tumors progress[100]. In this way, CD4$^+$ T-cell responses against a tumor can be impaired, even if MHC-II-restricted antigens are present. For example, it was recently demonstrated that tumor-specific CD4$^+$ T cells in a mouse prostate cancer model displayed a TCF-1$^+$ stem-like phenotype, and their differentiation into Th1 cells was impaired by Tregs. When Tregs were depleted, Th1 differentiation and CTL-based tumor control was improved[101]. In another recent study, proximity-dependent labeling in a mouse melanoma model showed that interactions between tumor-specific CD4$^+$ T cells and DCs in the TdLN decreased over the course of tumor progression[102]. In the same tumor model, the activation of cDC2s in the TME was inhibited by Tregs, leading to suboptimal priming of CD4$^+$ T cells in

the TdLN[103]. Also in a breast tumor model, CTLA4-mediated suppression by Tregs impaired proliferation and differentiation of tumor-specific CD4$^+$ T helper cells in the TdLN. Over the course of tumor progression, tumor-specific CD4$^+$ T cells acquired FOXP3 expression, indicative of Treg induction[99]. These findings suggest that tumors prime insufficient or dysfunctional CD4$^+$ T-cell responses, thereby leading to impaired CD4$^+$ T-cell help to CTLs.

In Chapter 6, we describe another possible underlying mechanism for impaired help in cancer, namely a lack of IFN-I signals in the TME. IFN-I is a crucial signal for initial cDC1 activation but also for delivery of CD4$^+$ T-cell help. Supported by current literature, we present an integrated model how IFN-I signals optimize CD4$^+$ T-cell help delivery by increasing cDC1 survival, antigen presentation on MHC-I and MHC-II, and expression of costimulatory molecules and cytokines. IFN-I also plays an important role in orchestrating the spatial localization of primed CD8$^+$ and CD4$^+$ T cells and cDC1s within the LN via the induction of chemokines, and formation of the help delivery platform. However, tumors often represent a IFN-I-poor environment, via suppression of IFN-I production by tumor cells or dysfunction of tumor-infiltrating immune cells. We propose that the lack of IFN-I signals in the TME could be an important underlying mechanism for the lack of CD4$^+$ T-cell help to tumor-specific CD8$^+$ T cells.

Help delivery in cancer

There are many different cancer types with different immune cell compositions and in certain types help delivery may take place in the TdLN and/or in the TME. For example, neoantigen-specific CD4$^+$ T cells were identified in human melanoma and correlated with improved CD8$^+$ T-cell activation and clinical responses[104–106]. In human kidney cancer, presence of CD4$^+$ Th1 cells in the TME or TdLN correlated with higher frequencies of effector CD8$^+$ T cells and response to immune therapy[101]. Intratumoral interactions between DCs, CD4$^+$ T cells and CD8$^+$ T cells, so-called 'triads', were found to be enriched in hepatocellular carcinoma and malignant plural mesothelioma patients that respond to ICB therapy[107,108]. Also tertiary lymphoid structures (TLS), which are more complex immune structures in close localization to the tumor where DCs and T cells colocalize, have been associated with better prognosis and response to ICB therapy in various human cancers[64,109]. These studies suggest that tumor-specific T cells can be primed or recurrently activated by APCs within intratumoral triads or TLS upon ICB therapy. They also suggests that the CD4$^+$ T-cell help scenario may play out within or close to the TME. However, to which extent this process happens spontaneously in treatment-naïve tumors remains to be investigated.

In recent years, efforts have intensified to characterize TIL populations or overall immune cell composition by transcriptome analysis across multiple types of human cancer. The aim in these studies is to identify overarching T-cell states, tumor immune archetypes or carcinoma ecotypes[8,110–112]. These pan-cancer analyses provide a wealth of information and may also be used to assess the presence or absence of spontaneous CD4$^+$ T-cell help in different TME types.

For example, a meta-analysis of about 6000 tumors representing 16 solid cancer types identified a specific carcinoma ecosystem (CE9) with co-localization of $CD8^+$ T cells, $CD4^+$ T cells and cDC1s, which were associated with the highest overall survival and response to PD-1 blockade therapy[110]. Among different ecosystems, CE9 contained the gene expression signature of helped human cDC1s[113], suggesting that in this type of TME help delivery takes place.

Is helped priming sufficient to eliminate a tumor?

Whether helped priming is necessary or sufficient to control tumor growth likely depends on the immunogenicity of the tumor. The total effect of the anti-tumor CTL response is determined by both the absolute numbers of raised $CD8^+$ T cells and their cytotoxic efficacy. In a highly immunogenic tumor setting which spontaneously raises a large and varied population of tumor-specific $CD8^+$ T cells, helpless priming of these cells may already be sufficient for tumor control, particularly at an early stage of tumorigenesis. For example, it was shown that poorly immunogenic PDAC-OVA tumors injected into the pancreas, but not highly immunogenic PDAC-OVA tumors injected subcutaneously, were dependent on $CD4^+$ T-cell help for tumor rejection[114]. In less immunogenic tumor settings, even helped CTL priming may not be sufficient to control tumor outgrowth, despite $CD4^+$ T-cell help improving the number and efficacy of the CTLs raised. For example, in a tumor model where helped $CD8^+$ T-cell responses were not sufficient for primary tumor control, they could protect against a secondary tumor after resection of the first[54]. Similar to infection, the amount of TCR/costimulatory/cytokine input tumor-specific $CD8^+$ T cells receive during first step of priming probably dictates to which extent the primary CTL response to the tumor relies on $CD4^+$ T-cell help.

It is important to realize that helped priming does not solve all problems regarding the required efficacy of tumor-specific CTL responses, since suppressive mechanisms in the TME may still impair helped CTL responses. Suppressive mechanisms include anti-inflammatory cytokines such as TGF-β or IL-10, inhibitory metabolites, limited nutrient availability and the presence of suppressive cells such as Tregs[115]. Tumor cell-intrinsic escape mechanisms may also occur, such as loss of MHC-I epitopes, downregulation of MHC-I or dysregulation of the antigen processing and presentation (APP) pathway[116]. Tumor cells that lose expression of an MHC-I epitope could in theory still induce help for priming of CTLs specific for other MHC-I restricted epitopes, as long as tumors retain expression of immunogenic MHC-II epitopes. Since MHC-II epitopes are presented by APCs rather than (generally) by the tumor cells themselves, MHC-II epitope loss from the tumor may be limited[96]. However, loss of MHC-II epitopes by tumor cells may indirectly lead to less efficient killing via the priming of helpless CTLs.

Clinical implications of the helpless dysfunction model

In the past decade, advances in immunotherapy have revolutionized cancer treatment, but clinical responses are still highly variable between patients. In order to improve immunotherapy strategies or to select the best immunotherapy regimen for different groups of patients, it is crucial to gain a better understanding of the various types of immune states or TMEs that can surround a tumor. In recent years, several large meta-analyses have been performed to profile different TME compositions across cancer types, in order to identify overlapping immune 'ecotypes' or 'archetypes' that can be used to guide immunotherapy strategies[8,110–112], but the presence or absence of $CD4^+$ T-cell help within these types of TMEs is not generally considered. Understanding $CD4^+$ T-cell help in cancer is important to make rational decisions on immune therapy, whether it is immune checkpoint blockade (ICB), adoptive cell therapy (ACT), or therapeutic vaccination.

$CD4^+$ T-cell help for ICB therapy

In Chapter 7, we link our findings to the mechanism of PD-(L)1 blockade therapy. Studies in mouse models of chronic LCMV infection[4–6] and cancer [117–119] have demonstrated that PD-(L)1 blockade acts on stem-like $CD8^+$ T cells by inducing their proliferation. We clarify the role of PD-1 signaling on the T-cell-cDC interface during priming in the LN, where it regulates TCR signaling and CD28 costimulation. We also outline several studies proving that the therapeutic effect of PD-(L)1 blockade is due to alleviating PD-1 mediated inhibition at the T cell-cDC1 interface and promoting CTL priming, rather than at the CTL/tumor cell interface and promoting CTL-mediated killing. In $CD4^+$ T-cell depleted mouse models of chronic LCMV infection, PD-(L)1 blockade drives expansion but also exhaustion of stem-like $CD8^+$ T cells, and is not sufficient to induce the differentiation of $CX3CR1^+$ effector CTLs[6,9]. In light of the helpless dysfunction model (Chapter 3, 4), we hypothesize in Chapter 7 that PD-(L)1 blockade transiently activates helpless/stem-like $CD8^+$ T cells. We suggest that PD-(L)1 blockade alone is not sufficient to completely 'mimic' or replace $CD4^+$ T-cell help signals that are needed for optimal effector differentiation.

However, recent data have led us to a somewhat different view. In melanoma patients, an increased frequency of $TCF\text{-}1^+$ stem-like $CD8^+$ TILs positively predicts clinical response to PD-1 targeted therapy[117,120]. More recent studies in various types of human cancer show that response to PD-(L)1 blockade therapy is associated with so-called 'triads' or 'immunity hubs' in the TME where T cells and DCs interact[107,108,121,122]. Upon PD-1 blockade therapy, breast cancer lesions showed an increase of $PD\text{-}1^+CXCL13^+$ $CD4^+$ T cells, which displayed a gene signature similar to tumor-specific $CD4^+$ T cells interacting with DCs in the TME or TdLN in mouse tumor models[121,123]. $CXCL13^+$ CD4 T cells in the TME showed expression of both Th1 and Tfh-related genes[107,123], which may suggest an uncommitted phenotype such as described in Chapter 5. In the TME of hepatocellular cancer patients that responded to PD-1 blockade, interactions were observed between stem-

like PD-1$^+$TCF-1$^+$ CD8$^+$ T cells, CXCL13$^+$ CD4$^+$ T cells and DCs with an activated phenotype that also express PD-L1[107]. Importantly, these so-called mature regulatory DCs (mregDCs)[124] shared their transcriptional signature with helped cDC1s as recently shown by our research group[113]. The presence of the helped cDC1 signature in melanoma patients positively correlated with response to PD-1 blockade therapy[113]. Taken together, these studies indicate that the hypothesis that PD-(L)1 blockade therapy acts on stem-like CD8$^+$ T cells by partially substituting for help signals, as described in Chapter 7, is probably incomplete. In addition, successful PD-(L)1 blockade therapy likely works via activating helper CD4$^+$ T cells in the TdLN and/or TME, allowing the CD4$^+$ T-cell help scenario to take place. This model is supported by clinical data from lung cancer, where CD8$^+$ T-cell proliferation and clinical response upon PD-(L)1 blockade was only observed in patients harboring functional systemic CD4$^+$ T-cell responses before treatment[125].

Fewer studies have focused on the role of CD4$^+$ T-cell help in CTLA-4 blockade therapy. CTLA-4-mediated suppression via downregulation of CD80/CD86 on APCs is a key suppressive mechanism of Tregs[100]. Some studies suggest that clinically effective tumor control by CTLA-4 blockade therapy may be achieved via depletion of Tregs rather than blocking CTLA-4-CD80/CD86 interactions[126–128]. Removing CTLA-4-mediated suppression during CD8$^+$ T-cell activation in the LN allows for CD28 costimulation and thereby to improved CTL priming. Recent studies in mouse tumor models also suggest a role for CD4$^+$ T-cell help during this scenario. For example, CTLA-4 expression on Tregs but also on tumor-specific CD4$^+$ T cells themselves was shown to mediate dysfunction of tumor-specific CD4$^+$ T cells, which resulted in impaired CD4$^+$ T-cell help delivery and tumor control. Treg depletion or CTLA-4 blockade resulted in increased numbers of cDC2s in the TdLN and higher expression of CD80 and CD86 on these cells, indicating that Tregs and CTLA-4 induce dysfunction of tumor-specific CD4$^+$ T cells by limiting CD28 signals for their activation[99]. These results are in line with an earlier study, showing that Treg-mediated suppression of cDC2s leads to suboptimal CD4$^+$ T-cell priming[103]. Using proximity-dependent labeling, it was recently shown that CTLA-4 blockade induced higher frequencies of cDC2s and more interactions between DCs and CD4$^+$ T cells in the TdLN and the TME[102]. Thus, CTLA-4 blockade may promote CD4$^+$ T-cell activation and subsequent help delivery by limiting Treg-mediated suppression of cDC2s.

CD4$^+$ T-cell help for ACT

ACT is a personalized cancer therapy that relies on the administration of tumor-specific CD8$^+$ T cells to a patient. These cells can be *ex vivo* expanded TILs, or T cells from blood that are genetically modified to express a tumor-specific TCR or chimeric antigen receptor (CAR). The persistence and anti-tumor activity of CD8$^+$ T cells used for ACT is highly dependent on their differentiation status. Clinical studies have shown that ACT using less differentiated CD8$^+$ T cells is associated with prolonged T-cell persistence and improved therapeutic control, while more differentiated effector-like CD8$^+$ T cells are more prone to become dysfunctional[129]. The role of CD4$^+$ T-cell help for the differentiation of tumor-specific CD8$^+$ T cells is not widely considered in

the ACT field, although there are clinical data showing that adoptive transfer of tumor-specific $CD4^+$ T cells along with $CD8^+$ T cells increases treatment efficacy[130,131].

In CAR-T cells, variable regions of the antibody heavy and light chains are linked to the intracellular signaling chain of CD3ζ and additional costimulatory domains such as CD28 or 4-1BB, which results in MHC-I-independent activation of CAR-T cells upon binding to surface antigens[132]. Thus, CAR-T cells are not activated by cDC1s in the way endogenous $CD8^+$ T cells are, and likely do not receive cDC1-mediated $CD4^+$ T-cell help. In solid tumors, CAR-T cell therapy has demonstrated low clinical efficacy, which is mediated by various factors such as low tumor infiltration, poor T-cell persistence, and CAR-T cells acquiring an exhausted phenotype[133]. These characteristics indeed match those of helpless $CD8^+$ T cells. Thus, understanding the molecular mechanisms underlying $CD4^+$ T-cell help delivery, and incorporating relevant costimulatory domains in CAR design to 'mimic' help signals, may improve CAR-T cell efficacy. For example, adding CD27 to CD28/4-1BB costimulation domains in CAR-T cells has recently been shown to enhance CAR-T cell persistence and tumor control in a xenograft mouse model, while reducing expression of exhaustion markers[134].

$CD4^+$ T-cell help for therapeutic vaccination

A possible strategy to overcome helpless priming in cancer is to specifically raise or activate $CD4^+$ T-cell responses along with $CD8^+$ T-cell responses, for example via vaccination. Several studies have demonstrated that the inclusion of helper epitopes improves vaccine efficacy against tumors[135–139]. Our research group previously showed that in a TC-1 tumor model, which expresses HPV-E7, vaccination with E7-Help but not with E7-No Help resulted in tumor clearance[13]. In these vaccines, which are also used in Chapter 2 and Chapter 4, MHC-II restricted T helper cell epitopes P30 and PADRE are E7-unrelated. Help can be delivered because upon vaccination, MHC-II restricted helper epitopes and MHC-I restricted E7-derived CTL epitope are expressed on the same transfected keratinocyte[59] and can therefore be presented on the same DC. In peptide vaccination studies, vaccination with coupled MHC-I and MHC-II epitopes raised more potent anti-tumor $CD8^+$ T-cell responses than combined vaccination with separate epitopes[140,141]. Also tumor cells expressing both MHC-I and MHC-II restricted epitopes induced stronger anti-tumor $CD8^+$ T-cell responses and better protection than tumors consisting of mixed cells expressing MHC-I or MHC-II epitopes only[108,142]. Taken together, these findings indicate that for therapeutic vaccination, both helper and CTL epitopes should be presented on the same DC in order to facilitate $CD4^+$ T-cell help delivery.

Most therapeutic vaccination strategies aim to raise both $CD4^+$ and $CD8^+$ T-cell responses by vaccination. Another strategy is to raise $CD4^+$ T cells by vaccination that can deliver help to endogenous $CD8^+$ T cells primed by the tumor. For example, neoantigen-specific $CD4^+$ T cells raised by vaccination could help $CD8^+$ T cells against tumor antigens not included in the vaccine in a mouse model of multiple myeloma[143]. Our own experiments so far suggest that vaccinating

tumor-bearing mice with tumor-unrelated helper epitopes does raise a CD4+ T-cell response, but does not effectively deliver help to tumor-primed CD8+ T cells. This is probably because the MHC-I epitopes from the tumor and the MHC-II epitopes from the vaccine are not presented by the same DC for help delivery. This is in line with studies reporting improved protection against tumor outgrowth by tumor-specific rather than tumor-unrelated memory CD4+ T cells, effects that depended on CD4+ T-cell help delivery to CTLs[95,137,144]. When tumor-specific helper epitopes are used for vaccination, it is more likely that DCs presenting tumor-derived antigens can benefit from the help of tumor-specific CD4+ T cells raised by the vaccination. However, tumor-specific helper epitopes may be weakly immunogenic and fail to induce CD8+ T-cell effector differentiation (Chapter 4). In this thesis, we focus on the effect of CD4+ T-cell help on differentiation of CTLs, however direct cytotoxic effects of CD4+ T cells could also contribute to tumor control in case of MHC-II expression by the tumor[145,146]. Alternatively, cytokines released by tumor-specific CD4+ T cells can act on tumor cells or immune cells in the TME, which may also contribute to anti-tumor immune responses[97,147].

A downside of using tumor-specific help for therapeutic vaccination is the challenge to select the right MHC-II neoepitopes to include in the vaccine. In several clinical trials using vaccination with neoantigen peptides, predominant CD4+ T-cell responses were observed without clinical benefit[148–150]. In contrast to mouse studies, where immunogenicity of neoepitopes can be tested, most clinical trials use only prediction algorithms, which may result in selection of suboptimal epitopes, especially for MHC-II[138]. Another possibility is that vaccination with tumor-specific MHC-II epitopes raises Tregs rather than helper CD4+ T cells, when vaccine-induced CD4+ T cells are converted into Tregs under tolerogenic or immune-suppressive conditions in the TME. Tumor-specific Treg induction as a result of therapeutic vaccination has been reported in preclinical and clinical studies[151–153] and was also observed in our experiments. These results underline the importance of selecting optimal administration routes and immune-stimulating adjuvants to induce proper DC activation and T-cell priming upon therapeutic vaccination[154].

Overall, the helpless dysfunction model provides a new perspective on the mechanism of T-cell priming in cancer, and understanding this mechanism is crucial to make rational decisions on novel or combination immune therapies. Gene expression signatures of helped or helpless CD8+ T cells could be used for immune profiling of tumors, in order to stratify patients for immune therapy treatment.

Concluding remarks

In summary, this thesis provides experimental evidence for a new conceptual model on $CD8^+$ T-cell differentiation, by showing that $CD4^+$ T-cell help shifts the CTL differentiation spectrum towards a more effector-like state. More importantly, it identifies helpless priming as underlying mechanism for the occurrence of stem-like and eventually exhausted $CD8^+$ T cells in cancer. These findings offer a new perspective to re-interpret studies on tumor-specific $CD8^+$ T-cell differentiation, and highlight the potential of stem-like/helpless $CD8^+$ T cells to still complete their CTL differentiation when provided with help signals. Presence or absence of $CD4^+$ T-cell help is an important aspect to consider as part of immune profiling of tumors, to tailor immune therapy for cancer patients.

References

1. Zajac, A. J. *et al.* Viral Immune Evasion Due to Persistence of Activated T Cells Without Effector Function. *Journal of Experimental Medicine* **188**, 2205–2213 (1998).
2. Wherry, E. J. & Ahmed, R. Memory CD8 T-Cell Differentiation during Viral Infection. *J. Virol.* **78**, 5535–5545 (2004).
3. Wu, T. *et al.* The TCF1-Bcl6 axis counteracts type I interferon to repress exhaustion and maintain T cell stemness. *Sci. Immunol.* **1**, eaai8593 (2016).
4. He, R. *et al.* Follicular CXCR5-expressing CD8+ T cells curtail chronic viral infection. *Nature* **537**, 412–416 (2016).
5. Utzschneider, D. T. *et al.* T Cell Factor 1-expressing memory-like CD8+T cells sustain the immune response to chronic viral infections. *Immunity* **45**, 415–427 (2016).
6. Im, S. J. *et al.* Defining CD8+ T cells that provide the proliferative burst after PD-1 therapy. *Nature* **537**, 417–421 (2016).
7. Pritykin, Y. *et al.* A unified atlas of CD8 T cell dysfunctional states in cancer and infection. *Mol. Cell* **81**, 2477–2493 (2021).
8. Zheng, L. *et al.* Pan-cancer single-cell landscape of tumor-infiltrating T cells. *Science (1979).* **374**, 6474 (2021).
9. Zander, R. *et al.* CD4+ T Cell Help Is Required for the Formation of a Cytolytic CD8+ T Cell Subset that Protects against Chronic Infection and Cancer. *Immunity* **51**, 1028–1042 (2019).
10. McManus, D. T. *et al.* An early precursor CD8+ T cell that adapts to acute or chronic viral infection. *Nature* **640**, 772–781 (2025).
11. Wu, R. & Murphy, K. M. DCs at the center of help: Origins and evolution of the three-cell-type hypothesis. *Journal of Experimental Medicine* **219**, 1–13 (2022).
12. Ahrends, T. *et al.* CD4+ T cell help confers a cytotoxic T cell effector program including coinhibitory receptor downregulation and increased tissue invasiveness. *Immunity* **47**, 848–861 (2017).
13. Ahrends, T. *et al.* CD27 Agonism Plus PD-1 Blockade Recapitulates CD4+ T-cell Help in Therapeutic Anticancer Vaccination. *Cancer Res.* **76**, 2921–2931 (2016).
14. Mueller, S. N., Gebhardt, T., Carbone, F. R. & Heath, W. R. Memory T Cell Subsets, Migration Patterns, and Tissue Residence. *Annu. Rev. Immunol.* **31**, 137–161 (2013).
15. Chen, Y., Zander, R., Khatun, A., Schauder, D. M. & Cui, W. Transcriptional and Epigenetic Regulation of Effector and Memory CD8 T Cell Differentiation. *Front. Immunol.* **9**, 2826 (2018).
16. Henning, A. N., Roychoudhuri, R. & Restifo, N. P. Epigenetic control of CD8+ T cell differentiation. *Nat. Rev. Immunol.* **18**, 340–356 (2018).
17. Youngblood, B., Hale, J. S. & Ahmed, R. T-cell memory differentiation: insights from transcriptional signatures and epigenetics. *Immunology* **139**, 277–284 (2013).
18. Kaech, S. M. *et al.* Selective expression of the interleukin 7 receptor identifies effector CD8 T cells that give rise to long-lived memory cells. *Nat. Immunol.* **4**, 1191–1198 (2003).
19. Joshi, N. S. *et al.* Inflammation Directs Memory Precursor and Short-Lived Effector CD8+ T Cell Fates via the Graded Expression of T-bet Transcription Factor. *Immunity* **27**, 281–295 (2007).
20. Restifo, N. P. & Gattinoni, L. Lineage relationship of effector and memory T cells. *Curr. Opin. Immunol.* **25**, 556–563 (2013).

21. Gattinoni, L., Speiser, D. E., Lichterfeld, M. & Bonini, C. T memory stem cells in health and disease. *Nat. Med.* **23**, 18–27 (2017).

22. Dogra, P., Ghoneim, H. E., Abdelsamed, H. A. & Youngblood, B. Generating long-lived CD8(+) T-cell memory: Insights from epigenetic programs. *Eur. J. Immunol.* **46**, 1548–62 (2016).

23. Pais Ferreira, D. *et al.* Central memory CD8+ T cells derive from stem-like Tcf7hi effector cells in the absence of cytotoxic differentiation. *Immunity* **53**, 985–1000 (2020).

24. Johnnidis, J. B. *et al.* Inhibitory signaling sustains a distinct early memory CD8+ T cell precursor that is resistant to DNA damage. *Sci. Immunol.* **6**, (2021).

25. Al Khabouri, S. & Gerlach, C. T cell fate mapping and lineage tracing technologies probing clonal aspects underlying the generation of CD8 T cell subsets. *Scand. J. Immunol.* **92**, (2020).

26. Bresser, K. *et al.* Replicative history marks transcriptional and functional disparity in the CD8+ T cell memory pool. *Nat. Immunol.* **23**, 791–801 (2022).

27. Böttcher, J. P. *et al.* Functional classification of memory CD8+ T cells by CX3CR1 expression. *Nat. Commun.* **6**, 8306 (2015).

28. Gerlach, C. *et al.* The Chemokine Receptor CX3CR1 Defines Three Antigen-Experienced CD8 T Cell Subsets with Distinct Roles in Immune Surveillance and Homeostasis. *Immunity* **45**, 1270–1284 (2016).

29. Herndler-Brandstetter, D. *et al.* KLRG1+ Effector CD8+ T Cells Lose KLRG1, Differentiate into All Memory T Cell Lineages, and Convey Enhanced Protective Immunity. *Immunity* **48**, 716-729.e8 (2018).

30. Sarkar, S. *et al.* Strength of stimulus and clonal competition impact the rate of memory CD8 T cell differentiation. *J. Immunol.* **179**, 6704–14 (2007).

31. Snell, L. M. *et al.* CD8+ T Cell Priming in Established Chronic Viral Infection Preferentially Directs Differentiation of Memory-like Cells for Sustained Immunity. *Immunity* **49**, 678–694 (2018).

32. Schober, K. *et al.* Reverse TCR repertoire evolution towards dominant low affinity clones during chronic CMV infection. *Nat. Immunol.* **21**, 434–441 (2020).

33. Kaech, S. M., Hemby, S., Kersh, E. & Ahmed, R. Molecular and Functional Profiling of Memory CD8 T Cell Differentiation. *Cell* **111**, 837–851 (2002).

34. Best, J. A. *et al.* Transcriptional insights into the CD8+ T cell response to infection and memory T cell formation. *Nat. Immunol.* **14**, 404–412 (2013).

35. Akondy, R. S. *et al.* Origin and differentiation of human memory CD8 T cells after vaccination. *Nature* **552**, 362–367 (2017).

36. Youngblood, B. *et al.* Effector CD8 T cells dedifferentiate into long-lived memory cells. *Nature* **552**, 404–409 (2017).

37. Giles, J. R. *et al.* Shared and distinct biological circuits in effector, memory and exhausted CD8+ T cells revealed by temporal single-cell transcriptomics and epigenetics. *Nat. Immunol.* 1–14 (2022) doi:10.1038/s41590-022-01338-4.

38. Abadie, K. *et al.* Reversible, tunable epigenetic silencing of TCF1 generates flexibility in the T cell memory decision. *Immunity* **57**, 271–286 (2024).

39. Wherry, E. J. *et al.* Lineage relationship and protective immunity of memory CD8 T cell subsets. *Nat. Immunol.* **4**, 225–234 (2003).

40. Bouneaud, C., Garcia, Z., Kourilsky, P. & Pannetier, C. Lineage relationships, homeostasis, and recall capacities of central- and effector-memory CD8 T cells in vivo. *Journal of Experimental Medicine* **201**, 579–590 (2005).

41. Wiesel, M. & Oxenius, A. From crucial to negligible: Functional CD8+ T-cell responses and their dependence on CD4+ T-cell help. *Eur. J. Immunol.* **42**, 1080–1088 (2012).

42. Matloubian, M., Concepcion, R. J. & Ahmed, R. CD4+ T cells are required to sustain CD8+ cytotoxic T-cell responses during chronic viral infection. *J. Virol.* **68**, 8056–8063 (1994).

43. von Herrath, M. G., Yokoyama, M., Dockter, J., Oldstone, M. B. & Whitton, J. L. CD4-deficient mice have reduced levels of memory cytotoxic T lymphocytes after immunization and show diminished resistance to subsequent virus challenge. *J. Virol.* **70**, 1072–1079 (1996).

44. Shedlock, D. J. & Shen, H. Requirement for CD4 T cell help in generating functional CD8 T cell memory. *Science (1979).* **300**, 337–9 (2003).

45. Janssen, E. M. *et al.* CD4+ T cells are required for secondary expansion and memory in CD8+ T lymphocytes. *Nature* **421**, 852–856 (2003).

46. Khanolkar, A., Fuller, M. J. & Zajac, A. J. CD4 T Cell-Dependent CD8 T Cell Maturation. *The Journal of Immunology* **172**, 2834–2844 (2004).

47. van der Heide, V. *et al.* Prolonged but finite antigen presentation promotes reversible defects of "helpless" memory CD8+ T cells. *Immunity* **58**, 1742-1761.e14 (2025).

48. Jobin, K. *et al.* A distinct priming phase regulates CD8 T cell immunity by orchestrating paracrine IL-2 signals. *Science (1979).* **388**, (2025).

49. Bedoui, S., Heath, W. R. & Mueller, S. N. CD4+ T-cell help amplifies innate signals for primary CD8+ T-cell immunity. *Immunol. Rev.* **272**, 52–64 (2016).

50. Gressier, E. *et al.* CD4+ T cell calibration of antigen-presenting cells optimizes antiviral CD8+ T cell immunity. *Nat. Immunol.* **24**, (2023).

51. Schoenberger, S. P., Toes, R. E. M., van der Voort, E. I. H., Offringa, R. & Melief, C. J. M. T-cell help for cytotoxic T lymphocytes is mediated by CD40–CD40L interactions. *Nature* **393**, 480–483 (1998).

52. Bennett, S. R. M. *et al.* Help for cytotoxic-T-cell responses is mediated by CD40 signalling. *Nature* **393**, 478–480 (1998).

53. Ridge, J. P., Di Rosa, F. & Matzinger, P. A conditioned dendritic cell can be a temporal bridge between a CD4+ T-helper and a T-killer cell. *Nature* **393**, 474–478 (1998).

54. Ferris, S. T. *et al.* cDC1 prime and are licensed by CD4+ T cells to induce anti-tumour immunity. *Nature* **584**, 624–629 (2020).

55. Cullen, J. G. *et al.* CD4+ T help promotes influenza virus-specific CD8+ T cell memory by limiting metabolic dysfunction. *Proc. Natl. Acad. Sci. U. S. A.* **116**, 4481–4488 (2019).

56. Kim, J. *et al.* Memory programming in CD8+ T-cell differentiation is intrinsic and is not determined by CD4 help. *Nat. Commun.* **6**, 7994 (2015).

57. Li, Y. *et al.* Persistent antigen and prolonged AKT–mTORC1 activation underlie memory CD8 T cell impairment in the absence of CD4 T cells. *The Journal of Immunology* **195**, 1591–1598 (2015).

58. Babala, N. *et al.* Subcellular Localization of Antigen in Keratinocytes Dictates Delivery of CD4 + T-cell Help for the CTL Response upon Therapeutic DNA Vaccination into the Skin. *Cancer Immunol. Res.* **6**, 835–847 (2018).

59. Bins, A. D. *et al.* A rapid and potent DNA vaccination strategy defined by in vivo monitoring of antigen expression. *Nat. Med.* **11**, 899–904 (2005).

60. Elsaesser, H., Sauer, K. & Brooks, D. G. IL-21 Is Required to Control Chronic Viral Infection. *Science (1979).* **324**, 1569–1572 (2009).

61. Fröhlich, A. *et al.* IL-21R on T Cells Is Critical for Sustained Functionality and Control of Chronic Viral Infection. *Science (1979).* **324**, 1576–1580 (2009).

62. Yi, J. S., Du, M. & Zajac, A. J. A Vital Role for Interleukin-21 in the Control of a Chronic Viral Infection. *Science (1979).* **324**, 1572–1576 (2009).

63. Tian, Y. *et al.* A Context-Dependent Role for IL-21 in Modulating the Differentiation, Distribution, and Abundance of Effector and Memory CD8 T Cell Subsets. *The Journal of Immunology* **196**, 2153–2166 (2016).

64. Schenkel, J. M. & Pauken, K. E. Localization, tissue biology and T cell state — implications for cancer immunotherapy. *Nat. Rev. Immunol.* **23**, 807–823 (2023).

65. Masopust, D., Vezys, V., Wherry, E. J., Barber, D. L. & Ahmed, R. Cutting Edge: Gut Microenvironment Promotes Differentiation of a Unique Memory CD8 T Cell Population. *The Journal of Immunology* **176**, 2079–2083 (2006).

66. Fonseca, R. *et al.* Developmental plasticity allows outside-in immune responses by resident memory T cells. *Nature Immunology 2020 21:4* **21**, 412–421 (2020).

67. Behr, F. M. *et al.* Tissue-resident memory CD8+ T cells shape local and systemic secondary T cell responses. *Nat. Immunol.* **21**, 1070–1081 (2020).

68. Laidlaw, B. J. *et al.* CD4+ T Cell Help Guides Formation of CD103+ Lung-Resident Memory CD8+ T Cells during Influenza Viral Infection. *Immunity* **41**, 633–645 (2014).

69. Mockus, T. E. *et al.* CD4 T cells control development and maintenance of brain-resident CD8 T cells during polyomavirus infection. *PLoS Pathog.* **14**, e1007365 (2018).

70. Ren, H. M. & Lukacher, A. E. IL-21 in Homeostasis of Resident Memory and Exhausted CD8 T Cells during Persistent Infection. *Int. J. Mol. Sci.* **21**, 6966 (2020).

71. Son, Y. M. *et al.* Tissue-resident CD4 + T helper cells assist the development of protective respiratory B and CD8 + T cell memory responses. *Sci. Immunol.* **6**, 55 (2021).

72. Philip, M. & Schietinger, A. CD8+ T cell differentiation and dysfunction in cancer. *Nat. Rev. Immunol.* **22**, 209–223 (2022).

73. Schietinger, A. *et al.* Tumor-specific T cell dysfunction is a dynamic antigen-driven differentiation program initiated early during tumorigenesis. *Immunity* **45**, 389–401 (2016).

74. Oliveira, G. *et al.* Phenotype, specificity and avidity of antitumour CD8+ T cells in melanoma. *Nature* **596**, 119–125 (2021).

75. Caushi, J. X. *et al.* Transcriptional programs of neoantigen-specific TIL in anti-PD-1-treated lung cancers. *Nature* **596**, 126–132 (2021).

76. Nagasaki, J. *et al.* PD-1 blockade therapy promotes infiltration of tumor-attacking exhausted T cell clonotypes. *Cell Rep.* **38**, 110331 (2022).

77. Chow, A., Perica, K., Klebanoff, C. A. & Wolchok, J. D. Clinical implications of T cell exhaustion for cancer immunotherapy. *Nat. Rev. Clin. Oncol.* **19**, 775–790 (2022).

78. Laumont, C. M., Banville, A. C., Gilardi, M., Hollern, D. P. & Nelson, B. H. Tumour-infiltrating B cells: immunological mechanisms, clinical impact and therapeutic opportunities. *Nat. Rev. Cancer* **22**, 414–430 (2022).

79. Cui, C. *et al.* Neoantigen-driven B cell and CD4 T follicular helper cell collaboration promotes anti-tumor CD8 T cell responses. *Cell* **184**, 6101-6118.e13 (2021).

80. Gebhardt, T., Park, S. L. & Parish, I. A. Stem-like exhausted and memory CD8+ T cells in cancer. *Nat. Rev. Cancer* **23**, 780–798 (2023).

81. Broomfield, B. J. & Groom, J. R. Defining the niche for stem-like CD8+ T cell formation and function. *Curr. Opin. Immunol.* **89**, 102454 (2024).

82. Hudson, W. H. *et al.* Proliferating Transitory T Cells with an Effector-like Transcriptional Signature Emerge from PD-1+ Stem-like CD8+ T Cells during Chronic Infection. *Immunity* **51**, 1043–1058 (2019).

83. Hanna, B. S. *et al.* Interleukin-10 receptor signaling promotes the maintenance of a PD-1int TCF-1+ CD8+ T cell population that sustains anti-tumor immunity. *Immunity* **54**, 2825–2841 (2021).

84. Dähling, S. *et al.* Type 1 conventional dendritic cells maintain and guide the differentiation of precursors of exhausted T cells in distinct cellular niches. *Immunity* 1–15 (2022) doi:10.1016/j.immuni.2022.03.006.

85. Beltra, J.-C. *et al.* Developmental relationships of four exhausted CD8+ T Cell subsets reveals underlying transcriptional and epigenetic landscape control mechanisms. *Immunity* **52**, 825–841 (2020).

86. Daniel, B. *et al.* Divergent clonal differentiation trajectories of T cell exhaustion. *Nat. Immunol.* **23**, 1614–1627 (2022).

87. Eberhardt, C. S. *et al.* Functional HPV-specific PD-1+ stem-like CD8 T cells in head and neck cancer. *Nature* **597**, 279–284 (2021).

88. Gueguen, P. *et al.* Contribution of resident and circulating precursors to tumor-infiltrating CD8 + T cell populations in lung cancer. *Sci. Immunol.* **6**, (2021).

89. Schenkel, J. M. *et al.* Conventional type I dendritic cells maintain a reservoir of proliferative tumor-antigen specific TCF-1+ CD8+ T cells in tumor-draining lymph nodes. *Immunity* **54**, 2338–2353 (2021).

90. Connolly, K. A. *et al.* A reservoir of stem-like CD8 + T cells in the tumor-draining lymph node preserves the ongoing antitumor immune response. *Sci. Immunol.* **6**, 64 (2021).

91. Li, Z. *et al.* In vivo labeling reveals continuous trafficking of TCF-1+ T cells between tumor and lymphoid tissue. *Journal of Experimental Medicine* **219**, e20210749 (2022).

92. Huang, Q. *et al.* The primordial differentiation of tumor-specific memory CD8+ T cells as bona fide responders to PD-1/PD-L1 blockade in draining lymph nodes. *Cell* **185**, 4049–4066 (2022).

93. Prokhnevska, N. *et al.* CD8+ T cell activation in cancer comprises an initial activation phase in lymph nodes followed by effector differentiation within the tumor. *Immunity* **56**, 107–124 (2023).

94. Medler, T. R. *et al.* Tumor resident memory CD8 T cells and concomitant tumor immunity develop independently of CD4 help. *Sci. Rep.* **13**, 6277 (2023).

95. Brightman, S. E. *et al.* Neoantigen-specific stem cell memory-like CD4+ T cells mediate CD8+ T cell-dependent immunotherapy of MHC class II-negative solid tumors. *Nat. Immunol.* **24**, 1345–1357 (2023).

96. Brightman, S. E., Naradikian, M. S., Miller, A. M. & Schoenberger, S. P. Harnessing neoantigen specific CD4 T cells for cancer immunotherapy. *J. Leukoc. Biol.* **107**, 625–633 (2020).

97. Speiser, D. E., Chijioke, O., Schaeuble, K. & Münz, C. CD4+ T cells in cancer. *Nat. Cancer* **4**, 317–329 (2023).

98. Wculek, S. K. *et al.* Dendritic cells in cancer immunology and immunotherapy. *Nat. Rev. Immunol.* **20**, 7–24 (2020).

99. Guo, M. *et al.* Molecular, metabolic, and functional CD4 T cell paralysis in the lymph node impedes tumor control. *Cell Rep.* **42**, 113047 (2023).

100. Tay, C., Tanaka, A. & Sakaguchi, S. Tumor-infiltrating regulatory T cells as targets of cancer immunotherapy. *Cancer Cell* **41**, 450–465 (2023).

101. Cardenas, M. A. *et al.* Differentiation fate of a stem-like CD4 T cell controls immunity to cancer. *Nature* 1–9 (2024) doi:10.1038/s41586-024-08076-7.

102. Chudnovskiy, A. *et al.* Proximity-dependent labeling identifies dendritic cells that drive the tumor-specific CD4+ T cell response. *Sci. Immunol.* **9**, 8843 (2024).

103. Binnewies, M. *et al.* Unleashing Type-2 Dendritic Cells to Drive Protective Antitumor CD4+ T Cell Immunity. *Cell* **177**, 556–571 (2019).

104. Linnemann, C. *et al.* High-throughput epitope discovery reveals frequent recognition of neo-antigens by CD4+ T cells in human melanoma. *Nat. Med.* **21**, 81–85 (2015).

105. Veatch, J. R. *et al.* Tumor-infiltrating BRAFV600E-specific CD4+ T cells correlated with complete clinical response in melanoma. *Journal of Clinical Investigation* **128**, 1563–1568 (2018).

106. Veatch, J. R. *et al.* Neoantigen-specific CD4+ T cells in human melanoma have diverse differentiation states and correlate with CD8+ T cell, macrophage, and B cell function. *Cancer Cell* **40**, 393–409 (2022).

107. Magen, A. *et al.* Intratumoral dendritic cell–CD4+ T helper cell niches enable CD8+ T cell differentiation following PD-1 blockade in hepatocellular carcinoma. *Nat. Med.* **29**, 1389–1399 (2023).

108. Espinosa-Carrasco, G. *et al.* Intratumoral immune triads are required for immunotherapy-mediated elimination of solid tumors. *Cancer Cell* 1–15 (2024) doi:10.1016/j.ccell.2024.05.025.

109. Schumacher, T. N. & Thommen, D. S. Tertiary lymphoid structures in cancer. *Science (1979).* **375**, eabf9419 (2022).

110. Luca, B. A. *et al.* Atlas of clinically distinct cell states and ecosystems across human solid tumors. *Cell* **184**, 5482–5496 (2021).

111. Combes, A. J. *et al.* Discovering dominant tumor immune archetypes in a pan-cancer census. *Cell* **185**, 184–203 (2022).

112. Chu, Y. *et al.* Pan-cancer T cell atlas links a cellular stress response state to immunotherapy resistance. *Nature Medicine 2023* **19**, 1–13 (2023).

113. Lei, X. *et al.* CD4+ helper T cells endow cDC1 with cancer-impeding functions in the human tumor micro-environment. *Nat. Commun.* **14**, 217 (2023).

114. Diamond, M. S., Lin, J. H. & Vonderheide, R. H. Site-dependent immune escape due to impaired dendritic cell cross-priming. *Cancer Immunol. Res.* **9**, 877–890 (2021).

115. Anderson, K. G., Stromnes, I. M. & Greenberg, P. D. Obstacles Posed by the Tumor Microenvironment to T cell Activity: A Case for Synergistic Therapies. *Cancer Cell* **31**, 311–325 (2017).

116. Dersh, D., Hollý, J. & Yewdell, J. W. A few good peptides: MHC class I-based cancer immunosurveillance and immunoevasion. *Nat. Rev. Immunol.* **21**, 116–128 (2021).

117. Miller, B. C. *et al.* Subsets of exhausted CD8+ T cells differentially mediate tumor control and respond to checkpoint blockade. *Nat. Immunol.* **20**, 326–336 (2019).

118. Siddiqui, I. *et al.* Intratumoral Tcf1+PD-1+CD8+ T cells with stem-like properties promote tumor control in response to vaccination and checkpoint blockade immunotherapy. *Immunity* **50**, 195–211 (2019).

119. Kurtulus, S. *et al.* Checkpoint blockade immunotherapy induces dynamic changes in PD-1 – CD8 + tumor-infiltrating T cells. *Immunity* **50**, 181–194 (2019).

120. Sade-Feldman, M. *et al.* Defining T Cell States Associated with Response to Checkpoint Immunotherapy in Melanoma. *Cell* **175**, 998–1013 (2018).

121. Cohen, M. *et al.* The interaction of CD4+ helper T cells with dendritic cells shapes the tumor microenvironment and immune checkpoint blockade response. *Nat. Cancer* **3**, 303–317 (2022).

122. Chen, J. H. *et al.* Human lung cancer harbors spatially organized stem-immunity hubs associated with response to immunotherapy. *Nat. Immunol.* **20**, 1–15 (2024).

123. Bassez, A. *et al.* A single-cell map of intratumoral changes during anti-PD1 treatment of patients with breast cancer. *Nat. Med.* **27**, 820–832 (2021).

124. Maier, B. *et al.* A conserved dendritic-cell regulatory program limits antitumour immunity. *Nature* **580**, 257–262 (2020).

125. Zuazo, M. *et al.* Functional systemic CD4 immunity is required for clinical responses to PD-L1/PD-1 blockade therapy. *EMBO Mol. Med.* **11**, e10293 (2019).

126. Simpson, T. R. *et al.* Fc-dependent depletion of tumor-infiltrating regulatory t cells co-defines the efficacy of anti-CTLA-4 therapy against melanoma. *Journal of Experimental Medicine* **210**, 1695–1710 (2013).

127. Selby, M. J. *et al.* Anti-CTLA-4 antibodies of IgG2a isotype enhance antitumor activity through reduction of intratumoral regulatory T cells. *Cancer Immunol. Res.* **1**, 32–42 (2013).

128. Du, X. *et al.* A reappraisal of CTLA-4 checkpoint blockade in cancer immunotherapy. *Cell Res.* **28**, 416–432 (2018).

129. Chan, J. D. *et al.* Cellular networks controlling T cell persistence in adoptive cell therapy. *Nat. Rev. Immunol.* **21**, 769–784 (2021).

130. Turtle, C. J. *et al.* CD19 CAR–T cells of defined CD4+:CD8+ composition in adult B cell ALL patients. *Journal of Clinical Investigation* **126**, 2123–2138 (2016).

131. Tran, E. *et al.* Cancer Immunotherapy Based on Mutation-Specific CD4+ T Cells in a Patient with Epithelial Cancer. *Science (1979).* **344**, 641–645 (2014).

132. Rosenberg, S. A. & Restifo, N. P. Adoptive cell transfer as personalized immunotherapy for human cancer. *Science (1979).* **348**, 62–68 (2015).

133. Yong, C. S. M. *et al.* CAR T-cell therapy of solid tumors. *Immunol. Cell Biol.* **95**, 356–363 (2017).

134. Zhang, C. *et al.* CD27 agonism coordinates with CD28 and 4-1BB signal to augment the efficacy of CAR-T cells in colorectal tumor. *Medical Oncology* **40**, 123 (2023).

135. Ossendorp, F., Mengedé, E., Camps, M., Filius, R. & Melief, C. J. M. Specific T Helper Cell Requirement for Optimal Induction of Cytotoxic T Lymphocytes against Major Histocompatibility Complex Class II Negative Tumors. *J. Exp. Med.* **187**, 693–702 (1998).

136. Aarntzen, E. H. J. G. *et al.* Targeting CD4+ T-Helper Cells Improves the Induction of Antitumor Responses in Dendritic Cell–Based Vaccination. *Cancer Res.* **73**, 19–29 (2013).

137. de Graaf, J. F. *et al.* Neoantigen-specific T cell help outperforms non-specific help in multi-antigen DNA vaccination against cancer. *Molecular Therapy: Oncology* **32**, 200835 (2024).

138. Huff, A. L. *et al.* CD4 T cell–activating neoantigens enhance personalized cancer vaccine efficacy. *JCI Insight* **8**, (2023).

139. Shibata, H. *et al.* Integrating CD4+ T cell help for therapeutic cancer vaccination in a preclinical head and neck cancer model. *Oncoimmunology* **10**, (2021).

140. Dolina, J. S. *et al.* Linked CD4+/CD8+ T cell neoantigen vaccination overcomes immune checkpoint blockade resistance and enables tumor regression. *Journal of Clinical Investigation* **133**, (2023).

141. Swartz, A. M. *et al.* A conjoined universal helper epitope can unveil antitumor effects of a neoantigen vaccine targeting an MHC class I-restricted neoepitope. *NPJ Vaccines* **6**, 12 (2021).

142. Alspach, E. *et al.* MHC-II neoantigens shape tumour immunity and response to immunotherapy. *Nature* **574**, 696–701 (2019).

143. Bekri, S. *et al.* Neoantigen vaccine-induced CD4 T cells confer protective immunity in a mouse model of multiple myeloma through activation of CD8 T cells against non-vaccine, tumor-associated antigens. *J. Immunother. Cancer* **10**, e003572 (2022).

144. Hos, B. J. *et al.* Cancer-specific T helper shared and neo-epitopes uncovered by expression of the MHC class II master regulator CIITA. *Cell Rep.* **41**, 111485 (2022).

145. Quezada, S. A. *et al.* Tumor-reactive CD4+ T cells develop cytotoxic activity and eradicate large established melanoma after transfer into lymphopenic hosts. *Journal of Experimental Medicine* **207**, 637–650 (2010).

146. Takeuchi, A. *et al.* CRTAM determines the CD4+ cytotoxic T lymphocyte lineage. *Journal of Experimental Medicine* **213**, 123–138 (2016).

147. Kruse, B. *et al.* CD4+ T cell-induced inflammatory cell death controls immune-evasive tumours. *Nature* **618**, 1033–1040 (2023).

148. Ott, P. A. *et al.* An immunogenic personal neoantigen vaccine for patients with melanoma. *Nature* **547**, 217–221 (2017).

149. Keskin, D. B. *et al.* Neoantigen vaccine generates intratumoral T cell responses in phase Ib glioblastoma trial. *Nature* **565**, 234–239 (2019).

150. Hu, Z. *et al.* Personal neoantigen vaccines induce persistent memory T cell responses and epitope spreading in patients with melanoma. *Nat. Med.* **27**, 515–525 (2021).

151. Schreiber, T. H., Wolf, D., Bodero, M. & Podack, E. Tumor antigen specific iTreg accumulate in the tumor microenvironment and suppress therapeutic vaccination. *Oncoimmunology* **1**, 642–648 (2012).

152. Zhou, G., Drake, C. G. & Levitsky, H. I. Amplification of tumor-specific regulatory T cells following therapeutic cancer vaccines. *Blood* **107**, 628–636 (2006).

153. Welters, M. J. P. *et al.* Success or failure of vaccination for HPV16-positive vulvar lesions correlates with kinetics and phenotype of induced T-cell responses. *Proceedings of the National Academy of Sciences* **107**, 11895–11899 (2010).

154. Saxena, M., van der Burg, S. H., Melief, C. J. M. & Bhardwaj, N. Therapeutic cancer vaccines. *Nature Reviews Cancer* vol. 21 360–378 Preprint at https://doi.org/10.1038/s41568-021-00346-0 (2021)

Appendix

Nederlandse Samenvatting

Hoe CD4⁺ T-cel hulp functionele en disfunctionele CD8⁺ T-cel differentiatie vormgeeft

Ons afweersysteem, of immuunsysteem, beschermt ons tegen infecties door bacteriën, virussen en parasieten. Dit gebeurt via het onschadelijk maken en opruimen van de ziekteverwekkers zelf, maar ook door het herkennen en doden van geïnfecteerde lichaamscellen. Ook kan het immuunsysteem kankercellen herkennen en doden, omdat kankercellen er anders uitzien dan gezonde lichaamscellen.

Het afweersysteem is een complexe samenwerking van verschillende soorten immuuncellen met elk hun eigen functie. Het kan worden opgedeeld in twee armen, de zogenaamde 'aangeboren afweer' en de 'verworven afweer'. Het aangeboren afweersysteem vormt de eerste barrière tegen ziekteverwekkers en geeft een snelle, brede respons die ook leidt tot de activatie van het verworven afweersysteem. Het verworven afweersysteem komt wat later op gang maar werkt heel gericht tegen een bepaalde ziekteverwekker. Het vormt ook een zogenaamd 'geheugen' waardoor het de volgende keer diezelfde ziekteverwekker nog sneller en efficiënter kan aanvallen. Dit principe van immunologisch geheugen wordt gebruikt bij vaccinatie. Tijdens vaccinatie wordt ons immuunsysteem blootgesteld aan een kleine hoeveelheid ziekteverwekkers, zoals deeltjes van een virus, wat zorgt voor het vormen van geheugencellen. Deze geheugencellen kunnen bij een tweede blootstelling aan hetzelfde virus direct een efficiënte immuunrespons in gang zetten die je beschermt tegen infectie. Je bent dan immuun.

Twee belangrijke soorten immuuncellen van het verworven afweersysteem zijn B cellen en T cellen. B cellen maken antilichamen, dat zijn moleculen die specifiek kunnen binden aan een bepaald doelwit, zoals een ziekteverwekker. Door de binding van antilichamen kunnen ziekteverwekkers onschadelijk worden gemaakt, of beter worden gezien en opgeruimd door cellen van het immuunsysteem. In mijn proefschrift focus ik op T cellen. T cellen kunnen specifiek lichaamscellen herkennen die er anders uitzien dan normaal, bijvoorbeeld omdat ze geïnfecteerd zijn met een virus, of omdat ze zijn veranderd in tumorcellen. T cellen spelen dus ook een belangrijke rol in de immuunrespons tegen kanker.

T cellen hebben een soort antenne, genaamd de T-cel receptor, waarmee ze kleine stukjes eiwit, genaamd antigeen, kunnen herkennen. De zogenaamde vechter T cellen, of $CD8^+$ T cellen, kunnen geïnfecteerde lichaamscellen of tumorcellen doden. Daarnaast heb je de helper T cellen, of $CD4^+$ T cellen, die hulp kunnen bieden aan $CD8^+$ T cellen of B cellen. Voor dit proefschrift heb ik onderzoek gedaan naar de rol van $CD4^+$ T cel hulp aan $CD8^+$ T cellen tijdens hun activatie.

Hoofdstuk 1

In dit hoofdstuk introduceer ik het onderwerp en leg ik uit hoe $CD4^+$ T cel hulp tijdens $CD8^+$ T cel activatie werkt.

Voordat een T cel zijn werk kan gaan doen moet hij eerst geactiveerd worden. Dit geldt zowel voor $CD8^+$ als voor $CD4^+$ T cellen. Ons lichaam kent een heel divers repertoire aan T cellen, die allemaal iets anders kunnen herkennen. Alleen de T cellen die specifiek een bepaald antigeen herkennen zullen worden geactiveerd wanneer dit antigeen in het lichaam aanwezig is. Dit heet een antigeen-specifieke T cel respons. T cellen die 'hun' antigeen nog nooit hebben gezien, noemen we naïeve T cellen.

Naïeve T cellen worden geactiveerd door andere immuuncellen, genaamd antigeen-presenterende cellen (APCs). Dendritische cellen (DCs), een bepaald soort APCs, kunnen in weefsel resten van dode cellen opeten. Ze verwerken de celresten, presenteren de antigenen die daarbij vrijkomen op hun oppervlakte en migreren vervolgens naar de lymfeknopen om daar de antigenen aan T cellen te laten zien. Naast het presenteren van antigenen geven de DCs ook andere activerende signalen door aan T cellen. Dit gebeurt via direct cel-cel contact (genaamd costimulatie) en via uitgescheiden moleculen (genaamd cytokines). Dit proces waarbij T cellen worden geactiveerd door DCs noemen we ook wel priming. Als een T cel geprimed is gaat hij zich vermenigvuldigen en ontwikkelt hij bepaalde eigenschappen die nodig zijn voor zijn functie. Dit ontwikkelproces heet T-cel differentiatie. Vervolgens verlaat de T cel de lymfeknoop en reist hij via het bloed naar de weefsels waar hij zijn werk kan doen.

De priming van $CD8^+$ T cellen gebeurt in twee stappen. Tijdens de eerste stap wordt de $CD8^+$ T cel wel geactiveerd door een DC, maar krijgt hij nog geen hulp. Bij de tweede stap kan een $CD4^+$ helper T cel hulp afleveren aan een DC, specifiek aan een subtype genaamd cDC1, die deze hulp vervolgens weer door kan geven aan de $CD8^+$ T cel. 'Hulp' bestaat hierbij uit meerdere activatiesignalen (costimulatie en cytokines) die worden doorgegeven tussen cellen. Eerdere onderzoeken hebben laten zien dat $CD4^+$ T-cel hulp heel belangrijk is voor het vormen van goede vechter $CD8^+$ T cellen tijdens virusinfecties en kanker.

Hoofdstuk 2

In dit hoofdstuk hebben we onderzocht wat de rol is van $CD4^+$ T-cel hulp voor de vorming van $CD8^+$ geheugencellen.

Zoals eerder genoemd kunnen cellen van het verworven afweersysteem, zoals $CD8^+$ T cellen, ook geheugencellen worden. In tegenstelling tot vechtercellen die maar kort leven, blijven de geheugencellen lang in leven, ook nog nadat een infectie is afgelopen. Bij een tweede

blootstelling aan hetzelfde antigeen komen de geheugencellen extra snel in actie. Centrale geheugencellen (T_{CM}) kunnen dan heel hard gaan delen, terwijl effector geheugencellen (T_{EM}) snel hun vechtersfunctie kunnen gaan uitoefenen.

Om te onderzoeken wat de rol is van $CD4^+$ T-cel hulp voor de formatie en functie van $CD8^+$ geheugencellen hebben we gebruikgemaakt van proefdieren, muizen, die werden gevaccineerd met twee soorten vaccins. Door het ene vaccin (Help) werden zowel $CD8^+$ T cellen als $CD4^+$ T cellen geactiveerd, waardoor de $CD4^+$ T cellen de $CD8^+$ T cellen konden gaan helpen. Door het andere vaccin (No Help) werden alleen de $CD8^+$ T cellen geactiveerd, die dus niet geholpen konden worden door $CD4^+$ T cellen. We zagen dat in muizen die gevaccineerd waren met het Help vaccin de geholpen T_{CM} cellen langer in stand gehouden werden, en dat er veel meer T_{EM} cellen gevormd werden. Geholpen T_{EM} cellen leken qua profiel erg op geholpen vechtercellen. Wanneer we de muizen een tweede keer vaccineerden, hoefden de geholpen $CD8^+$ T cellen niet nog een keer $CD4^+$ T-cel hulp te ontvangen maar konden ze meteen een robuuste respons geven. Kortom, $CD8^+$ T cellen die $CD4^+$ T-cel hulp hebben ontvangen tijdens hun priming, 'onthouden' dit en kunnen de volgende keer hulp-onafhankelijk reageren.

Hoofdstuk 3

In dit hoofdstuk laat ik zien dat ongeholpen $CD8^+$ T cellen erg lijken op zogenaamde 'stem-like' cellen in chronische infectie en kanker, en stel ik voor dat dit misschien wel dezelfde cellen zijn.

In chronische infectie en kanker werken $CD8^+$ T cellen vaak niet goed. Ze delen minder, ze zien er anders uit en ze kunnen niet goed hun doelwitcellen doden. Deze disfunctionele staat wordt uitputting genoemd, of 'exhaustion' in het Engels. Wetenschappers dachten vroeger dat uitgeputte $CD8^+$ T cellen worden gevormd door vechtercellen die te lang aan hun doelwit waren blootgesteld. Echter, in de afgelopen jaren heeft nieuw onderzoek aangetoond dat uitgeputte cellen niet ontstaan uit vechtercellen, maar uit voorloper cellen, die in het Engels 'stem-like' cellen genoemd worden. In dit hoofdstuk vat ik de wetenschappelijke literatuur samen over dit onderwerp. Vervolgens onderzoek ik in hoeverre stem-like cellen uit kanker of chronische infectie lijken op ongeholpen cellen zoals wij ze zien in ons vaccinatiemodel. Dit doe ik op basis van de genexpressieprofielen van deze cellen, dat laat zien welke genen (stukjes DNA) een cel op dat moment actief gebruikt om eiwitten van te maken. Het genexpressieprofiel zegt iets over de identiteit, differentiatiestaat en functie van een cel, en kan worden vergeleken tussen cellen. Door de profielen van onze ongeholpen cellen te vergelijken met die van stem-like en uitgeputte cellen, afkomstig uit gepubliceerde datasets van andere onderzoeksgroepen, kwam ik tot de conclusie dat stem-like cellen qua genexpressieprofiel erg lijken op ongeholpen cellen.

Op basis van de genexpressiedata en het literatuuronderzoek, stel ik in dit hoofdstuk een nieuwe theorie voor: De voorlopers van uitgeputte $CD8^+$ T cellen in chronische infectie en kanker, de stem-like cellen dus, worden gevormd als gevolg van priming zonder $CD4^+$ T-cel hulp. In dit model, wat ik het 'ongeholpen disfunctiemodel' noem, zijn stem-like cellen en ongeholpen cellen dus hetzelfde.

Hoofdstuk 4

In dit hoofdstuk hebben we het 'ongeholpen disfunctiemodel' uit Hoofdstuk 3 onderbouwd met experimenteel bewijs.

Door gebruik te maken van hetzelfde vaccinatiemodel als in Hoofdstuk 2, hebben we laten zien dat naïeve $CD8^+$ T cellen na priming een heel spectrum aan differentiatiestaten kunnen vormen. Van minst tot meest ontwikkeld bestaat dit spectrum uit T_{CM} cellen, stem-like cellen, T_{EM} cellen en als laatste de vechtercellen. $CD4^+$ T-cel hulp schuift dit spectrum op, in de richting van de vechtercellen. We laten zien dat in muizen die gevaccineerd worden zonder $CD4^+$ T-cel hulp de $CD8^+$ T cellen blijven steken in de stem-like staat. Echter, deze ongeholpen cellen kunnen zich alsnog verder ontwikkelen tot vechtercellen wanneer ze $CD4^+$ T-cel hulp ontvangen.

Vervolgens hebben we gekeken naar $CD8^+$ T-cel differentiatie in tumoren. In een immunogeen muismodel van darmkanker zagen we dat er wel tumor-specifieke stem-like $CD8^+$ T cellen, maar geen geholpen vechtercellen werden gevormd. Zelfs als we de tumorcellen expres $CD4^+$ T-cel activerende antigenen lieten maken, en de $CD4^+$ T cellen ook daadwerkelijk werden geactiveerd, dan nog ontstonden de geholpen vechtercellen niet. Deze resultaten suggereren dat in tumoren $CD4^+$ T-cel hulp waarschijnlijk niet goed wordt doorgegeven aan $CD8^+$ T cellen door DCs. Dit zou een belangrijke verklaring kunnen zijn waarom $CD8^+$ T cellen in kanker hun functie niet goed kunnen uitoefenen, en uiteindelijk uitgeput raken.

Hoofdstuk 5

In dit hoofdstuk hebben we de differentiatie van $CD4^+$ T cellen onderzocht, en gevonden dat voorloper $CD4^+$ T cellen zich kunnen ontwikkelen tot T helper 1 (Th1) cellen of folliculaire helper (Tfh) cellen, afhankelijk van hun interacties met andere immuuncellen.

Zoals eerder genoemd kunnen $CD4^+$ T cellen hulp bieden aan $CD8^+$ T cellen of aan B cellen. Dit wordt gedaan door verschillende subtypes van $CD4^+$ T cellen: Th1 cellen helpen $CD8^+$ T cellen bij hun differentiatie tot vechtercellen, en Tfh cellen helpen B cellen bij het maken van effectieve antilichamen. In dit hoofdstuk hebben we laten zien dat Th1 cellen en Tfh cellen afkomstig zijn uit dezelfde Th1/Tfh voorloper. Deze voorlopers worden gevormd wanneer naïeve $CD4^+$ T-cellen hun eerste stap van priming hebben doorlopen. Of ze vervolgens een Th1 of een Tfh cel worden hangt

af van de tweede stap van priming: Gebeurt dit door interactie met een cDC1 dan wordt de $CD4^+$ T cel een Th1 cel, maar gebeurt dit door interactie met een B cel dan wordt de $CD4^+$ T cel een Tfh cel. Ook de costimulatie signalen die worden doorgegeven verschillen tussen deze scenario's.

Hoofdstuk 6

In dit hoofdstuk hebben we literatuuronderzoek gedaan naar het belang van Type I interferon (IFN-I) voor het mogelijk maken van $CD4^+$ T-cel hulp aan $CD8^+$ T cellen in kanker.

IFN-I is een cytokine (signaalstof) die wordt uitgescheiden door immuuncellen of andere lichaamscellen op het moment dat ze ziekteverwekkers of schade tegenkomen. Dit signaal werkt als een soort alarmbel: hier is iets aan de hand, het immuunsysteem moet in actie komen! IFN-I zorgt ervoor dat DC (tumor)antigenen beter kunnen presenteren, gaan migreren naar de lymfeknopen en costimulatie moleculen op hun oppervlakte krijgen. Hierdoor kunnen ze beter T cellen activeren.

Ook in de lymfeknoop zelf speelt IFN-I een belangrijke rol, het zorgt er namelijk voor dat T cellen en cDC1 cellen het platform kunnen vormen waarbij $CD4^+$ T-cel hulp wordt doorgegeven via de cDC1 aan de $CD8^+$ T cel. Kortom, IFN-I is cruciaal voor $CD4^+$ T-cel hulp. Echter, in tumoren wordt er vaak maar weinig IFN-I geproduceerd. Dit zou een belangrijke onderliggende reden kunnen zijn waarom $CD4^+$ T-cel hulp aan tumor-specifieke $CD8^+$ T cellen niet goed op gang komt, en de $CD8^+$ T cellen dus disfunctioneel worden.

Hoofdstuk 7

In dit hoofdstuk hebben we literatuuronderzoek gedaan naar de werking van PD-1 blokkade, de op dit moment meest gebruikte en succesvolste immuuntherapie in kankerpatiënten. Ook leggen we uit hoe onze theorie over $CD4^+$ T-cel hulp bepaalde mechanismes achter de werking van PD-1 blokkade in kanker kan verklaren.

PD-1 is een receptor, dat wil zeggen een molecuul aan de buitenkant van de cel dat signalen door kan geven, op bepaalde T cellen en andere immuuncellen. Wanneer PD-1 bindt aan zijn bindingspartner PD-L1 wordt er een negatief signaal de cel in gestuurd wat de cel afremt in zijn functie. PD-1 is dus een remmende receptor. Door deze receptor te blokkeren valt de rem weg en zou bijvoorbeeld een $CD8^+$ T cel beter zijn werk kunnen gaan doen. PD-1 zit niet op alle $CD8^+$ T cellen, maar met name op uitgeputte cellen en op stem-like cellen. PD-L1 kan zitten op tumorcellen of op immuuncellen.

Vroeger werd gedacht dat PD-1 blokkerende immuuntherapie, die wordt gebruikt in kanker, werkt op uitgeputte $CD8^+$ T cellen in de tumor. De uitgeputte cellen zouden daardoor hun rem verliezen en weer actief kunnen worden. Recentere studies laten echter zien dat het niet de uitgeputte cellen, maar de stem-like cellen zijn die reageren op PD-1 blokkade. Volgens ons 'ongeholpen disfunctiemodel' zijn stem-like cellen gelijk aan ongeholpen cellen, en dit betekent dat juist ongeholpen $CD8^+$ T cellen baat hebben bij PD-1 blokkerende therapie. In dit hoofdstuk stellen we voor dat PD-1 blokkade de signalen van $CD4^+$ T-cel hulp deels kan nabootsen. Echter, sinds de publicatie van dit werk in 2021 zijn er weer nieuwe inzichten bijgekomen die erop wijzen dat PD-1 blokkade niet alleen $CD4^+$ T-cel hulp zou kunnen nabootsen, maar ook de $CD4^+$ T-cellen zelf zou kunnen activeren waardoor deze hulp kunnen bieden aan de $CD8^+$ T cellen.

Hoofdstuk 8

In dit hoofdstuk plaats ik de bevindingen en concepten uit dit proefschrift in de bredere context van de bestaande wetenschappelijke literatuur.

Ik ga dieper in op het 'ongeholpen disfunctiemodel' en benoem waar deze theorie aansluit, en waar hij juist botst met bevindingen van andere onderzoekers. Ik ga in op welke vragen er nu beantwoord zijn, en welke nog open liggen. Ook beschrijf ik de klinische relevantie van mijn werk: Wat betekent dit voor de behandeling van kankerpatiënten met immuuntherapie?

Samenvattend, in dit proefschrift stel ik een nieuwe theorie voor over $CD8^+$ T-cel differentiatie, en onderbouw ik deze theorie met experimenteel bewijs. Ik laat zien dat $CD4^+$ T-cel hulp het differentiatiespectrum van $CD8^+$ T cellen opschuift richting vechtercellen. Bovendien identificeer ik een gebrek aan $CD4^+$ T-cel hulp als belangrijk onderliggend mechanisme voor het vormen van stem-like en uiteindelijk uitgeputte $CD8^+$ T cellen in kanker. Deze bevindingen bieden een nieuw perspectief om eerder onderzoek over T cellen in kanker te herinterpreteren. Ook benadrukken ze dat $CD4^+$ T-cel hulp een belangrijk aspect is om te begrijpen en rekening mee te houden bij het ontwikkelen van nieuwe immuuntherapieën tegen kanker.

English Summary

How $CD4^+$ T-cell help shapes functional and dysfunctional $CD8^+$ T-cell differentiation

Our immune system protects us against infections by bacteria, viruses and parasites. This happens by attacking these pathogens themselves, but also by recognizing and killing infected body cells. The immune system can also recognize and kill cancer cells, because cancer cells look different than healthy cells.

The immune system is a complex interplay between different types of immune cells, each with their own function. It can be divided in two arms, the so-called 'innate immunity' and 'adaptive immunity'. The innate immune system forms the first barrier against pathogens and elicits a fast, broad response that also leads to the activation of the adaptive immune system. The adaptive immune system starts up a bit later but works very specifically against a certain pathogen. It also forms so-called 'memory', which enables it to attack the same pathogen even faster and more efficiently the next time. This principle of immunological memory is used in vaccination. During vaccination our immune system is exposed to a small amount of pathogen, such as virus particles, which drives the formation of memory cells. These memory cells can quickly induce an effective immune response upon a second exposure to the same virus, which protects you from infection. You are then immune.

Two important cell types of the adaptive immune system are B cells and T cells. B cells make antibodies, these are molecules that can bind specifically to a target, such as a pathogen. Binding of antibodies can disarm pathogens, or makes them more easy to be seen and killed by immune cells. In my thesis I focus on T cells. T cells can specifically recognize cells that look different from normal, for example because they have been infected by a virus, or because they have turned into tumor cells. Thus, T cells play an important role in the immune response against cancer.

T cells have a sort of antenna, called the T-cell receptor, which they use to recognize small pieces of protein, called antigens. The so-called cytotoxic T cells, or $CD8^+$ T cells, can kill infected body cells or tumor cells. In addition there are the helper T cells, or $CD4^+$ T cells, which can help $CD8^+$ T cells or B cells. In this thesis I investigated the role of $CD4^+$ T-cell help to $CD8^+$ T cells during their activation.

Chapter 1

In this chapter I introduce the subject and explain how $CD4^+$ T-cell help during $CD8^+$ T-cell activation works.

Before a T cell can do its job it needs to be activated. This is true for both $CD8^+$ and $CD4^+$ T cells. Our body has a diverse repertoire of T cells, that all recognize something different. Only the T cells that recognize a specific antigen will be activated when this antigen is present in the body.

This is called an antigen-specific T-cell response. T cells that have never seen 'their' antigen are called naïve T cells.

Naïve T cells are activated by other immune cells, called antigen-presenting cells (APCs). Dendritic cells (DCs), a subset of APCs, can take up parts of dead cells in tissues. They process the debris, present the antigens that are produced on their surface, and subsequently migrate to the lymph nodes to show the antigens to T cells. Besides presenting antigens, DCs also pass on other activating signals to T cells. This happens via direct cell-cell contact (called costimulation) and via secreted molecules (called cytokines). This process where T cells are activated by DCs is also called priming. If a T cell is primed, it starts to divide and develop specific traits that are necessary for its function. This development process is called T-cell differentiation. Next, the T cell leaves the lymph node and travels via the blood to the tissues where it can do its work.

The priming of $CD8^+$ T cells happens in two steps. During the first step the T cell becomes activated by a DC, but it does not yet receive help. During the second step, a $CD4^+$ T cell can deliver help to a DC, specifically to a subtype called cDC1, which subsequently can deliver this help to the $CD8^+$ T cell. In this scenario, 'help' consists of multiple activation signals (costimulation and cytokines) that are passed on between cells. Previous studies have shown that $CD4^+$ T-cell help is crucial to generate properly functional effector $CD8^+$ T cells during virus infections and cancer.

Chapter 2

In this chapter we investigated the role of $CD4^+$ T-cell help for the formation of $CD8^+$ memory T cells.

As mentioned previously, cells of the adaptive immune system, such as $CD8^+$ T cells, can also form memory cells. In contrast to cytotoxic effector cells, which are short-lived, memory cells are maintained long-term, even after an infection is cleared. Upon a second encounter with the same antigen, memory T cells respond extra quickly. Central memory (T_{CM}) cells start dividing a lot, while effector memory (T_{EM}) cells rapidly exert their cytotoxic effector function.

To investigate the role of $CD4^+$ T-cell help for the formation and function of $CD8^+$ memory T cells, we used laboratory animals, mice, which were vaccinated with two types of vaccines. One vaccine (Help) activated both $CD8^+$ and $CD4^+$ T cells, whereby $CD4^+$ T cells could provide help to the $CD8^+$ T cells. The other vaccine (No Help) only activated $CD8^+$ T cells, which could therefore not be helped by the $CD4^+$ T cells. In mice that were vaccinated with the Help vaccine, we saw that helped T_{CM} cells were maintained longer, and many more T_{EM} cells were formed. The profile of helped T_{EM} cells was very similar to helped effector $CD8^+$ T cells. When we vaccinated the mice a second time, the helped $CD8^+$ T cells did not need to receive $CD4^+$ T-cell help a second time, but

could already mount a robust response. Thus, $CD8^+$ T cells 'remember' that they have received $CD4^+$ T cells during priming, and can respond help-independently during a secondary challenge.

Chapter 3

In this chapter I show that helpless $CD8^+$ T cells resemble so-called 'stem-like' cells in chronic infection and cancer, and I propose that these may be the same cells.

In chronic infection and cancer, $CD8^+$ T cells often don't work very well. They divide less, they look different and they are unable to kill their target cells. This dysfunctional state is called exhaustion. Previously, researchers believed that exhausted $CD8^+$ T cells were generated from effector cells that were exposed to their target for too long. However, in the past years, new studies have shown that exhausted cells do not originate from effector cells, but from a precursor population called 'stem-like' cells. In this chapter I summarize the scientific literature on this subject. Next, I investigate to which extent stem-like cells from cancer or chronic infection resemble un-helped, or 'helpless' cells from our vaccination model. This is done based on the gene expression profiles of these cells, showing which genes (parts of DNA) are actively used by a cell to make proteins. The gene expression profile says something about identity, differentiation state and function of a cell, and can be compared between different cells. By comparing the profiles of our helpless cells to those of stem-like and exhausted cells, obtained from published datasets by other research groups, I concluded that stem-like cells strongly resemble helpless cells based on their gene expression profile.

Based on the gene expression data and literature review, in this chapter I propose a new theory: The precursors of exhausted $CD8^+$ T cells in chronic infection and cancer, which are the stem-like cells, are formed as a result of priming in absence of $CD4^+$ T-cell help. In this model, which I call the 'helpless dysfunction model', stem-like cells and helpless cells are the same.

Chapter 4

In this chapter we supported the 'helpless dysfunction model' from Chapter 3 with experimental evidence.

Using the same vaccination model as in Chapter 2, we showed that when naïve $CD8^+$ T cells are primed, they adopt a whole spectrum of differentiation states. From least to most developed, this spectrum consists of T_{CM} cells, stem-like cells, T_{EM} cells and lastly the cytotoxic effector cells. $CD4^+$ T-cell help shifts this spectrum, in the direction of more effector-like. We show that in mice that are vaccinated without $CD4^+$ T-cell help, $CD8^+$ T cells get stuck in the stem-like state. However, these helpless cells can still develop further into effector cells upon receiving $CD4^+$ T-cell help.

Next, we looked at $CD8^+$ T-cell differentiation in tumors. In an immunogenic mouse model of colon cancer, we saw formation of tumor-specific stem-like $CD8^+$ T cells, but not helped effector cells. Even when we manipulated the tumor cells to express $CD4^+$ T-cell activating antigens, and $CD4^+$ T cells were actually activated, still helped effector cells were not generated. These results suggest that in tumors, $CD4^+$ T-cell help delivery to $CD8^+$ T cells by DCs is probably impaired. This could be an important explanation why $CD8^+$ T cells do not exert their functions properly in cancer, and eventually become exhausted.

Chapter 5

In this chapter we investigated the differentiation of $CD4^+$ T cells, and found that precursor $CD4^+$ T cells can develop into T helper 1 (Th1) cells or follicular helper (Tfh) cells, depending on their interactions with other immune cells.

As mentioned previously, $CD4^+$ T cells can offer help to $CD8^+$ T cells or to B cells. This is done by different subtypes of $CD4^+$ T cells: Th1 cells help $CD8^+$ T cells differentiate into effector cells, and Tfh cells help B cells make effective antibodies. In this chapter we showed that Th1 cells and Tfh cells originate from the same Th1/Tfh precursor. These precursors are formed when naïve $CD4^+$ T cells undergo their first step of priming. Whether they become a Th1 or Tfh after this depends on the second step of priming: If this happens through interaction with a cDC1 the $CD4^+$ T cell becomes a Th1 cell, but if this happens through interaction with a B cells the CD4+ T cell becomes a Tfh cell. Also the costimulation signals that are passed on differ between these scenarios.

Chapter 6

In this chapter we reviewed the scientific literature about the importance of Type I interferon (IFN-I) for orchestrating $CD4^+$ T-cell help to $CD8^+$ T cells in cancer.

IFN-I is a cytokine (messenger molecule) which is secreted by immune cells or other cells when they encounter pathogens or damage. This signal works like an alarm bell: something is going on here, the immune system needs to be activated! IFN-I induces better (tumor) antigen presentation by DCs, as well as better migration to the lymph nodes and upregulation of costimulatory molecules. Due to these effects, DCs can activate T cells better.

Also within the lymph node IFN-I plays an important role, by allowing T cells and cDC1 cells to form the platform in which $CD4^+$ T-cell help is delivered through the cDC1 to the $CD8^+$ T cell. Thus, IFN-I is crucial for $CD4^+$ T-cell help. However, in tumors there is often a lack of IFN-I production. This could be an important underlying mechanism why $CD4^+$ T-cell help to tumor-specific $CD8^+$ T cells can not be delivered well, and the $CD8^+$ T cells become dysfunctional.

Chapter 7

In this chapter we reviewed the scientific literature about the mechanisms of action of PD-1 blockade, currently the most used and successful immune therapy in cancer patients. We also explain how our theory about $CD4^+$ T-cell help can explain certain mechanisms of action of PD-1 blockade in cancer.

PD-1 is a receptor, that means a molecule on the outside of a cell that can transmit signals into the cell, on certain types of T cells and other immune cells. When PD-1 binds to its binding partner PD-L1, a negative signal is sent into the cell, which inhibits it function. Thus, PD-1 is an inhibitory receptor. By blocking this receptor, the brake is released and this would enhance the function of for example a $CD8^+$ T cell. PD-1 is not present on all $CD8^+$ T cells, but especially on exhausted cells and on stem-like cells. PD-L1 can be on tumor cells or on immune cells.

Previously, it was thought that PD-1 blocking immune therapy, which is used in cancer, acts on exhausted $CD8^+$ T cells in the tumor. The exhausted cells would thereby lose their brake and become active again. However, more recent studies show that it is not the exhausted cells, but the stem-like cells that respond to PD-1 blockade. According to our 'helpless dysfunction model', stem-like cells equal helpless cells, and this means that it is the helpless $CD8^+$ T cells that benefit from PD-1 blocking therapy. In this chapter we suggest that PD-1 blockade can partly mimic the $CD4^+$ T-cell help signals. However, since the publication of this work in 2021, novel studies indicate that PD-1 blockade does not only mimic $CD4^+$ T-cell help signals but also activates $CD4^+$ T cells themselves, allowing for $CD4^+$ T-cell help delivery to take place.

Chapter 8

In this chapter I place the findings and concepts from this thesis in the broader context of the existing scientific literature.

I expand on the ' helpless dysfunction model' and discuss where this theory aligns, and where it opposes findings from other scientists. I discuss which questions are now answered, an which are still open. Also I describe the clinical relevance of my work: What does this mean for treatment of cancer patients with immune therapies?

In conclusion, in this thesis I propose a new theory about $CD8^+$ T-cell differentiation, and I support this theory with experimental evidence. I show that $CD4^+$ T-cell help shifts the differentiation spectrum of $CD8^+$ T cells in the direction of more effector-like. Moreover, I identify a lack of $CD4^+$ T-cell help as important underlying mechanism for the formation of stem-like, and eventually exhausted $CD8^+$ T cells in cancer. These findings offer a new perspective to re-interpret previous studies about $CD8^+$ T cells in cancer. They also highlight $CD4^+$ T-cell help as an important aspect to understand and consider during the development of new immune therapies against cancer.

Curriculum Vitae

Julia Laura Charlotte Busselaar was born on 10th January 1994 in Amsterdam, the Netherlands. She completed her pre-university education cum laude at the Vossius Gymnasium in Amsterdam in 2012. In the same year, Julia started her bachelor studies Biomedical Sciences at the University of Amsterdam, which she completed in 2015. In 2016, she took a gap year in which she worked for the university as supervisor for 1st and 2nd year bachelor students during their practical courses. Subsequently she enrolled in the master's Biomedical Sciences at the University of Amsterdam, with a specialization in oncology. During this time she performed her first internship in the group of Jannie Borst at the Netherlands Cancer Institute. Under supervision of Sander de Kivit, she developed a new *in vitro* platform for delivering deliberate costimulatory and coinhibitory signals to human T cells, which was later published. Julia performed her second internship at the VUmc Cancer Center Amsterdam in the group of Victor van Beusechem. Under supervision of Maxime Blijlevens, she studied the relationship between p53 transcriptional activity and cisplatin sensitivity in human lung cancer. This was followed by completing the Article 9 course for working with laboratory animals at the University of Amsterdam, and writing her master thesis in the group of Yvette van Kooyk at the VUmc, about therapeutic vaccinations in infection and cancer. After obtaining her Master's degree cum laude in 2018, Julia re-joined the group of Jannie Borst at the NKI as a PhD candidate. She continued her PhD research at the LUMC in Leiden, when the Borst lab moved there in 2019. The results of her studies are presented in this thesis. Currently, Julia works as a postdoctoral researcher in the group of Linde Meyaard at UMC Utrecht, where she investigates novel ways of blocking immune inhibitory receptors.

Portfolio

Factual narrative of the PhD trajectory

In September 2018, Julia joined the lab of professor Jannie Borst at the Netherlands Cancer Institute (NKI) as PhD candidate. She was appointed on a project on the molecular mechanisms of $CD4^+$ T-cell help to $CD8^+$ T cells, which was initiated by a previous PhD student, Tomasz Ahrends. Her first task was to analyse an RNA sequencing dataset generated by Tomasz just before he left the lab, and incorporate this data into the revision of his final paper. Unexpectedly, the results from this additional dataset shifted the interpretation of Tomasz's data and total concept of the paper. Julia generated and adapted figures, reinterpreted the data and wrote the revised version of the manuscript based on this new concept (Chapter 2 of this thesis), which was crucial for its acceptance for publication.

In May 2019, 8 months after Julia started, the Borst group moved from the NKI to the Leiden University Medical Center (LUMC). At that time Julia was the only group member that would be performing mouse experiments at the new institute, which meant that she also took care of all the paperwork, ethical approval of experimental protocols and the transfer of genetically modified mice to the LUMC. Together with Douwe Bosma, who joined the lab as a PhD student in October 2019, she re-established the murine *in vivo* DNA tattoo vaccination model, testing various strategies to optimize the induced T cell responses.

The process of moving to the LUMC took several months, which Julia used to dive deep into the literature on T cell biology. During this time she developed a new theory about T cell differentiation, namely that $CD4^+$ T-cell help shifts the differentiation spectrum of $CD8^+$ T cells, and that 'exhausted' $CD8^+$ T cells in cancer are formed from incompletely differentiated 'helpless' cells. Julia enthusiastically presented her theory to her promotor Jannie, who was initially reluctant to divert Julia's project but agreed to let her write a perspective article on it during the first Covid-19 lockdown in spring 2020. This resulted in a publication (Chapter 3 of this thesis), which also convinced Jannie of the new theory and its importance. Despite the highly competitive nature of the T-cell exhaustion field, Jannie agreed to let Julia divert her project and investigate her differentiation model experimentally.

Over the next few years, together with Douwe, Julia designed and performed experiments to test the new hypothesis. From the same *in vivo* mouse experiments, they both performed data-analysis individually, whereby Julia focused on the $CD8^+$ T cells and Douwe on the $CD4^+$ T cells (resulting in Chapter 4 and 5 of this thesis). When the research group generated a large single cell RNA and TCR sequencing dataset of $CD4^+$ and $CD8^+$ T cells but had no bioinformatician to analyse it, Julia taught herself R programming language so that she could perform the analyses independently. These data were used both in her own project and in the work of Douwe.

She also closely collaborated with PhD students Mo Staal and Elselien Frijlink, together forming the 'mouse team' of the Borst group. Julia followed several PhD courses and attended many scientific conferences, where she also presented her own work.

In the meantime, Julia kept up with all the literature in the exhaustion field, and noticed that many of other people's findings could be explained beautifully by the new differentiation model. In 2021, she contributed as a second author to an invited review written by her promotor Jannie, highlighting the importance of $CD4^+$ T-cell help for explaining the biological mechanisms of PD-1 blockade therapy (Chapter 7 of this thesis).

In 2022, Julia contributed substantially to the application for a new CCD licence for *in vivo* animal studies, which provided valuable insights into ethical and regulatory processes. In 2023, she supervised the writing assignment of Merel Sijbranda, a master student Infection and Immunity at Utrecht University. Julia later adapted this writing assignment into a review about the importance of Type-I interferon signaling in $CD4^+$ T-cell help delivery (Chapter 6 of this thesis), which was published in 2024.

In December 2024, Julia concluded her PhD at the LUMC. In 2025 she became a mother and focused on her new family, while also writing the revision of her final paper. This work, which provided substantial experimental evidence for the new T cell differentiation model (Chapter 4 of this thesis), was eventually published in 2026. Also the main work of Douwe, to which Julia contributed (Chapter 5 of this thesis), was published in 2026.

CRediT Table

CRediT table for the thesis of Julia Busselaar

Ch.	Type*	Short Title	Conceptualization	Data Curation	Formal Analysis	Funding Acquisition	Investigation	Methodology	Project Administration	Resources	Software	Supervision	Validation	Visualization	Writing – Original Draft	Writing – Review & Editing	Preregistered	Preprinted	Published with Peer Review
1	Introduction	Chapter 1. Introduction															☐	☐	☐
2	PhD project chapter	Chapter 2. Memory															☐	☐	☑
3	PhD project chapter	Chapter 3. Helpless dysfunction															☐	☐	☑
4	PhD project chapter	Chapter 4. CD8 differentiation															☐	☐	☑
5	PhD project chapter	Chapter 5. CD4 differentiation															☐	☐	☑
6	PhD project chapter	Chapter 6. IFN															☐	☐	☑
7	PhD project chapter	Chapter 7. PD-1															☐	☐	☑
8	Discussion	Chapter 8. Discussion															☐	☐	☐

*PhD project chapters are the direct result of the PhD project of the PhD candidate.
Some theses also include Collaboration Chapters, to which the PhD candidate has contributed but fall outside the PhD project.

Left to right colored:
Conceptualization, Data curation, Formal analysis, Funding acquisition, Investigation, Methodology, Project administration, Resources, Software, Supervision, Validation, Visualization, Writing – Original draft, Writing – Review and editing.

Color scale:

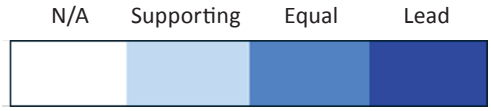

Left to right ticked:
Preregistered, Preprinted, Published with Peer Review

For more info, see: https://osf.io/download/6845fa0e26e4486cf1d539468/

List of Publications

1. **CD4⁺ T cell help creates memory CD8⁺ T cells with innate and help-independent recall capacities**
   Ahrends T, Busselaar J, Severson T, Babala N, de Vries E, Bovens A, Wessels L, van Leeuwen F, Borst J.
   Nature Communications 2019; 10(1): 553. doi: 10.1038/s41467-019-13438-1

2. **Helpless priming sends CD8⁺ T cells on the road to exhaustion**
   Busselaar J, Tian S, van Eenennaam H, Borst J.
   Frontiers in Immunology 2020; 11: 592569; doi: 10.3389/fimmu.2020.592569

3. **Mechanism of action of PD-1 receptor/ligand targeted cancer immunotherapy**
   Borst J, Busselaar J, Bosma DMT, Ossendorp F.
   European Journal of Immunology 2021; 51(8): 1911-1920. doi: 10.1002/eji.202048994

4. **The importance of type I interferon in orchestrating the cytotoxic T-cell response to cancer**
   Busselaar J*, Sijbranda M*, Borst J.
   Immunology Letters 2024; 270: 106938; doi: 10.1016/j.imlet.2024.106938

5. **PD-1 or CTLA-4 blockade promotes CD86-driven Treg responses upon radiotherapy of lymphocyte-depleted cancer in mice**
   Frijlink E, Bosma DMT, Busselaar J, Battaglia TW, Staal MD, Verbrugge I, Borst J.
   Journal of Clinical Investigation 2024; 134(6): e171154. doi: 10.1172/JCI171154.

6. **CD4⁺ T-cell help delivery to monocyte-derived dendritic cells promotes CD4⁺ effector differentiation of helper and cytotoxic T cells**
   Bosma DMT, Busselaar J, Staal M, Frijlink E, Mack M, Salerno F, Borst J.
   Immunology Letters 2025; 273: 107022. doi: 10.1016/j.imlet.2025.107022

7. **CD27 costimulation supports metabolic fitness of CD4⁺ T cells by enhancing de novo nucleotide and protein synthesis**
   Ngoc Minh TT*, Verleng LJ*, Schrama E, Busselaar J, de Vries E, Borst J, Berkers CR, Zaal EA, de Kivit S.
   The Journal of Immunology 2025; vkaf075. doi: 10.1093/jimmun/vkaf075

8. **Phagocytosis of necroptotic cells optimizes type 1 conventional dendritic cells for induction of a cytotoxic T-cell response**
   Staal MD, Wang Z, Bosma DMT, Busselaar J, Schrama E, de Vries E, Xiao Y, Borst J.
   Cell Death and Differentiation 2026; doi: 10.1038/s41418-026-01689-7.

9. **Stem-like PD-1⁺TCF-1⁺ CD8⁺ T cells result from helpless priming and rely on CD4⁺ T-cell help to complete their cytotoxic effector differentiation**
   Busselaar J*, Bosma DMT*, Staal MD, Lei X, Xiao Y, Borst J.
   The Journal of Immunotherapy of Cancer 2026; 14(4): e014041. doi: 10.1136/jitc-2025-014041

10. **Requirements for development of T-helper1 and T-follicular helper cells from a common precursor**
    Bosma DMT*, Busselaar J*, Staal MD, de Koning M, Reljić M, Lei X, de Wit T, Xiao Y, Borst J, Salerno F.
    Cell Reports 2026; 45(5): 117296. doi: 10.1016/j.celrep.2026.117296

List of submitted manuscripts

1. **Discerning and common features of CD4$^+$ conventional and regulatory T cells that determine human pregnancy success**
   Verleng L J, Busselaar J, Mensink M, Schrama E, Kapsenberg H, van der Keur C, Lei X, Eikmans M, Xiao Y, de Kivit S, Borst J.
   Manuscript submitted to Frontiers in Immunology

2. **CD8$^+$ T cell priming, CD4$^+$ T cell help and implications for cancer immunotherapy**
   Kastenmüller W, Busselaar J, Huang A, Borst J.
   Revised manuscript submitted to Immunity

Overview of completed courses and other training

Mandatory activities

Year	Title	Hours
2018	Laboratory Animal Science (Article 9)	80
2020	Leiden University Onboarding Programme Inform & Connect	10
2020	Workshop Scientific Conduct for PhDs	5
2021	Basic Methods and Reasoning in Biostatistics	42

Scientific courses, workshops, conferences and other training activities

Year	Title	Hours
2018	European Congress of Immunology (Amsterdam)	16
2019	Dutch Society for Immunology (NVVI) Symposium (Noordwijk)	16
2019	PhD Course Mouse Genetic Engineering (Leiden)	50
2019	IHB Science Retreat (Leiden)	8
2019	NVVI Annual Meeting (Lunteren)	16
2020	MACS T cell Exhaustion Meeting (Brussels, Belgium)	8
2020	NKI-LUMC Immunology Meeting (Leiden)	8
2020	IMMU Science Retreat (Leiden)	8
2020	NVVI Annual meeting (online)	16
2021	NVVI Symposium (online)	16
2021	Oncode Annual Meeting (online)	16
2021	Dutch Tumor Immunology Meeting (online)	16
2021	European Congress of Immunology (online)	16
2021	IMMU Science Retreat (Leiden)	8
2022	PhD Course Infection and Immunity (Leiden)	42
2022	NKI-LUMC Immunology meeting (Leiden)	8
2022	NVVI Annual Meeting (Lunteren)	16
2022	VIB Conference Immuno-Oncology (Leuven, Belgium)	16
2022	Oncode & HollandBio Meeting (Amsterdam)	5
2022	IMMU Science Retreat (Leiden)	8
2023	Joint Belgian-Dutch Immunology Meeting (Antwerp, Belgium)	16
2023	16th ENII EFIS EJI Summer School on Advanced Immunology (Alghero, Italy)	21

Presentations

Year	Title
2019-23	**Speaker (occasionally)**: Weekly department of Immunology (IMMU) meeting (Leiden)
2019-23	**Speaker (occasionally)**: Weekly Cancer Immunology meeting (Leiden)
2019	**Speaker:** NVVI Annual meeting (Lunteren)
2020	**Speaker:** IMMU Science Retreat (Leiden)
2021	**Poster:** IMMU Science Retreat (Leiden)
2022	**Poster:** NVVI Annual Meeting (Lunteren)
2023	**Poster:** IMMU Science Retreat (Leiden)
2023	**Poster:** 16th ENII EFIS EJI Summer School on Advanced Immunology (Alghero, Italy)

Teaching

Year	Title	Hours
2023	Supervision of writing assignment by Merel Sijbranda, second year master student Infection and Immunity at Utrecht University	20

Acknowledgements

Help is essential, not only for T cells but also for people. During my PhD, I was fortunate enough to receive help, guidance and support from so many people. Without you, this thesis would not have been possible.

First and foremost: Many thanks to my promotor Jannie. I have never learned as much from anyone as I have learned from you. Thank you for giving me the guidance, and the freedom, to conduct the science we are both so passionate about.

An enormous thanks to my closest colleagues. It was truly special to be part of such a great team, I could always rely on you and trust you blindly. Douwe, thank you for being my right-hand man, my sparring partner and overall my rock in the lab. All those hours tattooing, processing samples and FACSing were so much more enjoyable working side-by-side with you. Mo, thank you for all your help designing and producing the materials used in this project, and for always being ready to step in or take over during mouse experiments. Our shared passion for music, and attending each other's DJ gigs / classical concerts is something I really enjoyed.

Elselien, thank you for all your support, your scientific input during mouse meetings and for letting me be a part of the NKI B3 lab again every once in a while. I will miss our suspicious lab material exchanges outside Station Zuid.

Yanling, thank you for our warm bond and for sharing your knowledge with me, whether it was about DC biology or how to deal with difficult reviewers. Fiamma, thank you for all your scientific input, helpful career advice, and fresh energy you brought to the lab.

Many thanks to all my wonderful colleagues: Evert, always fun working with you, you are one of a kind. Sander, thank you for supervising me during my internship, I learned from the best. Mark, Lotte, Xin, Tom: I really enjoyed sharing an office with you. Thank you for our nice conversations and shared experiences. Ellen, thank you for always being there for us. Jorn, thank you for welcoming me at the LUMC, we had a great connection from day one. Eloisa, thank you for being a ray of sunshine in the lab, I have great memories of our dancing night out together. Laurens and Ben, thank you for always making me laugh. Dennis, Timo, Sander, Sabine, Yizhi, Mirna, Zhixian, Karel, Annick, Mylène, thank you for the great company and fun conversations we had during lunch and social activities. Merel, thank you for your hard work and dedication during the writing of your literature review.

To my second promotor Ferry and PhD guidance committee Ramon, Thorbald and Noel: Thank you for your interest, sharp questions and constructive feedback during my PhD progress meetings.

To the people from the IVD, PDC and FCF: Thank you for making this research possible. Also many thanks to Susan, Leon, Ioannis, Martijn and Vincent for helping me with the scRNAseq analysis.

My colleagues at NKI: Tomasz, thank you for trusting me with the revision of your memory paper, and for all the previous work you have done with the Help / No Help model. Without you, my project would not have been possible. Nika, Victoria and Astrid, thank you for taking me under your wings when I just started my PhD, and for teaching me all the ins & outs of the tattoo vaccination model. Inge, Andriy, Irene, Paula, Aldo, Ronak: Thank you for creating such a welcoming environment and for helping me find my way in the lab.

A huge thank you to my lovely friends for supporting me and for taking such a great interest in my research. Mijn lieve vriendinnen: Parand, Gabriëlle, Laetitia, Annemiek, Milena, Laura, Claartje, dank jullie wel voor het meeleven tijdens alle ups & downs. The CitizenM crew: Andrew, Lalit, Ivana, Panos, Dominic, Adrian, Wojciech, Kinga, thank you guys for all the fun we have together. Isabelle, Freya, Luc, Sara, Salina: Dank jullie wel voor jullie vriendschap en het samen muziek maken.

Mijn lieve tantes Cynthia en Atte: Dank jullie wel voor jullie oprechte interesse in mijn onderzoek. Lieve Sophia en Bart, dank jullie wel voor alle steun, gezelligheid en het helpen herinneren dat het leven niet alleen uit werken bestaat.

Mama, Papa, aan jullie heb ik alles te danken. Jullie hebben mij de best mogelijke start gegeven en mijn wetenschappelijke én persoonlijke ontwikkeling altijd aangemoedigd. Bedankt voor al jullie liefde en steun. Ik hou van jullie.

Altin, my love, I could never have done this without you. Thank you for supporting me in everything. You are an amazing husband to me and an amazing father to Nandini. I love you forever.

En tot slot: Nandini, mijn liefste. Dankjewel dat jij er bent.